UNIVERSITÀ DEGLI STUDI DI CAGLIARI

PhD Degree in Physics

CYCLE XXXIV

Transverse momentum dependent fragmentation functions and their role in spin-1/2 polarized hadron production

Scientific Disciplinary Sector(s)

FIS/02

PhD Student: Marco Zaccheddu

Supervisors: Prof. Umberto D'Alesio

Prof. Francesco Murgia

Final exam. Academic Year 2020-2021

Thesis defence: April 2022

Contents

Chapter 1.

Introduction

Until the first years of the 70s there was the common belief that, in hard scattering processes, the effects due to the transverse polarization of the particles involved were negligible. Precisely in those years the results of several measurements, totally unexpected, opened a new way to study transverse spin effects in hadron physics. During the mid 70s, indeed, significant Single Spin Asymmetries (SSAs) in pion inclusive production in proton-proton collisions, at center of mass energy of few GeV, were observed at the Argonne Laboratory synchrotron [1–3]. Moreover, during the same period at the Fermilab, Λ-hyperons produced in unpolarized pN collisions, at $\sqrt{s} \simeq 24\,\text{GeV}$ and moderate transverse momentum P_T (below 1.5 GeV), showed high values of their transverse polarization with respect to the production plane [4]. In general, the transverse Single Spin Asymmetry for an inclusive process like $A^{\uparrow}B \to C + X$ is defined as:

$$A_N = \frac{d\sigma^{\uparrow} - d\sigma^{\downarrow}}{d\sigma^{\uparrow} + d\sigma^{\downarrow}} = \frac{d\sigma^{\uparrow} - d\sigma^{\downarrow}}{2d\sigma^{\text{unpol}}}\,, \tag{1.1}$$

where $d\sigma^{\uparrow(\downarrow)}$ is the differential cross section for the production of a hadron C in the scattering of a upwards, $d\sigma^{\uparrow}$, or downwards, $d\sigma^{\downarrow}$, transversely polarized hadron A off an unpolarized hadron B. This asymmetry is also called "left-right asymmetry". Analogously to A_N, it is also possible to define the transverse

polarization for the process $AB \to C^{\uparrow} + X$, where C is a spin-1/2 hadron, as:

$$P_C = \frac{d\sigma^{\uparrow} - d\sigma^{\downarrow}}{d\sigma^{\uparrow} + d\sigma^{\downarrow}} = \frac{d\sigma^{\uparrow} - d\sigma^{\downarrow}}{d\sigma^{\text{unpol}}}, \tag{1.2}$$

where now the arrows in $d\sigma^{\uparrow(\downarrow)}$ represent the direction of the final-state hadron transverse polarization with respect to the production plane. Experimentally, for the Λ polarization, it is usually measured by observing the angular distribution of the Λ weak decay (see below).

Given the great importance of the study of the SSAs, the discoveries made during the 70s stimulated a large number of both theorical and experimental analyses. Among the first and most important experimental works we cite those, around the 90s, of the E704 Collaboration at the Fermilab, that gathered data on the SSAs for the production of several particles (photons, pions, Λ, η) in pp and $p\bar{p}$ collisions, employing polarized beams for the first time. They significantly contributed to the studies of such asymmetries, reaching a center of mass energy of $\sqrt{s} = 20\,\text{GeV}$ and improving the separation between the x_F ($x_F = 2P_L/\sqrt{s}$, where P_L is the final hadron longitudinal momentum) and P_T dependences of the SSAs [5–8]. Surprisingly, pion asymmetries reached values as large as 30-40% in size.

These results were then confirmed, lately, by the STAR, PHENIX and BRAHMS Collaborations at the Relativistic Heavy Ion Collider (RHIC), at center of mass energies up to $\sqrt{s} = 500\,\text{GeV}$ and covering a wider kinematical range in x_F and P_T [9–13]. The most surprising aspect is that the main features characterizing such SSAs kept on manifesting even at these energies. Similarly, the experimental data, that were gradually collected on the transverse polarization of the Λ-hyperons produced in unpolarized hadronic collisions, confirmed the extraordinarity of this kind of measurements. Even nowadays, for what concerns A_N, while the available measurements are increasingly more accurate and cover wider kinematic regions, their phenomenological interpretation is still under examination and debate.

On the theory side, indeed, we know that large values of the transverse polarization P_C (and similarly for A_N) cannot be explained within the framework of collinear QCD factorization, at leading twist, that in fact predicts negligible values [14]. Hyperon polarization, observed in unpolarized collisions, necessarily has to originate from non-perturbative effects, presumably in the hadronization process. For this reason, a study of the Λ polarization enables us to obtain important information on this non-perturbative mechanism.

The study of SSAs, in addition, is strongly related to our comprehension of the inner structure of the hadrons and their spin content, in terms of the orbital angular momentum and the partons spin. In such a context an important role, within the framework of pQCD, is played by the spin and transverse momentum dependent parton distribution functions (TMD-PDFs) and fragmentation functions (TMD-FFs), collectively referred to as TMDs.

For what concerns the theoretical development, the first approaches were based on a natural extension of the collinear parton model in pQCD, by generalizing the PDFs and the FFs with the inclusion of a dependence on the intrinsic transverse momentum of the partons with respect to their parent nucleon direction, or of the hadrons with respect to their fragmenting quark direction. Phenomenologically, the first and most studied TMD-PDFs are the unpolarized distribution and the Sivers function. This last function, introduced in [15, 16], correlates the azimuthal distribution of unpolarized quarks with the spin of their parent nucleon. Indeed, we can define a non-zero asymmetry of the following form:

$$\Delta\hat{f}_{a/A^\uparrow}(x, \boldsymbol{k}_\perp) = \hat{f}_{a/A^\uparrow}(x, \boldsymbol{k}_\perp) - \hat{f}_{a/A^\downarrow}(x, \boldsymbol{k}_\perp), \tag{1.3}$$

where the arrows $\uparrow$ ($\downarrow$) represent the transverse spin direction, upwards and downwards, of the hadron A with respect to its direction of motion. We can also notice that the function $\Delta\hat{f}_{a/A^\uparrow}$ should be, by parity conservation, proportional to $(\hat{\boldsymbol{p}}_A \times \boldsymbol{k}_\perp) \cdot \boldsymbol{S}_A$, where $\boldsymbol{p}_A$ and $\boldsymbol{S}_A$ are the hadron A momentum and spin, and $\boldsymbol{k}_\perp$ the parton transverse momentum.

It is worth noting that the this asymmetry enters in the expression of the unpolarized parton number density inside a transversely polarized hadron

$$\hat{f}_{a/A^\uparrow}(x, \boldsymbol{k}_\perp) = f_{a/A}(x, \boldsymbol{k}_\perp) + \frac{1}{2}\Delta^N f_{a/A^\uparrow}(x, k_\perp)(\hat{\boldsymbol{p}}_A \times \hat{\boldsymbol{k}}_\perp) \cdot \boldsymbol{S}_A \,, \tag{1.4}$$

where $\Delta^N f_{a/A^\uparrow}$, is the so-called Sivers function [17].

In the fragmenting sector, the most studied TMD functions are the unpolarized and the Collins fragmentation functions, where the latter gives the asymmetric azimuthal distribution of unpolarized hadrons produced in the fragmentation of a transversely polarized quark. Analogously to the Sivers function, we can write the fragmentation function of a polarized quark as follows:

$$\hat{D}_{C/c^\uparrow}(z, \boldsymbol{k}_\perp) = D_{C/c}(z, \boldsymbol{k}_\perp) + \frac{1}{2}\Delta^N D_{C/c^\uparrow}(z, k_\perp)(\hat{\boldsymbol{p}}_q \times \hat{\boldsymbol{k}}_\perp) \cdot \boldsymbol{s}_q \,, \tag{1.5}$$

where $\boldsymbol{p}_q$ and $\boldsymbol{s}_q$ are the quark momentum and spin, and $\Delta^N D_{C/c^\uparrow}$ is the so called Collins function [17], that can be also written as:

$$\Delta\hat{D}_{C/c^\uparrow}(z, \boldsymbol{k}_\perp) = \hat{D}_{C/c^\uparrow}(z, \boldsymbol{k}_\perp) - \hat{D}_{C/c^\downarrow}(z, \boldsymbol{k}_\perp) \,, \tag{1.6}$$

where $\uparrow$ ($\downarrow$) represents the transverse spin direction, upwards or downwards, of the fragmenting quark.

Subsequently, a systematic classification of the TMD-PDFs and TMD-FFs was carried out, leading to a total of eight different spin and transverse momentum dependent parton distribution and fragmentation functions (for spin-1/2 hadrons) [18, 19]. Among them, in the quark case we can also cite, besides the aforementioned Sivers [15, 16] and Collins functions [20], the Boer-Mulders distribution function, that was proposed initially as a usefull tool to explain the azimuthal asymmetries observed in the dilepton angular distribution in unpolarized Drell-Yan processes [21]. Similar functions can also be defined in the gluon sector, where, instead of transverse polarization, we refer to linearly polarized states.

In recent years, we have witnessed significant progress in the formulation of factorization theorems in terms of TMDs for a well defined class of processes [22–25], all characterized by the presence of two strongly ordered energy scales: namely, semi-inclusive deep inelastic scattering (SIDIS), Drell-Yan (DY) and e^+e^- annihilation processes, where the two scales are the virtuality of the exchanged boson (the larger one) and the transverse momentum of the final hadron (SIDIS), of the lepton-pair (DY) or of the hadron-pair in e^+e^- collisions (the smaller one).

Moreover, it has been proven that, unlike the collinear distributions and all TMD-FFs, the TMD-PDFs are not all strictly universal. The universality, indeed, is an important issue within TMD factorization theorems: it enables us to predict observables in any of the three abovementioned processes, once one of the functions is extracted from a phenomenological analysis. Another important aspect, strongly related to the factorization, is the scale dependence of the TMDs, that can be encoded in well-defined evolution equations. These eventually allow to give estimates of TMD observables in different kinematical situations.

Among the TMD-PDFs there are two, already mentioned, T-odd functions, the Sivers, $f_{1T}^{\perp}$, and the Boer-Mulders, $h_1^{\perp}$, functions that are process dependent or, in other words, manifest a modified universality. For what concerns the Sivers asymmetry, this emerges in SIDIS processes from the interactions between the quark in the final state and the proton remnants, while in DY processes we have an initial-state interaction between the spectator and the incoming quarks. This difference leads to the following relation between the Sivers function when probed in SIDIS and DY [26,27]:

$$f_{1T}^{\perp}(x,k_{\perp})_{\rm SIDIS} = -f_{1T}^{\perp}(x,k_{\perp})_{\rm DY}\,. \tag{1.7}$$

A similar relation holds also for the Boer-Mulder function.

The complete structure of azimuthal dependences for particle production in (un)polarized collisions, within a TMD approach, specifically for SIDIS [18,19,28], DY [29] processes and hadron-pair production in e^+e^- collisions [30] has been

formulated in full detail. In particular, in Ref. [28] the full decomposition in terms of the eight independent TMD-PDFs was obtained for the process $\ell p \to \ell' h\, X$ adopting the helicity formalism. This, indeed, allows for a direct probabilistic interpretation within a more intuitive picture, which splits the physical process in three phases, each of them described by the corresponding helicity amplitude: the inclusive emission of a parton by the initial hadron $p \to q\, X$, the perturbatively calculable hard interaction $\ell q \to \ell' q'$, and the emission of the final hadron by the outgoing quark, $q' \to h\, X$. We recall that in this study only spinless or unpolarized hadrons were considered. A somehow pioneering work in this direction, even if in the context of a process for which TMD factorization is assumed as a phenomenological ansatz, was presented in Ref. [31]. There, the focus was on transverse SSAs for inclusive particle production in pp collisions, and, within the helicity formalism, all leading-twist TMD-PDFs, for quark and gluons, were considered together with the two TMD-FFs for spinless (or unpolarized) hadrons.

A striking feature of SIDIS processes, which have played and still play a leading role in accessing TMDs, is the strong correlation between the transverse momentum dependence arising from the TMD-PDFs and TMD-FFs in the resulting and measurable transverse momentum of the final hadron [32]. In this respect DY and e^+e^- processes are of fundamental importance, being sensitive separately to TMD-PDFs and TMD-FFs, respectively. In a similar way to what was done for the TMD-PDFs, we will see that within the helicity formalism it is also possible to define eight TMD-FFs, with analogous properties, for a spin-1/2 hadron.

In this thesis, these TMD-FFs will directly appear in the azimuthal dependences for double-hadron prodution in unpolarized e^+e^- annihilation processes, for which we have a factorization theorem. In particular, the Belle Collaboration [33] has collected data for the transverse polarization of Λ-hyperons produced together with light mesons in an almost back-to-back configuration as well as for Lambda's inclusively produced, where the Λ transverse momentum is measured with respect to the thrust axis.

It is worth recalling that the Λ polarization is self-analyzing and therefore easily measurable. Its proton-pion weak decay enables, through its angular distribution measurement, to identify directly the Λ polarization in its reference frame. The angular distribution can be written as follows:

$$\hat{W}^{(1/2)}(\theta,\phi) = \frac{1}{4\pi}(1 + \alpha P_Y^\Lambda \sin\theta\cos\phi)\,, \tag{1.8}$$

where P_Y^Λ is the transverse polarization, α is the decay constant for the Λ weak decay, while θ and ϕ are the angles that identify the proton direction in the Λ reference frame.

To try to describe the Λ transverse polarization, we will see that we can use a still less explored, but not less important, fragmentation function. This TMD-FF, called *polarizing FF* (pFF), gives the distribution of a transversely polarized spin-1/2 hadron coming from the fragmentation of an unpolarized quark. It can be written as :

$$\Delta\hat{D}_{C^\uparrow/c}(z,\boldsymbol{k}_\perp) = \hat{D}_{C^\uparrow/c}(z,\boldsymbol{k}_\perp) - \hat{D}_{C^\downarrow/c}(z,\boldsymbol{k}_\perp) = \hat{D}_{C^\uparrow/c}(z,\boldsymbol{k}_\perp) - \hat{D}_{C^\uparrow/c}(z,-\boldsymbol{k}_\perp)\,, \tag{1.9}$$

that is the difference between the FFs, $\hat{D}_{C^\uparrow/c}$ and $\hat{D}_{C^\downarrow/c}$, for an unpolarized quark fragmenting into a spin-1/2 hadron with an upward or downward transverse polarization. Among its main properties, we recall that this pFF is T-odd, but chiral even, and this allows to access it directly without any unknown, chiral-odd, counterpart. Last but not least, like the Collins function, it is universal, implying that it should be the same when probed in e^+e^- or SIDIS processes [34].

The *polarizing FF* was introduced in Ref. [18] and it was studied phenomenologically in Ref. [35], where the longstanding puzzle of the transverse polarization data for the inclusive production of Λ hyperons in unpolarized hadron-hadron collisions [4,36] was considered. Within a simplified TMD model, some of its interesting features were tentatively extracted and a good description of data was achieved. Notice that for such processes, TMD factorization is not proven and other competing contributions could be at work.

After these pioneering works, the lack of additional experimental information prevented any further theory development. This until the new available data from the Belle Collaboration at KEK [33] on transverse $\Lambda/\bar{\Lambda}$ hyperon polarization in e^+e^- processes have triggered a renewed interest. In fact, we will see how this intriguing TMD-FF can be directly extracted, within different approaches, from Belle experimental data.

1.1. This Thesis

This thesis is partly based on the following pubblications:

1. U. D'Alesio, F. Murgia and M. Zaccheddu
   First extraction of the Λ polarizing fragmentation function from Belle e^+e^- data
   Phys.Rev.D 102 (2020) 5, 054001

2. U. D'Alesio, F. Murgia and M. Zaccheddu
   General helicity formalism for two-hadron production in e^+e^- annihilation within a TMD approach
   JHEP 10 (2021) 078

3. U. D'Alesio, L. Gamberg , F. Murgia and M. Zaccheddu
   Reanalysis of Belle e^+e^- data on transverse Λ polarization within the CSS framework
   in preparation

To give the thesis a more logical organization, we will not present the results of the papers following their chronological order. Rather, we will start giving an overview of the double-hadron production case in e^+e^- annihilation process, within the helicity formalism, presenting the results of the second paper. We will then discuss the phenomenological extraction of the *polarizing FF* from Belle e^+e^- data, and show how it can be used to give estimates for the transverse Λ polarization in SIDIS processes.

The thesis is organized as follows:

- in Chapter 2 we present the complete expressions for all leading-twist azimuthal dependences and polarization observables at "leading order" for double-hadron production in e^+e^- annihilation processes within the helicity formalism. Moreover, by adopting a factorized transverse momentum dependence in terms of Gaussian-like TMD-FFs we derive simplified expressions for all single- and double-polarized observables, useful in phenomenological analyses;

- in Chapter 3 we present the phenomenological analysis of Belle data, for the transverse $\Lambda/\bar{\Lambda}$ hyperon polarization in e^+e^- annihilation processes, leading to the first extraction of the Λ Polarizing Fragmentation Function;
- in Chapter 4 we present the kinematics and the expression for the production of a transversely polarized hadron in a Semi-inclusive Deep Inelastic Scattering. Moreover, we will give the $\Lambda/\bar{\Lambda}$ polarization estimates for typical energies reachable at the future Electron-Ion Collider (EIC);
- in Chapter 5 we discuss, by employing the CSS evolution equations, the formulation in terms of convolutions in b_T-space for double and single-inclusive hadron production in e^+e^- annihilation processes. These results will be used to re-analyze the Belle data within a proper TMD framework.
- Finally, conclusions will be drawn in Chapter 6.

A number of more technical derivations and results used in the thesis are presented in several appendices.

Chapter 2.

General helicity formalism for two-hadron production in e^+e^- annihilation within a TMD approach

2.1. Introduction

In this Chapter we apply the TMD approach, adopting the helicity formalism, to $e^+e^- \to h_1 h_2 X$ processes and derive the complete expressions for all leading-twist azimuthal dependences and polarization observables at leading order, adopting two commonly used reference frames. The case of single-hadron production within a jet, as pointed out in a series of recent papers [37–40], requires a more dedicated study and it will be partially addressed in the following Chapters.

We will present the complete set of all leading-twist TMD-FFs for spinless (or unpolarized) and spin-1/2 hadrons both for quarks and gluons, discussing their main properties and their physical meaning. Moreover, by adopting a factorized transverse momentum dependence in terms of Gaussian-like TMD-FFs we derive simplified expressions for all single- and double-polarized observables, useful in phenomenological analyses. The results are in perfect agreement with those of Ref. [30].

The motivations behind this study are several: from the theory point of view, it represents the extension of the helicity formalism to spin-1/2 hadron production in e^+e^- annihilations, providing the classification of all leading-twist quark and gluon TMD-FFs, and focusing, for the quark case, on their role in polarized hadron production; on the phenomenology side, it timely matches the renewed interest, triggered by recent data from the Belle Collaboration on the transverse Λ polarization [33], in the associated hadron production in e^+e^- annihilation processes. In this context, the first phenomenological analysis, as we will discuss in the following Chapter, within a TMD framework has been carried out in Ref. [41].

The Chapter is organized as follows: in Section 2.2 we present the main formulae for the computation, within the helicity formalism, of the azimuthal dependences for the production of (un)polarized hadron-pairs in e^+e^- collisions. In Section 2.3 we give the complete set of quark TMD-FFs for spin-1/2 hadrons at leading twist, while in Sec. 2.4 we collect the explicit expressions for unpolarized, single- and double-polarized hadron production. In Sec. 2.5 we present all convolutions in terms of the TMD-FFs for a specific kinematical configuration; in particular, in Sec. 2.5.4 we give the corresponding explicit analytical formulae assuming a factorized Gaussian dependence for the TMD-FFs. Our conclusions are gathered in Sec. 2.6. Several useful detailed results are derived and collected in the Appendices; in particular, in Appendix A we give the main properties of the helicity fragmentation amplitudes, in Appendix B we present the complete set of gluon TMD-FFs for spin-1/2 hadrons and in Appendix C the relation with other common notations is worked out. In Appendix D we discuss the tensorial analysis adopted to extract the observed azimuthal dependences. Useful relations and definitions on the helicity frames are given in Appendix E.

2.2. Production of two hadrons in e^+e^- annihilation

We consider the production of two almost back-to-back hadrons in the $e^+e^- \to h_1(S_1)\, h_2(S_2) + X$ process, where $S_{1,2}$ are the hadron spins, within a TMD ap-

proach and adopting the helicity formalism. Since we will be also interested in heavy baryon, like Λ's, production, we will pay special attention to hadron mass effects. Two reference frames are usually adopted for such a study: the "thrust frame", where one identifies the direction of the two opposite jets and measure the corresponding azimuthal distributions of the two hadrons within the jets; the "hadron frame", where one measures only the momenta of the two hadrons and the azimuthal distribution of one hadron with respect to the other.

More precisely, the thrust frame is chosen so that the $e^+e^- \to q\,\bar{q}$ scattering occurs in the $\hat{x}\hat{z}$ plane, with the back-to-back quark and antiquark moving along the $\hat{z}$-axis. This choice requires, experimentally, the reconstruction of the jet thrust axis, but it involves a very simple kinematics. In the configuration of Fig. 2.1, the four-momenta of the e^+, e^- leptons (respectively k^+, k^-) and of the $q, \bar{q}$ pair (q_1, q_2 respectively) are, neglecting all masses,

$$q_1 = \frac{\sqrt{s}}{2}(1,0,0,1) \qquad q_2 = \frac{\sqrt{s}}{2}(1,0,0,-1) \tag{2.1}$$

$$k^- = \frac{\sqrt{s}}{2}(1,-\sin\theta,0,\cos\theta) \qquad k^+ = \frac{\sqrt{s}}{2}(1,\sin\theta,0,-\cos\theta)\,, \tag{2.2}$$

where s is the center-of-mass energy squared. These define the leptonic plane. We will use the generic notation $\hat{\boldsymbol{x}}_L$, $\hat{\boldsymbol{y}}_L$, $\hat{\boldsymbol{z}}_L$ for the axes in this frame. The final hadrons h_1 and h_2 carry light-cone momentum fractions z_1 and z_2 and have intrinsic transverse momenta $\boldsymbol{p}_{\perp 1}$ and $\boldsymbol{p}_{\perp 2}$ with respect to the direction of the corresponding fragmenting quarks,

$$\boldsymbol{p}_{\perp 1} = p_{\perp 1}(\cos\varphi_1, \sin\varphi_1, 0) \qquad \boldsymbol{p}_{\perp 2} = p_{\perp 2}(\cos\varphi_2, \sin\varphi_2, 0)\,, \tag{2.3}$$

with $p_\perp = |\boldsymbol{p}_\perp|$, so that their four-momenta can be expressed as

$$P_{h_1} = \left(z_1 \frac{\sqrt{s}}{2}\Big(1 + \frac{a_{h_1}^2}{z_1^2}\Big), p_{\perp 1}\cos\varphi_1, p_{\perp 1}\,\sin\varphi_1,\; z_1\frac{\sqrt{s}}{2}\Big(1 - \frac{a_{h_1}^2}{z_1^2}\Big)\right) \tag{2.4}$$

$$P_{h_2} = \left(z_2 \frac{\sqrt{s}}{2}\Big(1 + \frac{a_{h_2}^2}{z_2^2}\Big), p_{\perp 2}\,\cos\varphi_2, p_{\perp 2}\,\sin\varphi_2, -z_2\frac{\sqrt{s}}{2}\Big(1 - \frac{a_{h_2}^2}{z_2^2}\Big)\right)\,, \tag{2.5}$$

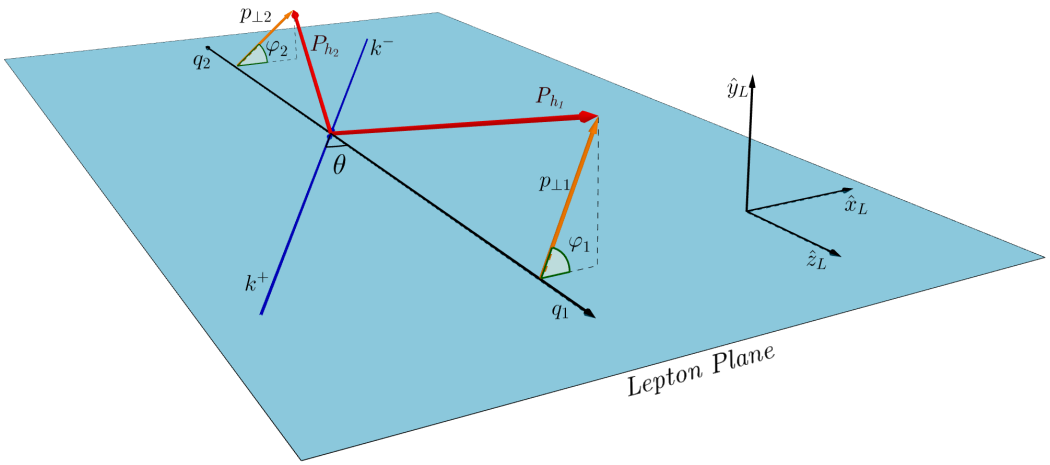

Figure 2.1.: Kinematics for the thrust-frame configuration.

where

$$a^2_{h_{1,2}} = \frac{p^2_{\perp 1,2} + M^2_{h_{1,2}}}{s} = \eta^2_{\perp 1,2} + \frac{M^2_{h_{1,2}}}{s}\,. \tag{2.6}$$

At large center of mass energies and not too small values of z, one can keep only the lowest-order contribution in $\eta_\perp$, with the whole mass dependence, and work with the much simpler kinematics:

$$P_{h_1} \simeq \left(z_1 \frac{\sqrt{s}}{2}\left(1 + \frac{M^2_{h_1}}{z_1^2 s}\right), p_{\perp 1}\cos\varphi_1, p_{\perp 1}\sin\varphi_1, z_1\frac{\sqrt{s}}{2}\left(1 - \frac{M^2_{h_1}}{z_1^2 s}\right)\right) \tag{2.7}$$

$$P_{h_2} \simeq \left(z_2 \frac{\sqrt{s}}{2}\left(1 + \frac{M^2_{h_2}}{z_2^2 s}\right), p_{\perp 2}\cos\varphi_2, p_{\perp 2}\sin\varphi_2, -z_2\frac{\sqrt{s}}{2}\left(1 - \frac{M^2_{h_2}}{z_2^2 s}\right)\right)\,. \tag{2.8}$$

It is important to stress that we will keep terms in $p_\perp/\sqrt{s}$ only when this is essential to give a non zero result. For massive hadrons, two further scaling variables are usually introduced: the energy fraction (often adopted in the experimental analyses)

$$z_h = 2E_h/\sqrt{s} \tag{2.9}$$

and the momentum fraction

$$z_p = 2|\boldsymbol{P}_h|/\sqrt{s}\,. \tag{2.10}$$

These are related to the light-cone momentum fractions as follows:

$$z_h = z\left(1+\frac{a_h^2}{z^2}\right) \simeq z\left(1+\frac{M_h^2}{z^2 s}\right) \tag{2.11}$$

$$z_p = z\left[\left(1-\frac{a_h^2}{z^2}\right)^2 + 4\frac{\eta_\perp^2}{z^2}\right]^{1/2} \simeq z\left(1-\frac{M_h^2}{z^2 s}\right) \tag{2.12}$$

$$z_p = z_h\left(1-4\,\frac{M_h^2}{z_h^2 s}\right)^{1/2}. \tag{2.13}$$

For later use we also define the following quantity:

$$\beta_{1,2}^2 = 1-4\,\frac{\eta_{\perp 1,2}^2}{z_{p_{1,2}}^2}\,. \tag{2.14}$$

Notice that, adopting the above variables, one can express the two hadron three-momenta as

$$\begin{aligned}\boldsymbol{P}_{h_1} &= |\boldsymbol{P}_{h_1}|\left(\frac{p_{\perp 1}}{|\boldsymbol{P}_{h_1}|}\cos\varphi_1, \frac{p_{\perp 1}}{|\boldsymbol{P}_{h_1}|}\sin\varphi_1, \sqrt{1-\frac{p_{\perp 1}^2}{|\boldsymbol{P}_{h_1}|^2}}\right)\\ &= |\boldsymbol{P}_{h_1}|\left(\frac{2\eta_{\perp 1}}{z_{p_1}}\cos\varphi_1, \frac{2\eta_{\perp 1}}{z_{p_1}}\sin\varphi_1, \beta_1\right)\end{aligned} \tag{2.15}$$

$$\begin{aligned}\boldsymbol{P}_{h_2} &= |\boldsymbol{P}_{h_2}|\left(\frac{p_{\perp 2}}{|\boldsymbol{P}_{h_2}|}\cos\varphi_2, \frac{p_{\perp 2}}{|\boldsymbol{P}_{h_2}|}\sin\varphi_2, -\sqrt{1-\frac{p_{\perp 2}^2}{|\boldsymbol{P}_{h_2}|^2}}\right)\\ &= |\boldsymbol{P}_{h_2}|\left(\frac{2\eta_{\perp 2}}{z_{p_2}}\cos\varphi_2, \frac{2\eta_{\perp 2}}{z_{p_2}}\sin\varphi_2, -\beta_2\right).\end{aligned} \tag{2.16}$$

Moving to the hadron frame, here one can fix the $\hat{z}$-axis in the opposite direction with respect to the observed hadron h_2 and the $\widehat{xz}$ letonic plane as determined by the lepton and the h_2 directions (with the e^+e^- axis at angle θ)[1]. There is

[1] We use the same angle as in the thrust frame for the sake of simplicity.

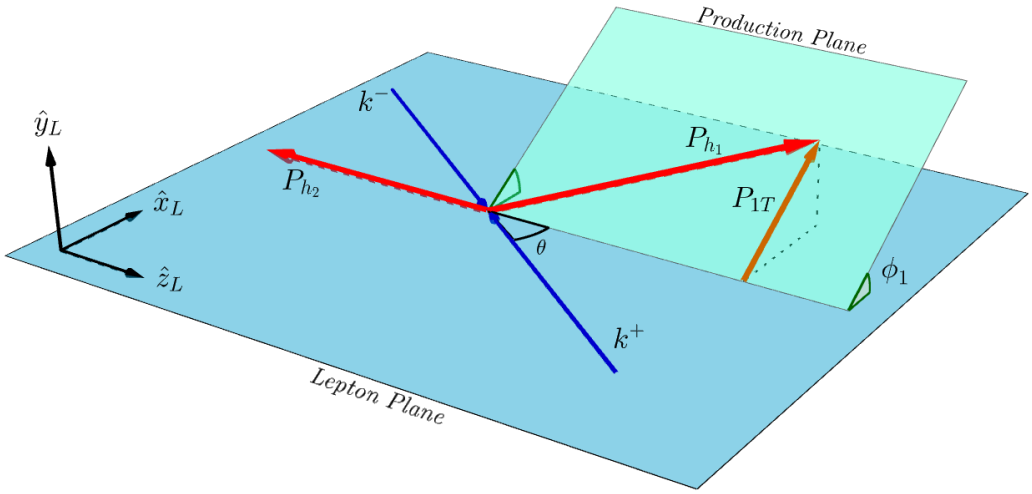

Figure 2.2.: Kinematics for the the hadron-frame configuration.

another relevant plane, the production one, determined by $\hat{z}$ and the direction of the other observed hadron h_1, at an angle ϕ_1 with respect to the $\hat{xz}$ plane. This kinematical configuration is shown in Fig. 2.2: it has the advantage of not requiring the reconstruction of the thrust axis. Also in this case we will use the notation $\hat{\boldsymbol{x}}_L$, $\hat{\boldsymbol{y}}_L$, $\hat{\boldsymbol{z}}_L$ for the axes in this frame, to which we refer generically to as the laboratory frame. Notice that the incoming particles entering the partonic process $e^+e^- \to q\bar{q}$ are still in a c.m. frame with $\boldsymbol{k}_1 = -\boldsymbol{k}_2$ and $\boldsymbol{q}_1 = -\boldsymbol{q}_2$ and lie on a plane, even if not coinciding with the lepton plane and depending on the intrinsic transverse momenta. In order to give it in a compact form we will use the relations among the three scaling variables defined above, as follows:

$$P_{h_2} = (E_2, 0, 0, -|\boldsymbol{P}_{h_2}|) = \frac{\sqrt{s}}{2} z_{h_2} \left(1, 0, 0, -\sqrt{1 - 4\frac{M_{h_2}^2}{z_{h_2}^2 s}}\right) = \frac{\sqrt{s}}{2}(z_{h_2}, 0, 0, -z_{p_2}) \tag{2.17}$$

$$\begin{aligned} q_2 &= (\frac{\sqrt{s}}{2}, -\frac{p_{\perp 2}}{z_{p_2}} \cos\varphi_2, -\frac{p_{\perp 2}}{z_{p_2}} \sin\varphi_2, -\frac{\sqrt{s}}{2}\beta_2) \\ &\simeq (\frac{\sqrt{s}}{2}, -\frac{p_{\perp 2}}{z_{p_2}} \cos\varphi_2, -\frac{p_{\perp 2}}{z_{p_2}} \sin\varphi_2, -\frac{\sqrt{s}}{2}) \end{aligned} \tag{2.18}$$

$$q_1 = \left(\frac{\sqrt{s}}{2}, \frac{p_{\perp 2}}{z_{p_2}}\cos\varphi_2, \frac{p_{\perp 2}}{z_{p_2}}\sin\varphi_2, \frac{\sqrt{s}}{2}\beta_2\right) \simeq \left(\frac{\sqrt{s}}{2}, \frac{p_{\perp 2}}{z_{p_2}}\cos\varphi_2, \frac{p_{\perp 2}}{z_{p_2}}\sin\varphi_2, \frac{\sqrt{s}}{2}\right) \tag{2.19}$$

$$\boldsymbol{P}_{h_1} = \left(P_{1T}\cos\phi_1, P_{1T}\sin\phi_1, z_{p_1}\frac{\sqrt{s}}{2}\sqrt{1-4\frac{\eta_{1T}^2}{z_{p_1}^2}}\right) \simeq \left(P_{1T}\cos\phi_1, P_{1T}\sin\phi_1, z_{p_1}\frac{\sqrt{s}}{2}\right) \tag{2.20}$$

$$\begin{aligned}
\boldsymbol{p}_{\perp 1} =& \boldsymbol{P}_{h_1} - z_{p_1}\beta_1\boldsymbol{q}_1 \\
=& \left(P_{1T}\cos\phi_1 - \frac{z_{p_1}}{z_{p_2}}p_{\perp 2}\beta_1\cos\varphi_2, P_{1T}\sin\phi_1 - \frac{z_{p_1}}{z_{p_2}}p_{\perp 2}\beta_1\sin\varphi_2,\right. \\
& \left. z_{p_1}\frac{\sqrt{s}}{2}\left(\sqrt{1-4\frac{\eta_{1T}^2}{z_{p_1}^2}} - \beta_1\beta_2\right)\right) \\
\simeq& \left(P_{1T}\cos\phi_1 - \frac{z_{p_1}}{z_{p_2}}p_{\perp 2}\cos\varphi_2, P_{1T}\sin\phi_1 - \frac{z_{p_1}}{z_{p_2}}p_{\perp 2}\sin\varphi_2, 0\right),
\end{aligned} \tag{2.21}$$

with $\eta_{1T} = \frac{P_{1T}}{\sqrt{s}}$ and where in the leading-order approximation in $\eta_\perp$ one consistently neglects second order corrections in η_{1T} as well. Notice that the approximate expressions in Eqs. (2.18) and (2.19) are valid for all scaling variables defined in Eqs. (2.11)-(2.13). In both configurations the master formula allowing to calculate, at leading order (LO), the most general spin configuration in the helicity formalism is given by

$$\begin{aligned}
&\rho^{h_1,S_1}_{\lambda_{h_1},\lambda'_{h_1}}\rho^{h_2,S_2}_{\lambda_{h_2},\lambda'_{h_2}}\frac{d\sigma^{e^+e^-\to h_1h_2X}}{d\cos\theta dz_1 d^2\boldsymbol{p}_{\perp 1}dz_2 d^2\boldsymbol{p}_{\perp 2}} \\
&= \sum_q\sum_{\{\lambda\}}\frac{1}{32\pi s}\frac{1}{4}\hat{M}_{\lambda_q\lambda_{\bar{q}},\lambda_+\lambda_-}\hat{M}^*_{\lambda'_q\lambda'_{\bar{q}},\lambda_+\lambda_-}\hat{D}^{\lambda_{h_1},\lambda'_{h_1}}_{\lambda_q,\lambda'_q}(z_1,\boldsymbol{p}_{\perp 1})\hat{D}^{\lambda_{h_2},\lambda'_{h_2}}_{\lambda_{\bar{q}},\lambda'_{\bar{q}}}(z_2,\boldsymbol{p}_{\perp 2}).
\end{aligned} \tag{2.22}$$

Let us clarify the physical meaning of Eq. (2.22) – our starting point – by making detailed comments on its notation and contents. The formula is written according to the TMD factorization theorem, separating the soft, long distance, from the hard, short distance, contributions. The hard part is computable in perturbative

QED, while information on the soft one has to be extracted from experiments and/or parameterized. More explicitly:

1. $\rho^{h,S_h}_{\lambda_h,\lambda'_h}$ is the helicity density matrix of the hadron h with spin S_h. It describes the spin orientation of the particle in *its helicity frame*; e.g. for a spin-1/2 particle, $\mathrm{Tr}(\sigma_i\rho) = P_i$ is the i-th component of the polarization vector $\boldsymbol{P}$ in the helicity frame of the particle;

2. the notation $\{\lambda\}$ implies a sum over all repeated helicity indices;

3. the $\hat{M}_{\lambda_q\lambda_{\bar{q}},\lambda_+\lambda_-}$'s are the helicity scattering amplitudes for the elementary process $e^+(\lambda_+) + e^-(\lambda_-) \to q(\lambda_q) + \bar{q}(\lambda_{\bar{q}})$, $q = u, d, s, \bar{u}, \bar{d}, \bar{s}$ (neglecting heavy flavours). They represent the hard contribution to the cross section and can be calculated perturbatively within QED.

4. $\hat{D}^{\lambda_h,\lambda'_h}_{\lambda_q,\lambda'_q}(z, \boldsymbol{p}_\perp)$ is a product of two helicity fragmentation amplitudes for the $q \to h + X$ process, and is directly related to the leading-twist TMD fragmentation functions for the hadron h. It represents the non-perturbative component of the cross section, as it will be discussed in detail in the next section. Here we recall only, referring now to a generic parton c, a quark or a gluon, that it is defined as

$$\hat{D}^{\lambda_h,\lambda'_h}_{\lambda_c,\lambda'_c}(z, \boldsymbol{p}_\perp) = \sum\!\!\!\!\!\!\int_{X,\lambda_X} \hat{\mathcal{D}}_{\lambda_h,\lambda_X;\lambda_c}(z, \boldsymbol{p}_\perp)\hat{\mathcal{D}}^*_{\lambda'_h,\lambda_X;\lambda'_c}(z, \boldsymbol{p}_\perp)\,, \tag{2.23}$$

where the $\sum\!\!\!\!\!\!\int_{X,\lambda_X}$ stands for a spin sum and phase space integration over all undetected particles, considered as a system X. The usual unpolarized fragmentation function $D_{h/c}(z)$, i.e. the number density of hadrons h resulting from the fragmentation of an unpolarized parton c and carrying a light-cone momentum fraction z, at tree level is given by

$$D_{h/c}(z) = \frac{1}{2}\sum_{\lambda_c,\lambda_h}\int d^2\boldsymbol{p}_\perp \hat{D}^{\lambda_h,\lambda_h}_{\lambda_c,\lambda_c}(z, \boldsymbol{p}_\perp)\,. \tag{2.24}$$

The expression in Eq. (2.22) has to be suitably integrated over the unobserved variables according to the chosen kinematical set-up. In the thrust frame, as discussed for instance in the context of spin-zero meson production for the study of the Collins effect [42], one changes the angular variables from (φ_1, φ_2) to $(\varphi_1, \varphi_1 + \varphi_2)$, integrates over the azimuthal angle φ_1 and, eventually, over the moduli of the intrinsic transverse momenta. In the hadron-frame configuration, where the parton momenta are not measurable, one has to integrate over them. For the most general case, i.e. the unpolarized, single-polarized, double-polarized hadron production, we will have

$$\begin{aligned}\frac{d\sigma^{e^+e^-\to h_1(S_1)h_2(S_2)\,X}}{d\cos\theta dz_1 dz_2 d^2\boldsymbol{P}_{1T}} &= \int d^2\boldsymbol{p}_{\perp 1}\, d^2\boldsymbol{p}_{\perp 2}\, \delta^{(2)}(\boldsymbol{p}_{\perp 1} - \boldsymbol{P}_{h_1} + z_{p_1}\,\beta_1\,\boldsymbol{q}_1) \\ &\times \frac{d\sigma^{e^+e^-\to h_1(S_1)h_2(S_2)\,X}}{d\cos\theta dz_1 d^2\boldsymbol{p}_{\perp 1} dz_2 d^2\boldsymbol{p}_{\perp 2}}\,,\end{aligned} \tag{2.25}$$

where $\boldsymbol{q}_1$ is given in terms of $\boldsymbol{p}_{\perp 2}$, see Eq. (2.19). At the lowest order in the transverse momentum dependence, $p_\perp/\sqrt{s}$, the above equation reads

$$\begin{aligned}\frac{d\sigma^{e^+e^-\to h_1(S_1)h_2(S_2)\,X}}{d\cos\theta dz_1 dz_2 d^2\boldsymbol{P}_{1T}} &= \int d^2\boldsymbol{p}_{\perp 1}\, d^2\boldsymbol{p}_{\perp 2}\, \delta^{(2)}(\boldsymbol{p}_{\perp 1} - \boldsymbol{P}_{1T} + \boldsymbol{p}_{\perp 2}\, z_{p_1}/z_{p_2}) \\ &\times \frac{d\sigma^{e^+e^-\to h_1(S_1)h_2(S_2)\,X}}{d\cos\theta dz_1 d^2\boldsymbol{p}_{\perp 1} dz_2 d^2\boldsymbol{p}_{\perp 2}}\,.\end{aligned} \tag{2.26}$$

In the next section we will discuss in details the soft contributions to the master formula.

2.3. Soft physics in the fragmentation process

The way the parton spin is transferred to the hadrons can be formally described, in general, by bilinear combinations of the helicity fragmentation amplitudes for the process $c \to h + X$. The hadron polarizations are, indeed, related to their parent parton polarizations. In this sense, one could equally well interpret

Eq. (2.22) either in terms of hadron polarizations or in terms of the fragmentation amplitudes.

We present here our results starting from the former approach, which is somewhat more direct and allows us to give a complete classification of the TMD fragmentation functions at leading twist. However, the latter approach offers a deeper understanding of some of the basic properties of our factorized scheme (e.g. the parity properties) and allows for a direct comparison with other formalisms adopted to describe the same spin effects.

For these reasons and for their relevance in the present study we will discuss the quark case in full detail here below. The corresponding gluon TMD-FFs can be found in Appendix B. The derivation of the explicit relations between our formalism and the one of the Amsterdam group is given in Appendix C.

2.3.1. Quark TMD fragmentation functions for spin-1/2 hadrons at leading twist

We start by introducing the TMD fragmentation function for a polarized quark, q, with spin s_q and polarization vector $\boldsymbol{P}^q$, fragmenting into an unpolarized hadron h: $\hat{D}_{h/q,s_q}(z,\boldsymbol{p}_\perp)$. This, together with the helicity density matrices of the quark and the hadron and the generalized fragmentation amplitudes defined in Eq. (2.23), allows us to give the complete set of leading-twist quark TMD-FFs. The quark and hadron helicity density matrices can be related as follows:

$$\rho^{h,S_h}_{\lambda_h,\lambda'_h}\hat{D}_{h/q,s_q}(z,\boldsymbol{p}_\perp)=\sum_{\lambda_q,\lambda'_q}\rho^{q}_{\lambda_q,\lambda'_q}\hat{D}^{\lambda_h,\lambda'_h}_{\lambda_q,\lambda'_q}(z,\boldsymbol{p}_\perp)\,. \tag{2.27}$$

The hadron helicity density matrix for a spin-1/2 hadron can be expressed in terms of the components of its polarization vector

$$\boldsymbol{P}^h=(P^h_X,P^h_Y,P^h_Z)=(P^h_T\cos\phi_{S_h},P^h_T\sin\phi_{S_h},P^h_L) \tag{2.28}$$

as [31]

$$\begin{aligned}\rho^{h,S_h}_{\lambda_h,\lambda'_h} &= \frac{1}{2}\begin{pmatrix}\rho^h_{++} & \rho^h_{+-}\\ \rho^h_{-+} & \rho^h_{--}\end{pmatrix}\\ &= \frac{1}{2}\begin{pmatrix}1+P^h_Z & P^h_X - iP^h_Y\\ P^h_X + iP^h_Y & 1-P^h_Z\end{pmatrix}\\ &= \frac{1}{2}\begin{pmatrix}1+P^h_L & P^h_T e^{-i\phi_{S_h}}\\ P^h_T e^{i\phi_{S_h}} & 1-P^h_L\end{pmatrix},\end{aligned} \tag{2.29}$$

where X, Y, Z are the axes directions in the hadron helicity reference frame. The above matrix elements have the following properties

$$\rho^h_{++} + \rho^h_{--} = 1 \tag{2.30}$$

$$\rho^h_{++} - \rho^h_{--} = P^h_Z = P^h_L \tag{2.31}$$

$$2\mathrm{Re}\rho^h_{-+} = 2\mathrm{Re}\rho^h_{+-} = P^h_X = P^h_T \cos\phi_{S_h} \tag{2.32}$$

$$2\mathrm{Im}\rho^h_{-+} = -2\mathrm{Im}\rho^h_{+-} = P^h_Y = P^h_T \sin\phi_{S_h}\,. \tag{2.33}$$

By using the above relations, we can write quantities of the form

$$P^h_J \hat{D}_{h/q,s_q} = \hat{D}^{h/q}_{S_J/s_q} - \hat{D}^{h/q}_{-S_J/s_q} \equiv \Delta\hat{D}^{h/q}_{S_J/s_q}\,, \tag{2.34}$$

where $J = X, Y, Z$. We will use the notations:

$$P^h_J\, \hat{D}_{h/q,s_T} = \hat{D}^{h/q}_{S_J/s_T} - \hat{D}^{h/q}_{-S_J/s_T} \equiv \Delta\hat{D}^{h/q}_{S_J/s_T}(z, \boldsymbol{p}_\perp) \tag{2.35}$$

$$P^h_J\, \hat{D}_{h/q,s_z} = \hat{D}^{h/q}_{S_J/+} - \hat{D}^{h/q}_{-S_J/+} \equiv \Delta\hat{D}^{h/q}_{S_J/+}(z, \boldsymbol{p}_\perp) = \Delta\hat{D}^{h/q}_{S_J/s_z} \tag{2.36}$$

$$\hat{D}_{h/q,s_T} = D_{h/q}(z, p_\perp) + \frac{1}{2}\,\Delta\hat{D}_{h/s_T}(z, \boldsymbol{p}_\perp)\,, \tag{2.37}$$

where s_T (s_z) stands for the quark transverse (longitudinal) spin component in its helicity frame.

These amount to eight independent quantities, which represent the $\boldsymbol{p}_\perp$-unintegrated fragmentation functions of hadron h with polarization $\boldsymbol{P}^h$ (defined in the hadron helicity frame) coming from a quark q with spin s_q (specified in the parton helicity frame).

All these functions have a simple and direct physical meaning: for instance, the X component of Eq. (2.35), $(P_X^h \, \hat{D}_{h/q,s_T})$ represents the amount of polarization along the X axis (in the hadron helicity frame) carried by hadrons h coming from the fragmentation of a transversely polarized quark q; $(P_Y^h \, \hat{D}_{h/q,s_T})$ is related to the $\boldsymbol{p}_\perp$-dependent transversity fragmentation function, which survives upon integration over $d^2\boldsymbol{p}_\perp$. Similarly, the Z component of Eq. (2.36) $(P_Z^h \, \hat{D}_{h/q,s_z})$ is the unintegrated helicity fragmentation function, which, once integrated over the transverse momentum, gives the TMD quark helicity fragmentation function $\Delta D^{h/q}_{S_Z/s_z}$.

Notice that two independent fragmentation functions appear in the definition of $\hat{D}_{h/q,s_T}$, Eq. (2.37), which is the only term in the sum over λ_h, λ_h' which corresponds to hadron h being unpolarized: $D_{h/q}(z, p_\perp)$, the unintegrated number density of unpolarized hadrons coming from the fragmentation of an unpolarized quark q, and $\Delta\hat{D}_{h/s_T}(z, \boldsymbol{p}_\perp)$, the Collins function [20]. The latter permits the distribution of unpolarized hadrons h to depend upon the transverse polarization of the parent quark q. In general, for a quark in a pure transverse spin state $\boldsymbol{s}_T$ and corresponding unit polarization vector, $\boldsymbol{P}^q$, we can also rewrite it as

$$\hat{D}_{h/q,s_T} = D_{h/q}(z, p_\perp) + \frac{1}{2}\Delta^N D_{h/q^\uparrow}(\hat{\boldsymbol{p}}_q \times \hat{\boldsymbol{p}}_\perp) \cdot \boldsymbol{P}^q \,, \tag{2.38}$$

where we have explicitly extracted the angular dependence, according to the so-called "Trento conventions" [17], and where $\hat{\boldsymbol{p}}_q$ is the unit vector along the quark three-momentum.

To deepen our understanding of the above eight TMD-FFs we can exploit Eq. (2.27) with the help of the helicity density matrix for quarks. In close analogy

to the hadron case we have

$$\begin{aligned}\rho^q_{\lambda_q,\lambda_q'} &= \frac{1}{2}\begin{pmatrix}\rho^q_{++} & \rho^q_{+-}\\ \rho^q_{-+} & \rho^q_{--}\end{pmatrix}\\ &= \frac{1}{2}\begin{pmatrix}1+P^q_z & P^q_x - iP^q_y\\ P^q_x + iP^q_y & 1-P^q_z\end{pmatrix}\\ &= \frac{1}{2}\begin{pmatrix}1+P^q_L & P^q_T e^{-i\phi_{s_q}}\\ P^q_T e^{i\phi_{s_q}} & 1-P^q_L\end{pmatrix},\end{aligned} \tag{2.39}$$

where x, y, z are the axes of the helicity reference frame of the quark and ϕ_{s_q} is the azimuthal angle of the quark spin.

By summing over the quark helicity indices on the right-hand side of Eq. (2.27) and keeping fixed those of the hadron density matrix on the left-hand side, we obtain:

$$\begin{aligned}\rho^{h,S_h}_{++}\hat{D}_{h/q,s_q} &= \frac{1}{2}(1+P^h_Z)\hat{D}_{h/q,s_q}\\ &= \frac{1}{2}(D^{++}_{++}+D^{++}_{--}) + \frac{1}{2}P^q_L(D^{++}_{++}-D^{++}_{--})\\ &+ P^q_T[\mathrm{Re}D^{++}_{+-}\cos(\phi_{s_q}-\phi_h) + \mathrm{Im}D^{++}_{+-}\sin(\phi_{s_q}-\phi_h)]\end{aligned} \tag{2.40}$$

$$\begin{aligned}\rho^{h,S_h}_{--}\hat{D}_{h/q,s_q} &= \frac{1}{2}(1-P^h_Z)\hat{D}_{h/q,s_q}\\ &= \frac{1}{2}(D^{++}_{++}+D^{++}_{--}) - \frac{1}{2}P^q_L(D^{++}_{++}-D^{++}_{--})\\ &- P^q_T[\mathrm{Re}D^{++}_{+-}\cos(\phi_{s_q}-\phi_h) - \mathrm{Im}D^{++}_{+-}\sin(\phi_{s_q}-\phi_h)]\end{aligned} \tag{2.41}$$

$$\begin{aligned}\rho^{h,S_h}_{+-}\hat{D}_{h/q,s_q} &= \frac{1}{2}(P^h_X - iP^h_Y)\hat{D}_{h/q,s_q}\\ &= i\mathrm{Im}D^{+-}_{++} + P^q_L\mathrm{Re}D^{+-}_{++}\\ &+ \frac{1}{2}P^q_T[(D^{+-}_{+-}+D^{+-}_{-+})\cos(\phi_{s_q}-\phi_h) - i(D^{+-}_{+-}-D^{+-}_{-+})\sin(\phi_{s_q}-\phi_h)],\end{aligned} \tag{2.42}$$

where ϕ_h is the azimuthal angle of the hadron h in the helicity reference frame of its fragmenting parton, and we have used the properties of $\hat{D}^{\lambda_h,\lambda'_h}_{\lambda_q,\lambda'_q}(z,\boldsymbol{p}_\perp)$ collected in Appendix A.

To better clarify the above as well as the following expressions, we recall that according to our "hat-convention" the quantities like $\hat{D}$ (or $\Delta\hat{D}$) depend on $\boldsymbol{p}_\perp$, including its phase, while quantities like D (or ΔD) do not depend on phases anymore, as such dependence has been explicitly factored out.

By combining these expressions we are able to find the eight fragmentation functions discussed above. For instance, by summing and subtracting Eqs. (2.40) and (2.41) we have respectively

$$\hat{D}_{h/q,s_q} = (D^{++}_{++} + D^{++}_{--}) + 2P^q_T \mathrm{Im} D^{++}_{+-} \sin(\phi_{s_q} - \phi_h) \tag{2.43}$$

$$P^h_Z \hat{D}_{h/q,s_q} = P^q_L (D^{++}_{++} - D^{++}_{--}) + 2P^q_T \mathrm{Re} D^{++}_{+-} \cos(\phi_{s_q} - \phi_h)\,. \tag{2.44}$$

Meanwhile from the real and imaginary part Eq. (2.42), we find respectively the fragmentation function for a hadron polarized along its X and Y helicity axes

$$P^h_X \hat{D}_{h/q,s_q} = 2P^q_L \mathrm{Re} D^{+-}_{++} + P^q_T (D^{+-}_{+-} + D^{+-}_{-+}) \cos(\phi_{s_q} - \phi_h) \tag{2.45}$$

$$P^h_Y \hat{D}_{h/q,s_q} = -2\mathrm{Im} D^{+-}_{++} + P^q_T (D^{+-}_{+-} - D^{+-}_{-+}) \sin(\phi_{s_q} - \phi_h)\,. \tag{2.46}$$

The two above relations can be expressed in a more compact form in terms of the transverse polarization of the final hadron

$$P^h_X = P^h_T \cos\phi_{S_h} \qquad P^h_Y = P^h_T \sin\phi_{S_h}\,. \tag{2.47}$$

By multiplying Eq. (2.45) by $\cos\phi_{S_h}$ and Eq. (2.46) by $\sin\phi_{S_h}$ and summing them up, we get

$$\begin{aligned} P^h_T \hat{D}_{h/q,s_q} = {} & -2\,\mathrm{Im} D^{+-}_{++} \sin\phi_{S_h} + 2P^q_L\,\mathrm{Re} D^{+-}_{++} \cos\phi_{S_h} \\ & + P^q_T \left[D^{+-}_{+-} \cos(\phi_{S_h} - \phi_{s_q} + \phi_h) + D^{-+}_{+-} \cos(\phi_{S_h} + \phi_{s_q} - \phi_h) \right]\,. \end{aligned} \tag{2.48}$$

Moreover, it is easy to show that the azimuthal angle of $\boldsymbol{P}^h$ in the hadron helicity frame, ϕ_{S_h}, and the same angle measured in the quark helicity frame, ϕ'_{S_h}, are related as follows

$$\phi_{S_h} = \phi'_{S_h} - \phi_h + \mathcal{O}(p_\perp^2/s)\,, \tag{2.49}$$

so that Eq. (2.48) can be recast as

$$\begin{aligned} P_T^h \hat{D}_{h/q,s_q} = &-2\,\mathrm{Im}D_{++}^{+-}\sin(\phi'_{S_h} - \phi_h) + 2\,P_L^q Re D_{++}^{+-}\cos(\phi'_{S_h} - \phi_h) \\ &+ P_T^q\left[D_{+-}^{+-}\cos(\phi'_{S_h} - \phi_{s_q}) + D_{+-}^{-+}\cos(\phi'_{S_h} + \phi_{s_q} - 2\phi_h)\right]. \end{aligned} \tag{2.50}$$

From the above equations, giving the hadron polarization in terms of the fragmentation amplitudes and the quark polarization, we can define the eight TMD-FFs as follows. Through Eq. (2.43) we have

$$\hat{D}_{h/q} = \hat{D}_{h/q,s_L} = (D_{++}^{++} + D_{--}^{++}) \equiv D_{h/q} \tag{2.51}$$

$$\hat{D}_{h/q,s_T} = (D_{++}^{++} + D_{--}^{++}) + 2\,\mathrm{Im}D_{+-}^{++}\sin(\phi_{s_q} - \phi_h)\,. \tag{2.52}$$

The first expression gives the fragmentation function for an unpolarized hadron generated by an unpolarized quark. This equals by parity the fragmentation function of a longitudinally polarized quark into an unpolarized hadron. In the second expression we have the TMD-FF of an unpolarized hadron generated by a transversely polarized quark. By using the following identity

$$\sin(\phi_{s_q} - \phi_h) = (\hat{\boldsymbol{p}}_q \times \hat{\boldsymbol{p}}_\perp)\cdot \boldsymbol{P}^q, \tag{2.53}$$

we recover the expression in Eq. (2.38) and, at the same time, we find the relation between $\mathrm{Im}D_{+-}^{++}$ and $\Delta^N D_{h/q^\uparrow}$. From Eq. (2.44) we have

$$P_Z^h \hat{D}_{h/q,s_L} = (D_{++}^{++} - D_{--}^{++}) = \Delta D_{S_Z/s_L}^{h/q} \tag{2.54}$$

$$P_Z^h \hat{D}_{h/q,s_T} = 2\,\mathrm{Re}D_{+-}^{++}\cos(\phi_{s_q} - \phi_h) = \Delta D_{S_Z/s_T}^{h/q}\cos(\phi_{s_q} - \phi_h)\,, \tag{2.55}$$

giving the FF for a longitudinally polarized hadron produced, respectively, by a longitudinally and a transversely polarized quark. Analogously, from Eq. (2.45) we get

$$P_X^h \hat{D}_{h/q,s_L} = 2\,\mathrm{Re} D_{++}^{+-} = \Delta D^{h/q}_{S_X/s_L} \tag{2.56}$$

$$P_X^h \hat{D}_{h/q,s_T} = (D_{+-}^{+-} + D_{-+}^{+-}) \cos(\phi_{s_q} - \phi_h) = \Delta D^{h/q}_{S_X/s_T} \cos(\phi_{s_q} - \phi_h)\,, \tag{2.57}$$

where we have the FF for a hadron transversely polarized along the X axis produced, respectively, longitudinally and a transversely polarized quark. Finally, from Eq. (2.46) we have

$$P_Y^h \hat{D}_{h/q,s_L} = P_Y^h \hat{D}_{h/q} = -2\mathrm{Im} D_{++}^{+-} = \Delta D^h_{S_Y/q} \tag{2.58}$$

$$\begin{aligned} P_Y^h \hat{D}_{h/q,s_T} &= -2\mathrm{Im} D_{++}^{+-} + (D_{+-}^{+-} - D_{-+}^{+-}) \sin(\phi_{s_q} - \phi_h) \\ &= \Delta D^h_{S_Y/q} + \Delta^- \hat{D}^{h/q}_{S_Y/s_T} = \Delta D^h_{S_Y/q} + \Delta^- D^{h/q}_{S_Y/s_T} \sin(\phi_{s_q} - \phi_h)\,, \end{aligned} \tag{2.59}$$

giving the TMD-FF for an unpolarized quark and for a transversely polarized quark fragmenting into a hadron transversely polarized along the Y axis. The first expression gives the so-called polarizing fragmentation function, introduced in Refs. [21, 30] and considered in a phenomenological study of transverse Λ polarization in inclusive hadron collisions [35] and in semi-inclusive deep inelastic processes [43]. It is also worth mentioning that the function $\Delta \hat{D}^{h/q}_{S_Y/s_T} \equiv P_Y^h \hat{D}_{h/q,s_T}$ entering the second equation can be decomposed into two terms, the polarizing FF term which is independent of the quark transverse polarization, and a term which changes sign when the quark polarization direction is reversed:

$$\Delta^- \hat{D}^{h/q}_{S_Y/s_T} = \frac{1}{2}[\Delta \hat{D}^{h/q}_{S_Y/s_T} - \Delta \hat{D}^{h/q}_{S_Y/-s_T}] = -\Delta^- \hat{D}^{h/q}_{S_Y/-s_T}. \tag{2.60}$$

Before concluding this section, we notice that the azimuthal dependence of the term involving the polarizing FF in Eq. (2.50) can be expressed as

$$\sin(\phi'_{S_h} - \phi_h) = (\hat{\boldsymbol{p}}_q \times \hat{\boldsymbol{p}}_\perp) \cdot \boldsymbol{P}^h\,. \tag{2.61}$$

Therefore, we can define, in close analogy to the Collins FF,

$$P_T^h \hat{D}_{h/q} = \Delta\hat{D}^h_{S_T/q} = \Delta^N D_{h^\uparrow/q}\,(\hat{\boldsymbol{p}}_q \times \hat{\boldsymbol{p}}_\perp)\cdot \boldsymbol{P}^h\,, \tag{2.62}$$

for the fragmentation of an unpolarized quark into a transversely polarized hadron. All the above results can be collected as follows:

$$\begin{aligned}
\hat{D}_{h/q}(z,\boldsymbol{p}_\perp) &= D_{h/q} = (D^{++}_{++} + D^{++}_{--}) \\
\Delta\hat{D}_{h/q,s_T}(z,\boldsymbol{p}_\perp) &= \Delta^N D_{h/q^\uparrow}\sin(\phi_{s_q}-\phi_h) = 4\mathrm{Im}D^{++}_{+-}\sin(\phi_{s_q}-\phi_h) \quad \text{[Collins FF]} \\
\Delta\hat{D}^{h/q}_{S_Z/s_L}(z,\boldsymbol{p}_\perp) &= \Delta D^{h/q}_{S_Z/s_L} = (D^{++}_{++} - D^{++}_{--}) \\
\Delta\hat{D}^{h/q}_{S_Z/s_T}(z,\boldsymbol{p}_\perp) &= \Delta D^{h/q}_{S_Z/s_T}\cos(\phi_{s_q}-\phi_h) = 2\mathrm{Re}D^{++}_{+-}\cos(\phi_{s_q}-\phi_h) \\
\Delta\hat{D}^{h/q}_{S_X/s_L}(z,\boldsymbol{p}_\perp) &= \Delta D^{h/q}_{S_X/s_L} = 2\mathrm{Re}D^{+-}_{++} \\
\Delta\hat{D}^{h/q}_{S_X/s_T}(z,\boldsymbol{p}_\perp) &= \Delta D^{h/q}_{S_X/s_T}\cos(\phi_{s_q}-\phi_h) = (D^{+-}_{+-} + D^{+-}_{-+})\cos(\phi_{s_q}-\phi_h) \\
\Delta\hat{D}^{h}_{S_Y/q}(z,\boldsymbol{p}_\perp) &= \Delta D^{h}_{S_Y/q} = \Delta^N D_{h^\uparrow/q} = -2\mathrm{Im}D^{+-}_{++} \quad \text{[Polarizing FF]} \\
\Delta^- \hat{D}^{h/q}_{S_Y/s_T}(z,\boldsymbol{p}_\perp) &= \Delta^- D^{h/q}_{S_Y/s_T}\sin(\phi_{s_q}-\phi_h) = (D^{+-}_{+-} - D^{+-}_{-+})\sin(\phi_{s_q}-\phi_h)\,.
\end{aligned} \tag{2.63}$$

2.4. Azimuthal dependences and polarization observables in $e^+e^- \to h_1h_2 + X$

We present here all possible azimuthal dependences and polarization observables for the case of unpolarized, single-polarized and double-polarized hadron production in $e^+e^- \to h_1h_2 + X$. To start with, we give the partonic helicity scattering amplitudes appearing in Eq. (2.22). From helicity conservation (with massless leptons and quarks), the only nonzero amplitudes for the process $ab \to cd$, are:

$$\hat{M}_{\lambda_c\lambda_d,\lambda_a\lambda_b} : \left\{\hat{M}_{+-,+-}; \hat{M}_{-+,-+}; \hat{M}_{+-,-+}; \hat{M}_{-+,+-}\right\}, \tag{2.64}$$

where, by parity conservation, only two of them are independent, since

$$\hat{M}_{+-,+-} = \hat{M}^*_{-+,-+} \equiv \hat{M}_2 \qquad \hat{M}_{-+,+-} = \hat{M}^*_{+-,-+} \equiv \hat{M}_3\,. \tag{2.65}$$

Once again the two kinematical configurations have to be treated differently. In the thrust frame, the partonic scattering process occurs on the xz plane of the center of mass frame and the helicity scattering amplitudes are the canonical ones. These are given as

$$\begin{aligned} \hat{M}_{+-,+-} &= \hat{M}^0_{+-,+-} = e^2 e_q \sqrt{3}\,(1+\cos\theta) \\ \hat{M}_{-+,+-} &= \hat{M}^0_{-+,+-} = e^2 e_q \sqrt{3}\,(1-\cos\theta)\,, \end{aligned} \tag{2.66}$$

where we have included the color factor. The corresponding helicity amplitudes for the hadron frame configuration are more complicated, since, even if still in the c.m. frame, the partonic scattering process occurs out of the $\widehat{xz}$ plane (containing the lepton and the hadron h_2 momenta). One could relate these to the canonical ones by following the procedure described in Ref. [31] (somehow simplified here since only rotations are involved). Instead, we prefer to give them as obtained by an explicit calculation in terms of the helicity spinors, using the kinematics as given in Eqs. (2.18) and (2.19) (with the help of Eq. (2.2), where now θ refers to the relative angle between the lepton-axis and the direction of the hadron h_2):

$$\begin{aligned} \hat{M}_{+-,+-} &= e^2 e_q \sqrt{3}\Big[\cos\varphi_2(1+\beta_2\cos\theta) - 2\frac{\eta_{\perp 2}}{z_{p_2}}\sin\theta + i\sin\varphi_2(\beta_2+\cos\theta)\Big] \\ \hat{M}_{-+,+-} &= e^2 e_q \sqrt{3}\Big[\cos\varphi_2(1-\beta_2\cos\theta) + 2\frac{\eta_{\perp 2}}{z_{p_2}}\sin\theta - i\sin\varphi_2(\beta_2-\cos\theta)\Big]\,. \end{aligned} \tag{2.67}$$

At the lowest order in $p_\perp/\sqrt{s}$, in which $\eta_{\perp 2} = 0$ and $\beta_2 = 1$, they simplify as

$$\begin{aligned} \hat{M}_{+-,+-} &\simeq e^2 e_q \sqrt{3}\,(1+\cos\theta)\,e^{i\varphi_2} \;\; = \hat{M}^0_{+-,+-}\,e^{i\varphi_2} \\ \hat{M}_{-+,+-} &\simeq e^2 e_q \sqrt{3}\,(1-\cos\theta)\,e^{-i\varphi_2} = \hat{M}^0_{-+,+-}\,e^{-i\varphi_2}\,. \end{aligned} \tag{2.68}$$

where φ_2 is the azimuthal angle of the two quarks (see Eqs. (2.19) and (2.18)).

2.4.1. Unpolarized hadron production

By summing over the diagonal indices of the helicity density matrices appearing on the left hand side of Eq. (2.22) we get the unpolarized cross section:

$$\frac{d\sigma^{e^+e^-\to h_1h_2X}}{d\cos\theta d\mathrm{PS}_{12}} = \frac{1}{128\pi s}\sum_q \Big\{2\Big(|\hat{M}_2|^2+|\hat{M}_3|^2\Big)D_{h_1/q}(z_1,p_{\perp 1})D_{h_2/\bar{q}}(z_2,p_{\perp 2}) + \Big[\mathrm{Re}[\hat{M}_2\hat{M}_3^*]\cos\Delta\phi - \mathrm{Im}[\hat{M}_2\hat{M}_3^*]\sin\Delta\phi\Big]\Delta^N D_{h_1/q^\uparrow}(z_1,p_{\perp 1})\Delta^N D_{h_2/\bar{q}^\uparrow}(z_2,p_{\perp 2})\Big\}, \tag{2.69}$$

where we have introduced the shorthand notation

$$d\mathrm{PS}_{12} = dz_1 d^2\boldsymbol{p}_{\perp 1} dz_2 d^2\boldsymbol{p}_{\perp 2} \tag{2.70}$$

and where $\Delta\phi = \phi_{h_1} - \phi_{h_2}$, with $\phi_{h_{1,2}}$ the azimuthal angles of the two hadrons in the corresponding helicity frames of their parent quarks. In the thrust frame we directly get

$$\frac{d\sigma^{e^+e^-\to h_1h_2X}}{d\cos\theta d\mathrm{PS}_{12}} = \frac{3\pi\alpha^2}{2s}\sum_q e_q^2\Big\{(1+\cos^2\theta)D_{h_1/q}(z_1,p_{\perp 1})D_{h_2/\bar{q}}(z_2,p_{\perp 2}) + \frac{1}{4}\sin^2\theta\Delta^N D_{h_1/q^\uparrow}(z_1,p_{\perp 1})\Delta^N D_{h_2/\bar{q}^\uparrow}(z_2,p_{\perp 2})\cos(\varphi_1+\varphi_2)\Big\}, \tag{2.71}$$

where we have used the relations in Eq. (2.66) and the fact that $\phi_{h_1} = \varphi_1$ and $\phi_{h_2} = 2\pi - \varphi_2$ (see Appendix E). For the hadron-frame configuration, by using the expressions of the helicity amplitudes in Eq. (2.68) and the fact that $\phi_{h_2} = 0$ (see Appendix E), we obtain

$$\frac{d\sigma^{e^+e^-\to h_1h_2X}}{d\cos\theta d\mathrm{PS}_{12}} = \frac{3\pi\alpha^2}{2s}\sum_q e_q^2\Big\{(1+\cos^2\theta)D_{h_1/q}(z_1,p_{\perp 1})D_{h_2/\bar{q}}(z_2,p_{\perp 2}) + \frac{1}{4}\sin^2\theta\Delta^N D_{h_1/q^\uparrow}(z_1,p_{\perp 1})\Delta^N D_{h_2/\bar{q}^\uparrow}(z_2,p_{\perp 2})\cos(2\varphi_2+\phi_{h_1})\Big\}. \tag{2.72}$$

This has then to be integrated according to Eq. (2.25). In such a case the angle ϕ_{h_1} can be expressed in terms of the integration variables as (see Eqs. (E.28) and (E.29) and their derivation)

$$\cos\phi_{h_1} = \frac{P_{1T}}{p_{\perp 1}}\beta_2\cos(\phi_1-\varphi_2) - \frac{z_{p_1}}{z_{p_2}}\frac{p_{\perp 2}}{p_{\perp 1}}\sqrt{1-4\,\frac{\eta_{1T}^2}{z_{p_1}^2}}$$
$$\simeq \frac{P_{1T}}{p_{\perp 1}}\cos(\phi_1-\varphi_2) - \frac{z_{p_1}}{z_{p_2}}\frac{p_{\perp 2}}{p_{\perp 1}} \tag{2.73}$$
$$\sin\phi_{h_1} = \frac{P_{1T}}{p_{\perp 1}}\sin(\phi_1-\varphi_2)\,, \tag{2.74}$$

where we have also given the lowest-order expressions in $\eta_{\perp,1T}/z_p$. Notice that ϕ_1, not to be confused with ϕ_{h_1}, is the observed azimuthal angle of the hadron momentum, $\boldsymbol{P}_1$, in the hadron frame. In the expression of the unpolarized cross section, in agreement with Ref. [42], we recognize, beside the ordinary contribution from the unpolarized TMD FFs, the azimuthal dependence coming from the Collins effect.

2.4.2. Single-polarized hadron production

In order to compute the polarization state for a single hadron, let us refer to h_1, one has to consider the diagonal part of the helicity density matrix for the second hadron, h_2, and take the proper combination of the matrix elements of hadron h_1, see Eq. (2.22). By a calculation analogous to the previous one :

$$P_{\rm X}^{h_1}\frac{d\sigma^{e^+e^-\to h_1h_2X}}{d\cos\theta d{\rm PS}_{12}} = \frac{1}{64\pi s}\sum_q\Big[{\rm Im}[\hat{M}_2\hat{M}_3^*]\cos\Delta\phi + {\rm Re}[\hat{M}_2\hat{M}_3^*]\sin\Delta\phi\Big]$$
$$\times\,\Delta D^{h_1/q}_{S_X/s_T}(z_1,p_{\perp 1})\Delta^N D_{h_2/\bar{q}^\uparrow}(z_2,p_{\perp 2}) \tag{2.75}$$

$$P_Y^{h_1}\frac{d\sigma^{e^+e^-\to h_1h_2X}}{d\cos\theta d\mathrm{PS}_{12}} = \frac{1}{64\pi s}\sum_q \Big\{ \Big(|\hat{M}_2|^2+|\hat{M}_3|^2\Big)\Delta^N D_{h_1^\uparrow/q}(z_1,p_{\perp 1})D_{h_2/\bar{q}}(z_2,p_{\perp 2}) + \Big[\mathrm{Re}[\hat{M}_2\hat{M}_3^*]\cos\Delta\phi - \mathrm{Im}[\hat{M}_2\hat{M}_3^*]\sin\Delta\phi\Big]\Delta^- D_{S_Y/s_T}^{h_1/q}(z_1,p_{\perp 1})\Delta^N D_{h_2/\bar{q}^\uparrow}(z_2,p_{\perp 2})\Big\} \tag{2.76}$$

$$P_Z^{h_1}\frac{d\sigma^{e^+e^-\to h_1h_2X}}{d\cos\theta d\mathrm{PS}_{12}} = \frac{1}{64\pi s}\sum_q \Big[\mathrm{Im}[\hat{M}_2\hat{M}_3^*]\cos\Delta\phi + \mathrm{Re}[\hat{M}_2\hat{M}_3^*]\sin\Delta\phi\Big] \times \Delta D_{S_Z/s_T}^{h_1/q}(z_1,p_{\perp 1})\Delta^N D_{h_2/\bar{q}^\uparrow}(z_2,p_{\perp 2}), \tag{2.77}$$

where we can recognize the contributions coming from a transversely polarized quark-antiquark pair, i.e. the coupling of the Collins function with $\Delta D_{S_X/s_T}^{h_1/q}$, Eq. (2.75), $\Delta^- D_{S_Y/s_T}^{h_1/q}$, Eq. (2.76) (second line), and $\Delta D_{S_Z/s_T}^{h_1/q}$, Eq. (2.77), as well as from an unpolarized quark-antiquark pair, first line of Eq. (2.76), involving the polarizing FF. To get the expressions in the two adopted frames it is enough to replace (as already done in the previous Section)

$$\mathrm{Re}[\hat{M}_2\hat{M}_3^*]\cos\Delta\phi - \mathrm{Im}[\hat{M}_2\hat{M}_3^*]\sin\Delta\phi = 3e_q^2(4\pi\alpha)^2\,\sin^2\theta\cos(\varphi_1+\varphi_2) \tag{2.78}$$

$$\mathrm{Im}[\hat{M}_2\hat{M}_3^*]\cos\Delta\phi + \mathrm{Re}[\hat{M}_2\hat{M}_3^*]\sin\Delta\phi = 3e_q^2(4\pi\alpha)^2\,\sin^2\theta\sin(\varphi_1+\varphi_2) \tag{2.79}$$

for the thrust frame, and

$$\mathrm{Re}[\hat{M}_2\hat{M}_3^*]\cos\Delta\phi - \mathrm{Im}[\hat{M}_2\hat{M}_3^*]\sin\Delta\phi = 3e_q^2(4\pi\alpha)^2\,\sin^2\theta\cos(2\varphi_2+\phi_{h_1}) \tag{2.80}$$

$$\mathrm{Im}[\hat{M}_2\hat{M}_3^*]\cos\Delta\phi + \mathrm{Re}[\hat{M}_2\hat{M}_3^*]\sin\Delta\phi = 3e_q^2(4\pi\alpha)^2\,\sin^2\theta\sin(2\varphi_2+\phi_{h_1}) \tag{2.81}$$

for the hadron frame. In both cases

$$|\hat{M}_2|^2+|\hat{M}_3|^2 = 6e_q^2\,(4\pi\alpha)^2\,(1+\cos^2\theta)\,. \tag{2.82}$$

Once again one has to properly integrate over the unobserved kinematical quantities, with ϕ_{h_1} given in Eqs. (2.73) and (2.74). For completeness we give also the

explicit expressions of the polarizations, both for the thrust-frame configuration,

$$P_X^{h_1}\frac{d\sigma^{e^+e^-\to h_1h_2X}}{d\cos\theta d\mathrm{PS}_{12}} = \frac{3\pi\alpha^2}{4s}\sum_q e_q^2\sin^2\theta\Delta D^{h_1/q}_{S_X/s_T}(z_1,p_{\perp 1})\Delta^N D_{h_2/\bar{q}^\uparrow}(z_2,p_{\perp 2})\sin(\varphi_1+\varphi_2) \tag{2.83}$$

$$P_Y^{h_1}\frac{d\sigma^{e^+e^-\to h_1h_2X}}{d\cos\theta d\mathrm{PS}_{12}} = \frac{3\pi\alpha^2}{2s}\sum_q e_q^2\Big\{(1+\cos^2\theta)\Delta^N D_{h_1^\uparrow/q}(z_1,p_{\perp 1})D_{h_2/\bar{q}}(z_2,p_{\perp 2}) + \frac{1}{2}\sin^2\theta\Delta^- D^{h_1/q}_{S_Y/s_T}(z_1,p_{\perp 1})\Delta^N D_{h_2/\bar{q}^\uparrow}(z_2,p_{\perp 2})\cos(\varphi_1+\varphi_2)\Big\} \tag{2.84}$$

$$P_Z^{h_1}\frac{d\sigma^{e^+e^-\to h_1h_2X}}{d\cos\theta d\mathrm{PS}_{12}} = \frac{3\pi\alpha^2}{4s}\sum_q e_q^2\sin^2\theta\Delta D^{h_1/q}_{S_Z/s_T}(z_1,p_{\perp 1})\Delta^N D_{h_2/\bar{q}^\uparrow}(z_2,p_{\perp 2})\sin(\varphi_1+\varphi_2)\,, \tag{2.85}$$

and for the hadron-frame case

$$P_X^{h_1}\frac{d\sigma^{e^+e^-\to h_1h_2X}}{d\cos\theta d\mathrm{PS}_{12}} = \frac{3\pi\alpha^2}{4s}\sum_q e_q^2\sin^2\theta\Delta D^{h_1/q}_{S_X/s_T}(z_1,p_{\perp 1})\Delta^N D_{h_2/\bar{q}^\uparrow}(z_2,p_{\perp 2})\sin(2\varphi_2+\phi_{h_1}) \tag{2.86}$$

$$P_Y^{h_1}\frac{d\sigma^{e^+e^-\to h_1h_2X}}{d\cos\theta d\mathrm{PS}_{12}} = \frac{3\pi\alpha^2}{2s}\sum_q e_q^2\Big\{(1+\cos^2\theta)\Delta^N D_{h_1^\uparrow/q}(z_1,p_{\perp 1})D_{h_2/\bar{q}}(z_2,p_{\perp 2}) + \frac{1}{2}\sin^2\theta\Delta^- D^{h_1}_{S_Y/s_T}(z_1,p_{\perp 1})\Delta^N D_{h_2/\bar{q}^\uparrow}(z_2,p_{\perp 2})\cos(2\varphi_2+\phi_{h_1})\Big\} \tag{2.87}$$

$$P_Z^{h_1}\frac{d\sigma^{e^+e^-\to h_1h_2X}}{d\cos\theta d\mathrm{PS}_{12}} = \frac{3\pi\alpha^2}{4s}\sum_q e_q^2\sin^2\theta\Delta D^{h_1/q}_{S_Z/s_T}(z_1,p_{\perp 1})\Delta^N D_{h_2/\bar{q}^\uparrow}(z_2,p_{\perp 2})\sin(2\varphi_2+\phi_{h_1})\,. \tag{2.88}$$

2.4.3. Double-polarized hadron production

In a very similar way, we can compute all possible double spin configurations for the production of two spin-1/2 hadrons. The following expressions are simply obtained by considering proper combinations of the helicity density matrices of the two hadrons and then exploiting the sum over the helicity indices of quarks and antiquarks in Eq. (2.22). The general formulas so obtained are:

$$\begin{aligned}
&P_X^{h_1} P_X^{h_2} \frac{d\sigma^{e^+e^-\to h_1 h_2 X}}{d\cos\theta d\mathrm{PS}_{12}} \\
&= \frac{1}{64\pi s} \sum_q \Big\{ -\Big(|\hat{M}_2|^2 + |\hat{M}_3|^2\Big) \Delta D^{h_1/q}_{S_X/s_L}(z_1, p_{\perp 1}) \Delta D^{h_2/\bar{q}}_{S_X/s_L}(z_2, p_{\perp 2}) \\
&+ 2\Big[\mathrm{Re}[\hat{M}_2 \hat{M}_3^*]\cos\Delta\phi - \mathrm{Im}[\hat{M}_2 \hat{M}_3^*]\sin\Delta\phi\Big] \Delta D^{h_1/q}_{S_X/s_T}(z_1, p_{\perp 1}) \Delta D^{h_2/\bar{q}}_{S_X/s_T}(z_2, p_{\perp 2}) \Big\}
\end{aligned} \tag{2.89}$$

$$\begin{aligned}
&P_X^{h_1} P_Y^{h_2} \frac{d\sigma^{e^+e^-\to h_1 h_2 X}}{d\cos\theta d\mathrm{PS}_{12}} = \frac{1}{32\pi s} \sum_q \Big\{ \Big[\mathrm{Im}[\hat{M}_2 \hat{M}_3^*]\cos\Delta\phi + \mathrm{Re}[\hat{M}_2 \hat{M}_3^*]\sin\Delta\phi\Big] \\
&\times \Delta D^{h_1/q}_{S_X/s_T}(z_1, p_{\perp 1}) \Delta^- D^{h_2/\bar{q}}_{S_Y/s_T}(z_2, p_{\perp 2}) \Big\}
\end{aligned} \tag{2.90}$$

$$\begin{aligned}
&P_X^{h_1} P_Z^{h_2} \frac{d\sigma^{e^+e^-\to h_1 h_2 X}}{d\cos\theta d\mathrm{PS}_{12}} \\
&= \frac{1}{64\pi s} \sum_q \Big\{ -\Big(|\hat{M}_2|^2 + |\hat{M}_3|^2\Big) \Delta D^{h_1/q}_{S_X/s_L}(z_1, p_{\perp 1}) \Delta D^{h_2/\bar{q}}_{S_Z/s_L}(z_2, p_{\perp 2}) \\
&+ 2\Big[\mathrm{Re}[\hat{M}_2 \hat{M}_3^*]\cos\Delta\phi - \mathrm{Im}[\hat{M}_2 \hat{M}_3^*]\sin\Delta\phi\Big] \Delta D^{h_1/q}_{S_X/s_T}(z_1, p_{\perp 1}) \Delta D^{h_2/\bar{q}}_{S_Z/s_T}(z_2, p_{\perp 2}) \Big\}
\end{aligned} \tag{2.91}$$

$$P_Y^{h_1} P_X^{h_2} \frac{d\sigma^{e^+e^-\to h_1h_2X}}{d\cos\theta d\mathrm{PS}_{12}} = \frac{1}{32\pi s}\sum_q \Big\{ -\Big[\mathrm{Im}[\hat{M}_2\hat{M}_3^*]\cos\Delta\phi + \mathrm{Re}[\hat{M}_2\hat{M}_3^*]\sin\Delta\phi\Big] \times \Delta^- D^{h_1/q}_{S_Y/s_T}(z_1,p_{\perp 1})\Delta D^{h_2/\bar{q}}_{S_X/s_T}(z_2,p_{\perp 2})\Big\} \tag{2.92}$$

$$P_Y^{h_1} P_Y^{h_2} \frac{d\sigma^{e^+e^-\to h_1h_2X}}{d\cos\theta d\mathrm{PS}_{12}} = \frac{1}{64\pi s}\sum_q \Big\{ \Big(|\hat{M}_2|^2+|\hat{M}_3|^2\Big)\Delta^N D_{h_1^\uparrow/q}(z_1,p_{\perp 1})\Delta^N D_{h_2^\uparrow/\bar{q}}(z_2,p_{\perp 2}) + 2\Big[\mathrm{Re}[\hat{M}_2\hat{M}_3^*]\cos\Delta\phi - \mathrm{Im}[\hat{M}_2\hat{M}_3^*]\sin\Delta\phi\Big]\Delta^- D^{h_1/q}_{S_Y/s_T}(z_1,p_{\perp 1})\Delta^- D^{h_2/\bar{q}}_{S_Y/s_T}(z_2,p_{\perp 2})\Big\} \tag{2.93}$$

$$P_Y^{h_1} P_Z^{h_2} \frac{d\sigma^{e^+e^-\to h_1h_2X}}{d\cos\theta d\mathrm{PS}_{12}} = \frac{1}{32\pi s}\sum_q \Big\{ -\Big[\mathrm{Im}[\hat{M}_2\hat{M}_3^*]\cos\Delta\phi + \mathrm{Re}[\hat{M}_2\hat{M}_3^*]\sin\Delta\phi\Big] \times \Delta^- D^{h_1/q}_{S_Y/s_T}(z_1,p_{\perp 1})\Delta D^{h_2/\bar{q}}_{S_Z/s_T}(z_2,p_{\perp 2})\Big\} \tag{2.94}$$

$$P_Z^{h_1} P_X^{h_2} \frac{d\sigma^{e^+e^-\to h_1h_2X}}{d\cos\theta d\mathrm{PS}_{12}} = \frac{1}{64\pi s}\sum_q \Big\{ -\Big(|\hat{M}_2|^2+|\hat{M}_3|^2\Big)\Delta D^{h_1/q}_{S_Z/s_L}(z_1,p_{\perp 1})\Delta D^{h_2/\bar{q}}_{S_X/s_L}(z_2,p_{\perp 2}) + 2\Big[\mathrm{Re}[\hat{M}_2\hat{M}_3^*]\cos\Delta\phi - \mathrm{Im}[\hat{M}_2\hat{M}_3^*]\sin\Delta\phi\Big]\Delta D^{h_1/q}_{S_Z/s_T}(z_1,p_{\perp 1})\Delta D^{h_2/\bar{q}}_{S_X/s_T}(z_2,p_{\perp 2})\Big\} \tag{2.95}$$

$$P_Z^{h_1} P_Y^{h_2} \frac{d\sigma^{e^+e^-\to h_1h_2X}}{d\cos\theta d\mathrm{PS}_{12}} = \frac{1}{32\pi s}\sum_q \Big\{ \Big[\mathrm{Im}[\hat{M}_2\hat{M}_3^*]\cos\Delta\phi + \mathrm{Re}[\hat{M}_2\hat{M}_3^*]\sin\Delta\phi\Big] \times \Delta D^{h_1/q}_{S_Z/s_T}(z_1,p_{\perp 1})\Delta^- D^{h_2/\bar{q}}_{S_Y/s_T}(z_2,p_{\perp 2})\Big\} \tag{2.96}$$

$$P_Z^{h_1} P_Z^{h_2} \frac{d\sigma^{e^+e^-\to h_1h_2X}}{d\cos\theta d\mathrm{PS}_{12}} = \frac{1}{64\pi s}\sum_q \Big\{ -\Big(|\hat{M}_2|^2+|\hat{M}_3|^2\Big)\Delta D^{h_1/q}_{S_Z/s_L}(z_1,p_{\perp 1})\Delta D^{h_2/\bar{q}}_{S_Z/s_L}(z_2,p_{\perp 2}) + 2\Big[\mathrm{Re}[\hat{M}_2\hat{M}_3^*]\cos\Delta\phi - \mathrm{Im}[\hat{M}_2\hat{M}_3^*]\sin\Delta\phi\Big]\Delta D^{h_1/q}_{S_Z/s_T}(z_1,p_{\perp 1})\Delta D^{h_2/\bar{q}}_{S_Z/s_T}(z_2,p_{\perp 2})\Big\}. \tag{2.97}$$

By using the expressions in Eqs. (2.78)-(2.82) one can directly obtain the results for the two kinematical configurations considered here.

2.5. Hadron frame: complete results

As already pointed out, while in the thrust frame at least in principle one can directly measure the azimuthal dependences on $\varphi_{1,2}$ entering the formulas of the previous section, in the hadron frame the partonic variables are not accessible and one has to properly extract the azimuthal dependences on ϕ_1. This can be done by employing proper projection techniques thanks to a simple tensorial analysis, as described in Appendix D, without formulating any particular assumption on the $p_\perp$ dependence of the fragmentation functions. This will also allow for a more direct comparison with the results of Ref. [30]. As discussed in Section 2.2 we will have to compute the following expression

$$\frac{d\sigma^{e^+e^-\to h_1(S_1)h_2(S_2)\,X}}{d\cos\theta dz_1 dz_2 d^2\boldsymbol{P}_{1T}} = \int d^2\boldsymbol{p}_{\perp 1}\, d^2\boldsymbol{p}_{\perp 2}\,\delta^{(2)}(\boldsymbol{p}_{\perp 1} - \boldsymbol{P}_{1T} + \boldsymbol{p}_{\perp 2}\, z_{p_1}/z_{p_2}) \times \frac{d\sigma^{e^+e^-\to h_1(S_1)h_2(S_2)\,X}}{d\cos\theta dz_1 d^2\boldsymbol{p}_{\perp 1} dz_2 d^2\boldsymbol{p}_{\perp 2}}\,. \tag{2.98}$$

To this aim, we define, for a generic couple of (un)polarized TMD-FFs, one referring to hadron h_1 (ΔD^{h_1}) and the other to hadron h_2 (ΔD^{h_2}), the following convolution over the intrinsic transverse momenta

$$\mathcal{C}[w\Delta D^{h_1}\Delta D^{h_2}] = \sum_q e_q^2 \int d^2\boldsymbol{p}_{\perp 1} d^2\boldsymbol{p}_{\perp 2}\,\delta^{(2)}(\boldsymbol{p}_{\perp 1} - \boldsymbol{P}_{1T} + \boldsymbol{p}_{\perp 2}\, z_{p_1}/z_{p_2}) \times w(\boldsymbol{p}_{\perp 2}, \boldsymbol{P}_{1T})\Delta D_{h_1/q}(z_1, p_{\perp 1})\Delta D_{h_2/\bar{q}}(z_2, p_{\perp 2})\,, \tag{2.99}$$

where the TMD-FFs depend only on the moduli of the intrinsic transverse momenta and the weight $w(\boldsymbol{p}_{\perp 2}, \boldsymbol{P}_{1T})$ depends on the specific azimuthal structure considered, as illustrated below. Notice that this expression differs from the corresponding one in Ref. [30] by a factor $1/z_2^2$, and by the definition of the

parton momenta, that we recall here below:

$$(-z\,\boldsymbol{k}_T)_{\text{Amsterdam}} = \boldsymbol{p}_\perp \tag{2.100}$$

$$(\hat{\boldsymbol{h}})_{\text{Amsterdam}} = \frac{\boldsymbol{P}_{1T}}{P_{1T}} = \hat{\boldsymbol{P}}_{1T}\,. \tag{2.101}$$

By means of this procedure one obtains the following hadron-frame azimuthal dependences for the (un)polarized cross sections.

2.5.1. Unpolarized case

$$\frac{d\sigma^{e^+e^-\to h_1h_2X}}{d\cos\theta dz_1dz_2d^2\boldsymbol{P}_{1T}} = \frac{3\pi\alpha^2}{2s}\left\{\left(1+\cos^2\theta\right)F_{UU} + \sin^2\theta\cos(2\phi_1)F_{UU}^{\cos(2\phi_1)}\right\}, \tag{2.102}$$

with

$$F_{UU} = \sum_q e_q^2 \int d^2\boldsymbol{p}_{\perp 2}\, D_{h_1/q}(z_1,p_{\perp 1})D_{h_2/\bar{q}}(z_2,p_{\perp 2}) = \mathcal{C}[D_1\bar{D}_1] \tag{2.103}$$

$$\begin{aligned}
&\cos(2\phi_1)\,F_{UU}^{\cos(2\phi_1)}\\
&= \sum_q e_q^2 \int d^2\boldsymbol{p}_{\perp 2}\frac{1}{4}\Big[\frac{P_{1T}}{p_{\perp 1}}\cos(\phi_1+\varphi_2) - \frac{z_{p_1}}{z_{p_2}}\frac{p_{\perp 2}}{p_{\perp 1}}\cos(2\varphi_2)\Big]\Delta^N D_{h_1/q^\uparrow}\Delta^N D_{h_2/\bar{q}^\uparrow}\\
&= \cos(2\phi_1)\,\mathcal{C}\left[\frac{1}{4}\left\{\frac{P_{1T}}{p_{\perp 1}}\,\hat{\boldsymbol{p}}_{\perp 2}\cdot\hat{\boldsymbol{P}}_{1T} - \frac{z_{p_1}}{z_{p_2}}\frac{p_{\perp 2}}{p_{\perp 1}}\left[2\left(\hat{\boldsymbol{p}}_{\perp 2}\cdot\hat{\boldsymbol{P}}_{1T}\right)^2-1\right]\right\}\Delta^N D_{h_1/q^\uparrow}\Delta^N D_{h_2/\bar{q}^\uparrow}\right]\\
&= \cos(2\phi_1)\,\mathcal{C}\left[\left\{\frac{\boldsymbol{p}_{\perp 2}\cdot\boldsymbol{P}_{1T}}{z_1z_2} - \left[2\left(\frac{\boldsymbol{p}_{\perp 2}\cdot\hat{\boldsymbol{P}}_{1T}}{z_2}\right)^2 - \frac{p_{\perp 2}^2}{z_2^2}\right]\right\}\frac{H_1^\perp\bar{H}_1^\perp}{M_{h_1}M_{h_2}}\right],
\end{aligned} \tag{2.104}$$

where the second line is obtained by using Eqs. (E.28) and (E.29), and in the third line, neglecting terms in $M_h/\sqrt{s}$, we have switched to the Amsterdam notation (see Appendix C) for a more direct comparison with Ref. [30].

2.5.2. Single-polarized case

Let us start with the longitudinal polarization

$$P_Z^{h_1}\frac{d\sigma^{e^+e^-\to h_1h_2X}}{d\cos\theta dz_1dz_2d^2\boldsymbol{P}_{1T}}=\frac{3\pi\alpha^2}{2s}\sin^2\theta\sin(2\phi_1)F_{LU}^{\sin(2\phi_1)} \tag{2.105}$$

$$\begin{aligned}
&\sin(2\phi_1)\,F_{LU}^{\sin(2\phi_1)}\\
&=\sum_q e_q^2\int d^2\boldsymbol{p}_{\perp 2}\frac{1}{2}\Big[\frac{P_{1T}}{p_{\perp 1}}\sin(\phi_1+\varphi_2)-\frac{z_{p_1}}{z_{p_2}}\frac{p_{\perp 2}}{p_{\perp 1}}\sin(2\varphi_2)\Big]\Delta D_{S_Z/s_T}^{h_1/q}\Delta^N D_{h_2/\bar{q}^\uparrow}\\
&=\sin(2\phi_1)\,\mathcal{C}\left[\frac{1}{2}\left\{\frac{P_{1T}}{p_{\perp 1}}\,\hat{\boldsymbol{p}}_{\perp 2}\cdot\hat{\boldsymbol{P}}_{1T}-\frac{z_{p_1}}{z_{p_2}}\frac{p_{\perp 2}}{p_{\perp 1}}\left[2\big(\hat{\boldsymbol{p}}_{\perp 2}\cdot\hat{\boldsymbol{P}}_{1T}\big)^2-1\right]\right\}\Delta D_{S_Z/s_T}^{h_1/q}\Delta^N D_{h_2/\bar{q}^\uparrow}\right]\\
&=-\sin(2\phi_1)\,\mathcal{C}\left[\left\{\frac{\boldsymbol{p}_{\perp 2}\cdot\boldsymbol{P}_{1T}}{z_1z_2}-\left[2\left(\frac{\boldsymbol{p}_{\perp 2}\cdot\hat{\boldsymbol{P}}_{1T}}{z_2}\right)^2-\frac{p_{\perp 2}^2}{z_2^2}\right]\right\}\frac{H_{1L}^\perp\bar{H}_1^\perp}{M_{h_1}M_{h_2}}\right],
\end{aligned} \tag{2.106}$$

where once again the last equality is valid in the Amsterdam notation and neglecting hadron mass effects. For the transverse polarization, firstly we have to express it in the hadron frame, the laboratory (L) frame:

$$\boldsymbol{P}_T^{h_1}=P_X^{h_1}\,\hat{\boldsymbol{X}}_{h_1}+P_Y^{h_1}\,\hat{\boldsymbol{Y}}_{h_1}=P_{x_L}^{h_1}\,\hat{\boldsymbol{x}}_L+P_{y_L}^{h_1}\,\hat{\boldsymbol{y}}_L=P_T^{h_1}(\cos\phi_{S_1}^L\,\hat{\boldsymbol{x}}_L+\sin\phi_{S_1}^L\,\hat{\boldsymbol{y}}_L) \tag{2.107}$$

adopting Eqs. (E.31) and (E.32). By combining the transverse polarization components in the lab frame as

$$P_T^{h_1}=P_{x_L}^{h_1}\cos\phi_{S_1}^L+P_{y_L}^{h_1}\sin\phi_{S_1}^L\,, \tag{2.108}$$

where $\phi_{S_1}^L$ is the azimuthal angle of the hadron spin in the laboratory frame, we then get

$$P_T^{h_1}\frac{d\sigma^{e^+e^-\to h_1h_2X}}{d\cos\theta dz_1dz_2d^2\boldsymbol{P}_{1T}}=\frac{3\pi\alpha^2}{2s}\Bigg\{\Big(1+\cos^2\theta\Big)\sin(\phi_1-\phi_{S_1}^L)F_{TU}^{\sin(\phi_1-\phi_{S_1}^L)}$$
$$+\sin^2\theta\Bigg(\sin(\phi_1+\phi_{S_1}^L)F_{TU}^{\sin(\phi_1+\phi_{S_1}^L)}+\sin(3\phi_1-\phi_{S_1}^L)F_{TU}^{\sin(3\phi_1-\phi_{S_1}^L)}\Bigg)\Bigg\}, \tag{2.109}$$

where

$$\begin{aligned}
&\sin(\phi_1-\phi_{S_1}^L)\,F_{TU}^{\sin(\phi_1-\phi_{S_1}^L)}\\
&=\sum_q e_q^2\int d^2\boldsymbol{p}_{\perp 2}\Big[\frac{z_{p_1}}{z_{p_2}}\frac{p_{\perp 2}}{p_{\perp 1}}\sin(\varphi_2-\phi_{S_1}^L)-\frac{P_{1T}}{p_{\perp 1}}\sin(\phi_1-\phi_{S_1}^L)\Big]\Delta^N D_{h_1^\uparrow/q}D_{h_2/\bar q}\\
&=\sin(\phi_1-\phi_{S_1}^L)\,\mathcal{C}\left[\left(\frac{z_{p_1}}{z_{p_2}}\frac{p_{\perp 2}}{p_{\perp 1}}\,\hat{\boldsymbol{p}}_{\perp 2}\cdot\hat{\boldsymbol{P}}_{1T}-\frac{P_{1T}}{p_{\perp 1}}\right)\Delta^N D_{h_1^\uparrow/q}D_{h_2/\bar q}\right]\\
&=\sin(\phi_1-\phi_{S_1}^L)\,\mathcal{C}\left[\left(\frac{\boldsymbol{p}_{\perp 2}\cdot\hat{\boldsymbol{P}}_{1T}}{z_2}-\frac{P_{1T}}{z_1}\right)\frac{D_{1T}^\perp\bar D_1}{M_{h_1}}\right]
\end{aligned} \tag{2.110}$$

$$\begin{aligned}
&2\sin(\phi_1+\phi_{S_1}^L)\,F_{TU}^{\sin(\phi_1+\phi_{S_1}^L)}\\
&=\sum_q e_q^2\int d^2\boldsymbol{p}_{\perp 2}\sin(\varphi_2+\phi_{S_1}^L)\frac{1}{2}\big(\Delta D_{S_X/s_T}^{h_1/q}+\Delta^- D_{S_Y/s_T}^{h_1/q}\big)\,\Delta^N D_{h_2/\bar q^\uparrow}\\
&=\sin(\phi_1+\phi_{S_1}^L)\,\mathcal{C}\left[(\hat{\boldsymbol{p}}_{\perp 2}\cdot\hat{\boldsymbol{P}}_{1T})\frac{1}{2}\big(\Delta D_{S_X/s_T}^{h_1/q}+\Delta^- D_{S_Y/s_T}^{h_1/q}\big)\Delta^N D_{h_2/\bar q^\uparrow}\right]\\
&=2\sin(\phi_1+\phi_{S_1}^L)\,\mathcal{C}\left[\left(\frac{\boldsymbol{p}_{\perp 2}\cdot\hat{\boldsymbol{P}}_{1T}}{z_2}\right)\frac{H_1\bar H_1^\perp}{M_{h_2}}\right]
\end{aligned} \tag{2.111}$$

$$
\begin{aligned}
&2\sin(3\phi_1-\phi_{S_1}^L)\,F_{TU}^{\sin(3\phi_1-\phi_{S_1}^L)}\\
&=\sum_q e_q^2\int d^2\boldsymbol{p}_{\perp 2}\Bigg\{\frac{P_{1T}^2}{p_{\perp 1}^2}\sin(\varphi_2+2\phi_1-\phi_{S_1}^L)-2\frac{z_{p_1}}{z_{p_2}}\frac{P_{1T}p_{\perp 2}}{p_{\perp 1}^2}\sin(2\varphi_2+\phi_1-\phi_{S_1}^L)\\
&+\frac{z_{p_1}^2}{z_{p_2}^2}\frac{p_{\perp 2}^2}{p_{\perp 1}^2}\sin(3\varphi_2-\phi_{S_1}^L)\Bigg\}\frac{1}{2}\left(\Delta D_{S_X/s_T}^{h_1/q}-\Delta^- D_{S_Y/s_T}^{h_1/q}\right)\Delta^N D_{h_2/\bar{q}^\uparrow}\\
&=\sin(3\phi_1-\phi_{S_1}^L)\,\mathcal{C}\Bigg[\Bigg\{\frac{z_{p_1}^2}{z_{p_2}^2}\frac{p_{\perp 2}^2}{p_{\perp 1}^2}\Big[4\big(\hat{\boldsymbol{p}}_{\perp 2}\cdot\hat{\boldsymbol{P}}_{1T}\big)^3-3\left(\hat{\boldsymbol{p}}_{\perp 2}\cdot\hat{\boldsymbol{P}}_{1T}\right)\Big]+\frac{P_{1T}^2}{p_{\perp 1}^2}\left(\hat{\boldsymbol{p}}_{\perp 2}\cdot\hat{\boldsymbol{P}}_{1T}\right)\\
&-2\frac{z_{p_1}}{z_{p_2}}\frac{p_{\perp 2}P_{1T}}{p_{\perp 1}^2}\Big[2\big(\hat{\boldsymbol{p}}_{\perp 2}\cdot\hat{\boldsymbol{P}}_{1T}\big)^2-1\Big]\Bigg\}\frac{1}{2}\left(\Delta D_{S_X/s_T}^{h_1/q}-\Delta^- D_{S_Y/s_T}^{h_1/q}\right)\Delta^N D_{h_2/\bar{q}^\uparrow}\Bigg]\\
&=2\sin(3\phi_1-\phi_{S_1}^L)\,\mathcal{C}\Bigg[\Bigg\{\Bigg[4\left(\frac{\boldsymbol{p}_{\perp 2}\cdot\hat{\boldsymbol{P}}_{1T}}{z_2}\right)^3-3\frac{p_{\perp 2}^2}{z_2^2}\left(\frac{\boldsymbol{p}_{\perp 2}\cdot\hat{\boldsymbol{P}}_{1T}}{z_2}\right)\Bigg]\\
&+\left(\frac{\boldsymbol{p}_{\perp 2}\cdot\boldsymbol{P}_{1T}}{z_1 z_2}\right)\frac{P_{1T}}{z_1}-2\Bigg[2\left(\frac{\boldsymbol{p}_{\perp 2}\cdot\hat{\boldsymbol{P}}_{1T}}{z_2}\right)^2-\frac{p_{\perp 2}^2}{z_2^2}\Bigg]\frac{P_{1T}}{z_1}\Bigg\}\frac{H_{1T}^\perp\bar{H}_1^\perp}{2M_{h_1}^2 M_{h_2}}\Bigg]\,.
\end{aligned}
\tag{2.112}
$$

A relevant projection, often adopted in experimental analyses, is the polarization orthogonal to the hadron plane, that is along

$$
\hat{\boldsymbol{n}}\equiv(\cos\phi_n,\sin\phi_n,0)=\frac{-\boldsymbol{P}_2\times\boldsymbol{P}_1}{|\boldsymbol{P}_2\times\boldsymbol{P}_1|}=-\sin\phi_1\hat{\boldsymbol{x}}_L+\cos\phi_1\hat{\boldsymbol{y}}_L\,,
\tag{2.113}
$$

implying

$$
\phi_n=\phi_1+\frac{\pi}{2}\,.
\tag{2.114}
$$

The polarization along $\hat{\boldsymbol{n}}$ can be directly obtained by identifying $\phi_{S_1}^L=\phi_n$ in Eq. (2.109) as follows

$$
\begin{aligned}
&P_n^{h_1}\frac{d\sigma^{e^+e^-\to h_1h_2X}}{d\cos\theta dz_1dz_2d^2\boldsymbol{P}_{1T}}\equiv P_T^{h_1}(\phi_{S_1}^L=\phi_n)\,\frac{d\sigma^{e^+e^-\to h_1h_2X}}{d\cos\theta dz_1dz_2d^2\boldsymbol{P}_{1T}}\\
&=\frac{3\pi\alpha^2}{2s}\Bigg\{-\left(1+\cos^2\theta\right)F_{TU}^{\sin(\phi_1-\phi_{S_1}^L)}+\sin^2\theta\cos(2\phi_1)\left(F_{TU}^{\sin(\phi_1+\phi_{S_1}^L)}-F_{TU}^{\sin(3\phi_1-\phi_{S_1}^L)}\right)\Bigg\}\,.
\end{aligned}
\tag{2.115}
$$

In such a case, by integrating over $\boldsymbol{P}_{1T}$, and therefore over the azimuthal angle ϕ_1, one is sensitive only to the structure function $F_{TU}^{\sin(\phi_1-\phi_{S_1}^L)}$, Eq. (2.110), that is given as a convolution of the polarizing TMD-FF for hadron h_1 with the unpolarized TMD-FF for hadron h_2. Notice that also in the unpolarized cross section, Eq. (2.102), only the term F_{UU}, Eq. (2.103), survives. The final expression, simplifying a common factor $(1+\cos^2\theta)$, reads

$$P_n^{h_1}(z_1,z_2) = -\frac{F_{TU}^{\sin(\phi_1-\phi_{S_1}^L)}}{F_{UU}}\,. \tag{2.116}$$

This is indeed the strategy adopted in the recent phenomenological analysis performed in Ref. [41] that will be presented in the next Chapter 3.

2.5.3. Double-polarized case

In the following cases we give directly the expressions in terms of convolutions.

$$P_Z^{h_1}P_Z^{h_2}\frac{d\sigma^{e^+e^-\to h_1h_2X}}{d\cos\theta dz_1dz_2d^2\boldsymbol{P}_{1T}} = \frac{3\pi\alpha^2}{2s}\left\{-\Big(1+\cos^2\theta\Big)F_{LL} + \sin^2\theta\cos(2\phi_1)F_{LL}^{\cos(2\phi_1)}\right\}, \tag{2.117}$$

where

$$F_{LL} = \mathcal{C}\left[G_{1L}\bar{G}_{1L}\right] \tag{2.118}$$

$$\begin{aligned} F_{LL}^{\cos(2\phi_1)} &= \mathcal{C}\left[\left\{\frac{P_{1T}}{p_{\perp 1}}\,\hat{\boldsymbol{p}}_{\perp 2}\cdot\hat{\boldsymbol{P}}_{1T} - \frac{z_{p_1}}{z_{p_2}}\frac{p_{\perp 2}}{p_{\perp 1}}\left[2\big(\hat{\boldsymbol{p}}_{\perp 2}\cdot\hat{\boldsymbol{P}}_{1T}\big)^2-1\right]\right\}\Delta D_{S_Z/s_T}^{h_1/q}\Delta D_{S_Z/s_T}^{h_2/\bar{q}}\right] \\ &= \mathcal{C}\left[\left\{\frac{\boldsymbol{p}_{\perp 2}\cdot\boldsymbol{P}_{1T}}{z_1z_2} - \left[2\left(\frac{\boldsymbol{p}_{\perp 2}\cdot\hat{\boldsymbol{P}}_{1T}}{z_2}\right)^2 - \frac{p_{\perp 2}^2}{z_2^2}\right]\right\}\frac{H_{1L}^{\perp}\bar{H}_{1L}^{\perp}}{M_{h_1}M_{h_2}}\right]. \end{aligned} \tag{2.119}$$

For the case of a transversely-longitudinally polarized hadron pair we have

$$P_T^{h_1} P_Z^{h_2} \frac{d\sigma^{e^+e^-\to h_1 h_2 X}}{d\cos\theta dz_1 dz_2 d^2\boldsymbol{P}_{1T}} = \frac{3\pi\alpha^2}{2s}\Bigg\{\Big(1+\cos^2\theta\Big)\cos(\phi_1-\phi_{S_1}^L)F_{TL}^{\cos(\phi_1-\phi_{S_1}^L)} + \sin^2\theta\Big[\cos(\phi_1+\phi_{S_1}^L)F_{TL}^{\cos(\phi_1+\phi_{S_1}^L)} + \cos(3\phi_1-\phi_{S_1}^L)F_{TL}^{\cos(3\phi_1-\phi_{S_1}^L)}\Big]\Bigg\}, \quad (2.120)$$

where

$$\begin{aligned} F_{TL}^{\cos(\phi_1-\phi_{S_1}^L)} &= \mathcal{C}\left[\left(\frac{z_{p_1}}{z_{p_2}}\frac{p_{\perp 2}}{p_{\perp 1}}\,\hat{\boldsymbol{p}}_{\perp 2}\cdot\hat{\boldsymbol{P}}_{1T} - \frac{P_{1T}}{p_{\perp 1}}\right)\Delta D_{S_X/s_L}^{h_1/q}\Delta D_{S_Z/s_L}^{h_2/\bar{q}}\right] \\ &= -\mathcal{C}\left[\left(\frac{\boldsymbol{p}_{\perp 2}\cdot\hat{\boldsymbol{P}}_{1T}}{z_2} - \frac{P_{1T}}{z_1}\right)\frac{G_{1T}\bar{G}_{1L}}{M_{h_1}}\right] \end{aligned} \quad (2.121)$$

$$\begin{aligned} F_{TL}^{\cos(\phi_1+\phi_{S_1}^L)} &= \mathcal{C}\left[(\hat{\boldsymbol{p}}_{\perp 2}\cdot\hat{\boldsymbol{P}}_{1T})\frac{1}{2}\left(\Delta D_{S_X/s_T}^{h_1/q} + \Delta^- D_{S_Y/s_T}^{h_1/q}\right)\Delta D_{S_Z/s_T}^{h_2/\bar{q}}\right] \\ &= -\mathcal{C}\left[\left(\frac{\boldsymbol{p}_{\perp 2}\cdot\hat{\boldsymbol{P}}_{1T}}{z_2}\right)\frac{H_1\bar{H}_{1L}^\perp}{M_{h_2}}\right] \end{aligned} \quad (2.122)$$

$$\begin{aligned} &2\,F_{TL}^{\cos(3\phi_1-\phi_{S_1}^L)} \\ &= \mathcal{C}\Bigg[\Bigg\{\frac{z_{p_1}^2}{z_{p_2}^2}\frac{p_{\perp 2}^2}{p_{\perp 1}^2}\Big[4\big(\hat{\boldsymbol{p}}_{\perp 2}\cdot\hat{\boldsymbol{P}}_{1T}\big)^3 - 3\big(\hat{\boldsymbol{p}}_{\perp 2}\cdot\hat{\boldsymbol{P}}_{1T}\big)\Big] + \frac{P_{1T}^2}{p_{\perp 1}^2}\left(\hat{\boldsymbol{p}}_{\perp 2}\cdot\hat{\boldsymbol{P}}_{1T}\right) \\ &- 2\,\frac{z_{p_1}}{z_{p_2}}\frac{p_{\perp 2}P_{1T}}{p_{\perp 1}^2}\Big[2\big(\hat{\boldsymbol{p}}_{\perp 2}\cdot\hat{\boldsymbol{P}}_{1T}\big)^2 - 1\Big]\Bigg\}\left(\Delta D_{S_X/s_T}^{h_1/q} - \Delta^- D_{S_Y/s_T}^{h_1/q}\right)\Delta D_{S_Z/s_T}^{h_2/\bar{q}}\Bigg] \\ &= -\mathcal{C}\Bigg[\Bigg\{\Bigg[4\left(\frac{\boldsymbol{p}_{\perp 2}\cdot\hat{\boldsymbol{P}}_{1T}}{z_2}\right)^3 - 3\frac{p_{\perp 2}^2}{z_2^2}\left(\frac{\boldsymbol{p}_{\perp 2}\cdot\hat{\boldsymbol{P}}_{1T}}{z_2}\right)\Bigg] + \left(\frac{\boldsymbol{p}_{\perp 2}\cdot\boldsymbol{P}_{1T}}{z_1 z_2}\right)\frac{P_{1T}}{z_1} \\ &- 2\left[2\left(\frac{\boldsymbol{p}_{\perp 2}\cdot\hat{\boldsymbol{P}}_{1T}}{z_2}\right)^2 - \frac{p_{\perp 2}^2}{z_2^2}\right]\frac{P_{1T}}{z_1}\Bigg\}\frac{H_{1T}^\perp\bar{H}_{1L}^\perp}{M_{h_1}^2 M_{h_2}}\Bigg], \end{aligned} \quad (2.123)$$

where the minus signs appearing when switching to the Amsterdam notation come from the relative signs between the definition of the corresponding TMD-FFs. Finally, when both hadrons are transversely polarized we have

$$
\begin{aligned}
&P_T^{h_1} P_T^{h_2} \frac{d\sigma^{e^+e^-\to h_1 h_2 X}}{d\cos\theta dz_1 dz_2 d^2\boldsymbol{P}_{1T}} = \frac{3\pi\alpha^2}{2s} \\
&\times \left\{ \left(1+\cos^2\theta\right)\frac{1}{2}\Big[\cos(2\phi_1 - \phi_{S_1}^L - \phi_{S_2}^L) F_{TT}^{\cos(2\phi_1-\phi_{S_1}^L-\phi_{S_2}^L)} - \cos(\phi_{S_1}^L - \phi_{S_2}^L) F_{TT}^{\cos(\phi_{S_1}^L-\phi_{S_2}^L)} \Big] \right. \\
&+ \sin^2\theta \Big[\cos(\phi_{S_1}^L + \phi_{S_2}^L) F_{TT}^{\cos(\phi_{S_1}^L+\phi_{S_2}^L)} + \cos(2\phi_1 + \phi_{S_1}^L - \phi_{S_2}^L) F_{TT}^{\cos(2\phi_1+\phi_{S_1}^L-\phi_{S_2}^L)} \\
&\left. + \cos(2\phi_1 - \phi_{S_1}^L + \phi_{S_2}^L) F_{TT}^{\cos(2\phi_1-\phi_{S_1}^L+\phi_{S_2}^L)} + \cos(4\phi_1 - \phi_{S_1}^L - \phi_{S_2}^L) F_{TT}^{\cos(4\phi_1-\phi_{S_1}^L-\phi_{S_2}^L)} \Big] \right\},
\end{aligned}
\tag{2.124}
$$

where

$$
F_{TT}^{\cos(\phi_{S_1}^L+\phi_{S_2}^L)} = \mathcal{C}\left[\frac{1}{2}\left(\Delta D_{S_X/s_T}^{h_1/q} + \Delta^- D_{S_Y/s_T}^{h_1/q}\right) \frac{1}{2}\left(\Delta D_{S_X/s_T}^{h_2/\bar{q}} + \Delta^- D_{S_Y/s_T}^{h_2/\bar{q}}\right) \right] = \mathcal{C}\left[H_1 \bar{H}_1\right]
\tag{2.125}
$$

$$
\begin{aligned}
F_{TT}^{\cos(2\phi_1-\phi_{S_1}^L-\phi_{S_2}^L)} &= \mathcal{C}\left[\left\{ \frac{P_{1T}}{p_{\perp 1}} \hat{\boldsymbol{p}}_{\perp 2}\cdot\hat{\boldsymbol{P}}_{1T} - \frac{z_{p_1}}{z_{p_2}}\frac{p_{\perp 2}}{p_{\perp 1}}\left[2\left(\hat{\boldsymbol{p}}_{\perp 2}\cdot\hat{\boldsymbol{P}}_{1T}\right)^2 - 1\right] \right\} \right. \\
&\qquad \left. \times \left(\Delta^N D_{h_1^\uparrow/q} \Delta^N D_{h_2^\uparrow/\bar{q}} - \Delta D_{S_X/s_L}^{h_1/q} \Delta D_{S_X/s_L}^{h_2/\bar{q}} \right) \right] \\
&= \mathcal{C}\left[\left\{ \frac{\boldsymbol{p}_{\perp 2}\cdot\boldsymbol{P}_{1T}}{z_1 z_2} - \left[2\left(\frac{\boldsymbol{p}_{\perp 2}\cdot\hat{\boldsymbol{P}}_{1T}}{z_2} \right)^2 - \frac{p_{\perp 2}^2}{z_2^2} \right] \right\} \frac{D_{1T}^\perp \bar{D}_{1T}^\perp - G_{1T}\bar{G}_{1T}}{M_{h_1} M_{h_2}} \right]
\end{aligned}
\tag{2.126}
$$

$$
\begin{aligned}
&F_{TT}^{\cos(\phi_{S_1}^L-\phi_{S_2}^L)} \\
&= \mathcal{C}\left[\left\{\frac{P_{1T}}{p_{\perp 1}}\,\hat{\boldsymbol{p}}_{\perp 2}\cdot\hat{\boldsymbol{P}}_{1T}-\frac{z_{p_1}}{z_{p_2}}\frac{p_{\perp 2}}{p_{\perp 1}}\right\}\left(\Delta^N D_{h_1^\uparrow/q}\Delta^N D_{h_2^\uparrow/\bar{q}}+\Delta D_{S_X/s_L}^{h_1/q}\Delta D_{S_X/s_L}^{h_2/\bar{q}}\right)\right] \\
&= \mathcal{C}\left[\left\{\frac{\boldsymbol{p}_{\perp 2}\cdot\boldsymbol{P}_{1T}}{z_1 z_2}-\frac{p_{\perp 2}^2}{z_2^2}\right\}\frac{D_{1T}^\perp \bar{D}_{1T}^\perp+G_{1T}\bar{G}_{1T}}{M_{h_1}M_{h_2}}\right]
\end{aligned}
\tag{2.127}
$$

$$
\begin{aligned}
F_{TT}^{\cos(2\phi_1+\phi_{S_1}^L-\phi_{S_2}^L)} &= \mathcal{C}\left[\left\{2\left(\hat{\boldsymbol{p}}_{\perp 2}\cdot\hat{\boldsymbol{P}}_{1T}\right)^2-1\right\}\frac{1}{2}\left(\Delta D_{S_X/s_T}^{h_1/q}+\Delta^- D_{S_Y/s_T}^{h_1/q}\right)\right. \\
&\quad\left.\times\frac{1}{2}\left(\Delta D_{S_X/s_T}^{h_2/\bar{q}}-\Delta^- D_{S_Y/s_T}^{h_2/\bar{q}}\right)\right] \\
&= \mathcal{C}\left[\left\{2\left(\frac{\boldsymbol{p}_{\perp 2}\cdot\hat{\boldsymbol{P}}_{1T}}{z_2}\right)^2-\frac{p_{\perp 2}^2}{z_2^2}\right\}\frac{H_1\bar{H}_{1T}^\perp}{2M_{h_2}^2}\right]
\end{aligned}
\tag{2.128}
$$

$$
\begin{aligned}
F_{TT}^{\cos(2\phi_1-\phi_{S_1}^L+\phi_{S_2}^L)} &= \mathcal{C}\left[\left\{\frac{P_{1T}^2}{p_{\perp 1}^2}+\frac{z_{p_1}^2}{z_{p_2}^2}\frac{p_{\perp 2}^2}{p_{\perp 1}^2}\left[2\left(\hat{\boldsymbol{p}}_{\perp 2}\cdot\hat{\boldsymbol{P}}_{1T}\right)^2-1\right]-2\frac{z_{p_1}}{z_{p_2}}\frac{p_{\perp 2}P_{1T}}{p_{\perp 1}^2}\left(\hat{\boldsymbol{p}}_{\perp 2}\cdot\hat{\boldsymbol{P}}_{1T}\right)\right\}\right. \\
&\quad\left.\times\frac{1}{2}\left(\Delta D_{S_X/s_T}^{h_1/q}-\Delta^- D_{S_Y/s_T}^{h_1/q}\right)\frac{1}{2}\left(\Delta D_{S_X/s_T}^{h_2/\bar{q}}+\Delta^- D_{S_Y/s_T}^{h_2/\bar{q}}\right)\right] \\
&= \mathcal{C}\left[\left\{\frac{P_{1T}^2}{z_1^2}+\left[2\left(\frac{\boldsymbol{p}_{\perp 2}\cdot\hat{\boldsymbol{P}}_{1T}}{z_2}\right)^2-\frac{p_{\perp 2}^2}{z_2^2}\right]-2\left(\frac{\boldsymbol{p}_{\perp 2}\cdot\boldsymbol{P}_{1T}}{z_1 z_2}\right)\right\}\frac{H_{1T}^\perp\bar{H}_1}{2M_{h_1}^2}\right]
\end{aligned}
\tag{2.129}
$$

$$
\begin{aligned}
&F_{TT}^{\cos(4\phi_1-\phi_{S_1}^L-\phi_{S_2}^L)} \\
&= \mathcal{C}\Bigg[\Bigg\{8\frac{z_{p_1}^2}{z_{p_2}^2}\frac{p_{\perp 2}^2}{p_{\perp 1}^2}\Bigg[\left(\hat{\boldsymbol{p}}_{\perp 2}\cdot\hat{\boldsymbol{P}}_{1T}\right)^4-\left(\hat{\boldsymbol{p}}_{\perp 2}\cdot\hat{\boldsymbol{P}}_{1T}\right)^2+\frac{1}{8}\Bigg]-8\frac{z_{p_1}}{z_{p_2}}\frac{p_{\perp 2}P_{1T}}{p_{\perp 1}^2}\left(\hat{\boldsymbol{p}}_{\perp 2}\cdot\hat{\boldsymbol{P}}_{1T}\right)^3 \\
&+\frac{P_{1T}^2}{p_{\perp 1}^2}\left[2\left(\hat{\boldsymbol{p}}_{\perp 2}\cdot\hat{\boldsymbol{P}}_{1T}\right)^2-1\right]+6\frac{z_{p_1}}{z_{p_2}}\frac{P_{1T}p_{\perp 2}}{p_{\perp 1}^2}\left(\hat{\boldsymbol{p}}_{\perp 2}\cdot\hat{\boldsymbol{P}}_{1T}\right)\Bigg\} \\
&\times\frac{1}{2}\left(\Delta D_{S_X/s_T}^{h_1/q}-\Delta^- D_{S_Y/s_T}^{h_1/q}\right)\frac{1}{2}\left(\Delta D_{S_X/s_T}^{h_2/\bar{q}}-\Delta^- D_{S_Y/s_T}^{h_2/\bar{q}}\right)\Bigg] \\
&= \mathcal{C}\Bigg[\Bigg\{8\Bigg[\left(\frac{\boldsymbol{p}_{\perp 2}\cdot\hat{\boldsymbol{P}}_{1T}}{z_2}\right)^4-\frac{p_{\perp 2}^2}{z_2^2}\left(\frac{\boldsymbol{p}_{\perp 2}\cdot\hat{\boldsymbol{P}}_{1T}}{z_2}\right)^2+\frac{p_{\perp 2}^4}{8z_2^4}\Bigg]-8\frac{P_{1T}}{z_1}\left(\frac{\boldsymbol{p}_{\perp 2}\cdot\hat{\boldsymbol{P}}_{1T}}{z_2}\right)^3 \\
&+\frac{P_{1T}^2}{z_1^2z_2^2}\left[2\left(\boldsymbol{p}_{\perp 2}\cdot\hat{\boldsymbol{P}}_{1T}\right)^2-p_{\perp 2}^2\right]+6\frac{P_{1T}p_{\perp 2}^2}{z_1z_2^2}\left(\frac{\boldsymbol{p}_{\perp 2}\cdot\hat{\boldsymbol{P}}_{1T}}{z_2}\right)\Bigg\}\frac{H_{1T}^{\perp}\bar{H}_{1T}^{\perp}}{4M_{h_1}^2M_{h_2}^2}\Bigg]. \qquad (2.130)
\end{aligned}
$$

2.5.4. A Gaussian model

The above results can be cast in a more explicit and simplified form by adopting a suitable functional $p_\perp$ dependence for the TMD-FFs involved. We focus for its relevance and complexity on the hadron-frame configuration, since for the thrust-frame case the intrinsic transverse momentum dependence of the two hadrons is completely factorized. In this respect the use of a Gaussian-like dependence together with the leading-order approximation in $p_\perp/\sqrt{s}$ (for not too small z values), allow us to carry out, analytically, all the integrations over the intrinsic transverse momenta, leading to simplified expressions.

We consider explicitly three cases that represent the TMD-FFs appearing in the present study. For a generic fragmentation function of a quark into a hadron h, that is the unpolarized and any of the single- or double-polarized FF we will therefore assume respectively the following form

$$D_h^{\text{unp}}(z,p_\perp) = D_h^{\text{unp}}(z)\,g(p_\perp) \qquad (2.131)$$

$$\Delta D_h(z,p_\perp) = \Delta D_h(z)\,g^{(i)}(p_\perp)\,, \qquad (2.132)$$

with $i = 0, 1, 2$. Our parameterizations are required to respect angular momentum conservation in the forward direction, therefore we define

$$g^{(i)}(p_\perp) = \left(\frac{p_\perp}{M}\right)^i h^{(i)}(p_\perp)\,. \tag{2.133}$$

In particular, $g(p_\perp)$ is a simple Gaussian normalized to unity:

$$g(p_\perp) = \frac{1}{\pi\langle\, p_\perp^2\,\rangle}\, e^{-p_\perp^2/\langle p_\perp^2\rangle}\,, \tag{2.134}$$

while

$$g^{(i)}(p_\perp) = \left(\frac{p_\perp}{M}\right)^i h^{(i)}(p_\perp) = K_i\,\left(\frac{p_\perp}{M}\right)^i e^{-p_\perp^2/\langle p_\perp^2\rangle_\Delta}\,, \qquad i = 0, 1, 2\,, \tag{2.135}$$

where $\langle p_\perp^2\rangle_\Delta$ is the $p_\perp$ width of the corresponding ΔD. Notice that $g^{(0)}(p_\perp)$ is still a simple Gaussian, parametrizing the transverse momentum dependence of double polarized TMD-FFs surviving in the collinear limit.

The normalization constants, K_i, can be chosen to properly fulfill the positivity bounds, that can be expressed as:

$$\frac{|D^\uparrow - D^\downarrow|}{D^\uparrow + D^\downarrow} \leq 1 \tag{2.136}$$

where $\uparrow$ / $\downarrow$ represent opposite transverse/longitudinal polarization states of the polarized particle, either the hadron or the fragmenting quark. A simple way is to impose the bound separately on the $p_\perp$- and the z-dependent components of the FFs. The first is trivial since we can use the explicit functional form. For instance, for the unpolarized and the single-polarized TMD-FF, like the Collins (C) and the polarizing (p) FF, we have

$$D_{h/q}(z, p_\perp) = D_{h/q}(z)\frac{e^{-p_\perp^2/\langle p_\perp^2\rangle}}{\pi\langle p_\perp^2\rangle} \tag{2.137}$$

$$\Delta D_{h/q}^{C,p}(z, p_\perp) = \Delta D_{h/q}^{C,p}(z)\sqrt{2e}\,\frac{p_\perp}{M_{C,p}}\,\frac{e^{-p_\perp^2/\langle p_\perp^2\rangle_{C,p}}}{\pi\langle p_\perp^2\rangle}\,, \tag{2.138}$$

where

$$\langle p_\perp^2 \rangle_{C,p} = \frac{\langle p_\perp^2 \rangle M_{C,p}^2}{\langle p_\perp^2 \rangle + M_{C,p}^2} \,. \tag{2.139}$$

These expressions fulfill the positivity bounds of the TMD-FFs by simply imposing the corresponding bound on the z-dependent parts.

Here below we present the results for the azimuthal dependences and polarization observables in the hadron frame entering Eq. (2.25) and the convolutions defined in Sec. 2.5, limiting ourselves to the unpolarized and single-polarized cases. These indeed are at present the most interesting from the phenomenological point of view. We list here all expressions:

$$F_{UU} = D_{h_1/q}(z_1) D_{h_2/\bar{q}}(z_2) \frac{e^{-P_{1T}^2/\langle p_\perp^2 \rangle_{12}}}{\pi \langle p_\perp^2 \rangle_{12}} \tag{2.140}$$

$$\begin{aligned} F_{UU}^{\cos(2\phi_1)} = {} & \frac{1}{4} \Delta^N D_{h_1/q^\uparrow}(z_1) \Delta^N D_{h_2/\bar{q}^\uparrow}(z_2) \\ & \times \frac{2e}{M_{C_1} M_{C_2}} \frac{e^{-P_{1T}^2/\langle p_\perp^2 \rangle_{C_1,C_2}}}{\pi \langle p_\perp^2 \rangle_{C_1,C_2}} \frac{z_{p_1}}{z_{p_2}} \frac{P_{1T}^2}{\langle p_\perp^2 \rangle_{C_1,C_2}^2} \frac{\langle p_\perp^2 \rangle_{C_1}^2 \langle p_\perp^2 \rangle_{C_2}^2}{\langle p_\perp^2 \rangle_1 \langle p_\perp^2 \rangle_2} \,, \end{aligned} \tag{2.141}$$

where

$$\langle p_\perp^2 \rangle_{12} = \frac{z_{p_2}^2 \langle p_\perp^2 \rangle_1 + z_{p_1}^2 \langle p_\perp^2 \rangle_2}{z_{p_2}^2} \tag{2.142}$$

$$\langle p_\perp^2 \rangle_{C_1,C_2} = \frac{z_{p_2}^2 \langle p_\perp^2 \rangle_{C_1} + z_{p_1}^2 \langle p_\perp^2 \rangle_{C_2}}{z_{p_2}^2} \,, \tag{2.143}$$

and

$$\Delta^N D_{h_1/q^\uparrow}(z) \equiv \Delta D_{h_1/q}^C(z) \,. \tag{2.144}$$

Notice that for Gaussian widths independent of the scaling variables and for hadrons of the same kind, the above formulae simplify and coincide with the results of Ref. [42]. For its later use, we define

$$\langle p_\perp^2 \rangle_{\Delta_1,\Delta_2} = \frac{z_{p_2}^2 \langle p_\perp^2 \rangle_{\Delta_1} + z_{p_1}^2 \langle p_\perp^2 \rangle_{\Delta_2}}{z_{p_2}^2}\,, \tag{2.145}$$

and, in order to have more compact expressions,

$$\mathcal{G}(\Delta_1,\Delta_2) \equiv \frac{1}{\pi \langle p_\perp^2 \rangle_{\Delta_1,\Delta_2}} \exp\Big[-\frac{P_{1T}^2}{\langle p_\perp^2 \rangle_{\Delta_1,\Delta_2}}\Big]\,. \tag{2.146}$$

Moving to the single-polarized hadron production we have

$$F_{LU}^{\sin(2\phi_1)} = \frac{1}{2}\Delta D_{S_Z/s_T}^{h_1/q}(z_1)\Delta^N D_{h_2/\bar{q}^\uparrow}(z_2)\frac{2e\,\mathcal{G}(LT_1,C_2)}{M_{LT_1}M_{C_2}}\frac{P_{1T}^2}{\langle p_\perp^2 \rangle_{LT_1,C_2}^2}\frac{z_{p_1}}{z_{p_2}}\frac{\langle p_\perp^2 \rangle_{LT_1}^2 \langle p_\perp^2 \rangle_{C_2}^2}{\langle p_\perp^2 \rangle_1 \langle p_\perp^2 \rangle_2}\,, \tag{2.147}$$

where we have adopted the following parametrization

$$\Delta D_{S_Z/s_T}^{h/q}(z,p_\perp) = \Delta D_{S_Z/s_T}^{h/q}(z)\sqrt{2e}\frac{p_\perp}{M_{LT}}\frac{e^{-p_\perp^2/\langle p_\perp^2 \rangle_{LT}}}{\pi \langle p_\perp^2 \rangle}\,. \tag{2.148}$$

Notice that at the lowest order in η_{1T} this is also the longitudinal polarization in the laboratory frame. For the computation of the transverse polarization it is more convenient to parametrize the transversely polarized TMD-FFs as follows

$$D_{+-}^{+-}(z,p_\perp) \equiv H_1(z,p_\perp) = H_1(z)\frac{e^{-p_\perp^2/\langle p_\perp^2 \rangle_T}}{\pi \langle p_\perp^2 \rangle_T} \tag{2.149}$$

$$D_{-+}^{+-}(z,p_\perp) \equiv \frac{p_\perp^2}{2z^2M_h^2}H_{1T}^\perp(z,p_\perp) = H_{1T}^\perp(z)\,e\,\frac{p_\perp^2}{M_{TT}^2}\frac{e^{-p_\perp^2/\langle p_\perp^2 \rangle_{TT}}}{\pi \langle p_\perp^2 \rangle}\,, \tag{2.150}$$

where in the second equation we have kept distinct the mass parameter entering the relation between the two standard notations and the one related to the $p_\perp$

dependence to be extracted from data. This leads to the following results

$$F_{TU}^{\sin(\phi_1-\phi_{S_1}^L)} = -\Delta^N D_{h_1^\uparrow/q}(z_1) D_{h_2/\bar{q}}(z_2)\, \frac{\sqrt{2e}\,\mathcal{G}(p_1,2)}{M_{p_1}} \frac{P_{1T}}{\langle p_\perp^2\rangle_{p_1,2}} \frac{\langle p_\perp^2\rangle_{p_1}^2}{\langle p_\perp^2\rangle_1} \tag{2.151}$$

$$F_{TU}^{\sin(\phi_1+\phi_{S_1}^L)} = \frac{1}{2} H_1(z_1) \Delta^N D_{h_2/\bar{q}^\uparrow}(z_2)\, \frac{\sqrt{2e}\mathcal{G}(T_1,C_2)}{M_{C_2}} \frac{P_{1T}}{\langle p_\perp^2\rangle_{T_1,C_2}} \frac{\langle p_\perp^2\rangle_{C_2}^2}{\langle p_\perp^2\rangle_2} \frac{z_{p_1}}{z_{p_2}} \tag{2.152}$$

$$F_{TU}^{\sin(3\phi_1-\phi_{S_1}^L)} = \frac{1}{2}\, H_{1T}^\perp(z_1) \Delta^N D_{h_2/\bar{q}^\uparrow}(z_2)\, \frac{\sqrt{2e}\, e\, \mathcal{G}(TT_1,C_2)}{M_{TT_1}^2 M_{C_2}} \frac{P_{1T}^3}{\langle p_\perp^2\rangle_{TT_1,C_2}^3} \frac{z_{p_1}}{z_{p_2}} \frac{\langle p_\perp^2\rangle_{C_2}^2 \langle p_\perp^2\rangle_{TT_1}^3}{\langle p_\perp^2\rangle_2 \langle p_\perp^2\rangle_1}\,, \tag{2.153}$$

where we have restored the standard notation also for the polarizing FF

$$\Delta^N D_{h_1^\uparrow/q}(z_1) \equiv \Delta D_{h_1/q}^p(z_1)\,. \tag{2.154}$$

For its relevance we give here the result for the transverse polarization along $\hat{\boldsymbol{n}}$, integrated over $\boldsymbol{P}_{1T}$, Eq. (4.17), adopting the Gaussian parametrizations (see Eqs. (2.151) and (2.140)):

$$\begin{aligned}\mathcal{P}_n^{h_1}(z_1,z_2) = \sqrt{\frac{e\pi}{2}} \frac{1}{M_p} \frac{\langle p_\perp^2\rangle_{p_1}^2}{\langle p_\perp^2\rangle_1} \frac{z_2}{\left\{[z_1(1-M_{h_1}^2/(z_1^2 s))]^2 \langle p_\perp^2\rangle_2 + z_2^2 \langle p_\perp^2\rangle_{p_1}\right\}^{1/2}} \\ \times \frac{\sum_q e_q^2\, \Delta^N D_{h_1^\uparrow/q}(z_1) D_{h_2/\bar{q}}(z_2)}{\sum_q e_q^2\, D_{h_1/q}(z_1) D_{h_2/\bar{q}}(z_2)}\,.\end{aligned} \tag{2.155}$$

2.6. Conclusions

The study of hadron production in e^+e^- annihilations is definitely the most powerful tool to access the parton-to-hadron fragmentation mechanism in a

direct and clear way. When azimuthal modulations are considered, together with the polarization states in the case of spin-1/2 hadrons, the information we can extract is extremely rich and, within a TMD approach, could allow to disentangle important spin-momentum correlations and shed light on interesting effects.

We have presented, within a TMD approach and adopting the helicity formalism, the complete structure of all leading-twist azimuthal and polarization observables for almost back-to-back hadron-pair production in e^+e^- annihilation processes. This approach, extremely intuitive, gives indeed a more direct probabilistic picture and allows one to follow the underlying processes at the partonic level. It is important to stress how our helicity amplitudes for the different factorized steps lead to final results perfectly equivalent to those obtained within the TMD factorization at leading order [30].

We have considered both spinless and spin-1/2 hadrons, discussing in detail the classification and properties of the full set of leading-twist TMD fragmentation functions for quarks and gluons. For completeness we have also shown the connection with the Amsterdam notation, widely adopted in the literature.

We have presented our results adopting two reference frames: the thrust frame, which requires the reconstruction of the jet thrust axis and allows for the analysis of the azimuthal dependences of the hadron pair around this direction; the hadron frame, defined only in terms of the two hadron momenta. For the latter case we have shown as, by means of a simple tensorial analysis, one can extract the measurable azimuthal dependences. All expressions for single- and double-polarized hadron production have been presented, adopting a conventional form in terms of structure functions.

Special attention has been devoted to the proper expressions of all quantities when moving from the particle helicity frames to the configurations accessible in the measurements.

Moreover, by employing a Gaussian ansatz for the transverse momentum dependence of the TMD-FFs, we have obtained simple expressions for the struc-

ture functions, useful in phenomenological analyses. In particular, we have re-derived the explicit formula for the single transverse polarization of spin-1/2 hadron production in $e^+e^- \to h_1^{\uparrow} h_2 + X$ processes, which has allowed for the first ever extraction of the polarizing FF for Λ hyperons from Belle data [41], and that will be used in the next Chapter. Among the features of the Gaussian model, as shown also in previous phenomenological analyses, we have that it is able to describe fairly well the $p_\perp$-dependence of the TMDs, and it is extremely effective in their extraction from experimental data at a fixed hard scale Q. Since Belle data are at a single hard scale Q, the effects due to the TMD evolution have a small impact on the TMDs extraction, and so, as we will see, the Gaussian turns out to be good enough to extract the polarizing fragmentation function.

This study follows analogous studies already developed for the SIDIS processes [28], where once again the presence of two ordered energy scales guarantees the validity of a TMD factorization scheme. There the complete expressions for all the SIDIS spin asymmetries and the cross section azimuthal dependences were presented. In this respect the present work represents a sort of complementary study in the fragmentation sector, leading to an overall and complete picture within the helicity formalism of the realm of leading-twist TMDs and the ways to access them.

Chapter 3.

Extraction of the Λ polarizing fragmentation function from e^+e^- data

3.1. Introduction

As we will show in this Chapter, Belle data allow for the first ever extraction of the pFF in a clear way. Since no other contribution from the initial state could play a role, this is the best process to access this TMD-FF. A preliminary phenomenological study, even though in a simplified scheme, has been discussed in Ref. [44]. Here we present a detailed analysis[1] of Belle data at a level of accuracy very close to that of current studies on other relevant TMDs.

We will start by fitting the associated production ($\Lambda\, h$) data set alone, for which TMD factorization holds. For completeness, in a separate full-data fit we include also the Λ-jet data. Even if this configuration presents some difficulties experimentally and could imply a more complex TMD factorization structure [38–40, 46, 47], it represents a unique source of information on the explicit $p_\perp$ dependence of the TMD pFF. For this reason, and in order to verify the possibility to have a simultaneous extraction within a parton model approach,

[1] See also Ref. [45] for a similar study.

we will study it adopting a simplified and phenomenological TMD scheme. This approach will be revised in Chapter 5 where we will discuss the CSS formalism.

The Chapter is organized as follows: in Section 3.2 we summarize the theoretical formalism already presented in detail in Chapter 2, while in Section 3.3 we show the results of the fits to Belle data, discussing in detail our main findings. Finally, in Section 3.4 we gather our concluding remarks.

3.2. Formalism

We consider the processes $e^+e^- \to h_1 h_2 + X$ and $e^+e^- \to h_1(\text{jet}) + X$, where h_1 is a spin-1/2 hadron and the second (light and unpolarized) hadron, h_2, is produced almost back-to-back with respect to h_1. Here we focus only on the very intriguing case of the transverse hyperon polarization. This quantity is defined as

$$\mathcal{P}_T = \frac{d\sigma^{\uparrow} - d\sigma^{\downarrow}}{d\sigma^{\uparrow} + d\sigma^{\downarrow}} = \frac{d\sigma^{\uparrow} - d\sigma^{\downarrow}}{d\sigma^{\text{unp}}}, \tag{3.1}$$

where $d\sigma^{\uparrow(\downarrow)}$ is the differential cross section for the production of a hadron transversely polarized along the up(down) direction w.r.t. the production plane and $d\sigma^{\text{unp}}$ is the corresponding unpolarized cross section.

For inclusive production (within a jet), the polarization is measured orthogonally to the *thrust plane*, containing the jet (more precisely the thrust axis, $\hat{\boldsymbol{T}}$) and the spin-1/2 hadron momentum, $\boldsymbol{P}_{h_1}$, that is along $\hat{\boldsymbol{T}} \times \boldsymbol{P}_{h_1}$. For the associated production with a light hadron, h_2, one considers the *hadron plane*, containing the two hadrons, and the transverse polarization is measured along $(-\boldsymbol{P}_{h_2} \times \boldsymbol{P}_{h_1})$.

For the first case, in a leading order approach, we choose a frame so that the $e^+e^- \to q\bar{q}$ scattering occurs in the $\hat{x}\hat{z}$ plane, with θ being the angle between the back-to-back quark-antiquark (identifying the z axis) and e^+e^- directions. The three-momentum of the hadron h_1, with mass M_{h_1}, light-cone momentum fraction z_1, and intrinsic transverse momentum $\boldsymbol{p}_{\perp 1}$, w.r.t. the direction of the

fragmenting quark, is given as

$$\boldsymbol{P}_{h_1} = \left(p_{\perp 1} \cos\varphi_1, p_{\perp 1} \sin\varphi_1, z_1 \frac{\sqrt{s}}{2}(1 - a_{h_1}^2/z_1^2) \right), \tag{3.2}$$

with $p_{\perp 1} = |\boldsymbol{p}_{\perp 1}|$ and $a_{h_1}^2 = (p_{\perp 1}^2 + M_{h_1}^2)/s$. For such a configuration, $d\sigma^{\uparrow}$ in Eq. (3.1) stands for $d\sigma^{e^+e^- \to h_1^{\uparrow}(\text{jet})+X}/d\cos\theta dz_1 d^2\boldsymbol{p}_{\perp 1}$.

The transverse polarization, simplifying a common factor $(1 + \cos^2\theta)$ in the numerator and the denominator, can be given then within a phenomenological parton model approach as

$$\mathcal{P}_T(z_1, p_{\perp 1}) = \frac{\sum_q e_q^2 \, \Delta D_{h_1^{\uparrow}/q}(z_1, p_{\perp 1})}{\sum_q e_q^2 \, D_{h_1/q}(z_1, p_{\perp 1})}, \tag{3.3}$$

where the sum runs over quark and antiquarks, and $\Delta D_{h_1^{\uparrow}/q}$ is the pFF, also denoted as $D_{1T}^{\perp q}$. These are related as follows [17]:

$$\Delta D_{h^{\uparrow}/q}(z, p_{\perp}) = \frac{p_{\perp}}{z M_h} D_{1T}^{\perp q}(z, p_{\perp}) \,. \tag{3.4}$$

We recall that, for a hadron with polarization vector $\hat{\boldsymbol{P}} \equiv \uparrow$, coming from the fragmentation of a quark with momentum $\boldsymbol{p}_q$, the pFF is defined as (see Eq. (1.9)):

$$\Delta\hat{D}_{h^{\uparrow}/q}(z, \boldsymbol{p}_{\perp}) \equiv \hat{D}_{h^{\uparrow}/q}(z, \boldsymbol{p}_{\perp}) - \hat{D}_{h^{\downarrow}/q}(z, \boldsymbol{p}_{\perp}) = \Delta D_{h^{\uparrow}/q}(z, p_{\perp}) \, \hat{\boldsymbol{P}} \cdot (\hat{\boldsymbol{p}}_q \times \hat{\boldsymbol{p}}_{\perp}) \,. \tag{3.5}$$

Eq. (3.3) is obtained by integrating the numerator and the denominator in Eq. (3.1) over φ_1 and refers to the transverse polarization in the hadron helicity frame (i.e. transverse w.r.t. the plane containing the fragmenting quark and the hadron h_1). At leading order, this coincides with the thrust-plane frame defined above.

For massive hadrons, we use properly the two scaling variables presented in Chapter 2: the energy fraction z_h, Eq. (2.9), adopted in Belle analysis, and the

momentum fraction z_p, Eq. (2.10). We recall that, these are related as follows (see Eqs. (2.11, 2.12, 2.13)):

$$z_{h,p} \simeq z\left(1 \pm \frac{M_h^2}{z^2 s}\right) \tag{3.6}$$

$$z_p = z_h\left(1 - 4\,\frac{M_h^2}{z_h^2 s}\right)^{1/2}. \tag{3.7}$$

We will use for Λ hyperons, the full dependence on M_h. For the associated production we adopt the configuration represented in Fig. 2.2: the produced unpolarized hadron, h_2, identifies the $\hat{\boldsymbol{z}}_L$ direction

$$\boldsymbol{P}_{h_2} = -|\boldsymbol{P}_{h_2}|\,\hat{\boldsymbol{z}}_L\,, \tag{3.8}$$

and the $\hat{xz}$ plane is determined by the lepton and the h_2 directions (with the e^+e^- axis at angle θ). The other plane is determined by $\hat{\boldsymbol{z}}_L$ and the direction of the spin-1/2 hadron, h_1,

$$\boldsymbol{P}_{h_1} = (P_{1T}\cos\phi_1, P_{1T}\sin\phi_1, P_{1L})\,. \tag{3.9}$$

For such a case, $d\sigma^{\uparrow}$ in Eq. (3.1) stands for

$$\frac{d\sigma^{e^+e^-\to h_1^{\uparrow} h_2 + X}}{d\cos\theta_2 dz_1 dz_2 d^2\boldsymbol{P}_{1T}}\,. \tag{3.10}$$

More details on the kinematics for the almost back-to-back double-hadron production can be found in Chapter 2 and in Refs. [42, 48].

In this case, the transverse polarization of h_1, in its helicity frame, as reached from the helicity frame of the fragmenting quark, is not directed along $\hat{\boldsymbol{n}} \propto (-\boldsymbol{P}_{h_2} \times \boldsymbol{P}_{h_1})$ and has therefore to be projected out along this direction. Moreover, two independent contributions appear: one driven by the pFF for h_1, convoluted with the unpolarized TMD-FF for the hadron h_2, and another one driven by the Collins FF for the hadron h_2. The last manifests specific modulations in ϕ_1 and vanishes upon integrating over it, like in the present analysis and as presented

in Chapter 2. Here we give directly the final expression for the transverse polarization along $\hat{\boldsymbol{n}}$, integrated over $\boldsymbol{P}_{1T}$ and adopting a Gaussian Ansatz for the TMD-FFs. This choice, largely adopted in TMD phenomenology, allows to carry out the integrations over intrinsic transverse momenta analytically and, at the same time, is good enough to describe the low-$p_\perp$ dependence. As it will be shown below, this is indeed the region where the observed transverse Λ polarization is sizeable. In particular we use:

$$D_{h/q}(z, p_\perp) = D_{h/q}(z)\,\frac{e^{-p_\perp^2/\langle p_\perp^2\rangle}}{\pi\langle p_\perp^2\rangle}\,, \tag{3.11}$$

$$\Delta D_{h^\uparrow/q}(z, p_\perp) = \Delta D_{h^\uparrow/q}(z)\frac{\sqrt{2e}\,p_\perp}{M_{\rm p}}\frac{e^{-p_\perp^2/\langle p_\perp^2\rangle_{\rm p}}}{\pi\langle p_\perp^2\rangle}, \tag{3.12}$$

with $\langle p_\perp^2\rangle_{\rm p} = \frac{M_{\rm p}^2}{M_{\rm p}^2+\langle p_\perp^2\rangle}\,\langle p_\perp^2\rangle$. By imposing $|\Delta D(z)| \le D(z)$ the positivity bound for the pFF, Eq. (3.5), is automatically fulfilled. As shown in Chapter 2, the transverse polarization, simplifying again a common factor $(1+\cos^2\theta_2)$, is then given as

$$\begin{aligned}\mathcal{P}_n(z_1, z_2) = \sqrt{\frac{e\pi}{2}}\frac{1}{M_{\rm p}}\frac{\langle p_\perp^2\rangle_{\rm p}^2}{\langle p_{\perp 1}^2\rangle}\,\frac{z_2}{\left\{[z_1(1-M_{h_1}^2/(z_1^2 s))]^2\langle p_{\perp 2}^2\rangle + z_2^2\langle p_\perp^2\rangle_{\rm p}\right\}^{1/2}} \\ \times\frac{\sum_q e_q^2\,\Delta D_{h_1^\uparrow/q}(z_1)D_{h_2/\bar q}(z_2)}{\sum_q e_q^2\,D_{h_1/q}(z_1)D_{h_2/\bar q}(z_2)}\,.\end{aligned} \tag{3.13}$$

For its importance we also give the first $p_\perp$-moment of the pFF:

$$\begin{aligned}\Delta D^{(1)}_{h^\uparrow/q}(z) &= \int d^2\boldsymbol{p}_\perp\frac{p_\perp}{2zM_h}\Delta D_{h^\uparrow/q}(z, p_\perp) = D_{1T}^{\perp(1)}(z) \\ &= \sqrt{\frac{e}{2}}\frac{1}{zM_h}\frac{1}{M_{\rm p}}\frac{\langle p_\perp^2\rangle_{\rm p}^2}{\langle p_\perp^2\rangle}\Delta D_{h^\uparrow/q}(z)\,,\end{aligned} \tag{3.14}$$

where the last expression is obtained by using Eq. (3.12). Notice that $\mathcal{P}_n$, Eq. (3.13), is directly sensitive to this quantity.

3.3. Fit and results

We can now proceed, using Eqs. (3.3) and (3.13), with the analysis of Belle polarization data for Λ and $\bar{\Lambda}$ production, measured at $\sqrt{s} = 10.58$ GeV [33]. As already said, two data sets are available: one for the associated production with light hadrons (π and K), as a function of z_Λ and $z_\pi(z_K)$ (128 data points) and one for the inclusive production as a function of $p_\perp$ (the Λ transverse momentum w.r.t. the thrust axis), for different energy fractions, z_Λ (32 data points). Notice that here we consider the transverse polarization for inclusive Λ particles, namely those directly produced from $q\bar{q}$ fragmentation and those indirectly produced from strong decays. We parameterize the z-dependent part of the polarizing Fragmentation Function as

$$\Delta D_{\Lambda^\uparrow/q}(z) = N_q z^{a_q}(1-z)^{b_q} \frac{(a_q+b_q)^{(a_q+b_q)}}{a_q^{a_q} b_q^{b_q}} D_{\Lambda/q}(z)\,, \tag{3.15}$$

where $|N_q| \leq 1$ and $q = u, d, s,$ sea. This guaranties that $|\Delta D(z)| \leq D(z)$.

For the unpolarized FFs we adopt the DSS07 set [49], for pions and kaons, and the AKK08 set [50] for Λ's. Since all data are at fixed energy scale no evolution is implied in this extraction. For the unpolarized Gaussian widths we use $\langle p_\perp^2 \rangle = 0.2$ GeV^2 [51], both for light and heavy hadrons (varying this value has little effect in the final results). Concerning the Λ FF set, all available parameterizations are given for $\Lambda + \bar{\Lambda}$, including the AKK08 set, which adopts z_p as scaling variable. We then separate the two contributions assuming

$$D_{\bar{\Lambda}/q}(z_p) = D_{\Lambda/\bar{q}}(z_p) = (1-z_p)\, D_{\Lambda/q}(z_p)\,. \tag{3.16}$$

This is a common way to take into account the expected difference between the quark and antiquark FF with a suppressed Λ sea at large z_p w.r.t. the valence component. Other similar choices have a very little impact on the fit. Notice that all transformations among the different scaling variables (z, z_h, z_p) involved, Eqs. (2.11), (2.12) and (2.13), are properly taken into account.

In order to access the $p_\perp$ dependence of the pFF, data in the thrust-plane frame would be ideal. On the other hand, the experimental accuracy in extracting them, requiring the reconstruction of the thrust axis, is more problematic. Moreover, as already pointed out, the use of a TMD approach is technically more subtle [38–40, 46, 47]. This problem will be properly addressed in Chapter 5, where we will consider the recent theoretical devolopments devised within the full TMD framework.

The analysis of associated production data, extremely powerful in accessing flavor separation, experimentally easier and on a more firm theoretical ground, is however phenomenologically more complex. We have therefore performed first a fit of the associated production data alone and then attempted a full fit of both data sets, paying special attention to large-z_h data. In particular, for the associated production we exclude data where the energy fractions for both hadrons are too large, while for the inclusive production we cut out the largest z_Λ bin (0.5-0.9). We have then imposed the following cuts: $z_{\pi,K} \leq 0.5$ for the associated production and $z_\Lambda \leq 0.5$ for the Λ-jet data set. This leaves us with 96+24 = 120 data points, still allowing to probe, at least in the Λh data set, large values of z_Λ. Notice that the cut on z_π has no impact on the quality of the fit.

Concerning the z-dependent part of the Λ pFF, Eq. (3.15), the best fit is obtained adopting the following parameter set:

$$N_u,\ N_d,\ N_s,\ N_{\rm sea},\ a_s,\ b_u,\ b_{\rm sea}\,, \tag{3.17}$$

with all other a and b parameters set to zero. This means that, with $\langle p_\perp^2 \rangle_{\rm p}$ (Eq. (3.12)), we have 8 free parameters. We have indeed tried many different combinations of parameter sets and this choice represents a sort of balance between the number of parameters and the statistical significance of the fit. Notice that *simpler* fits with only two pFFs, for $u = d$ and s quarks, or without any sea contribution, give much higher $\chi^2_{\rm dof}$'s. The same happens if no appropriate modulation in z is included. See comments below.

$N_u = 0.47^{+0.32}_{-0.20}$	$N_d = -0.32^{+0.13}_{-0.13}$
$N_s = -0.57^{+0.29}_{-0.43}$	$N_{\text{sea}} = -0.27^{+0.12}_{-0.20}$
$a_s = 2.30^{+1.08}_{-0.91}$	
$b_u = 3.50^{+2.33}_{-1.82}$	$b_{\text{sea}} = 2.60^{+2.60}_{-1.74}$
$\langle p_\perp^2 \rangle_{\text{p}} = 0.10^{+0.02}_{-0.02}\ \text{GeV}^2$	

Table 3.1.: Best values of the 8 free parameters fixing the pFF (Eqs. (3.12), (3.15)) for u, d, s and sea quarks, as obtained by fitting the full set of Belle data [33]. The statistical errors correspond to the shaded uncertainty areas in Figs. 3.1, 3.4 and 3.2, as explained in the text.

Table 3.1 reports the values of the best-fit parameters for the full-data analysis. The corresponding estimates, compared to Belle data [33], are shown in Figs. 3.1 and 3.4, respectively for the inclusive and associated Λ hadron ($\pi^\pm$, $K^\pm$) production. Considering this preliminary stage, the quality of the fit is reasonable, with a $\chi^2_{\text{dof}} = 1.94$ and with $\chi^2_{\text{points}} = 2.75, 1.55, 1.61$ for jet, pion and kaon data subsets. Notice that a fit of associated production data alone gives a $\chi^2_{\text{dof}} = 1.26$ with $\chi^2_{\text{points}} = 0.8, 1.5$ for pion and kaon data subsets. The

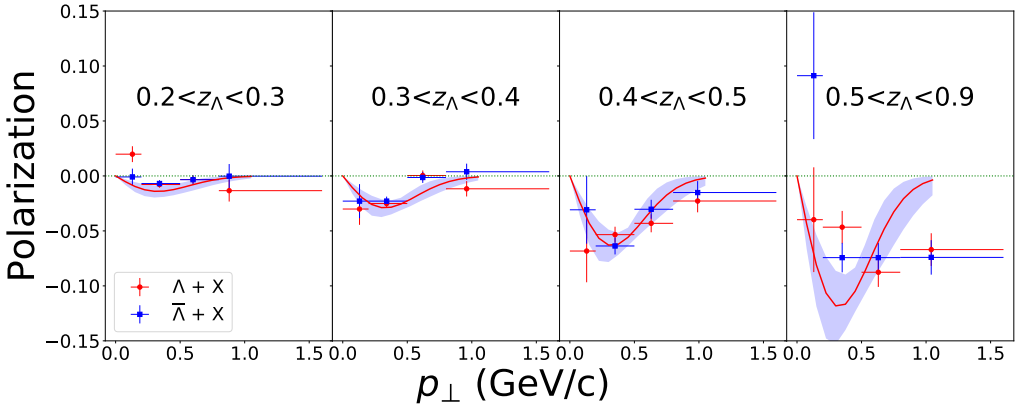

Figure 3.1.: Best-fit estimates of the transverse polarization for inclusive Λ and $\bar{\Lambda}$ production in $e^+e^- \to \Lambda(\text{jet}) + \text{X}$ (thrust-plane frame) as a function of $p_\perp$ for different z_Λ bins, compared against Belle data [33]. The statistical uncertainty bands, at 2σ level, are also shown. Notice that curves for Λ and $\bar{\Lambda}$ coincide and data in the rightmost panel are not included in the fit.

shaded areas, corresponding to a 2σ uncertainty, are computed according to the procedure explained in the Appendix of Ref. [52] and result in the statistical errors quoted in Table 3.1. More precisely, we have allowed the set of best fit parameters to vary, in order to generate around five hundred thousand new parameter sets, and we selected only those sets such that their corresponding $\chi^2 \leq \chi^2_{\rm min} + \Delta\chi^2$. All the curves associated to these sets (around two hundred thousand), lie inside the shaded area. The chosen value of $\Delta\chi^2 = 15.79$, for our eight-parameter fit, is such that the probability to find the "true" result inside the shaded band is 95.45%.

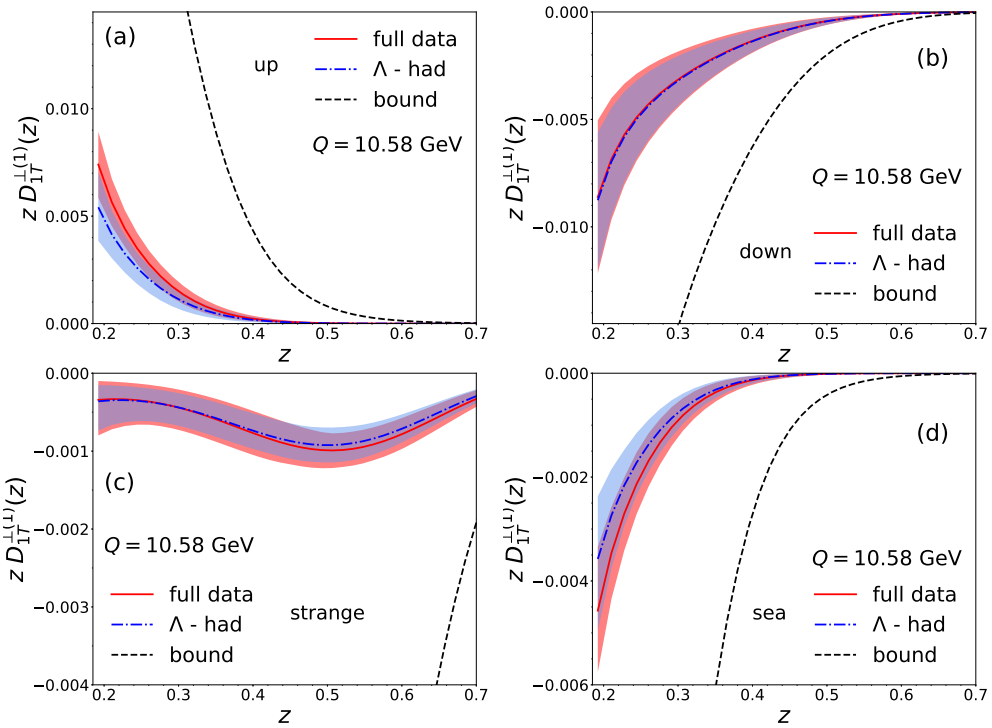

Figure 3.2.: First moments of the pFFs, see Eq. (3.14), for the up (a), down (b), strange (c) and sea (d) quarks, as obtained from the full-data fit (red solid lines) and the Λ-hadron fit (blue dot-dashed lines). The corresponding statistical uncertainty bands (at 2σ level), as well as the positivity bounds (black dashed lines), are shown.

As mentioned above, a fit restricted only to associated production data gives a much better result. Even though the resulting best-fit parameters are a bit different, the corresponding first moment, Eq. (3.14), is quite stable and the two extractions lead to consistent results. This is shown in Fig. 3.2, where we present the first moments of the Λ pFF as obtained in the full-data fit (red solid lines) and by fitting only the associated production data (blue dot-dashed lines), together with their positivity bounds (black dotted lines). As one can see, they are well consistent within their uncertainty bands, and in two cases (down and strange quarks) almost indistinguishable. In Fig. 3.3, we show, for the full-data fit, the ratios of the absolute value of the first moments w.r.t. their positivity bounds.

Some comments are in order. For the inclusive production case, the description is clearly less good. On the other hand, one would expect $\mathcal{P}_T = 0$ at $p_\perp = 0$, as well as $\mathcal{P}_T(\bar{\Lambda}) = \mathcal{P}_T(\Lambda)$, a feature not clearly visible in the data (Fig. 3.1). This increases the tension with the other data set, reducing the quality of the full-data fit. Moving to the associated production data set, we observe that charge conjugation symmetry implies $\mathcal{P}_n(\Lambda h^+) = \mathcal{P}_n(\bar{\Lambda} h^-)$; in this respect data are quite consistent (Fig. 3.4). Focusing on medium $z_{\pi,K}$ values, where the valence unpolarized FFs dominate, the Fig 3.5 (for $\Lambda\pi^-$(a), ΛK^-(b), $\Lambda\pi^+$(c) and ΛK^+(d) data) gives direct information on the pFFs respectively for *u* (red solid line), *d* (blue dashed line), *s* (purple dot-dashed) and *sea* (green dotted line) quarks (We represented best-fit estimates for Λ transverse polarization with a light-blue solid line, that coincide with those in Fig. 3.4). In fact, in this region $\mathcal{P}_n(\Lambda\pi^-)$ is positive (see Fig. 3.4a and Fig. 3.5a) and dominated by the contribution from the up quark pFF, while $\mathcal{P}_n(\Lambda\pi^+)$ is negative and dominated by the down quark pFF, at small-medium z_π, and by the pFFs of the down and the strange quarks, at large z_π (Figs. 3.2a, 3.2b and 3.5c). Moreover, the strong reduction in size of $\mathcal{P}_n(\Lambda\pi^-)$ with increasing z_Λ implies a large suppression of the up pFF for such values, see Figs. 3.3, 3.5a (red solid line), in contrast to the down quark pFF. At small z_Λ, sea quark FFs (green dotted line) start playing some role, becoming important around $z_\Lambda \leq 0.3$. For instance, for $\mathcal{P}_n(\Lambda\pi^+)$, where the up and down pFF contributions almost cancel each other for these z_Λ values, it is the negative sea polarizing FF that leads to large, and negative, values of the transverse polar-

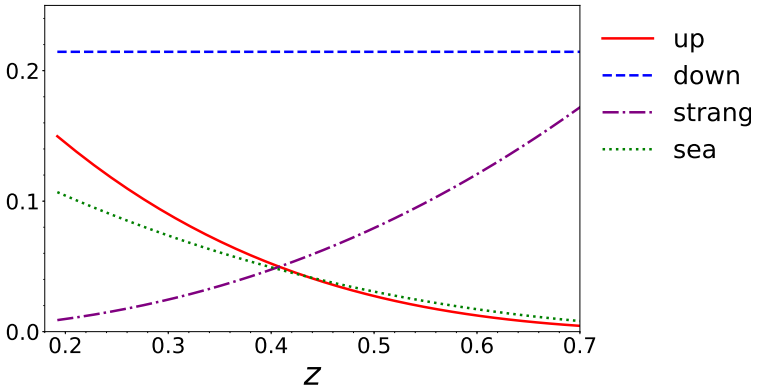

Figure 3.3.: Ratios of the absolute values of the first moments of the pFFs w.r.t. their positivity bounds for the u (red solid line), d (blue dashed line), s (purple dot-dashed line) and sea (green dotted line) quarks, as obtained from the full-data fit.

ization. Similarly, in $\mathcal{P}_n(\Lambda\pi^-)$, still for $z_\Lambda \leq 0.3$, this pFF is responsible for the partial reduction of the very large piece driven by the up polarizing FF, coupled to the favoured unpolarized π^- FF and weighted by a large relative charge factor. We can then understand the emerging of a negative sea polarizing FF (Fig. 3.2d) and its strong suppression at large z (Fig. 3.3, green dotted line). The description of Λ-kaon data follows a similar pattern. We can easily understand the negative values of $\mathcal{P}_n(\Lambda K^+)$ at medium z_Λ, being driven by a sizeable and negative $\Delta D_{\Lambda^\uparrow/s}$ (Figs. 3.2c and 3.5d, purple dot-dashed line), coupled to the leading FF $D_{K^+/\bar{s}}$. When moving to smaller z_Λ, this contribution is suppressed (see Figs. 3.3 and 3.5d) and once again it is the negative sea quark polarizing FF, $\Delta D_{\Lambda^\uparrow/\bar{u}}$, which leads to large and negative $\mathcal{P}_n(\Lambda K^+)$ values. For $\mathcal{P}_n(\Lambda K^-)$ (see Fig. 3.5b) at medium-large z_Λ all contributions are almost negligible, mainly for two reasons: i) the large-z suppression of the up and sea quark polarizing FFs coupled to the leading unpolarized kaon FFs; ii) the coupling of the other pFFs to sub-leading sea unpolarized K^- FFs. On the other hand, at small z_Λ the up quark pFF dominates, leading to large and positive $\mathcal{P}_n$, slightly reduced by the negative sea polarizing FF, $\Delta D_{\Lambda^\uparrow/\bar{s}}$, coupled to the leading unpolarized FF $D_{K^-/s}$. Similar reasonings apply to the $\bar{\Lambda}h$ data set. These quantitative findings are in perfect agreement with the qualitative expectations discussed in Ref. [33], with extra information on the size of the down pFF.

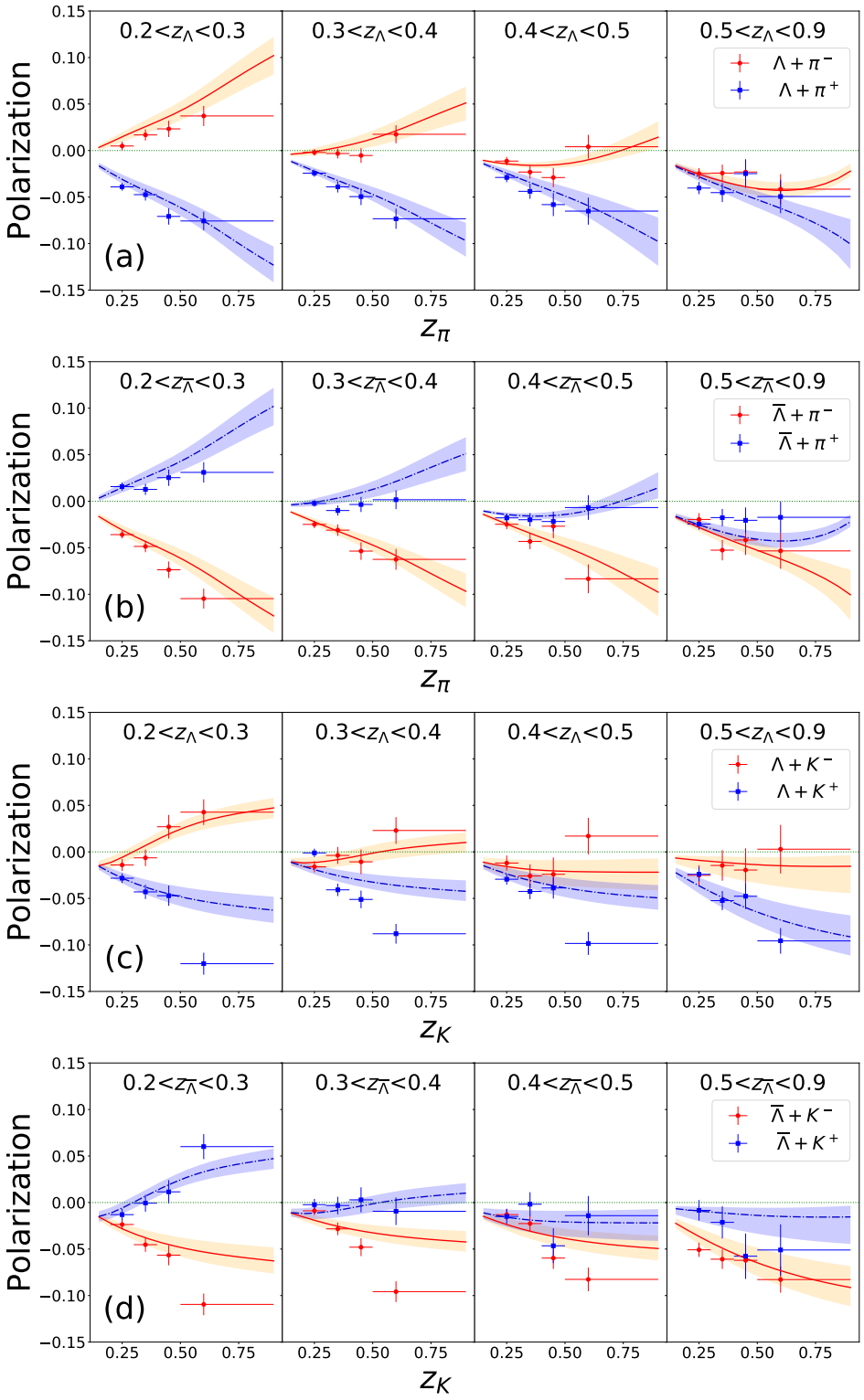

Figure 3.4.: Best-fit estimates, based on the full-data set, of the transverse polarization for Λ and $\bar{\Lambda}$ production in $e^+e^- \to \Lambda(\bar{\Lambda})h + X$, for $\Lambda\pi^\pm$ (a), $\bar{\Lambda}\pi^\pm$ (b), $\Lambda K^\pm$ (c), $\bar{\Lambda}K^\pm$ (d), as a function of z_h (of the associated hadron) for different z_Λ bins. Data are from Belle [33]. The statistical uncertainty bands, at 2σ level, are also shown. Data for $z_{\pi,K} > 0.5$ are not included in the fit.

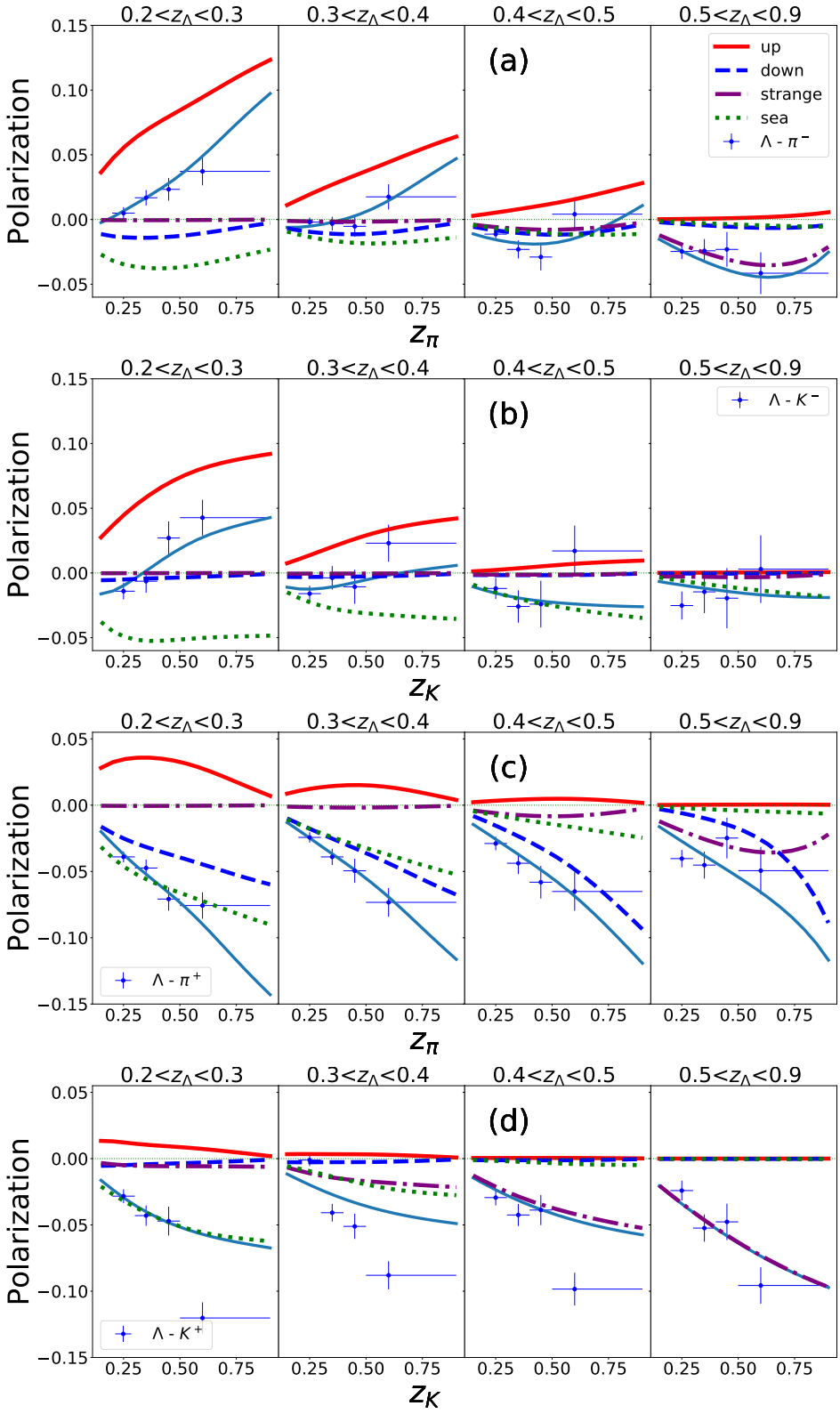

Figure 3.5.: Partial contributions of quark flavors, based on the full-data set, to the transverse polarization for Λ production in $e^+e^- \to \Lambda h + X$, for $\Lambda\pi^+$ (a), ΛK^+ (b), $\Lambda\pi^-$ (c) and ΛK^- (d): u (red solid line), d (blue dashed line), s (purple dot-dashed line) and sea (green dotted line). Best-fit estimates of the Λ transverse polarization are also represented (light-blue solid line), that coincide with those in Fig. 3.4.

3.4. Conclusions

The recent data from Belle Collaboration for the transverse $\Lambda/\bar{\Lambda}$ polarization have been used, within a TMD approach, to extract, for the first time, the polarizing fragmentation function of Λ hyperons. A clear separation in flavors has been achieved, supporting the need for three different valence pFFs, with their relative sign and size determined quite accurately. The need of a sea-quark pFF is well supported. By employing a phenomenological Gaussian Ansatz we obtained a first indication on their $p_\perp$ dependence have been extracted. New data with higher statistics, as well as complementary studies in other processes, will certainly help towards a deeper understanding of this important TMD-FF, and eventually, in solving the longstanding puzzle of the observed spontaneous transverse hyperon polarization.

Chapter 4.

Transversely polarized hadron production in Semi-inclusive DIS

4.1. Introduction

Semi-inclusive Deep Inelastic Scattering is one of the processes for which TMD factorization is proven that have played and still play a leading role in accessing TMDs. Thanks to the strong entanglements between the transverse momentum dependence of both the TMD-PDFs and FFs, SIDIS allows to extract simultaneously information about the inner structure of hadrons and the hadronization mechanism of partons.

It has been widely studied over the years [18, 19, 28], and the complete structure of azimuthal dependences for hadron production in (un)polarized collisions has been formulated in full detail. In particular, in Ref. [28] the authors presented the full decomposition of all azimuthal dependences, in terms of the eight TMD-PDFs, for unpolarized hadron production in $lp \to l'h + X$ processes, adopting the helicity formalism.

In this Chapter, following Ref. [28], we present the analogous expressions within the helicity formalism for the transverse polarization of a spin-1/2 hadron produced in unpolarized SIDIS processes. These results will be used, by exploit-

ing the previoulsy extracted Λ polarizing FF, to give estimates for the $\Lambda/\bar{\Lambda}$ transverse polarization.

The Chapter is organized as follows: in Section 4.2 we present the kinematics for the SIDIS process and the expression, within the helicity formalism, of the transverse polarization for the final state spin-1/2 hadron, following what was done in Ref. [28] for the unpolarized hadron production in case. In Section 4.3 we will give estimates for the transverse polarization of $\Lambda/\bar{\Lambda}$ hyperons, for kinematic configurations and energies reachable at the future Electron-Ion Collider (EIC).

4.2. Kinematics

We start considering the kinematics of Deep Inelastic Scattering processes (see Ref. [51]) in the $\gamma^* P$ c.m. frame, as shown in Fig. 4.1. We consider the photon and the proton colliding along the z axis with momenta $\boldsymbol{q}$ (along $+z$) and $\boldsymbol{P}$ (along $-z$) respectively; the lepton plane coincides with the x-z plane (following the so called "Trento conventions" [17]). We adopt the usual DIS variables (neglecting the lepton mass):

$$\begin{gathered} s = (P+l)^2 \qquad Q^2 = -q^2 \qquad (P+q)^2 = W^2 = \frac{1-x_B}{x_B} Q^2 + m_p^2 \\ x_B = \frac{Q^2}{2P\cdot q} = \frac{Q^2}{W^2 + Q^2 - m_p^2}\,. \end{gathered} \tag{4.1}$$

If we neglect also the proton mass m_p the four-momenta involved can be written as:

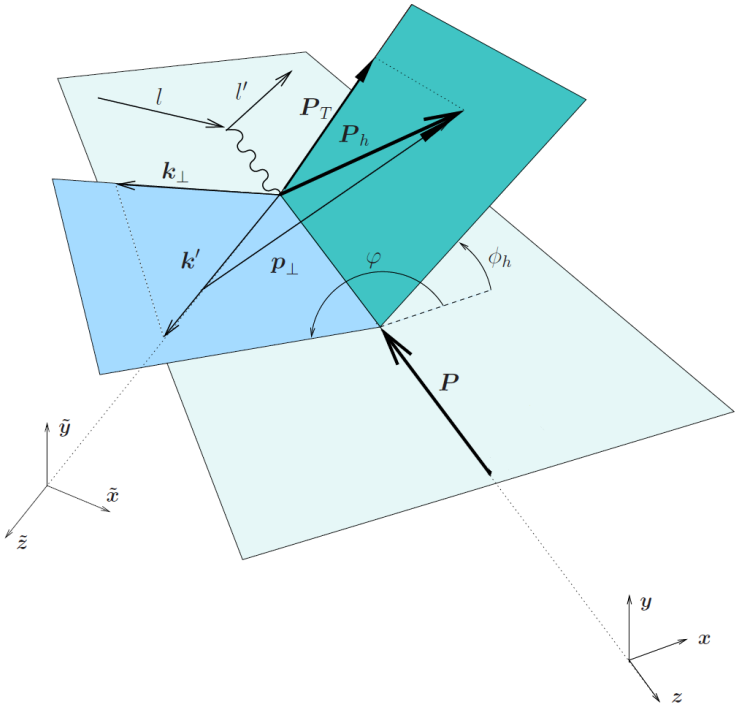

Figure 4.1.: Three dimensional kinematics of the SIDIS process.

$$
\begin{aligned}
q &= \frac{1}{2}\left(W - \frac{Q^2}{W}, 0, 0, W + \frac{Q^2}{W}\right), \\
P &= P_0(1, 0, 0, -1), \\
P_0 &= \frac{1}{2}\left(W + \frac{Q^2}{W}\right).
\end{aligned}
\tag{4.2}
$$

At leading order in QCD the lepton scatters off a quark and, taking intrinsic motion into account, the initial and final quark four-momenta are given by:

$$
k = \left(xP_0 + \frac{k_\perp^2}{4xP_0}, \boldsymbol{k}_\perp, -xP_0 + \frac{k_\perp^2}{4xP_0}\right), \qquad k' = k + q, \tag{4.3}
$$

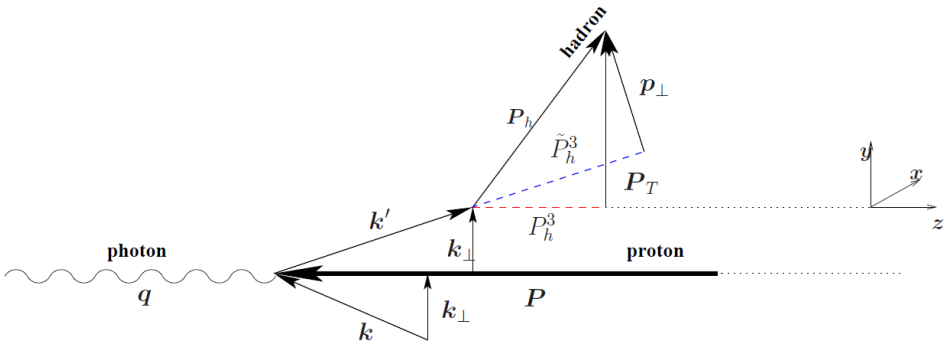

Figure 4.2.: Kinematics of photon-proton collision and of the fragmentation process.

where $x = k^-/P^-$ is the light-cone fraction of the proton momentum carried by the parton, $\boldsymbol{k}_\perp = k_\perp(\cos\varphi, \sin\varphi, 0)$ is the parton transverse momentum, with $k_\perp \equiv |\boldsymbol{k}_\perp|$ and k' is the four-momentum of the final-state quark fragmenting into the final-state hadron. It can also be proved [51] that the on-shell condition for the final quark, $k'^2 = 0$, implies

$$x = \frac{1}{2}x_B\left(1 + \sqrt{1 + \frac{4k_\perp^2}{Q^2}}\right) \simeq x_B + \mathcal{O}\left(\frac{k_\perp^2}{Q^2}\right). \tag{4.4}$$

Notice that when terms $\mathcal{O}(k_\perp^2/Q^2)$ are neglected in the above equations one recovers the usual relations $x = x_B$ and $k = x_B P + k_\perp$, moreover, the transverse momentum $\boldsymbol{k}'_\perp$ of the final quark in the laboratory frame is equal to the one of the initial quark, $\boldsymbol{k}'_\perp = \boldsymbol{k}_\perp$ (see Fig. 4.2).

In order to compute the polarization of the final-state hadron, we proceed with the definition of the the final-state quark and hadron momenta. The four-momenta of the final-state quark is:

$$
\begin{aligned}
k' &= (k'^0, \boldsymbol{k}_\perp, k'^3)\,, \\
k'^0 &= \frac{W}{2}\left(\frac{x - 2x_B + 1}{1 - x_B} + \frac{x_B}{x}\frac{k_\perp^2}{Q^2}\right), \\
k'^3 &= \frac{W}{2}\left(\frac{1 - x}{1 - x_B} + \frac{x_B}{x}\frac{k_\perp^2}{Q^2}\right).
\end{aligned}
\tag{4.5}
$$

Moreover, we can define the three-momentum of the final hadron in the laboratory frame as:

$$
\begin{aligned}
\boldsymbol{P}_h &= (P_T \cos\phi_h, P_T \sin\phi_h, P_L) \\
&= E_h\left(P_T \cos\phi_h, P_T \sin\phi_h, \sqrt{1 - \frac{M_h^2 + P_T^2}{E_h^2}}\right),
\end{aligned}
\tag{4.6}
$$

where E_h is the energy of the final-state hadron, P_T is the transverse momentum with respect to the initial-state hadron direction and $\boldsymbol{p}_\perp$ the transverse momentum with respect to its parent quark k', as shown in Fig. 4.1. As in the case of the initial particles, we can define the light-cone momentum fraction $z = P^+/k'^+$ and another variable commonly used in SIDIS processes, $z_h = (P \cdot P_h)/(P \cdot q)$. One finds [51] that the two scaling variables are related as follows:

$$
z \simeq z_h + \mathcal{O}\left(\frac{k_\perp^2}{Q^2}\right). \tag{4.7}
$$

For massive hadrons, two further scaling variables can be introduced: the energy fraction

$$
\xi_E = \frac{E_h}{\hat{k}'^0}\,, \tag{4.8}
$$

and the momentum fraction

$$\xi_p = \frac{\boldsymbol{P}_h \cdot \hat{\boldsymbol{k}}'}{k'^0}\,. \tag{4.9}$$

These are related to the light-cone momentum fractions as follows:

$$\begin{aligned} z_h &= \frac{1}{2}(\xi_p + \xi_E)\,, \\ \xi_p &= \xi_E \sqrt{1 - \frac{M_h^2 + p_\perp^2}{\xi_E^2 |k'^0|^2}} \simeq \xi_E \sqrt{1 - \frac{M_h^2}{\xi_E^2 |k'^0|^2}}\,, \\ \xi_p &\simeq z_h \left(1 - \frac{M_h^2}{4 z_h^2 |k'^0|^2}\right) \simeq z_h \left(1 - \frac{M_h^2}{z_h^2 Q^2} \frac{x_B}{1 - x_B}\right). \end{aligned} \tag{4.10}$$

Adopting the above variables, one can express the hadron and quark three-momenta as

$$\begin{aligned} \boldsymbol{P}_h &= |k'^0|^2 \xi_p \left(\frac{\eta_T}{\xi_p} \cos\phi_h, \frac{\eta_T}{\xi_p} \sin\phi_h, \sqrt{1 - \frac{\eta_T^2}{\xi_p^2}}\right), \\ \boldsymbol{k}' &= k'^0 (\eta_\perp \cos\varphi, \eta_\perp \sin\varphi, k'^3/k'^0)\,, \\ \boldsymbol{p}_\perp &= \boldsymbol{P}_h - \xi_p \boldsymbol{k}' \simeq \boldsymbol{P}_T - \xi_p \boldsymbol{k}_\perp \\ &\simeq \left(P_T \cos\phi_h - \xi_p k_\perp \cos\varphi, P_T \sin\phi_h - \xi_p k_\perp \sin\varphi, 0\right), \end{aligned} \tag{4.11}$$

We have also defined the quantities $\eta_{\perp,T}$ as:

$$\eta_\perp = \frac{k_\perp}{k'^0}\,, \quad \eta_T = \frac{P_T}{k'^0}\,, \tag{4.12}$$

with $P_T \equiv |\boldsymbol{P}_T|$. Now we can proceed to give the expression of the unit vectors identifying the axes of the final hadron helicity frame, as reached from the parent

quark helicity frame, in the laboratory frame adopted here. They are usually defined as follows:

$$\begin{aligned}\hat{\boldsymbol{X}}_h &= \hat{\boldsymbol{Y}}_h \times \hat{\boldsymbol{Z}}_h \\ \hat{\boldsymbol{Y}}_h &= \frac{\hat{\boldsymbol{k}}' \times \hat{\boldsymbol{P}}_h}{|\hat{\boldsymbol{k}}' \times \hat{\boldsymbol{P}}_h|} \\ \hat{\boldsymbol{Z}}_h &= \frac{\boldsymbol{P}_h}{|\boldsymbol{P}_h|}\,,\end{aligned} \tag{4.13}$$

and in our particular case we can write them, in the laboratory frame, in terms of the variables defined above:

$$\begin{aligned}\hat{\boldsymbol{X}}_h &\simeq \left(\frac{\eta_T}{\eta_{\perp h}}\cos\phi_h - \xi_p\frac{\eta_\perp}{\eta_{\perp h}}\cos\varphi, \frac{\eta_T}{\eta_{\perp h}}\sin\phi_h - \xi_p\frac{\eta_\perp}{\eta_{\perp h}}\sin\varphi, 0\right) \\ \hat{\boldsymbol{Y}}_h &\simeq \left(\xi_p\frac{\eta_\perp}{\eta_{\perp h}}\sin\varphi - \frac{\eta_T}{\eta_{\perp h}}\sin\phi_h, \frac{\eta_T}{\eta_{\perp h}}\cos\phi_h - \xi_p\frac{\eta_\perp}{\eta_{\perp h}}\cos\varphi, 0\right) \\ \hat{\boldsymbol{Z}}_h &= \left(\frac{\eta_T}{\xi_p}\cos\phi_h, \frac{\eta_T}{\xi_p}\sin\phi_h, \sqrt{1-\frac{\eta_T^2}{\xi_p^2}}\right),\end{aligned} \tag{4.14}$$

where $\eta_{\perp h} = p_\perp/k'^0$ and $p_\perp \equiv |\boldsymbol{p}_\perp|$. For the transverse polarization of the final hadron, firstly we have to express it in the hadron frame, the laboratory (L) frame:

$$\boldsymbol{P}_T^h = P_X^h\,\hat{\boldsymbol{X}}_h + P_Y^h\,\hat{\boldsymbol{Y}}_h = P_{x_L}^h\,\hat{\boldsymbol{x}}_L + P_{y_L}^h\,\hat{\boldsymbol{y}}_L = P_T^h(\cos\phi_{S_h}^L\,\hat{\boldsymbol{x}}_L + \sin\phi_{S_h}^L\,\hat{\boldsymbol{y}}_L)\,, \tag{4.15}$$

where $(\hat{\boldsymbol{x}}_L, \hat{\boldsymbol{y}}_L, \hat{\boldsymbol{z}}_L)$ are the unit vectors of the laboratory frame. By combining the transverse polarization components in the laboratory frame as

$$P_T^h = P_{x_L}^h\cos\phi_{S_h}^L + P_{y_L}^h\sin\phi_{S_h}^L\,. \tag{4.16}$$

By adopting the previous relations, also for this process, one can express the transverse polarization for the final hadron as a ratio of two convolutions

$$P_n^{h_1}(z_1, z_2) = \frac{\int d^2\boldsymbol{P}_T F_{TU}^{\sin(\phi_1 - \phi_{S_h}^L)}}{\int d^2\boldsymbol{P}_T F_{UU}}\,, \tag{4.17}$$

with

$$\begin{aligned} F_{UU} &= \sum_q e_q^2 \int d^2\boldsymbol{k}_\perp d^2\boldsymbol{p}_\perp \delta^{(2)}(\boldsymbol{P}_T - \xi_p \boldsymbol{k}_\perp - \boldsymbol{p}_\perp) f_{q/p}(x, k_\perp) D_{h/q}(z, p_\perp) \\ &= \mathcal{C}\left[f_1 D_1\right] \end{aligned} \tag{4.18}$$

$$\begin{aligned} F_{TU}^{\sin(\phi_1 - \phi_{S_h}^L)} =& \sum_q e_q^2 \int d^2\boldsymbol{k}_\perp d^2\boldsymbol{p}_\perp \delta^{(2)}(\boldsymbol{P}_T - \xi_p \boldsymbol{k}_\perp - \boldsymbol{p}_\perp) \\ &\times \left[\xi_p \frac{\boldsymbol{k}_\perp \cdot \hat{\boldsymbol{P}}_T}{p_\perp} - \frac{P_T}{p_\perp}\right] f_{q/p}(x, k_\perp) \Delta^N D_{h^\uparrow/q}(z, p_\perp) \\ =& \mathcal{C}\left[\left(\xi_p \frac{\boldsymbol{k}_\perp \cdot \hat{\boldsymbol{P}}_T}{p_\perp} - \frac{P_T}{p_\perp}\right) f_{q/p} \Delta^N D_{h^\uparrow/q}\right] \\ =& \mathcal{C}\left[\left(\boldsymbol{k}_\perp \cdot \hat{\boldsymbol{P}}_T - \frac{P_T}{z_h}\right) \frac{f_1 D_{1T}^\perp}{M_h}\right], \end{aligned} \tag{4.19}$$

where we used the notation used in Ref. [28] for a generic convolution on transverse momenta of a TMD-PDF with a TMD-FF:

$$\begin{aligned} \mathcal{C}[wfD] = \sum_q e_q^2 \int d^2\boldsymbol{k}_\perp d^2\boldsymbol{p}_\perp \delta^{(2)}(\boldsymbol{P}_T - \xi_p \boldsymbol{k}_\perp - \boldsymbol{p}_\perp) \\ \times w(\boldsymbol{k}_\perp, \boldsymbol{P}_T) f(x, k_\perp) D(z, p_\perp)\,. \end{aligned} \tag{4.20}$$

In Eqs. (4.18) and (4.19), $f_{q/p}$ and $D_{h/q}$ are respectively the unpolarized TMD parton distribution and fragmentation function, and $\Delta^N D_{h^\uparrow/q}$ is the polarizing fragmentation function. We also switched, in the last line of the $F_{TU}^{\sin(\phi_1 - \phi_{S_h}^L)}$

convolution, to the Amsterdam notation, neglecting terms in M_h/Q, for a more direct comparison with Ref. [53]. Assuming the same Gaussian parameterization as in Chapter 2, and considering the projection of the polarization along the $\hat{\boldsymbol{n}}$ direction (that is perpendicular to the production plane), defined as

$$\hat{\boldsymbol{n}} \equiv (\cos\phi_n, \sin\phi_n, 0) = \frac{-\boldsymbol{P}\times\boldsymbol{P}_h}{|\boldsymbol{P}\times\boldsymbol{P}_h|} = -\sin\phi_h\hat{\boldsymbol{x}}_L + \cos\phi_h\hat{\boldsymbol{y}}_L\,, \tag{4.21}$$

we find, for the polarization of the final-state hadron, the following expression:

$$\begin{aligned}\mathcal{P}_n^h(x_B, z_h) = \frac{\sqrt{2e\pi}}{2M_p}\frac{\langle p_\perp^2\rangle_{\rm p}^2}{\langle p_\perp^2\rangle_h}\frac{1}{\sqrt{\langle p_\perp^2\rangle_{\rm p} + \xi_p^2\langle k_\perp^2\rangle}} \\ \times \frac{\sum_q e_q^2 f_{q/p}(x_B)\Delta^N D_{h^\uparrow/q}(z_h)}{\sum_q e_q^2 f_{q/p}(x_B) D_{h/q}(z_h)}\,,\end{aligned} \tag{4.22}$$

where $\langle p_\perp^2\rangle_h$ and $\langle k_\perp^2\rangle$ are the Gaussian widths of, respectively, the unpolarized fragmentation function and the unpolarized parton distribution function, and $\langle p_\perp^2\rangle_{\rm p}$ is the width of the polarizing fragmentation function. After integration over all the transverse momenta, the polarization depends only on the fractions x_B and z_h, also via the variable

$$\xi_p \simeq z_h\left(1 - \frac{M_h^2}{z_h^2 Q^2}\frac{x_B}{1-x_B}\right). \tag{4.23}$$

4.3. Transversely polarized $\Lambda/\bar{\Lambda}$ production in Semi-inclusive Deep Inelastic Scattering

Employing Eq. (4.22) and the $\Lambda/\bar{\Lambda}$ polarizing fragmentation function for, extracted in [41] and presented in Chapter 3, we can give estimates of the polarization of $\Lambda/\bar{\Lambda}$, produced in $e^- p \to \Lambda/\bar{\Lambda}\, e^- + X$, as a function of z_h at fixed values of $x_B = (0.1, 0.3)$ and $Q = 10\,\text{GeV}$, which are consistent with the kinematics

reachable at the future Electron Ion Collider. This choice allows us to use the extracted polarizing FF without any evolution effect.

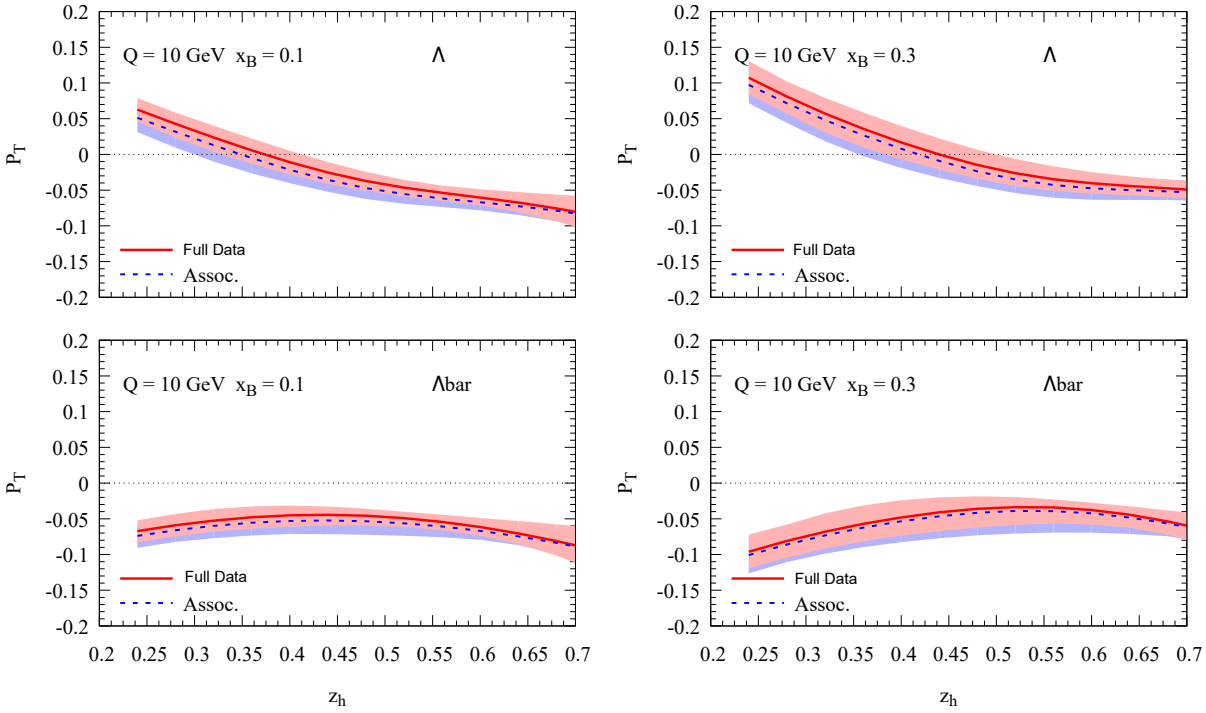

Figure 4.3.: Estimates of the transverse polarization for Λ and $\bar{\Lambda}$ production in $e^- p \to \Lambda/\bar{\Lambda}\ e^- + X$, as a function of z_h for different values of x_B and at $Q = 10\,\text{GeV}$. In red the estimates obtained adopting the Λ polarizing fragmentation functions extracted from the full data fit and in blue the ones from the associated production data fit.

In Fig. 4.3 we show the $\Lambda/\bar{\Lambda}$ transverse polarization estimates. We have adopted the CTEQ6 set [54] for the unpolarized collinear proton PDFs, the AKK set [50] for the unpolarized $\Lambda/\bar{\Lambda}$ FFs, and the polarizing FF extracted from Belle data, presented in [41] and in the previous Chapter 3.

The polarization reaches values around 10% in size for both particles and is of the same magnitude as the one measured by the Belle Collaboration in e^+e^- annihilation processes. This could mean that it should be measurable at the future EIC. The estimates related to the full data fit and the associated production fit are consistent, leading to estimates of almost the same size.

The Λ polarization is positive for a small range of z_h and decreases until it reaches negative values. Notice that the range of z_h, for which it is positive, increases for larger values of x_B. On the other hand for the $\bar{\Lambda}$ polarization is always negative, keeping almost a constant value as z_h increases.

4.4. Conclusions

We have presented the kinematic configuration and the expressions of the cross section, within the helicity formalism, for the production of a transversely polarized spin-1/2 hadron in SIDIS processes, following the approach already discussed in [28]. By adopting the $\Lambda/\bar{\Lambda}$ polarizing FFs extracted in [41], we have given estimates for the $\Lambda/\bar{\Lambda}$ transverse polarization for different values of z_h and x_B compatible with those reachable at the future EIC. This kind of estimates will enable us to test, in future measurements, one of the main features of TMD factorization: the universality of the polarizing FF.

Chapter 5.

Transverse Λ polarization within the CSS framework and TMD evolution of the polarizing fragmentation function

5.1. Introduction

One of the critical issues on the analysis of Belle data discussed in Chapter 3 is that we have not used the proper factorization theorems and the evolution equations for both the double and the single-inclusive hadron production cross sections. Indeed, the extraction of the Λ polarizing FF has been made at fixed scale ($Q = 10.58\,\mathrm{GeV}$) and this, if from one side does not need any evolution effects, from the other side does not enables us to make predictions at different energy scales.

Moreover, and more relevant, in the analysis we used a simplified and phenomenological model to study the transversely polarized Λ, produced in a single-inclusive processes, due to the lack of a formalism, at that time, that could describe this kind of processes. In fact, unlike the cross section for double-hadron production in e^+e^- annihilation processes, only recently new advancements in

the TMD factorization of the cross section for single-inclusive production processes have appeared. Among them, we can mention the works of Refs. [38, 47], where the factorization has been formulated within an effective theory context, and the ones in Refs. [39, 40, 55], where the Collins-Soper-Sterman (CSS) formalims has been adopted.

The purpose of this Chapter is therefore to present a renewed analys of Belle data by exploiting the TMD framework in its full glory, paying special attention to scale evolution effects.

The Chapter is organised as follows: in Section 5.2 we present the main convolutions and the cross section for the production of a transversely polarized spin-1/2 hadron, in association with a light hadron, in e^+e^- annihilation processes, and how they can be expressed in the impact parameter space. Then in Section 5.3 we show how these convolutions can be treated within TMD factorization, by employing the CSS evolution equations. In Section 5.4 we summarize the results already presented in Ref. [38], giving expressions for the cross sections for single-inclusive hadron production and for the transverse polarization. All these results will be exploited to re-analyze the Belle data in Section 5.5, where we show the outcomes of the fits for the double-hadron production data alone and the combined fit of both data set, discussing our main findings. Lastly, in Section 5.6, we collect our concluding remarks.

5.2. Double hadron production

5.2.1. Kinematics and cross section

We start illustrating here the kinematics and the expression for the cross section for the process $e^+e^- \to h_1(S_1)h_2(S_2) + X$ where h_1 and h_2 are two spin-1/2 hadrons and $S_{1,2}$ are the spins of the hadrons. We consider the two hadrons as produced almost back-to-back, where the second hadron, h_2, moves along $\hat{z}_L$, in the laboratory frame, and the first one, h_1, moves in the opposite direction, with

a small transverse momentum $\boldsymbol{P}_{1T}$ with respect to the second hadron direction. This kinematical configuration is shown in Fig. 5.1, where $(\hat{\boldsymbol{x}}_L, \hat{\boldsymbol{y}}_L, \hat{\boldsymbol{z}}_L)$ are the unit vectors in the laboratory frame and $\boldsymbol{P}_{h_1}$ and $\boldsymbol{P}_{h_2}$ are the momenta of, respectively, the first and second hadron.

The kinematic configuration, in Fig. 5.1, has the unit vectors $(\hat{x}_L, \hat{y}_L, \hat{z}_L)$ in the Laboratory frame inverted with respect to those of the hadron frame adopted in [56] and in Chapter 2. This choice is made for the sake of semplicity, because we will employ directly the convolutions adopted in Ref. [18]. These ones, as we will see, have a straighter connection with the convolutions in $\boldsymbol{b}_T$-space.

Moreover, we define two planes: the *Lepton Plane*, determined by the leptons and the hadron h_2, and the *Production Plane*, determined by the momenta of the two observed hadron, $h_{1,2}$, at an angle ϕ_1 with respect to the *Lepton Plane*. In this

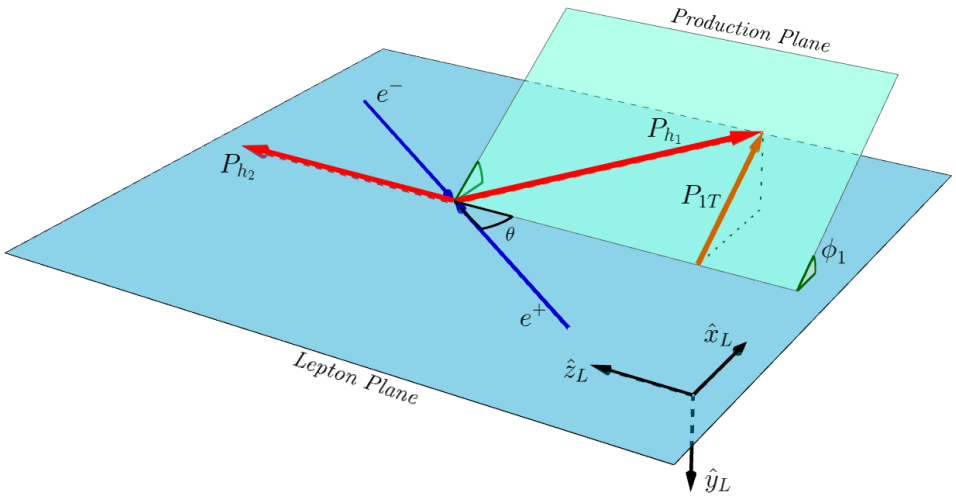

Figure 5.1.: Kinematics for the the hadron-frame configuration.

configuration, called "hadron frame", where one measures only the momenta of the two hadrons and the azimuthal distribution of the hadron h_1, the cross section

$$\frac{d\sigma^{e^+e^- \to h_1(S_1)h_2(S_2)\,X}}{d\cos\theta dz_1 dz_2 d^2\boldsymbol{q}_T} \tag{5.1}$$

depends on the transverse momentum of the virtual photon $\boldsymbol{q}_T$, and on the light-cone momentum fractions $z_{1,2}$ of the final-state hadrons. We recall that the transverse momentum of the photon, $\boldsymbol{q}_T$, is related to the transverse momentum of the first hadron, see Appendix F, as

$$\boldsymbol{P}_{1T} = -z_1 \boldsymbol{q}_T \,. \tag{5.2}$$

These two scaling variables, $z_{1,2}$, are defined as

$$z_1 = \frac{P_{h_1}^-}{k^-}, \qquad z_2 = \frac{P_{h_2}^+}{p^+}\,, \tag{5.3}$$

where k and p are the four-momenta of the first and second quark[1]. We can also introduce two further scaling variables that can be related to the light-cone momentum fraction: the energy fraction

$$z_{h_i} = \frac{P_i^0}{l^0} = z_i\left(1 + \frac{M_{h_i}^2}{2z_i^2 Q^2}\right), \tag{5.4}$$

often adopted in the experimental analyses, and the longitudinal momentum fraction

$$z_{p_i} = \frac{P_i^3}{l^3} = z_i\left(1 - \frac{M_{h_i}^2}{2z_i^2 Q^2}\right), \tag{5.5}$$

[1]For a generic four-vector a, we have $a^{\pm} = (a^0 \pm a^3)/\sqrt{2}$

where l is the four-momenta of the quark fragmenting into the hadron h_i, M_{h_i} is the mass of the hadron and Q is the center-of-mass energy of the process. It is such that $Q^2 = q^2$, with q the four momentum of the virtual photon. In both scaling variables we are keeping a kinematic power correction factor M^2/Q^2, usefull for the study of massive hadron production.

In general, the cross sections can be written as convolutions of two generic TMD fragmentation functions [18,56], as follows

$$\mathcal{F}[\omega D\bar{D}] = \sum_q e_q^2 \int d^2\boldsymbol{k}_T d^2\boldsymbol{p}_T\, \delta^{(2)}(\boldsymbol{k}_T + \boldsymbol{p}_T - \boldsymbol{q}_T)\, \omega(\boldsymbol{k}_T, \boldsymbol{p}_T) D(z_1, \boldsymbol{k}_\perp)\bar{D}(z_2, \boldsymbol{p}_\perp)\,, \tag{5.6}$$

where D and $\bar{D}$ are the fragmentation functions of the first and second hadron, $\boldsymbol{k}_T$ and $\boldsymbol{p}_T$ are the transverse momenta of the quark/antiquark with respect to the hadron h_1 and h_2. The two fragmentation functions depend explicitly on $\boldsymbol{k}_\perp$ and $\boldsymbol{p}_\perp$ that are the transverse momenta of the hadrons with respect to their own parent quarks. These two couples of transverse momenta are related, as shown in Appendix F, through the following relations:

$$\boldsymbol{k}_T = -\frac{\boldsymbol{k}_\perp}{z_{p_1}}; \qquad \boldsymbol{p}_T = -\frac{\boldsymbol{p}_\perp}{z_{p_2}}\,, \tag{5.7}$$

where z_p is the longitudinal momentum fractions of the hadron with respect to its fragmenting quark.

5.2.2. Transversely polarized hadron production

We now consider the associated production of a transversely polarized spin-1/2 hadron, h_1, with an unpolarized hadron, or meson, h_2. If the polarization is measured only as a function of the energy fractions of the two final state hadrons,

with the proper use of Eqs. (5.4) and (5.5) to relate the scaling variables, we can give it as the ratio of two $\boldsymbol{q}_T$-integrated convolutions

$$P_T^h(z_1, z_2) = -\sin(\phi_1 - \phi_{S_1}) \frac{\int d^2\boldsymbol{q}_T \, F_{TU}^{\sin(\phi_1 - \phi_{S_1})}}{\int d^2\boldsymbol{q}_T \, F_{UU}}, \tag{5.8}$$

that are defined as follows:

$$\begin{aligned} F_{UU} &= \mathcal{F}[D_1 \bar{D}_1] \\ F_{TU}^{\sin(\phi_1 - \phi_{S_1})} &= \mathcal{F}\left[\frac{\hat{\boldsymbol{h}} \cdot \boldsymbol{k}_T}{M_{h_1}} D_{1T}^{\perp} \bar{D}_1\right], \end{aligned} \tag{5.9}$$

where $D_1(z, k_\perp)$ is the unpolarized fragmentation function, $D_{1T}^{\perp}(z, k_\perp)$ is the polarizing fragmentation function, M_{h_1} is the mass of the first hadron and $\hat{\boldsymbol{h}} = \boldsymbol{P}_{1T}/|\boldsymbol{P}_{1T}|$. ϕ_{S_1} is the azimuthal angle of the spin of the hadron h_1 and, when the polarization is measured perpendicularly to the production plane, that is along the unit vector $\hat{\boldsymbol{n}}$ defined as:

$$\hat{\boldsymbol{n}} \equiv (\cos\phi_n, \sin\phi_n, 0) = \frac{-\boldsymbol{P}_{h_2} \times \boldsymbol{P}_{h_1}}{|\boldsymbol{P}_{h_2} \times \boldsymbol{P}_{h_1}|} = -\sin\phi_1 \hat{\boldsymbol{x}}_L + \cos\phi_1 \hat{\boldsymbol{y}}_L, \tag{5.10}$$

the factor entering Eq. (5.8) [56] simplifies as

$$-\sin(\phi_1 - \phi_{S_1}) = 1. \tag{5.11}$$

Generally, it is possible to define the TMD fragmentation functions in the conjugate $\boldsymbol{b}_T$-space as the Fourier transform of the fragmentation function in $\boldsymbol{k}_T$-space. By employing the integral definition of the Dirac's delta function

$$\delta^{(2)}(\boldsymbol{k}_T + \boldsymbol{p}_T - \boldsymbol{q}_T) = \int \frac{d^2\boldsymbol{b}_T}{(2\pi)^2}\, e^{i\boldsymbol{b}_T\cdot(\boldsymbol{k}_T+\boldsymbol{p}_T-\boldsymbol{q}_T)}\,, \tag{5.12}$$

we can write the convolutions, Eq. (5.9), in terms of the FF defined in the conjugate $\boldsymbol{b}_T$-space. The Fourier transform of the unpolarized FF is defined as:

$$\widetilde{D}_1(z, b_T) = \int d^2\boldsymbol{k}_T\, e^{i\boldsymbol{b}_T\cdot\boldsymbol{k}_T} D_1(z, k_\perp) = 2\pi \int dk_T\, k_T J_0(b_T k_T) D_1(z, k_\perp)\,, \tag{5.13}$$

where we have used Eq. (G.4), the integral definition of the J_0, the Bessel function of the first kind of order zero. With the above relation, the F_{UU} convolution in $\boldsymbol{b}_T$-space can be written as:

$$\begin{aligned} F_{UU} =& \mathcal{F}[D_1\bar{D}_1] = \mathcal{B}_0\Big[\widetilde{D}\widetilde{\bar{D}}\Big] \\ =& \sum_q e_q^2 \int \frac{db_T}{(2\pi)}\, b_T J_0(b_T\, q_T)\widetilde{D}_1(z_1, b_T)\widetilde{\bar{D}}_1(z_2, b_T)\,. \end{aligned} \tag{5.14}$$

Regarding the $\boldsymbol{b}_T$-space convolution of $F_{TU}^{\sin(\phi_1-\phi_S)}$, we first define the Fourier transform of the product of the polarizing fragmentation function with k_T^i, the i-th component of the quark transverse momentum with respect to the hadron direction, see Appendix G:

$$\int d^2\boldsymbol{k}_T\, \frac{k_T^i}{M_{h_1}} e^{i\boldsymbol{b}_T\cdot\boldsymbol{k}_T} D_{1T}^{\perp}(z_1, k_\perp) = i b_T^i M_{h_1} \widetilde{D}_{1T}^{\perp(1)}(z_1, b_T)\,. \tag{5.15}$$

Here we have introduced $\widetilde{D}_{1T}^{\perp(1)}(z_1, b_T)$, the first moment of the polarizing fragmentation function in $\boldsymbol{b}_T$-space, defined as

$$\widetilde{D}_{1T}^{\perp(1)}(z_1, b_T) = -\frac{2}{M_{h_1}^2}\frac{\partial}{\partial b_T^2}\widetilde{D}_{1T}^{\perp}(z_1, b_T)\,, \tag{5.16}$$

where $\widetilde{D}_{1T}^{\perp}(z_1, b_T)$ is the Fourier transform of the polarizing FF, Eq. (G.9). The first moment in $\boldsymbol{k}_T$-space, $D_{1T}^{\perp(1)}(z_1)$, defined as a weighted integral on $\boldsymbol{k}_\perp$,

$$D_{1T}^{\perp(1)}(z_1) = \int d^2\boldsymbol{k}_\perp \left(\frac{\boldsymbol{k}_\perp^2}{2z_1^2 M_h^2}\right) D_{1T}^{\perp}(z_1, k_\perp)\,, \tag{5.17}$$

can be related to that in $\boldsymbol{b}_T$-space, Eq. (5.16), as follows:

$$\lim_{b_T \to 0} \widetilde{D}_{1T}^{\perp(1)}(z_1, b_T) = \frac{1}{z_1^2} D_{1T}^{\perp(1)}(z_1)\,. \tag{5.18}$$

Employing the above equations and using the integral definition of the Bessel function J_1, Eq. (G.18), we can find the expression of $F_{TU}^{\sin(\phi_1 - \phi_{S_1})}$ in $\boldsymbol{b}_T$-space:

$$\begin{aligned} F_{TU}^{\sin(\phi_1-\phi_{S_1})} =& \mathcal{F}\left[\frac{\hat{\boldsymbol{h}}\cdot\boldsymbol{k}_T}{M_{h_1}} D_{1T}^{\perp} \bar{D}_1\right] = M_{h_1}\mathcal{B}_1\left[\widetilde{D}_{1T}^{\perp(1)}\widetilde{\bar{D}}_1\right] \\ =& M_{h_1}\sum_q e_q^2 \int \frac{db_T}{2\pi}\, b_T^2 J_1(q_T\, b_T)\widetilde{D}_{1T}^{\perp(1)}(z_1, b_T)\widetilde{\bar{D}}_1(z_2, b_T)\,. \end{aligned} \tag{5.19}$$

Finally, we can re-write the polarization of the final hadron, Eq. (5.8), along the $\hat{\boldsymbol{n}}$ direction as the ratio of the two convolutions in $\boldsymbol{b}_T$-space:

$$P_n^h(z_1, z_2) = \frac{\int d^2\boldsymbol{q}_T\, F_{TU}^{\sin(\phi_1-\phi_{S_1})}}{\int d^2\boldsymbol{q}_T\, F_{UU}} = \frac{M_{h_1}\int dq_T\, q_T\, d\phi_1\, \mathcal{B}_1\left[\widetilde{D}_{1T}^{\perp(1)}\widetilde{\bar{D}}_1\right]}{\int dq_T\, q_T\, d\phi_1\, \mathcal{B}_0\left[\widetilde{D}_1\widetilde{\bar{D}}_1\right]}\,, \tag{5.20}$$

where

$$\mathcal{B}_0\Big[\widetilde{D}_1\widetilde{\bar{D}}_1\Big] = \sum_q e_q^2 \int \frac{db_T}{2\pi}\, b_T J_0(b_T\, q_T)\widetilde{D}_1(z_1, b_T)\widetilde{\bar{D}}_1(z_2, b_T) \tag{5.21}$$

$$\mathcal{B}_1\Big[\widetilde{D}_{1T}^{\perp(1)}\widetilde{\bar{D}}_1\Big] = \sum_q e_q^2 \int \frac{db_T}{2\pi}\, b_T^2 J_1(q_T\, b_T)\widetilde{D}_{1T}^{\perp(1)}(z_1, b_T)\widetilde{\bar{D}}_1(z_2, b_T)\,. \tag{5.22}$$

The last step is to integrate both convolutions on $\boldsymbol{q}_T$. The integration over the azimuthal dependence $d\phi_1$ gives a factor of 2π that cancels in the polarization definition. Meanwhile for the radial part, since the only terms inside the convolutions that depend on q_T are the Bessel functions, we can separately integrate them from the rest of the terms, over the interval $[0, q_{T_{\max}}]$ (see below for the meaning of $q_{T_{\max}}$), obtaining the following results:

$$\int_0^{q_{T_{\max}}} dq_T\, q_T J_0(b_T\, q_T) = \frac{q_{T_{\max}}}{b_T} J_1(b_T\, q_{T_{max}}) \tag{5.23}$$

$$\begin{aligned}&\int_0^{q_{T_{\max}}} dq_T\, q_T J_1(b_T\, q_T)\\ =&\frac{\pi q_{T_{\max}}}{2b_T}\{J_1(b_T\, q_{T_{\max}})\boldsymbol{H}_0(b_T\, q_{T_{max}}) - J_0(b_T\, q_{T_{\max}})\boldsymbol{H}_1(b_T\, q_{T_{\max}})\}\end{aligned} \tag{5.24}$$

where $\boldsymbol{H}_{0,1}$ are the Struve functions of order zero and one respectively. To fulfill the conditions of validity for the TMD factorization [57] $q_{T_{\max}} \ll Q$. In the phenomenological analysis, Section 5.5, we will perform various tests adopting different values of the ratio $q_{T_{\max}}/Q$.

5.3. Double hadron production: CSS formalism

In this Section we extend the discussion of the convolutions, presented in Section 5.2, with the proper treatment of the scale evolution within the Collins-Soper-Sterman (CSS) approach and we will summarize the results presented

in [24, 57, 58]. According to the CSS formalism, the full form of the two convolutions, Eqs. (5.21), (5.22), is given by:

$$\mathcal{B}_0\left[\widetilde{D}_1\widetilde{\bar{D}}_1\right] = \sum_q e_q^2\,\mathcal{H}^{(e^+e^-)}(Q) \times \int \frac{db_T}{(2\pi)}\, b_T J_0(b_T\, q_T)\widetilde{D}_{1,q/h_1}(z_1, b_T; \zeta_1, \mu)\widetilde{\bar{D}}_{1,\bar{q}/h_2}(z_2, b_T; \zeta_2, \mu) \tag{5.25}$$

$$\mathcal{B}_1\left[\widetilde{D}_{1T}^{\perp(1)}\widetilde{\bar{D}}_1\right] = \sum_q e_q^2\,\mathcal{H}^{(e^+e^-)}(Q) \times \int \frac{db_T}{2\pi}\, b_T^2 J_1(q_T\, b_T)\widetilde{D}_{1T,q/h_1}^{\perp(1)}(z_1, b_T; \zeta_1, \mu)\widetilde{\bar{D}}_{1,\bar{q}/h_2}(z_2, b_T; \zeta_2, \mu) \tag{5.26}$$

where $\mathcal{H}^{(e^+e^-)}(Q)$ is the hard scattering part, for the massless on-shell process $e^+e^- \to q\bar{q}$, at the center-of-mass energy Q. This term is process dependent and in this particular case, for unpolarized $q\bar{q}$ production, the two convolutions share the same hard term. With respect to the previous expressions, the two fragmentation functions have two scale arguments: the renormalization scale μ and the ζ scale, that describes the effect of the recoil against the emission of soft gluons into an energy range determined approximately by μ and ζ. The fragmentation functions dependence on these two scales is regulated by the CSS and Renormalization Group (RG) equations.

5.3.1. Evolution equations for TMD fragmentation functions

The CSS evolution equation for the ζ dependence of the unpolarized TMD-FF has the following form:

$$\frac{\partial \ln \widetilde{D}_1(z_1, b_T; \zeta_1, \mu)}{\partial \ln \sqrt{\zeta_1}} = \widetilde{K}(b_T; \mu)\,, \tag{5.27}$$

where $\widetilde{K}$ is the CSS kernel and derived from the soft factor, that takes into account all the effects due to soft gluons [24]. It is independent of the flavor and spin of the quark, of the nature of the final-state hadron and of the light-cone momentum fraction z. However, since it depends on the color representation carried by the parton, it is different for quark and gluon FFs. The RG equation for the kernel is

$$\frac{d\widetilde{K}(b_T; \mu)}{d \ln \mu} = -\gamma_K(g(\mu))\,, \tag{5.28}$$

where the anomalous dimension γ_K has no dependence on b_T, since the UV divergences only arise from virtual graphs [24]. Meanwhile for the fragmentation function the RG equation is

$$\frac{d \ln \widetilde{D}_1(z_1, b_T; \zeta_1, \mu)}{d \ln \mu} = \gamma_D(g(\mu); \zeta_1/\mu^2)\,, \tag{5.29}$$

where, unlike the DGLAP equation, there is no convolution in the fraction z, although the anomalous dimension, γ_D, depends on it via the variable ζ [24]. Since the differentiation of the fragmentation function with respect to μ commutes with the differentiation with respect to ζ, we can finally obtain the energy dependence of γ_D, that is:

$$\gamma_D(g(\mu); \zeta_1/\mu^2) = \gamma_D(g(\mu); 1) - \frac{1}{2}\gamma_K(g(\mu)) \ln \frac{\zeta_1}{\mu^2}\,. \tag{5.30}$$

In addition, the anomalous dimensions and the CSS Kernel can be computed order by order perturbatively. Hence, by solving Eq. (5.27), we get the evolution from the reference scale $\zeta_{1,0}$ to the scale ζ_1 of the fragmentation functions:

$$\widetilde{D}_1(z_1, b_T; \zeta_1, \mu) = \widetilde{D}_1(z_1, b_T; \zeta_{1,0}, \mu) \exp\left\{\frac{1}{2}\widetilde{K}(b_T; \mu) \ln\frac{\zeta_1}{\zeta_{1,0}}\right\}. \tag{5.31}$$

This can be used in turn in Eq. (5.29) in order to get the evolution from the reference energy scale, μ_0, to μ, (notice that μ_0 has to be in the pertubative region so that the lowest-order perturbative calculations of γ_D and γ_K are reliable):

$$\begin{aligned}
\widetilde{D}_1(z_1, b_T; \zeta_1, \mu) &= \widetilde{D}_1(z_1, b_T; \zeta_1, \mu_0) \exp\left\{\int_{\mu_0}^{\mu} \frac{d\mu'}{\mu'} \gamma_D(g(\mu'); \zeta_1/\mu'^2)\right\} \\
&= \widetilde{D}_1(z_1, b_T; \zeta_1, \mu_0) \exp\left\{\int_{\mu_0}^{\mu} \frac{d\mu'}{\mu'} \left[\gamma_D(g(\mu'); 1) - \frac{1}{2}\gamma_K(g(\mu')) \ln\frac{\zeta_1}{\mu'^2}\right]\right\} \\
&= \widetilde{D}_1(z_1, b_T; \zeta_{1,0}, \mu_0) \exp\left\{\frac{1}{2}\widetilde{K}(b_T; \mu_0) \ln\frac{\zeta_1}{\zeta_{1,0}}\right\} \\
&\times \exp\left\{\int_{\mu_0}^{\mu} \frac{d\mu'}{\mu'} \left[\gamma_D(g(\mu'); 1) - \frac{1}{2}\gamma_K(g(\mu')) \ln\frac{\zeta_1}{\mu'^2}\right]\right\}.
\end{aligned} \tag{5.32}$$

The dependence on ζ_1 involves the function $\widetilde{K}$, implying an energy dependence on the shape of the transverse momentum distribution. Moreover, the function $\widetilde{D}_1$, at its reference scales $\zeta_{1,0}$ and μ_0, can be thought as the Fourier transform of an intrinsic transverse momentum distribution of the hadron with respect to its parent parton. The term that multiplies this function, cointaining the CSS Kernel, mimics the effect of the energy-dependent recoil against the emission of soft gluons.

The full solution of the evolution equations in terms of the anomalous dimensions and the CSS Kernel, and all the results above, can also be extended to the $\widetilde{D}_{1T}^{\perp(1)}$ function [24].

5.3.2. Small-b_T expansion

The first term of the last line in Eq. (5.32) is the TMD FF at the reference energy scale, and it is related to the short distance and small $\boldsymbol{b}_T$ behaviour of D_1 and therefore computable in perturbation theory. So at small-$\boldsymbol{b}_T$, the unpolarized TMD fragmentation function can be expressed in terms of the corresponding integrated fragmentation function $d_{j/h}(z;\mu)$ using an Operator Product Expansion (OPE):

$$\begin{aligned}&\widetilde{D}_{1,q/h}(z_1, b_T; \zeta_{1,0}, \mu_0)\\ &= \sum_j \int_{z_1}^1 \frac{d\hat{z}}{\hat{z}^{3-2\epsilon}} \widetilde{C}_{j/q}(z_1/\hat{z}, b_T; \zeta_{1,0}, \mu_0, g(\mu_0))\, d_{j/h}(\hat{z};\mu_0) + \mathcal{O}[(mb_T)^p]\,,\end{aligned} \tag{5.33}$$

where the error term is suppressed by some power of the transverse position. The sum is over all parton types j , including gluons and antiquarks. When b_T is small, the coefficient function $\widetilde{C}_{j/q}$ can be expanded in perturbation theory and calculated from Feynmann graphs with external on-shell partons of type j, with a double-counting subtraction in order to cancel all collinear contributions [24]. The lowest-order coefficient is unitary:

$$\widetilde{C}_{j/q}(z_1/\hat{z}, b_T; \zeta_1, \mu, g(\mu)) = \delta_{jq}\delta(z_1/\hat{z} - 1) + \mathcal{O}(g^2)\,. \tag{5.34}$$

An OPE of the same kind applies also to the other collinear fragmentation functions, e.g G_{1L} and H_{1T}, but they generally have different coefficient functions beyond lowest-order. For the other, polarization-dependent, TMD fragmentation

functions, like the Collins and the (single)polarizing fragmentation functions, it is possible to generalize the OPE involving quantities that are associated with matrix elements of higher-twist operators [59], like in the case of the Sivers function with the Qiu-Sterman function [60, 61].

5.3.3. Matching perturbative and non-perturbative $\mathbf{b}_T$ dependence for TMD fragmentation

In order to combine information on the $\boldsymbol{b}_T$ dependence coming from perturbative calculations, valid at small $\boldsymbol{b}_T$, and the one from the non-perturbative part, that must be extracted from experimental data, it is necessary to introduce a matching procedure. Note that the perturbatively calculable functions, like the CSS Kernel and the anomalous dimensions, appear in an exponent, thus any error in a perturbative calculation can be magnified by large logarithms.

Firstly it is necessary to choose a parameter $b_{\max}$, representing the maximum distance at which perturbation theory is to be trusted; it could be taken within an interval of $[0.5 - 1.5]\,\mathrm{GeV}^{-1}$. Then we define a function $\boldsymbol{b}_*(\boldsymbol{b}_T)$ with the properties that for small b_T it reduces to $\boldsymbol{b}_T$, and that at larger b_T it is not bigger than $b_{\max}$:

$$\boldsymbol{b}_*(\boldsymbol{b}_T) \to \begin{cases} b_T & b_T \ll b_{\max} \\ b_{\max} & b_T \gg b_{\max} \end{cases} . \tag{5.35}$$

A standard choice is the following:

$$\boldsymbol{b}_* = \frac{\boldsymbol{b}_T}{\sqrt{1 + b_T^2/b_{\max}^2}} . \tag{5.36}$$

Then one re-defines the CSS Kernel as:

$$\widetilde{K}(b_T;\mu) = \widetilde{K}(b_*;\mu) - g_K(b_T;b_{\max})\,, \tag{5.37}$$

where $\widetilde{K}(b_*;\mu)$ is always defined in a region where perturbation theory is appropriate and the correction term g_K is only important at large b_T. This last term, g_K, which has to be fitted to data in a phenomenological analysis, is a functions of b_T and can depend explicitly or not on the parameter $b_{\max}$. Since it is the difference of $\widetilde{K}$ calculated at two values of its position argument, it is RG invariant and has to vanish as $b_T \to 0$.

If we want to match the perturbative and non-perturbative part of the unpolarized fragmentation function $\widetilde{D}_1$, we can use $\boldsymbol{b}_*$ defined in Eq. (5.43). Generalizing Eq. (5.37), it is possibile to introduce an intrinsically non-perturbative part with the following decomposition:

$$\begin{aligned}
&\widetilde{D}_{1,q/h}(z_1,b_T;\zeta_1,\mu)\\
=&\widetilde{D}_{1,q/h}(z_1,b_*;\zeta_1,\mu)\left[\frac{\widetilde{D}_{1,q/h}(z_1,b_T;\zeta_1,\mu)}{\widetilde{D}_{1,q/h}(z_1,b_*;\zeta_1,\mu)}\right]\\
=&\widetilde{D}_{1,q/h}(z_1,b_*;\zeta_1,\mu)\exp\left[-g_{q/h}(z_1,b_T;b_{\max}) - g_K(b_T;b_{\max})\ln\frac{\sqrt{\zeta_1}}{\sqrt{\zeta_{1,0}}}\right]\\
=&\widetilde{D}_{1,q/h}(z_1,b_*;\zeta_1,\mu)\exp\left[-g_{q/h}(z_1,b_T;b_{\max}) - g_K(b_T;b_{\max})\ln\frac{\sqrt{\zeta_1}z_1}{M_{h_1}}\right].
\end{aligned} \tag{5.38}$$

In the second line we can find $\widetilde{D}(b_*)$, that can now be calculated perturbatively, and in the last line we have used the reference value $\zeta_{1,0} = M_{h_1}^2/z_1^2$ [24]. By employing Eq. (5.32), the anomalous dimensions, γ_D and γ_K, cancel between numerator and denominator. Meanwhile it survives only g_K, the correction and

"non-perturbative" term of $\widetilde{K}$. The remaining factor, written as an exponential, $e^{-g_{q/h}}$, that is introduced with the following definition [58]

$$e^{-g_{q/h}(z_1,b_T;b_{\max})} = \frac{\widetilde{D}_{1,q/h}(z_1,b_T;\zeta_1,\mu)}{\widetilde{D}_{1,q/h}(z_1,b_*;\zeta_1,\mu)} e^{g_K(b_T;b_{\max})\ln\sqrt{\zeta_1}/\sqrt{\zeta_{1,0}}}, \tag{5.39}$$

can be interpreted as the non-perturbative part of the intrinsic transverse momentum distribution. Both g_K and $g_{q/h}$ vanish approximately as b_T^2 at small b_T [24], and become significant when b_T approaches $b_{\max}$ and beyond. Both functions are independent of ζ and μ, being invariant under the application of the CSS and RG equations; moreover they depend on the choice of the value of $b_{\max}$. But despite this, the full TMD fragmentation function and the function $\widetilde{K}$ are independent of $b_{\max}$ and of the use of the b_* prescription. The flavor and z dependences of g_K and $g_{q/h}$ follow from those of the corresponding parent functions, respectively $\widetilde{K}$ and the TMD fragmentation functions [58]. Since $\widetilde{K}$ is independent of the quark's and hadron's flavor, polarization and fraction z, so is g_K. The same, of course, is not true in general for the TMD fragmentation functions and therefore for $e^{-g_{q/h}}$. In addition, this last term is usually written as $M_D(b_T;b_{\max})$ or $D_{NP}(b_T;b_{\max})$, a generic function of b_T, since it could assume also a non-exponential functional form, still preserving its properties, and the fact that it vanishes like b_T^2 at small b_T; it is usually referred to as the non-perturbative model of the fragmentation function, and within a parton model, can be seen as the Fourier transform of the transverse momentum distribution. As already said for the g_K, the function M_D can depend explicitly or not on the parameter $b_{\max}$. In a more general way, the phenomenological extraction of both non-perturbative functions is affected by the choice of the $b_{\max}$ value.

To use the perturbative small-b_T result from Eq. (5.33), it is necessary to evolve the $\widetilde{D}$ term in Eq. (5.38), with the b_* prescription, from a region where no large kinematic ratios appear in the coefficient function $\widetilde{C}$, whose logarithms would prevent the effective use of perturbation theory [24]. The standard choice is to replace μ_0 by:

$$\mu_b = \frac{C_1}{b_*(b_T)}\,, \tag{5.40}$$

where $C_1 = 2e^{-\gamma_E}$ (where γ_E is the Euler-Mascheroni constant), and replace the reference value $\zeta_{1,0}$ by μ_b^2. Then the TMD fragmentation function can be written as:

$$\begin{aligned}
&\widetilde{D}_{1,q/h}(z_1, b_T; \zeta_1, \mu) \\
&= \sum_j \int_{z_1}^1 \frac{d\hat{z}}{\hat{z}^{3-2\epsilon}} \widetilde{C}_{j/q}(z_1/\hat{z}, b_*; \mu_b^2, \mu_b, g(\mu_b))\, d_{j/h}(\hat{z}; \mu_b) \\
&\times M_D(b_T, z_1; b_{\max}) \exp\left\{ - g_K(b_T; b_{\max}) \ln \frac{\sqrt{\zeta_1} z_1}{M_{h_1}} \right\} \\
&\times \exp\left\{ \frac{1}{2} \widetilde{K}(b_*; \mu_b) \ln \frac{\zeta_1}{\mu_b^2} + \int_{\mu_b}^{\mu} \frac{d\mu'}{\mu'} \left[\gamma_D(g(\mu'); 1) - \frac{1}{2} \gamma_K(g(\mu')) \ln \frac{\zeta_1}{\mu'^2} \right] \right\}.
\end{aligned} \tag{5.41}$$

Finally, we need to modify the $\boldsymbol{b}_T$ definition using [62]:

$$b_c(b_T) = \sqrt{b_T^2 + b_{\min}^2}\,, \tag{5.42}$$

where $b_{\min} = 2e^{-\gamma_E}/Q$ and decreases like $1/Q$ in contrast to $b_{\max}$ which remains fixed. This definition reduces to b_T when $b_T \gg 1/Q$ but it is of order $1/Q$ when b_T is small, thereby providing a cutoff at small b_T. Naturally b_* has to be replaced by:

$$b_*(b_c(b_T)) = \sqrt{\frac{b_T^2 + b_{\min}^2}{1 + b_T^2/b_{\max}^2 + b_{\min}^2/b_{\max}^2}}\,, \tag{5.43}$$

which has the following behaviour:

$$b_*(b_c(b_T)) \to \begin{cases} b_{\min} & b_T \ll b_{\min} \\ b_T & b_{\min} \ll b_T \ll b_{\max} \\ b_{\max} & b_T \gg b_{\max} \end{cases}\,. \tag{5.44}$$

Lastly, instead of μ_b, we use the new scale:

$$\bar{\mu}_b(b_c(b_T)) = \frac{C_1}{b_*(b_c(b_T))}\,, \tag{5.45}$$

implying a maximum cutoff on the renormalization scale equal to $\bar{\mu}_b \simeq C_1/b_{\min}$. Recollecting all the above results we can now write the TMD fragmentation function, Eq. (5.41), employing the new definitions of $\boldsymbol{b}_T$, as:

$$\begin{aligned}
&\widetilde{D}_{1,q/h}(z_1, b_c(b_T); \zeta_1, \mu) \\
&= \sum_j \int_{z_1}^1 \frac{d\hat{z}}{\hat{z}^{3-2\epsilon}} \widetilde{C}_{j/q}(z_1/\hat{z}, b_*(b_c(b_T)); \bar{\mu}_b^2, \bar{\mu}_b, g(\bar{\mu}_b))\, d_{j/h}(\hat{z}; \bar{\mu}_b) \\
&\times M_D(b_c(b_T), z_1; b_{\max}) \exp\left\{ - g_K(b_c(b_T); b_{\max}) \ln \frac{\sqrt{\zeta_1} z_1}{M_{h_1}} \right\} \\
&\times \exp\left\{ \frac{1}{2} \widetilde{K}(b_*; \bar{\mu}_b) \ln \frac{\zeta_1}{\bar{\mu}_b^2} + \int_{\bar{\mu}_b}^{\mu} \frac{d\mu'}{\mu'} \left[\gamma_D(g(\mu'); 1) - \frac{1}{2} \gamma_K(g(\mu')) \ln \frac{\zeta_1}{\mu'^2} \right] \right\},
\end{aligned} \tag{5.46}$$

where, in addition, we will perform the following substitutions $\zeta_1 = Q^2$ and $\mu = Q$, leading to:

$$\begin{aligned}
&\widetilde{D}_{1,q/h}(z_1, b_c(b_T); Q^2, Q) \\
&= \sum_j \int_{z_1}^1 \frac{d\hat{z}}{\hat{z}^{3-2\epsilon}} \widetilde{C}_{j/q}(z_1/\hat{z}, b_*(b_c(b_T)); \bar{\mu}_b^2, \bar{\mu}_b, g(\bar{\mu}_b))\, d_{j/h}(\hat{z}; \bar{\mu}_b) \\
&\times M_D(b_c(b_T), z_1; b_{\max}) \exp\left\{ - g_K(b_c(b_T); b_{\max}) \ln \frac{Q z_1}{M_{h_1}} \right\} \\
&\times \exp\left\{ \frac{1}{2} \widetilde{K}(b_*; \bar{\mu}_b) \ln \frac{Q^2}{\bar{\mu}_b^2} + \int_{\bar{\mu}_b}^{Q} \frac{d\mu'}{\mu'} \left[\gamma_D(g(\mu'); 1) - \frac{1}{2} \gamma_K(g(\mu')) \ln \frac{Q^2}{\mu'^2} \right] \right\}.
\end{aligned} \tag{5.47}$$

5.3.4. Convolutions

Thanks to the evolution equations and the matching procedure, we can write the full form of the convolutions in Eqs. (5.25) and (5.26). For the convolution $\mathcal{B}_0$ we have:

$$\begin{aligned}
&\mathcal{B}_0\left[\widetilde{D}\widetilde{\bar{D}}\right] \\
&= \mathcal{H}^{(e^+e^-)}(Q) \sum_q e_q^2 \int \frac{db_T}{(2\pi)}\, b_T J_0(b_T\, q_T) \widetilde{D}(z_1, b_T; \zeta_1, \mu) \widetilde{\bar{D}}(z_2, b_T; \zeta_2, \mu) \\
&= \frac{\mathcal{H}^{(e^+e^-)}(Q)}{z_1^2 z_2^2} \sum_q e_q^2 \int \frac{db_T}{(2\pi)}\, b_T J_0(b_T\, q_T)\, d_{q/h_1}(z_1; \bar{\mu}_b) d_{\bar{q}/h_2}(z_2; \bar{\mu}_b) \\
&\times M_{D_1}(b_c(b_T); b_{\max})\, M_{D_2}(b_c(b_T); b_{\max}) \exp\left\{ - g_K(b_c(b_T); b_{\max}) \ln\left(\frac{Q^2 z_1 z_2}{M_{h_1} M_{h_2}} \right) \right\} \\
&\times \exp\left\{ \widetilde{K}(b_*; \bar{\mu}_b) \ln \frac{Q^2}{\bar{\mu}_b^2} + \int_{\bar{\mu}_b}^{Q} \frac{d\mu'}{\mu'} \left[2\gamma_D(g(\mu'); 1) - \gamma_K(g(\mu')) \ln \frac{Q^2}{\mu'^2} \right] \right\},
\end{aligned} \tag{5.48}$$

where in the second line we have used the lowest-order coefficient, Eq. (5.34), of the OPE expression for both the fragmentation functions, and we have adopted the notation M_{D_j} for the non-perturbative b_T-models for the two unpolarized fragmentation functions. Similarly, for the convolution $\mathcal{B}_1$ we have:

$$
\begin{aligned}
&\mathcal{B}_1\left[\widetilde{D}_{1T}^{\perp(1)}\widetilde{\bar{D}}_1\right] \\
=&\mathcal{H}^{(e^+e^-)}(Q)\sum_q e_q^2\int\frac{db_T}{(2\pi)}\,b_T^2 J_1(b_T\,q_T)\widetilde{D}_{1T}^{\perp(1)}(z_1,b_T;\zeta_1,\mu)\widetilde{\bar{D}}(z_2,b_T;\zeta_2,\mu) \\
=&\frac{\mathcal{H}^{(e^+e^-)}(Q)}{z_1^2 z_2^2}\sum_q e_q^2\int\frac{db_T}{(2\pi)}\,b_T^2 J_1(b_T\,q_T)\widetilde{D}_{1T}^{\perp(1)}(z_1;\bar{\mu}_b)\,d_{\bar{q}/h_2}(z_2;\bar{\mu}_b) \\
\times\, &M_D^{\perp}(b_c(b_T);b_{\max})\,M_{D_2}(b_c(b_T);b_{\max})\exp\left\{-g_K(b_c(b_T);b_{\max})\ln\left(\frac{Q^2 z_1 z_2}{M_{h_1}M_{h_2}}\right)\right\} \\
\times\, &\exp\left\{\widetilde{K}(b_*;\bar{\mu}_b)\ln\frac{Q^2}{\bar{\mu}_b^2}+\int_{\bar{\mu}_b}^{Q}\frac{d\mu'}{\mu'}\left[2\gamma_D(g(\mu');1)-\gamma_K(g(\mu'))\ln\frac{Q^2}{\mu'^2}\right]\right\},
\end{aligned}
\tag{5.49}
$$

where again we have used the lowest-order coefficient for the OPEs and $M_D^{\perp}$ as the non-perturbative function for the polarizing fragmentation function.

The last lines of Eq. (5.48) and (5.49) are usually referred to as perturbative Sudakov factors and, as explained above, they can be computed analytically. The anomalous dimension of the fragmentation functions at order $\alpha_s(\mu)$, with $\alpha_s(\mu) = g^2(\mu)/4\pi$, is [62]:

$$
\gamma_D(\alpha_s(\mu);\zeta_1/\mu^2) = 4C_F\left(\frac{3}{2}-\ln\frac{\zeta_1}{\mu^2}\right)\left(\frac{\alpha_s(\mu)}{4\pi}\right)+\mathcal{O}(\alpha_s^2(\mu))\,, \tag{5.50}
$$

where $C_F = 4/3$. Meanwhile the anomalous dimension of the CSS Kernel $\widetilde{K}$ at one-loop order is:

$$\gamma_K(\alpha_s(\mu)) = 8C_F\left(\frac{\alpha_s(\mu)}{4\pi}\right) + \mathcal{O}(\alpha_s^2(\mu))\,, \tag{5.51}$$

with $\widetilde{K} = 0$ at the first order. For the running coupling [62] we use the form:

$$\alpha_s(\mu) = \frac{A}{2\ln(\mu/\Lambda_{QCD})}\,, \tag{5.52}$$

with

$$A = \frac{1}{\beta_0} = \frac{12\pi}{33 - 2n_f}\,, \tag{5.53}$$

where n_f is the number of active flavors and the used value of Λ_{QCD} is 0.2123 GeV. With these results we can then analytically integrate the perturbative Sudakov factor, obtaining:

$$\begin{aligned}&\widetilde{K}(b_*;\bar{\mu}_b)\ln\frac{Q^2}{\bar{\mu}_b^2} + \int_{\bar{\mu}_b}^{Q}\frac{d\mu'}{\mu'}\left[2\gamma_D(g(\mu');1) - \gamma_K(g(\mu'))\ln\frac{Q^2}{\mu'^2}\right]\\ =&\frac{2A}{\pi}\left[\ln\left(\frac{\ln(Q/\Lambda_{QCD})}{\ln(\bar{\mu}_b/\Lambda_{QCD})}\right) - \frac{4}{3}\ln(Q/\Lambda_{QCD})\ln\left(\frac{\ln(Q/\Lambda_{QCD})}{\ln(\bar{\mu}_b/\Lambda_{QCD})}\right) + \frac{4}{3}\ln(Q/\bar{\mu}_b)\right].\end{aligned} \tag{5.54}$$

5.3.5. Non-perturbative models: $g_K(b_T; b_{\max})$

The non-perturbative functions, introduced in the previous subsection, cannot be computed from first principles; therefore, they must be obtained through a

phenomenological analysis. However, as shown in [58], it is possible to extract some of their properties from perturbative calculations. Indeed, we have that the lowest-order formula for $\widetilde{K}$ gives:

$$g_K(b_T, b_{\max}) = \frac{\alpha_s(C_1/b_*)C_F}{\pi} \ln(1 + b_T^2/b_{\max}^2)\,, \tag{5.55}$$

that has a b_T^2 behaviour at small b_T, but a slower rise above $b_{\max}$. A similar functional form has been used and extracted in [62, 63] with the following expression

$$g_K(b_T; b_{\max}) = g_2 \ln\left(\frac{b_T}{b_*}\right), \tag{5.56}$$

with an extracted value of $g_2 = 0.84$. For large b_T values, Eq. (5.55) is not expected to be an accurate parametrization of $g_K(b_T)$. Indeed, it is an extrapolation of a lowest-order perturbative calculation and it depends strongly on $b_{\max}$ at large b_T. The b_T^2 behaviour at small b_T can be found expanding Eq. (5.55) at small b_T, obtaining:

$$g_K(b_T; b_{\max}) = \frac{C_F}{\pi}\frac{b_T^2}{b_{\max}^2}\alpha_s(\mu_{b_*})\,, \tag{5.57}$$

with an explicit quadratic form of the g_K function. This justifies the use of the following expression:

$$g_K(b_T; b_{\max}) = \frac{g_2 b_T^2}{2}\,, \tag{5.58}$$

employed and fitted to data by BLNY [64] and KN [65] where they found, respectively, a value of $g_2 = 0.68\,\mathrm{GeV}^2$, with $b_{\max} = 0.5\,\mathrm{GeV}^{-1}$, and a value of $g_2 = 0.18\,\mathrm{GeV}^2$, with $b_{\max} = 1.5\,\mathrm{GeV}^{-1}$.

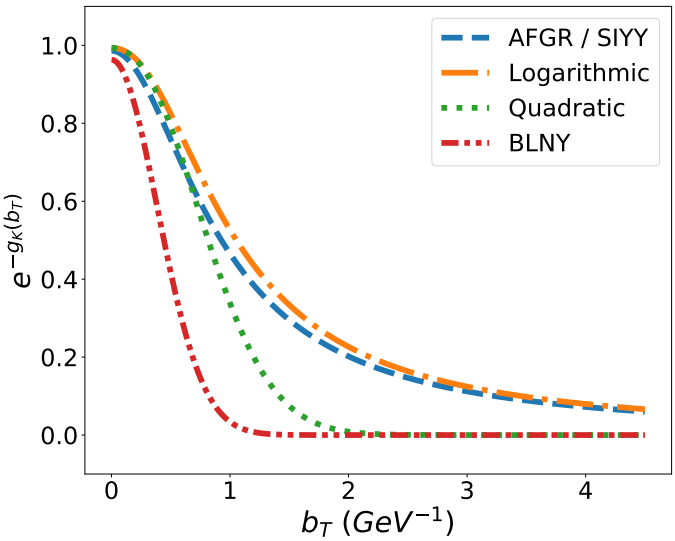

Figure 5.2.: Graphical representation of the different form of the g_K non-perturbative function listed in Eq. (5.60).

Since the real non-perturbative physics is at larger b_T, one wants to extract $g_K(b_T; b_{\max})$ with a more general parametrization and be sure that the data used to extract it are sensitive to high values of b_T. Moreover, the complete TMD factorization formalism is $b_{\max}$ independent and, in principle, optimized fits should not depend on its choice. A proposed functional form [58] that is $b_{\max}$ independent in the asymptotic small and large-b_T limit, and that goes to a constant at large b_T is:

$$g_K(b_T; b_{\max}) = g_0(b_{\max})\left(1 - \exp\left[-\frac{C_F \alpha_s(\mu_{b_*}) b_T^2}{\pi g_0(b_{\max}) b_{\max}^2}\right]\right). \tag{5.59}$$

In the phenomenological analysis, discussed in Section 5.5, we will employ the following functional forms of the non-perturbative function, g_K, see Fig. 5.2:

$$\begin{aligned}
g_K(b_T; b_{\max}) &= \frac{g_2 b_T^2}{2}\,; \quad g_2 = 0.68\,\mathrm{GeV}^2 \qquad \text{BLNY} \\
g_K(b_T; b_{\max}) &= \frac{C_F}{\pi}\frac{b_T^2}{b_{\max}^2}\alpha_s(\mu_{b_*}) \qquad \text{Quadratic} \\
g_K(b_T; b_{\max}) &= \frac{\alpha_s(C_1/b_*)C_F}{\pi}\ln(1 + b_T^2/b_{\max}^2) \qquad \text{Logarithmic} \\
g_K(b_T; b_{\max}) &= g_2 \ln\left(\frac{b_T}{b_*}\right) \quad g_2 = 0.84 \qquad \text{AFGR / SIYY}\,.
\end{aligned} \tag{5.60}$$

Thanks to their universality they can be used to predict observables or be supportive in the extraction of other non-perturbative functions, in processes like e^+e^- collisions, Semi-inclusive DIS and Drell-Yan.

5.3.6. Non-perturbative models: $M_D(b_T; b_{\max})$ and $M_D^\perp(b_T; b_{\max})$

In [58] it has been shown that the arguments for the approximately quadratic behaviour of $g_K(b_T)$ at small b_T are also valid for the function $g_{q/h}(b_T)$, and this corresponds, after an exponentiation, to a Gaussian model for the TMD fragmentation function:

$$M_D(b_T; b_{\max}) = \exp\left(-\frac{a b_T^2}{2}\right). \tag{5.61}$$

Hence this justifies the use of the following parameterization:

$$M_D(b_T; b_{\max}) = \exp\left(-\frac{\langle p_\perp^2\rangle b_T^2}{4 z_p^2}\right), \tag{5.62}$$

where $\langle p_\perp^2 \rangle$ is the Gaussian width in the $\boldsymbol{p}_\perp$-space[2], where this model corresponds to the following expression:

$$\widetilde{M}_D(p_\perp) = \frac{e^{-p_\perp^2/\langle p_\perp^2 \rangle}}{\pi \langle p_\perp^2 \rangle}. \tag{5.63}$$

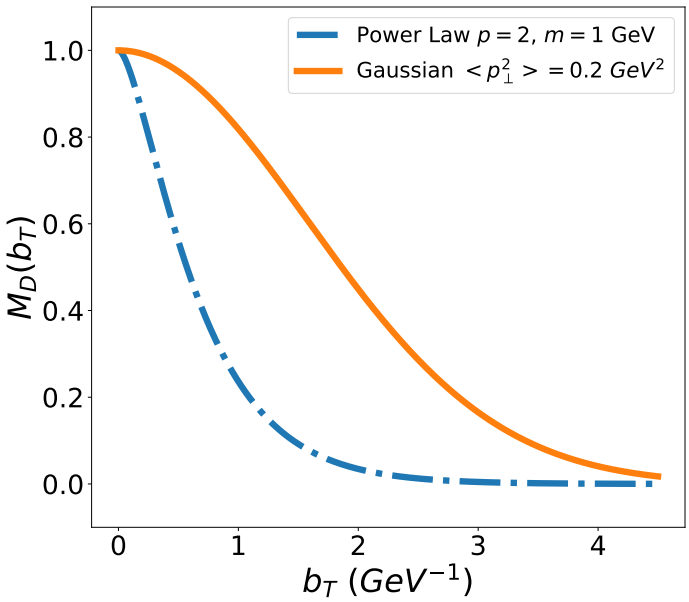

Figure 5.3.: Representation of non-perturbative hadronic models for $M_D(b_T)$: in orange (solid line) the Gaussian model and in blue (dash-dotted line) the Power-Law model.

The commonly assumed quadratic behaviour of $g_K(b_T)$ and the Gaussian behaviour of the TMD fragmentation function can only be a valid approximation, at best, for moderate b_T. Appropriate parametrizations for the non-perturbative large-b_T behaviour of TMD fragmentation functions and of the CSS Kernel need to be inferred from the general principles of quantum field theory [58], that suggest an exponentially decaying behaviour for large b_T. From many one-loop

[2]This space is equivalent to the $\boldsymbol{k}_\perp$-space used in previous sections.

calculations of the TMD quantities of interest, we know that a typical integral giving the proper b_T dependence is of the form

$$\int d^2\boldsymbol{p}_T \frac{e^{i\boldsymbol{p}_T\cdot\boldsymbol{b}_T}}{p_T^2+m^2}\,. \tag{5.64}$$

One possible functional form that generalizes, in $\boldsymbol{b}_T$-space, the Fourier transform of the previous equation, and preserves the quadratic behaviour at small b_T, used in [39, 66], is the following:

$$M_D(b_T,p,m;b_{\max}) = \frac{2^{2-p}}{\Gamma(p-1)}\,(b_T m/z_p)^{p-1}K_{p-1}(b_T m/z_p)\,, \tag{5.65}$$

where K_{p-1} is a Bessel function of the second kind, with the condition $p>1$. Its Fourier transform in $\boldsymbol{p}_\perp$-space is given by:

$$\widetilde{M}_D(p_\perp) = \frac{\Gamma(p)}{\pi\Gamma(p-1)}\frac{m^{2(p-1)}}{(p_\perp^2+m^2)^p}\,. \tag{5.66}$$

These two functional forms, Eqs. (5.62) and (5.65), shown in Fig. 5.3, will be used to parametrize the non-perturbative component of the polarizing fragmentation function in the phenomenological analysis presented in Section 5.5.

5.4. Single-inclusive hadron production and polarization

We summarize here the kinematics and give the expression of the cross section, already presented in [38, 67], for the process $e^+e^-\to h_1(S_{h_1})+X$, that is the single-inclusive production of an unpolarized or transversely polarized spin-1/2

hadron in e^+e^- annihilations. In this configuration, shown in Fig. 5.4, the hadron is produced with a certain energy fraction :

$$z_{h_1} = \frac{2P_{h_1} \cdot q}{Q^2}, \tag{5.67}$$

where q is the virtual photon four-momentum and $Q^2 = q^2 = s$. The hadron has transverse momentum $\boldsymbol{j}_\perp$ measured with respect to the thrust axis $\hat{\boldsymbol{T}}$, defined as the vector, $\hat{\boldsymbol{T}}$, which maximizes the thrust variable T

$$T = \frac{\sum_i |\boldsymbol{p}_i \cdot \hat{\boldsymbol{T}}|}{\sum_i |\boldsymbol{p}_i|}, \tag{5.68}$$

where $\boldsymbol{p}_i$ represent the three-momenta of the measured final-state particles. This is referred to as the *thrust frame* configuration. We have, moreover, that the full phase space is divided into two hemispheres by the plane perpendicular to the thrust axis at the e^+e^- interaction point.

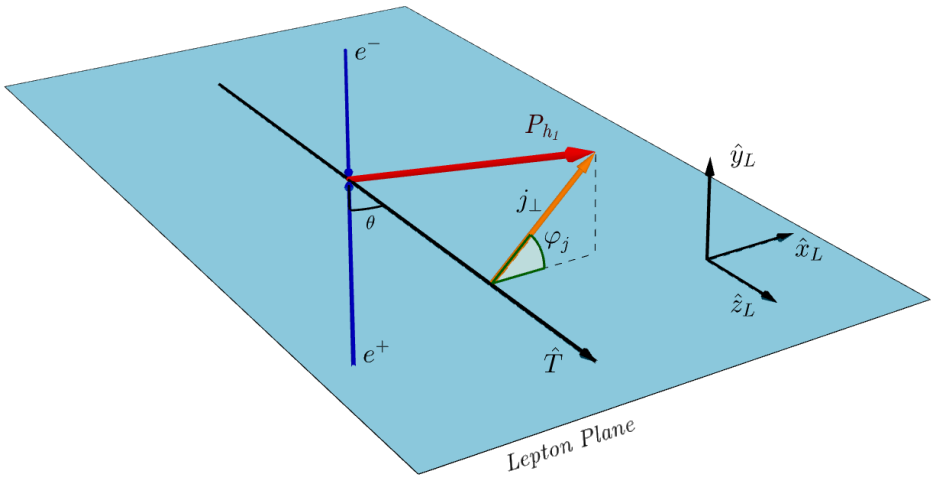

Figure 5.4.: Kinematics of the *thrust frame* configuration.

For this process, the single-inclusive measurement is carried out only in the hemisphere that contains the thrust axis, while the other hemisphere is fully inclusive. Thus, only soft radiation which is emitted into the hemisphere containing the thrust axis will contribute to $\boldsymbol{j}_\perp$. Indeed the factorized expression, used in [67] and given at next-to-leading logarithm accuracy (NLL) in [38], introduces the hemisphere soft function S_{hemi}, that is different from the typical soft function S usually defined to describe the almost back-to-back double hadron production in e^+e^- collisions. On the other hand, as demonstrated in [38], since S_{hemi} at one-loop order accuracy is equal to $\sqrt{S}$, both the unpolarized and polarizing FFs, in the single-inclusive process, are the same FFs that appear in the double-hadron production process. The cross section for the unpolarized hadron production is then given by:

$$\begin{aligned}\frac{d\sigma}{dz_1 d^2\boldsymbol{j}_\perp} =& \frac{\sigma_0}{z_1^2}\sum_q e_q^2 \int \frac{db_T}{(2\pi)}\, b_T J_0(b_T\, q_T) d_{q/h_1}(z_1;\bar{\mu}_b)\, U_{NG}(\bar{\mu}_b, Q) \\ &\times M_{D_1}(b_c(b_T);b_{\max})\, \exp\left\{ - g_K(b_c(b_T);b_{\max}) \ln\left(\frac{Qz_1}{M_{h_1}}\right)\right\} \\ &\times \exp\left\{ \tilde{K}(b_*;\bar{\mu}_b)\ln\frac{Q}{\bar{\mu}_b} + \int_{\bar{\mu}_b}^{Q}\frac{d\mu'}{\mu'}\left[\gamma_D(g(\mu'),1) - \gamma_K(g(\mu'))\ln\frac{Q}{\mu'}\right]\right\},\end{aligned} \tag{5.69}$$

where z_1 is the hadron light-cone momentum fraction, related to z_{h_1} as shown in Eq. (5.4), and where

$$\sigma_0 = \frac{4N_c\pi\alpha_{em}^2}{3Q^2}\,. \tag{5.70}$$

Here we find the same elements already presented in Section 5.3: d_{q/h_1} is the integrated unpolarized fragmentation functions, M_D and g_K are the non-perturbative models, and in the third line we have the perturbative Sudakov factor. Similarly, the cross section for the transversely polarized hadron production has the

following form:

$$\frac{d\Delta\sigma}{dz_1 d^2\boldsymbol{j}_\perp} = \sin(\phi_{S_{h_1}} - \phi_j)\frac{\sigma_0}{z_1^2}\sum_q e_q^2 \int \frac{db_T}{(2\pi)}\, b_T^2 J_1(b_T\, q_T)\widetilde{D}_{1T}^{\perp(1)}(z_1,\bar{\mu}_b)\, U_{NG}(\bar{\mu}_b, Q)$$
$$\times M_D^\perp(b_c(b_T); b_{\max})\, \exp\left\{ - g_K(b_c(b_T); b_{\max}) \ln\left(\frac{Qz_1}{M_{h_1}}\right)\right\}$$
$$\times\, \exp\left\{\tilde{K}(b_*;\bar{\mu}_b)\ln\frac{Q}{\bar{\mu}_b} + \int_{\bar{\mu}_b}^{Q}\frac{d\mu'}{\mu'}\left[\gamma_D(g(\mu'),1) - \gamma_K(g(\mu'))\ln\frac{Q}{\mu'}\right]\right\}, \tag{5.71}$$

where $\widetilde{D}_{1T}^{\perp(1)}$ is the small-b_T limit of the first moment of the polarizing fragmentation function.

Since the soft radiation is restricted to only one hemisphere, the cross section is a non-global observable. The factorization formula for this kind of observables have been derived within an effective field theory context [68–71], where a multi-Wilson-line structure [72–74] is the key ingredient to capture the non-linear QCD evolution effects from the so-called *non-global logarithms*. For this reason in both cross sections, Eqs. (5.69) and (5.71), we have introduced the function U_{NG} (see Ref. [38]), which accounts for the effects of such non-global logarithms.

In the following we will use the parametrization given in Ref. [75]

$$U_{NG}(\bar{\mu}_b, Q) = \exp\left[- C_A C_F \frac{\pi^2}{3} u^2 \frac{1+(au)^2}{1+(bu^c)}\right], \tag{5.72}$$

with $a = 0.85\, C_A$, $b = 0.86\, C_A$, $c = 1.33$ and

$$u = \frac{1}{\beta_0}\ln\left[\frac{\alpha_s(\bar{\mu}_b)}{\alpha_s(Q)}\right], \tag{5.73}$$

where $\beta_0 = \frac{11}{3}C_A - \frac{4}{3}T_F n_f$, with $T_F = 1/2$ and n_f is the number of the active flavors. In addition, when the polarization is measured along the axis $\hat{\boldsymbol{n}} = \hat{\boldsymbol{T}} \times \hat{\boldsymbol{P}}_{h_1}$, the spin and transverse momentum azimuthal angles are such that

$\sin(\phi_{S_{h_1}} - \phi_j) = 1$. Finally, the expression of the transverse polarization can be given as:

$$\mathcal{P}(z_1, p_\perp) = \frac{d\Delta\sigma/dz_1 d^2\boldsymbol{j}_\perp}{d\sigma/dz_1 d^2\boldsymbol{j}_\perp}\,, \tag{5.74}$$

that will be used to fit the Belle data. This will allows us to extract the first moment of the polarizing fragmentation function and its non-perturbative function.

5.5. Phenomenological analysis

We can now proceed with the analysis of Belle data [33], for the transverse Λ polarization measured in e^+e^- collisions, employing the approach presented in the previous sections. Two data sets are provided: one where the Λ particle is produced almost back-to-back with respect to a light unpolarized hadron, that we will refer to as double-hadron production (2-h) data set, and one where the Λ transverse momentum is measured with respect to the thrust axis, the single-inclusive production (1-h) data set. We will start considering the double-hadron production data alone and present the corresponding results. In a second phase, we will include in the study also the single-inclusive hadron production case.

5.5.1. Double-hadron production data fit

In this section, by employing Eqs. (5.20), (5.23), (5.24), (5.48) and (5.49), we present the analysis of the $\Lambda/\bar{\Lambda}$ polarization produced with a light hadron, $\pi^\pm$ or $K^\pm$, measured at $\sqrt{s} = 10.58\,\text{GeV}$. The 128 data points are given [33] as a function of z_Λ and $z_{\pi/K}$, the energy fractions of the $\Lambda/\bar{\Lambda}$ and π/K particles, but for the current analysis we impose a cut for large values of the light-hadrons energy fractions, $z_{\pi/K} < 0.5$, keeping only 96 data points. Notice that here we consider the transverse polarization for inclusive Λ particles, namely those

directly produced from $q\bar{q}$ fragmentation and those indirectly produced from strong decays. The purpose of the analysis is to extract $\widetilde{D}^{\perp(1)}_{1T,\Lambda/q}$ and $M^{\perp}_{D,\Lambda}$, the first moment and the non-perturbative function of the polarizing fragmentation function of the $\Lambda/\bar{\Lambda}$ particle. We will use the following expression to parametrize the z dependence of $\widetilde{D}^{\perp(1)}_{1T,\Lambda/q}$:

$$\widetilde{D}^{\perp(1)}_{1T,\Lambda/q}(z;\mu_b) = \mathcal{N}^p_q(z) d_{q/\Lambda}(z;\mu_b)\,, \tag{5.75}$$

with $q = u$, d, s, *sea*, and where z is the light-cone momentum fraction defined in Eq. (5.3). $\mathcal{N}^p_q(z)$ parametrized as:

$$\mathcal{N}^p_q(z) = N_q z^{a_q}(1-z)^{b_q}\frac{(a_q+b_q)^{(a_q+b_q)}}{a_q^{a_q} b_q^{b_q}}\,, \tag{5.76}$$

without imposing any constraint on the parameters entering $\mathcal{N}^p_q(z)$. $d_{q/\Lambda}$ is the collinear unpolarized fragmentation function of the Λ for which we employ, here and in the convolutions, the AKK08 set [50]. This set adopts the longitudinal momentum fraction, z_p, as scaling variable and the parametrization is given for $\Lambda + \bar{\Lambda}$. In order to separate the two contributions we assume[3]

$$d_{q/\bar{\Lambda}} = d_{\bar{q}/\Lambda} = (1-z_p) d_{q/\Lambda}\,. \tag{5.77}$$

This is a common way to take into account the expected difference between the quark and antiquark FF with a suppressed sea at large z_p with respect to the valence component. Other similar choiches have a very little impact on the fit. Concerning the non-perturbative function $M^{\perp}_{D,\Lambda}$ we employ two different functional forms. The first is the Gaussian model, Eq. (5.62):

[3]Notice that, in Chapter 3, we used the notation $D_{\Lambda/q}$ for the Λ unpolarized fragmentation function, see Eq. (3.16).

$$M^{\perp}_{D,\Lambda}(b_T) = \exp\left(-\frac{\langle p_\perp^2\rangle_{\rm p} b_T^2}{4z_p^2}\right), \tag{5.78}$$

where z_p is the longitudinal momentum fraction and $\langle p_\perp^2\rangle_{\rm p}$, the Gaussian width, is a free parameter that we extract from the fit. The second model is the Power-Law model, Eq. (5.65):

$$M^{\perp}_{D,\Lambda}(b_T) = \frac{2^{2-p}}{\Gamma(p-1)}\,(b_T m/z_p)^{p-1} K_{p-1}(b_T m/z_p)\,, \tag{5.79}$$

where we will extract the values of p and m (with the condition $p > 1$). Regarding the collinear FFs of the unpolarized light hadrons, π and K, we adopt the DSS07 set [49], meanwhile for M_D, their non-perturbative function, we assume a Gaussian model, compatible with previous extractions, with $\langle p_\perp^2\rangle = 0.2\,\text{GeV}^2$ [51]. For what concerns the non-perturbative function of the unpolarized FF of the Λ we use either a Gaussian model, with the same width as for the light hadrons, or a Power-Law model, Eq. (5.65), with the parameters values $p = 2$ and $m = 1\,\text{GeV}$. These are represented in Fig. 5.3. Notice that all the conversions among the different scaling variables (z, z_h, z_p) involved, Eqs. (5.3), (5.4) and (5.5), are properly taken into account. Concerning the g_K function, we use the four functions presented in Section 5.3, in Eq. (5.60) and Fig. 5.2, listed below:

$$\begin{aligned}
g_K(b_T; b_{\rm max}) &= \frac{g_2 b_T^2}{2}\,; \quad g_2 = 0.68\,\text{GeV}^2 \qquad \text{BLNY} \\
g_K(b_T; b_{\rm max}) &= \frac{C_F}{\pi}\frac{b_T^2}{b_{\rm max}^2}\alpha_s(\mu_{b_*}) \qquad \text{Quadratic} \\
g_K(b_T; b_{\rm max}) &= \frac{\alpha_s(C_1/b_*)C_F}{\pi}\ln(1 + b_T^2/b_{\rm max}^2) \qquad \text{Logarithmic} \\
g_K(b_T; b_{\rm max}) &= g_2 \ln\left(\frac{b_T}{b_*}\right) \quad g_2 = 0.84 \qquad \text{AFGR / SIYY}\,.
\end{aligned} \tag{5.80}$$

In all non-perturbative functions and in the $\boldsymbol{b}_*$-prescription, we have used:

$$b_{\min} = 2e^{-\gamma_E}/Q\,; \qquad b_{\max} = 0.6\,\mathrm{GeV}^{-1}\,,$$

with $Q = 10.58\,\mathrm{GeV}$. Bearing in mind that the larger is the value of $b_{\max}$, the smaller is the value assumed by μ_b (that is the energy scale at which we call the AKK routine), we chose the value of $b_{\max}$ to be as large as possible, taking into account that the AKK set lower scale is $Q = 1\,\mathrm{GeV}$.

Along with the already mentioned non-perturbative functions that can be used for M_D, for the unpolarized pions and kaons, and for the g_K function, there are those extracted in [76] from SIDIS, Drell-Yan and Z-boson production. Although these functions are an important source of informations for what concerns non-perturbative effects, we will not use them in the current analysis because they were extracted by employing a different $\boldsymbol{b}_*$-prescription and a larger value of $b_{\max}$.

Lastly, for the upper limit of the integration in Eqs. (5.23) and (5.24), we use $q_{T_{\max}} = 0.25\,Q$, checking also the impact of different values of $q_{T_{\max}}/Q$. To perform the phenomenological analysis we use *iMINUIT* [77] as a minimizer for the χ^2 function, and for the Fourier transforms we employ the *Fast Bessel Transform* algorithm presented in [78].

5.5.2. Fit results

Concerning the first moment of the polarizing FF, Eqs. (5.75) and (5.76), we adopt the same parameter choice already considered in Chapter 3 and Ref. [41], that is:

$$N_u, \quad N_d, \quad N_s, \quad N_{\mathrm{sea}}, \quad a_s, \quad b_u, \quad b_{\mathrm{sea}}\,, \tag{5.81}$$

with all other a and b parameters set to zero. All the considerations in Section 3.3 on the choice and number of these parameters are also valid in this analysis.

Regarding the non-perturbative functions, we have used various combinations of them, for a total of 36 fits. We have also considered different initial values of the p parameter[4] of the Power-Law model, noticing that this leads to different chi-square minimum values. This means that we have 8 or 9 free parameters depending on whether we use the Gaussian or the Power-Law model for the polarizing non-perturbative function. The best results for the double-hadron production case are found, as reported in Tab. 5.1, using the *Logarithmic* function for g_K, the *Power-Law* model for the unpolarized Λ FF and a Gaussian or Power-Law model for the polarizing FF, leading to a $\chi^2_{\rm dof}$ around 1.2.

Polarizing	Unpolarized	g_K	$\chi^2_{\rm dof}$ (2-h)	$\chi^2_{\rm dof}$ (2-h + 1-h)
Gaussian	Power-Law	Logarithmic	1.192	2.813
Power-Law	Power-Law	Logarithmic	1.21	2.39

Table 5.1.: Values of the $\chi^2_{\rm dof}$ obtained fitting the double hadron production data set only (column 2-h), and those obtained for the combined fit (column 2-h + 1-h).

As reported in Tab. 5.2, the parameters values extracted employing the Gaussian or Power-Law models are totally consistent and, similarly, the two polarizing non-perturbative models $M_D^\perp$ are compatible as shown in Fig. 5.5. As in the case of the previous extraction, we find that only the first moment of the up quark is positive, confirming, moreover, that the contributions to the transverse polarization given by the up and the down quarks are opposite in sign.

In Fig. 5.7 we show the estimates of the transverse Λ polarization, produced in association with a light-hadron, compared to Belle data [33], adopting the parameters extracted with the Gaussian model. The shaded areas, corresponding to a 2σ uncertainty, are computed according to the procedure explainded in the Appendix of Ref. [52].

It is important to notice that, unlike the other experimental data points not included in the fit, the ΛK^+ and $\bar{\Lambda} K^-$ data with $z_K > 0.5$, can be described

[4] *iMINUIT allows the users to choose the starting values of the parameters that will be extracted.*

Parameters	Gaussian	Power-Law
N_u	$0.093^{-0.052}_{+0.092}$	$0.100^{-0.054}_{+0.095}$
N_d	$-0.100^{-0.036}_{+0.035}$	$-0.107^{-0.041}_{+0.036}$
N_s	$-0.117^{-0.09}_{+0.059}$	$-0.115^{-0.089}_{+0.057}$
N_{sea}	$-0.055^{-0.058}_{+0.033}$	$-0.058^{-0.062}_{+0.034}$
a_s	$2.19^{-0.83}_{+1.07}$	$2.12^{-1.0}_{+1.5}$
b_u	$3.5^{-2.2}_{+2.8}$	$3.5^{-1.9}_{+2.8}$
b_{sea}	$2.3^{-1.8}_{+2.5}$	$2.3^{-1.9}_{+2.7}$
$\langle p_\perp^2 \rangle_p$	$0.066^{-0.031}_{+0.039}$	
p		$3.0^{-1.4}_{+2.5}$
m		$0.35^{-0.22}_{+0.3}$

Table 5.2.: Best values of the parameters for the polarizing first moment and for the two non-perturbative functions used to fit the double hadron data set.

neither by the previous fit, see Ref. [41] (also presented in Chapter 3), nor by the present new extraction. This points out that even including evolution effects we cannot describe these experimental points. Thus, further investigation, probably with the inclusion of heavier quark flavors, is needed.

In Tab. 5.3 we report the $\chi^2_{\rm dof}$ range of values, for the different fits performed; we notice that the extractions are consistent and stable when we employ the same g_K. Moreover, we see that the best fits are found when we make use of the *Logarithmic* g_K function, meanwhile the *Quadratic* and *AFGR* functional forms give worse $\chi^2_{\rm dof}$ and return similar results. Finally, the worst $\chi^2_{\rm dof}$s, are obtained with the *BLNY* functional form.

In Fig. 5.6 we show the impact of choosing different values of $q_{T_{\rm max}}/Q$ on the quality of the fit obtained using the Power-Law and the Gaussian models. In general, the Gaussian model gives a smaller $\chi^2_{\rm dof}$ values than the Power-Law one. Both models reach their minimum $\chi^2_{\rm dof}$ value at $q_{T_{\rm max}}/Q = 0.22$. The growth of

g_K	χ^2_{dof} range
Logarithmic	1.192 - 1.287
Quadratic	1.4 - 1.472
AFGR	1.474 - 1.514
BLNY	1.67 - 1.783

Table 5.3.: Range of the χ^2_{dof} values for different non-perturbative g_K functions.

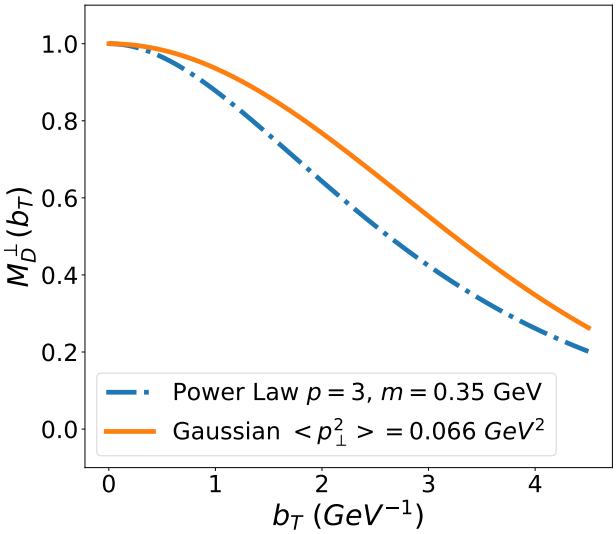

Figure 5.5.: Representation of the two non-perturbative functions extracted from the double-hadron data fit: Gaussian model (orange solid line) and Power-Law model (blue dash-dotted line).

the χ^2_{dof}, as $q_{T_{\max}}/Q$ increases, can be explained considering that we are gradually going out of the validity region of the TMD factorization. Meanwhile, the growth for lower values of $q_{T_{\max}}/Q$ can be attributed to the fact that the smaller is the value of $q_{T_{\max}}/Q$, the larger is the distance between the nodes of Bessel functions. Hence, the *Fast Bessel Transform* algorithm [78] is not able to sample sufficiently well the integrand, whose Fourier transform is to be computed.

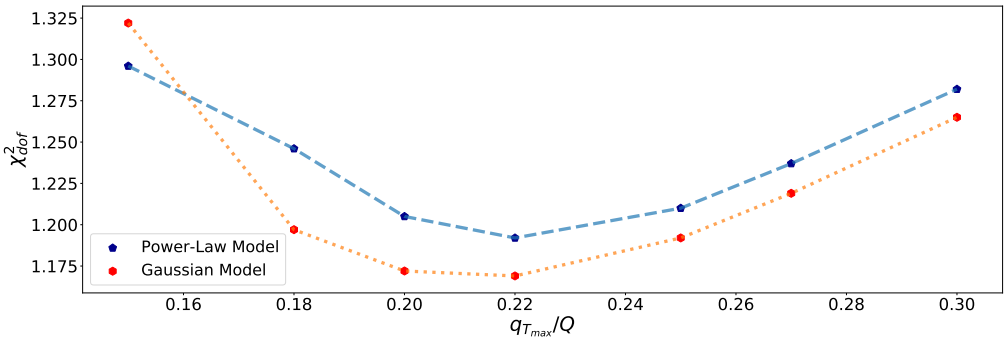

Figure 5.6.: χ^2_{dof} values for the fits obtained with the Power-Law model (blue dashed line) and with the Gaussian model (red dashed line) as a function of $q_{T_{\text{max}}}/Q$ values.

5.5.3. Combined fit: double and single-inclusive hadron production data

In this section we discuss the combined fit of both data sets. Employing Eqs. (5.69), (5.71) and (5.74), we first tried to check if, using the parameters extracted from the double-hadron production fit (Tab. 5.2), we can describe the single-inclusive hadron production data. This data set is presented as a function of $p_\perp$, the transverse momentum of the $\Lambda/\bar{\Lambda}$ particle with respect to the thrust axis, that coincides with $j_\perp$ in Eqs. (5.69) and (5.71), for different bins of the energy fraction z_Λ [33]. As shown in Fig. 5.8 the two models cannot fully describe the pattern and the size of the polarization. Indeed, if the single-inclusive hadron data set is included in the fit we obtain a higher χ^2_{dof} as shown in the last column of Tab. 5.1. In addition, we have also performed the combined fit using all the other different combinations of non-perturbative models, as we have done in the double-hadron production section, obtaining χ^2_{dof} values ranging from 2.4 to 5.4. Since the first moment of the polarizing FF is a collinear quantity, it should be the same in both the double hadron and the single-inclusive cross sections. Therefore, the fact that the two data set cannot be fitted simultaneously could point out that these processes cannot be described by the same factorization theorems and/or by the same $M_D^\perp$ non-perturbative functions.

5.5.4. Combined fit: different non-perturbative function $M_D^\perp$

In order to investigate the possible reasons why the combined fit is not satisfactory and why the parametrizations extracted in the double-hadron fit cannot describe the single-inclusive polarization data, we try to fit both data sets using the same parametrizations for the first moment of the polarizing FF and the same functional form for $M_D^\perp$, but with two different sets of parameters. In the case of the Gaussian model we fit two gaussian widths, while in the case of the Power-Law model we fit two different pairs of (p, m), one for the 2-h data set and one for the 1-h data set. Concerning g_K and the unpolarized non-perturbative functions we use the same functions as in Tab. 5.1. As we can see in Tab. 5.4, with this approach we can find χ^2_{dof}s lower than the ones presented in the last column of Tab. 5.1. Indeed, we have a $\chi^2_{\text{dof}} = 1.801$ for the Gaussian model and a $\chi^2_{\text{dof}} = 1.565$ for the Power-Law model.

Gaussian			Power-Law		
$\chi^2_{\text{dof}} = 1.801$			$\chi^2_{\text{dof}} = 1.565$		
	2-h	1-h		2-h	1-h
$\langle p_\perp^2 \rangle_p$	$0.04^{-0.02}_{+0.03}$	$0.2^{-0.01}_{+0}$	p	$1.352^{-0.055}_{+0.068}$	$1.623^{-0.011}_{+0.011}$
			m	$0.151^{-0.024}_{+0.026}$	$0.48^{-0.005}_{+0.005}$

Table 5.4.: Values of the best fit non-perturbative function parameters using a double set of parameters for the Gaussian and Power-Law model.

Focusing on the results obtained with the Power-Law model, since it has a better χ^2_{dof}, we can see how the estimates for the single-inclusive polarization, Fig. 5.9, describe the experimental data better than the estimates in Fig. 5.8, and how the two data sets are better described when using two different pairs of (p, m), which values are reported in Tab. 5.4.

Comparing the two Power-Law models for the 2-h and 1-h data sets in Fig. 5.10, we can see that they reach the same value at small b_T, as expected since the

two fragmentation functions should be the same in the collinear limit, but they differ as b_T increases: the model related to the 2-h data set, blue solid line, is wider than the model related to the 1-h data set, orange dash-dotted line. This corresponds in $\boldsymbol{p}_\perp$-space to have a similar behaviour for large $p_\perp$ values, Fig. 5.11, while differing at small $p_\perp$: this could suggest the fact that the two models are probably convoluted with different soft factors and that the effects of the recoil against emission of soft gluons are different in the two cross sections.

The fragmentation functions of the single-inclusive hadron production, in the factorization scheme presented in Ref. [38], coincide only with those in the double-hadron production at one-loop order. Indeed, we have that exclusively in this case the hemisphere soft factor, S_{hemi}, corresponds to the soft factor, $\sqrt{S}$, convoluted with one of the fragmentation functions in the double-hadron production cross sections.

Hence in future analysis, a possible way to have a better combined fit, without using artificially two different sets of parameters, would be to calculate and employ the S_{hemi} beyond the one-loop order. Otherwise, another manner would be to exploit the cross sections formulated in Ref. [47], within an effective theory context, or in [40, 55], which derivation is based on the CSS approach.

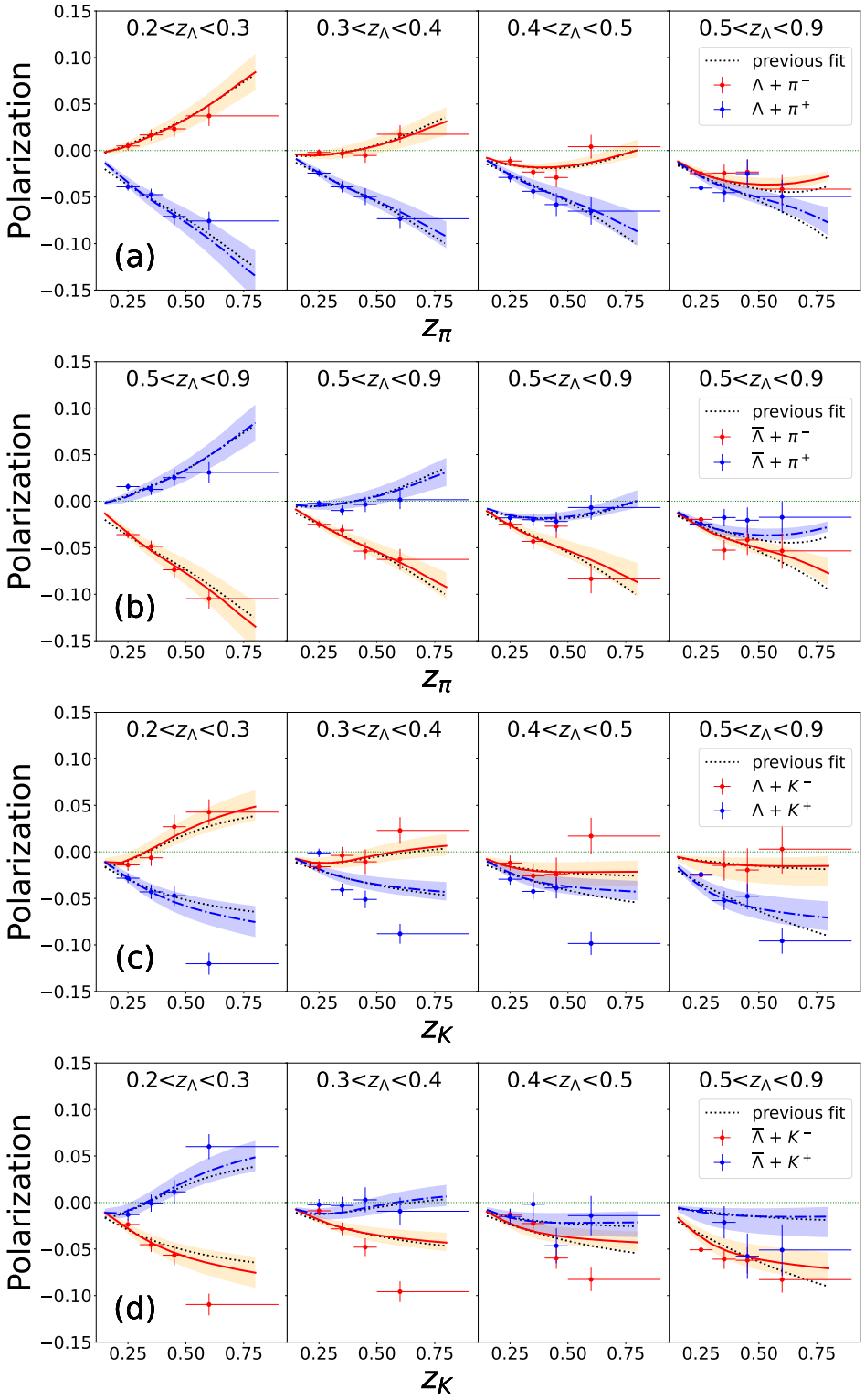

Figure 5.7.: Best-fit estimates, using the Gaussian model and the parameters in Tab. 5.2, of the transverse polarization for Λ and $\bar{\Lambda}$ produced in $e^+e^- \to \Lambda(\bar{\Lambda})h + X$, for $\Lambda\pi^\pm$ (a), $\bar{\Lambda}\pi^\pm$ (b), $\Lambda K^\pm$ (c), $\bar{\Lambda}K^\pm$ (d), as a function of z_h (of the associated hadron) for different z_Λ bins. Data are from Belle [33]. The statistical uncertainty bands, at 2σ level, are also shown. Data for $z_{\pi,K} > 0.5$ are not included in the fit.

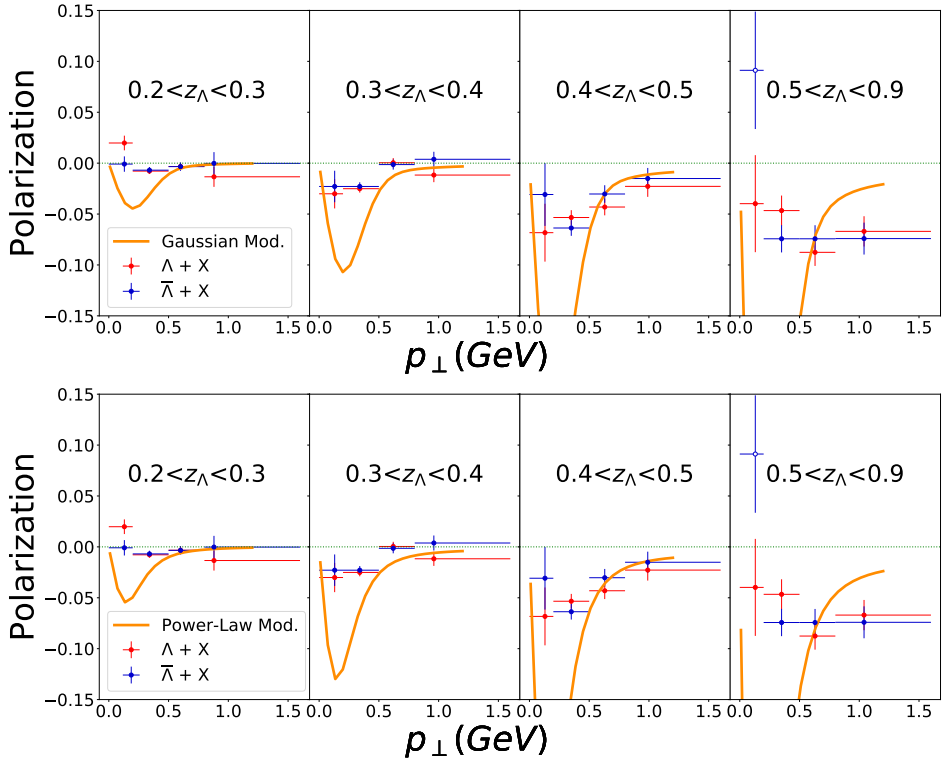

Figure 5.8.: Estimates of the transverse polarization in the single-inclusive Λ production. The results are obtained using the Eqs. (5.69), (5.71) and (5.74) and with the parameter values of Tab. 5.2, found with the Gaussian model (upper plot) and with the Power-Law model (lower plot).

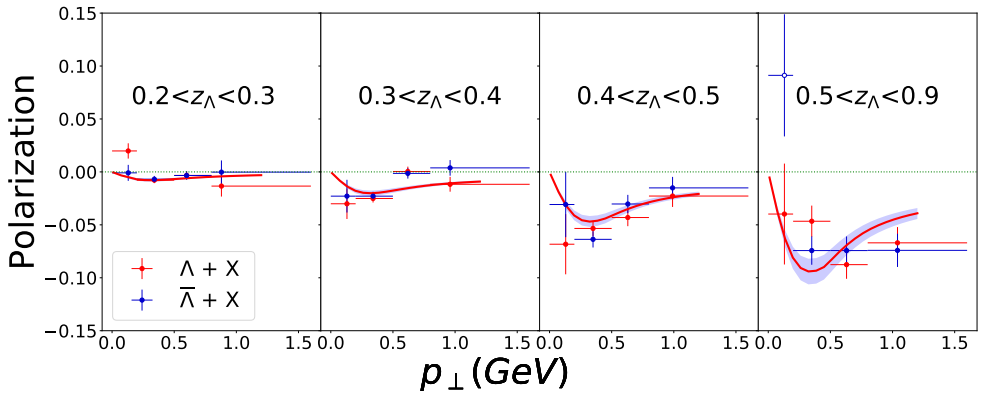

Figure 5.9.: Estimates of the single-inclusive polarization with the Power-Law model.

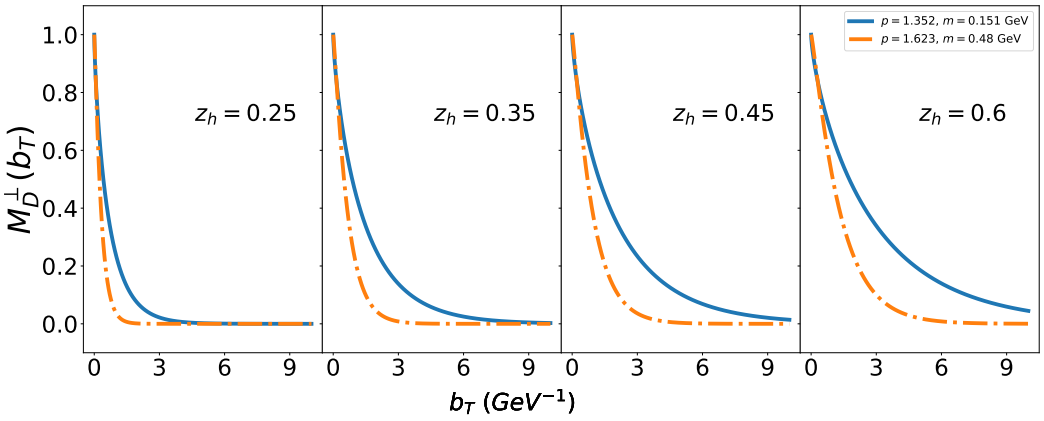

Figure 5.10.: Representation of the two Power-Law models in the double model fit in b_T-space: the 2-h in blue solid line and the 1-h in orange dash-dotted line.

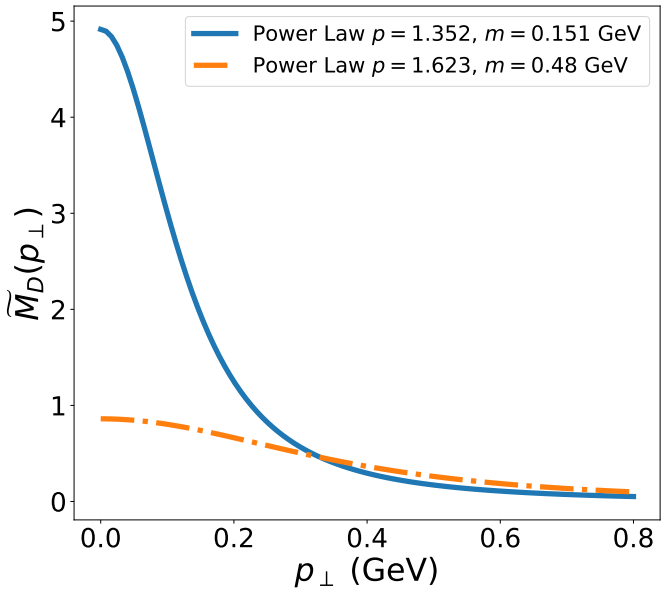

Figure 5.11.: Representation of the two Power-Law models in the double model fit in $p_\perp$-space: the 2-h (blue solid line) and the 1-h (orange dash-dotted line). The functional form is presented in Eq. (G.25).

5.6. Conclusions

The analysis of Belle data through the TMD factorization theorems and the CSS evolution equations has allowed to confirm the results previously obtained in a former extraction of the Λ polarizing FF, and to have deeper insights on the transverse polarization mechanism of Λ hyperons. The double-hadron production data can be well described through different combinations of non-perturbative functions, showing also that the $M_D^\perp$ functions extracted, with the Gaussian and with the Power-Law model, are totally compatible. However, for what concerns the non-perturbative function g_K, the smallest χ^2_{dof}s are found by employing the *Logarithmic* functional form. On the other hand, none of the models extracted from the double-hadron production data can describe either the size or the pattern of the Λ transverse polarization data in the single-inclusive production.

It is worth recalling that, the ΛK^+ and $\bar{\Lambda} K^-$ polarization data, with $z_K > 0.5$, cannot be described even employing the CSS evolution equations. As shown in a recent work [79], data could be possibly fitted by including heavier quark contributions, like charm quarks, and imposing a SU(2) symmetry for the up and down pFFs. The preservation of this symmetry has not been observed in our analysis (where we have not included charm quark contributions) and for this reason a further investigation and a comparison with future experimental data are required.

The combined fit of the double and the single-inclusive hadron production data sets, by extracting the same or two different sets of parameters for the $M_D^\perp$ function, brings to light that these two kinds of processes could not be formulated within the same factorization scheme. Indeed, the discrepancy between the two models extracted separately from the two data sets, in Fig. 5.10, could highlight that there are different effects of recoil against emission of soft gluons, and distinct polarization mechanisms for Λ hyperons between double and single-inclusive hadron production processes.

Future analysis and further theoretical developments will be necessary to understand/unveil the contrasting hadronization mechanisms involved in these two processes.

Chapter 6.

Conclusions

Single Spin Asymmetries and transverse polarization phenomena are an important source of information for our understanding on the inner structure of the hadrons and on hadronization mechanism, in terms of parton distribution and fragmentation functions. Since large values of SSAs and of transverse polarization could not be explained within the framework of collinear QCD factorization at leading twist, the first approaches were based on an extension of the collinear parton model in pQCD. By including a dependence on the spin and the transverse momentum, the TMD-PDFs and the TMD-FFs were introduced.

Only years later, a formulation of the TMD factorization was devised, mainly for three hadronic processes: Drell-Yan (DY), semi-inclusive deep inelastic scattering (SIDIS), and almost back-to-back double-hadron production in e^+e^- annihilation processes. These results have been a breakthrough both from the theoretical and the phenomenological point of view, as they have extended and generalized the original factorization theorems sensitive only to collinear momentum fractions.

Among the processes for which the factorization is proven, the double-hadron production in e^+e^- annihilation processes plays an important role. Indeed, it allows to access cleanly the parton-to-hadron fragmentation mechanism and polarization effects for spin-1/2 hadrons. In this thesis we have focused on a detailed theoretical study of $e^+e^- \to h_1\, h_2 + X$, as well as on a phenomenological

analysis of Belle data for the transverse polarization of $\Lambda/\bar{\Lambda}$ hyperons. The single-inclusive hadron production process, $e^+e^- \to h_1 + X$, has been also considered, firstly within a simplified approach and then by employing a proper TMD factorization scheme.

In Chapter 2 we presented, adopting a TMD approach and within the helicity formalism, the complete expressions for all leading-twist azimuthal dependences and polarization observables for double-hadron production in e^+e^- annihilation processes. Moreover, by adopting a Gaussian model for the transverse momentum dependence of TMD-FFs, we derived the expression for the transverse polarization of a spin-1/2 hadron, which has been exploited, in Chapter 3, for a phenomenological analysis of Belle data for the transverse $\Lambda/\bar{\Lambda}$ polarization. Belle data have been used to extract, for the first time, the polarizing fragmentation function of Λ hyperons, leading to a clear separation of different contributions from the quark flavors. The analysis shows how it is necessary to have different pFFs for the up, down and strange quarks, as well as a contribution from the sea quarks. Simpler fits with only two pFFs, the same for up/down and one for strange quarks, or without any sea contribution, would give much higher $\chi^2_{\rm dof}$. Higher statistics for experimental data and further analysis in the future, as well as complementary studies in other processes, will certainly allow to have a deeper understanding on the role of quark flavors, and if contributions from heavier quarks could be relevant.

In Chapter 4 we provided the expression for the transverse polarization of a spin-1/2 hadron produced in SIDIS processes. Through the polarizing FF extracted from Belle data, we were able to give estimates for the transverse Λ polarization at energy fractions, z_h and x_B, reachable at the future Electron-Ion Collider. This kind of studies will play an important role in testing the universality of the Λ pFF.

By employing a simplified phenomenological model, we have also considered Belle single-inclusive hadron production data, obtaining the first preliminary indication on the transverse momentum dependence of the Λ pFF. On the other hand, since double and single-inclusive hadron production processes, according

to new theoretical developments, should be studied with two different factorization frameworks, in Chapter 5 we have presented a re-analysis of Belle data, keeping into account the Collins-Soper-Sterman (CSS) evolution equations and proper factorization theorems. The convolutions in b_T-space and the expressions for the transverse polarization for the double and single-inclusive production of a spin-1/2 hadron, which have been used in the phenomenological analysis, were given in detail.

The analysis of double-hadron production data confirms the main features of the previous results, leading to four different first moments of the polarizing FF for the up, down, strange and sea quarks, and coming up with estimates of the transverse polarization compatible with those of the former analysis. At the same time, it allowed us to extend our knowledge on the non-perturbative functions, showing how these data can be described by several combinations of those functions, all compatible with each other. Data with higher statistics and further analysis will help in the future to extract different non-perturbative functions, $M_D^\perp$, for each quark flavors.

The combined fit of double and single-inclusive data brings to light that these two processes can be described neither by the same $M_D^\perp$ function nor formulated within the same TMD factorization approach. The estimates for transverse Λ polarization in single-inclusive hadron production, obtained by employing the fit results extracted from double-hadron data are in fact incompatible with data. As shown, the two models, obtained separately from a combined fit, have a common behaviour only at small b_T. Thus, the two processes, even though they look very similar, could apparently give place to different hadronization mechanisms and polarization phenomena.

In the future, further theoretical developments and a systematic comparison among different processes, in which the transverse momentum of final state hadrons is measured with respect to a reference hadron, like in SIDIS and e^+e^- annihilation processes, or with respect to the thrust axis, will let us to better understand the diffences between these hadronization mechanisms. Moreover, new measurements for the transverse Λ polarization in SIDIS processes, at the

future EIC, will have a strong impact on our comprehension about the role of heavy quarks on the transverse polarization, and if the SU(2) symmetry, for up and down pFFs, is preserved in the fragmentation process of transversely polarized Λ's.

All of this will allow us to take a step forward in the comprehension of the long-standing problem of the spontaneous Λ transverse polarization.

Appendix A.

Fragmentation amplitudes for spin-1/2 hadrons and their properties

As mentioned in Section 2.2, for a fragmentation process we can introduce a hadron fragmentation density matrix or a generalized fragmentation function. Following the approach adopted in Ref. [31], we define

$$\hat{D}^{\lambda_h,\lambda'_h}_{\lambda_c,\lambda'_c}(z,\boldsymbol{p}_\perp) = \sum\!\!\!\!\!\!\int_{X,\lambda_X} \hat{\mathcal{D}}_{\lambda_h,\lambda_X;\lambda_c}(z,\boldsymbol{p}_\perp)\hat{\mathcal{D}}^*_{\lambda'_h,\lambda_X;\lambda'_c}(z,\boldsymbol{p}_\perp)\,, \tag{A.1}$$

where $\hat{\mathcal{D}}_{\lambda_h,\lambda_X;\lambda_c}$ is the fragmentation amplitude for the process $c \to h + X$, with $z = \frac{P_h^+}{p_c^+}$ the hadron light-cone momentum fraction, and $\boldsymbol{p}_\perp$ the transverse momentum of the hadron with respect to the parton.

Defining ϕ_h as the azimuthal angle of the hadron h in the helicity reference frame of the parton c we can rewrite the fragmentation function as [31, 80]

$$\hat{\mathcal{D}}_{\lambda_h,\lambda_X;\lambda_c}(z,\boldsymbol{p}_\perp) = \mathcal{D}_{\lambda_h,\lambda_X;\lambda_c}(z,p_\perp)e^{i\lambda_c\phi_h}\,, \tag{A.2}$$

that allows us to write the generalized fragmentation function in the following way

$$\hat{D}^{\lambda_h,\lambda'_h}_{\lambda_c,\lambda'_c}(z,\boldsymbol{p}_\perp) = D^{\lambda_h,\lambda'_h}_{\lambda_c,\lambda'_c}(z,p_\perp)\exp[i(\lambda_c-\lambda'_c)\phi_h]\,. \tag{A.3}$$

The function $D^{\lambda_h,\lambda'_h}_{\lambda_c,\lambda'_c}(z,p_\perp)$ has the same definition of Eq. (A.1), with $\hat{\mathcal{D}}$ replaced by $\mathcal{D}$, but without any phase dependence.

From Eq. (A.1) we can get the following relation, valid both for quarks and gluons,

$$\left(\hat{D}^{\lambda'_h,\lambda_h}_{\lambda'_c,\lambda_c}\right)^* = \hat{D}^{\lambda_h,\lambda'_h}_{\lambda_c,\lambda'_c}\,, \tag{A.4}$$

which, in particular, gives

$$(\hat{D}^{+-}_{+-})^* = \hat{D}^{-+}_{-+} \qquad (\hat{D}^{+-}_{-+})^* = \hat{D}^{-+}_{+-} \tag{A.5}$$

$$(D^{++}_{+-})^* = D^{++}_{-+} \qquad (D^{+-}_{++})^* = D^{-+}_{++}\,. \tag{A.6}$$

Concerning the parity properties of the $\mathcal{D}$ amplitudes they are the usual ones valid for the helicity amplitudes in the $\phi_h = 0$ plane, that is [80]

$$\mathcal{D}_{-\lambda_h,-\lambda_X;-\lambda_c} = \eta\, e^{i\pi(s_c-S_h-S_X)}\, e^{i\pi(\lambda_c-\lambda_h+\lambda_X)}\, \mathcal{D}_{\lambda_h,\lambda_X;\lambda_c}\,, \tag{A.7}$$

where η is an intrinsic parity factor such that $\eta^2 = 1$. This implies that

$$D^{-\lambda_h,-\lambda'_h}_{-\lambda_c,-\lambda'_c}(z,p_\perp) = e^{i\pi[(\lambda_c-\lambda'_c)-(\lambda_h-\lambda'_h)]}\, D^{\lambda_h,\lambda'_h}_{\lambda_c,\lambda'_c}(z,p_\perp)\,. \tag{A.8}$$

Notice that the extra factor makes a difference between quarks and gluons.

Indeed, by exploiting the above relation, we get for quark (upper signs) e gluon (lower signs) fragmentation functions:

$$D^{++}_{++} = D^{--}_{--} \qquad D^{++}_{--} = D^{--}_{++} \tag{A.9}$$

$$D^{++}_{+-} = \mp D^{--}_{-+} \qquad D^{++}_{-+} = \mp D^{--}_{+-} \tag{A.10}$$

$$D^{+-}_{++} = -D^{-+}_{--} \qquad D^{-+}_{++} = -D^{+-}_{--} \tag{A.11}$$

$$D^{+-}_{+-} = \pm D^{-+}_{-+} \qquad D^{+-}_{-+} = \pm D^{-+}_{+-}\,. \tag{A.12}$$

By using the above relations we see that there are six independent quantities

$$D_{++}^{++}, D_{--}^{++}, D_{+-}^{++}, D_{++}^{+-}, D_{+-}^{+-}, D_{-+}^{+-}. \tag{A.13}$$

These are in principle complex quantities, however: D_{++}^{++} and D_{--}^{++} are real since, as we can see from Eq. (A.1), they are moduli squared; D_{+-}^{+-} and D_{-+}^{+-} are purely real for quarks and purely imaginary for gluons, see Eqs. (A.6) and (A.12); and, eventually, D_{+-}^{++} and D_{++}^{+-} are both complex, giving us four additional real quantities. This leaves us with eight independent real quantities.

Appendix B.

Gluon TMD fragmentation functions for spin-1/2 hadrons

Even if not directly relevant for the study of hadron production in e^+e^- collisions, that at LO involves only quark contributions, we present the gluon TMD-FFs for spin-1/2 hadrons, at leading twist, following the same procedure as for the quark ones. We start again with

$$\rho^{h,S_h}_{\lambda_h,\lambda_h'}\hat{D}_{h/g,P_g}(z,\boldsymbol{p}_\perp) = \sum_{\lambda_g,\lambda_g'}\rho^{g}_{\lambda_g,\lambda_g'}\hat{D}^{\lambda_h,\lambda_h'}_{\lambda_g,\lambda_g'}(z,\boldsymbol{p}_\perp)\,, \tag{B.1}$$

where now we have defined the fragmentation function for a massless gluon with polarization state P_g, $\hat{D}_{h/g,P_g}(z,\boldsymbol{p}_\perp)$, fragmenting into an unpolarized hadron. Notice that for a spin-1 parton, like a gluon, it is more convenient to refer to the polarization states (i.e. to circular and/or linear polarizations).

Indeed for the gluon helicity density matrix we have

$$\begin{aligned}\rho^g_{\lambda_g,\lambda'_g} &= \frac{1}{2}\begin{pmatrix}\rho^g_{++} & \rho^g_{+-}\\ \rho^g_{-+} & \rho^g_{--}\end{pmatrix}\\ &= \frac{1}{2}\begin{pmatrix}1+P^g_z & \mathcal{T}^g_1 - i\mathcal{T}^g_2\\ \mathcal{T}^g_1 + i\mathcal{T}^g_2 & 1-P^g_z\end{pmatrix}\\ &= \frac{1}{2}\begin{pmatrix}1+P^g_{\rm circ} & -P^g_{\rm lin}e^{-i2\phi}\\ -P^g_{\rm lin}e^{i2\phi} & 1-P^g_{\rm circ}\end{pmatrix}.\end{aligned} \tag{B.2}$$

In this case we can still define longitudinally, P^g_z, or circularly, $P^g_{\rm circ}$, polarization states, keeping in mind that the off-diagonal elements are now related to the linear polarization in the xy plane with an angle ϕ with respect to the x axis [31].

Once again the x, y, z axes are those of the helicity frame of the gluon, where its four-momentum is $p^\mu_g = (p, 0, 0, p)$. $P^g_{\rm lin}$ is expressed in terms of the parameters $\mathcal{T}^g_1$ and $\mathcal{T}^g_2$, which are closely related to the Stokes' parameters used in classical optics; formally their role is analogous to that played by the x and y components of the quark polarization vectors. The use of the $\mathcal{T}^g_1$ and $\mathcal{T}^g_2$ parameters makes the gluon fragmentation functions formally similar to those of the quarks and simplifies all formulas for the spin asymmetries.

Before exploiting the sum over the gluon helicity indices on the right hand side of Eq. (B.1), let us show how one can define the eight gluon TMD-FFs in close analogy with the quark case:

$$P^h_J \hat{D}_{h/q,P_g} = \hat{D}^{h/g}_{S_J/P_g} - \hat{D}^{h/g}_{-S_J/P_g} \equiv \Delta\hat{D}^{h/g}_{S_J/P_g}, \tag{B.3}$$

where $J = X, Y, Z$. We will use again the notations:

$$P_J^h \, \hat{D}_{h/g,P_{\rm lin}} = \Delta\hat{D}^{h/g}_{S_J/P_{\rm lin}} = \hat{D}^{h/g}_{S_J/P_{\rm lin}} - \hat{D}^{h/g}_{-S_J/P_{\rm lin}} \equiv \Delta\hat{D}^{h/g}_{S_J/P_{\rm lin}}(z, \boldsymbol{p}_\perp) \tag{B.4}$$

$$P_J^h \, \hat{D}_{h/g,s_z} = \Delta\hat{D}^{h/g}_{S_J/s_z} = \hat{D}^{h/g}_{S_J/+} - \hat{D}^{h/g}_{-S_J/+} \equiv \Delta\hat{D}^{h/g}_{S_J/+}(z, \boldsymbol{p}_\perp) \tag{B.5}$$

$$\hat{D}_{h/g,P_{\rm lin}} = \hat{D}_{h/g}(z, p_\perp) + \frac{1}{2}\,\Delta\hat{D}_{h/P_{\rm lin}}(z, \boldsymbol{p}_\perp)\,, \tag{B.6}$$

where, in the second line, for the circular or longitudinal polarization, we have used s_z, fixed as $+$.

These amount to eight gluon TMD-FFs. Analogously, to what has been done for quarks, we now exploit the sum in the right hand side of Eq. (B.1). Thus we can obtain the following three expressions:

$$\begin{aligned}
\rho^{h,S_h}_{++}\hat{D}_{h/g,P_g} &= \frac{1}{2}(1 + P_Z^h)\hat{D}_{h/g,P_g} \\
&= \frac{1}{2}(D^{++}_{++} + D^{++}_{--}) + \frac{1}{2}P^g_{\rm circ}(D^{++}_{++} - D^{++}_{--}) \\
&- P^g_{\rm lin}[{\rm Re}D^{++}_{+-}\cos\left[2(\phi - \phi_h)\right] + {\rm Im}D^{++}_{+-}\sin\left[2(\phi - \phi_h)\right]]
\end{aligned} \tag{B.7}$$

$$\begin{aligned}
\rho^{h,S_h}_{--}\hat{D}_{h/g,P_g} &= \frac{1}{2}(1 - P_Z^h)\hat{D}_{h/g,P_g} \\
&= \frac{1}{2}(D^{++}_{++} + D^{++}_{--}) - \frac{1}{2}P^g_{\rm circ}(D^{++}_{++} - D^{++}_{--}) \\
&- P^g_{\rm lin}[{\rm Re}D^{++}_{+-}\cos\left[2(\phi - \phi_h)\right] - {\rm Im}D^{++}_{+-}\sin\left[2(\phi - \phi_h)\right]]
\end{aligned} \tag{B.8}$$

$$\begin{aligned}
\rho^{h,S_h}_{+-}\hat{D}_{h/g,P_g} &= \frac{1}{2}(P_X^h - iP_Y^h)\hat{D}_{h/g,P_g} \\
&= i{\rm Im}D^{+-}_{++} + P^g_{\rm circ}{\rm Re}D^{+-}_{++} \\
&- \frac{1}{2}P^g_{\rm lin}[i({\rm Im}D^{+-}_{+-} + {\rm Im}D^{+-}_{-+})\cos\left[2(\phi - \phi_h)\right] \\
&+ ({\rm Im}D^{+-}_{+-} - {\rm Im}D^{+-}_{-+})\sin\left[2(\phi - \phi_h)\right]]\,,
\end{aligned} \tag{B.9}$$

where once again we have used the properties of the generalized fragmentation functions, $\hat{D}^{\lambda_h,\lambda_h'}_{\lambda_g,\lambda_g'}(z,\boldsymbol{p}_\perp)$, discussed in Appendix A.

By suitably combining the above expressions, we can find the eight gluon TMD-FFs for a spin-1/2 hadron. For instance, by summing or subtracting Eqs. (B.7) and (B.8) we obtain respectively the TMD-FF for an unpolarized and a longitudinally polarized hadron

$$\hat{D}_{h/g,P_g} = (D^{++}_{++} + D^{++}_{--}) - 2P^g_{\rm lin}{\rm Re}D^{++}_{+-}\cos\left[2(\phi-\phi_h)\right] \tag{B.10}$$

$$P^h_Z\hat{D}_{h/g,P_g} = P^g_{\rm circ}(D^{++}_{++} - D^{++}_{--}) - 2P^g_{\rm lin}{\rm Im}D^{++}_{+-}\sin\left[2(\phi-\phi_h)\right]. \tag{B.11}$$

As we can see from Eq. (B.10), we can have an unpolarized hadron coming from the fragmentation of an unpolarized or a linearly polarized gluon: this last case, in analogy with the quark one, is referred to as the *Collins-like* gluon TMD-FF. By taking the real or the imaginary part of Eq. (B.9) we get the FF for a hadron transversely polarized along, respectively, its X or Y helicity axis as coming from a polarized gluon

$$P^h_X\hat{D}_{h/g,P_g} = 2P^g_{\rm circ}{\rm Re}D^{+-}_{++} - P^g_{\rm lin}({\rm Im}D^{+-}_{+-} - {\rm Im}D^{+-}_{-+})\sin[2(\phi-\phi_h)] \tag{B.12}$$

$$P^h_Y\hat{D}_{h/g,P_g} = -2{\rm Im}D^{+-}_{++} + P^g_{\rm lin}({\rm Im}D^{+-}_{+-} + {\rm Im}D^{+-}_{-+})\cos\left[2(\phi-\phi_h)\right]. \tag{B.13}$$

Once again we can combine the two above expressions as follows

$$\begin{aligned} P^h_T\hat{D}_{h/g,P_g} = &-2{\rm Im}D^{+-}_{++}\sin\phi_{S_h} + 2P^g_{\rm circ}{\rm Re}D^{+-}_{++}\cos\phi_{S_h} \\ &+ P^g_{\rm lin}[{\rm Im}D^{+-}_{+-}\sin(\phi_{S_h} - 2(\phi-\phi_h)) + {\rm Im}D^{+-}_{-+}\sin(\phi_{S_h} + 2(\phi-\phi_h))]\,, \end{aligned} \tag{B.14}$$

and by using Eq. (2.49) we have

$$P_T^h \hat{D}_{h/g,P_g} = -2\mathrm{Im}D_{++}^{+-}\sin(\phi'_{S_h}-\phi_h) + 2P_{\mathrm{circ}}^g \mathrm{Re}D_{++}^{+-}\cos(\phi'_{S_h}-\phi_h) + P_{\mathrm{lin}}^g[\mathrm{Im}D_{+-}^{+-}\sin(\phi'_{S_h}-2\phi+\phi_h)) + \mathrm{Im}D_{-+}^{+-}\sin(\phi'_{S_h}+2\phi-3\phi_h))]\,. \tag{B.15}$$

By fixing now the gluon polarization we can recover the eight TMD-FFs discussed above. Using Eq. (B.10) we have

$$\hat{D}_{h/g} = \hat{D}_{h/g,P_{\mathrm{circ}}} = D_{++}^{++} + D_{--}^{++} \equiv D_{h/g}\,, \tag{B.16}$$

giving the TMD-FF for an unpolarized (or circularly polarized) gluon fragmenting into an unpolarized hadron, and

$$\hat{D}_{h/g,P_{\mathrm{lin}}} = \hat{D}_{h/g} - 2\mathrm{Re}D_{+-}^{++}\cos\left[2(\phi-\phi_h)\right] \tag{B.17}$$

$$= \hat{D}_{h/g} + \frac{1}{2}\Delta^N D_{h/g,P_{\mathrm{lin}}}\cos\left[2(\phi-\phi_h)\right], \tag{B.18}$$

giving the TMD-FF for a linearly polarized gluon fragmenting into an unpolarized hadron.

Through Eq. (B.11) we get

$$P_Z^h \hat{D}_{h/g,P_{\mathrm{circ}}} = D_{++}^{++} - D_{--}^{++} = \Delta D_{S_Z/P_{\mathrm{circ}}}^{h/g} \tag{B.19}$$

$$P_Z^h \hat{D}_{h/g,P_{\mathrm{lin}}} = -2\mathrm{Im}D_{+-}^{++}\,\sin\left[2(\phi-\phi_h)\right] = \Delta D_{S_Z/P_{\mathrm{lin}}}^{h/g}\sin\left[2(\phi-\phi_h)\right], \tag{B.20}$$

giving, respectively, the TMD-FFs for a circularly and for a linearly polarized gluon fragmenting into a longitudinally polarized hadron. Analogously from Eq. (B.12) we have the FF for a hadron transversely polarized, along its X helicity axis, produced by a circularly and a linearly polarized gluon

$$P_X^h \hat{D}_{h/g,P_{\mathrm{circ}}} = 2\,\mathrm{Re}D_{++}^{+-} = \Delta D_{S_X/P_{\mathrm{circ}}}^{h/g} \tag{B.21}$$

$$P_X^h \hat{D}_{h/g,P_{\mathrm{lin}}} = -(\mathrm{Im}D_{+-}^{+-} - \mathrm{Im}D_{-+}^{+-})\sin\left[2(\phi-\phi_h)\right] = \Delta D_{S_X/P_{\mathrm{lin}}}^{h/g}\sin\left[2(\phi-\phi_h)\right]. \tag{B.22}$$

Finally, from Eq. (B.13) we have the TMD-FF for a hadron transversely polarized along its Y direction coming from, respectively, a circularly and linearly polarized gluon

$$P_Y^h \hat{D}_{h/g,P_{\rm circ}} = -2{\rm Im}D_{++}^{+-} = \Delta D_{S_Y/g}^h \tag{B.23}$$

$$P_Y^h \hat{D}_{h/g,P_{\rm lin}} = -2{\rm Im}D_{++}^{+-} + ({\rm Im}D_{+-}^{+-} + {\rm Im}D_{-+}^{+-})\cos\left[2(\phi-\phi_h)\right] \tag{B.24}$$

$$= \Delta D_{S_Y/g}^h + \Delta^- \hat{D}_{S_Y/P_{\rm lin}}^{h/g} = \Delta D_{S_Y/g}^h + \Delta^- D_{S_Y/P_{\rm lin}}^{h/g}\cos\left[2(\phi-\phi_h)\right]. \tag{B.25}$$

Also in this case we have introduced the function $\Delta^- \hat{D}_{S_Y/P_{\rm lin}}^{h/g}$, analogously to Eq. (2.60), that changes sign if the gluon linear polarization has an off-set of $\pi/2$. Thus, as for the quark case, we are able to collect all TMD-FFs as follows

$$\begin{aligned}
\hat{D}_{h/g}(z,\boldsymbol{p}_\perp) &= D_{h/g} = (D_{++}^{++} + D_{--}^{++}) \\
\Delta\hat{D}_{h/g,P_{\rm lin}}(z,\boldsymbol{p}_\perp) &= \Delta^N D_{h/g,P_{\rm lin}}\cos\left[2(\phi-\phi_h)\right] = -4\,{\rm Re}D_{+-}^{++}\cos\left[2(\phi-\phi_h)\right] \\
\Delta\hat{D}_{S_Z/P_{\rm circ}}^{h/g}(z,\boldsymbol{p}_\perp) &= \Delta D_{S_Z/P_{\rm circ}}^{h/g} = (D_{++}^{++} - D_{--}^{++}) \\
\Delta\hat{D}_{S_Z/P_{\rm lin}}^{h/g}(z,\boldsymbol{p}_\perp) &= \Delta D_{S_Z/P_{\rm lin}}^{h/g}\sin\left[2(\phi-\phi_h)\right] = -2{\rm Im}D_{+-}^{++}\sin\left[2(\phi-\phi_h)\right] \\
\Delta\hat{D}_{S_X/P_{\rm circ}}^{h/g}(z,\boldsymbol{p}_\perp) &= \Delta D_{S_X/P_{\rm circ}}^{h/g} = 2{\rm Re}D_{++}^{+-} \\
\Delta\hat{D}_{S_X/P_{\rm lin}}^{h/g}(z,\boldsymbol{p}_\perp) &= \Delta D_{S_X/P_{\rm lin}}^{h/g}\sin\left[2(\phi-\phi_h)\right] = -({\rm Im}D_{+-}^{+-} - {\rm Im}D_{-+}^{+-})\sin\left[2(\phi-\phi_h)\right] \\
\Delta\hat{D}_{S_Y/g}^{h}(z,\boldsymbol{p}_\perp) &= \Delta D_{S_Y/g}^{h} = -2{\rm Im}D_{++}^{+-} \\
\Delta^-\hat{D}_{S_Y/P_{\rm lin}}^{h/g}(z,\boldsymbol{p}_\perp) &= \Delta^- D_{S_Y/P_{\rm lin}}^{h/g}\cos\left[2(\phi-\phi_h)\right] = ({\rm Im}D_{+-}^{+-} + {\rm Im}D_{-+}^{+-})\cos\left[2(\phi-\phi_h)\right].
\end{aligned} \tag{B.26}$$

Appendix C.

Comparison with other notations

In the literature another notation is also commonly used for the eight leading-twist quark TMD-FFs, referred to as the Amsterdam notation [21,30]. There the main quantity, corresponding to our $\hat{D}^{\lambda_h,\lambda_h'}_{\lambda_q,\lambda_q'}(z,\boldsymbol{p}_\perp)$, is the quark-hadron correlator $\Delta(z,\boldsymbol{k}_T)$ and all mass effects are neglected. It is important to notice that $\boldsymbol{k}_T$ is the transverse three-momentum of the fragmenting quark w.r.t. the produced hadron, which implies $\boldsymbol{k}_T \simeq -\boldsymbol{p}_\perp/z$ (valid in the massless hadron limit). We will also use the spin-polarization vector $\boldsymbol{P}^h = (P_L^h, \boldsymbol{P}_T^h)$ to allow for a more direct comparison.

For the case of an unpolarized quark fragmenting into a spin-1/2 hadron and a transversely polarized quark fragmenting into an unpolarized or spinless hadron we recover the results of the "Trento Conventions", see Ref. [17]. Following Ref. [21] we have

$$\Delta(z,\boldsymbol{k}_T) = \frac{1}{2}\Bigg\{ D_1 \not{n}^- + D_{1T}^\perp \frac{\epsilon^{\mu\nu\rho\sigma}\gamma_\mu n_\nu^- k_{T\rho} P_{T\sigma}^h}{M_h} + \Big(P_L^h G_{1L} + G_{1T}\,\frac{\boldsymbol{k}_T\cdot\boldsymbol{P}_T^h}{M_h}\Big)\gamma_5 \not{n}^- \\ + H_{1T} i\sigma^{\mu\nu}\gamma_5 n_\mu^- P_{T\nu}^h + \Big(P_L^h H_{1L}^\perp + H_{1T}^\perp\,\frac{\boldsymbol{k}_T\cdot\boldsymbol{P}_T^h}{M_h}\Big)\frac{i\sigma^{\mu\nu}\gamma_5 n_\mu^- k_{T\nu}}{M_h} + H_1^\perp \frac{\sigma^{\mu\nu} k_{T\mu} n_\nu^-}{M_h}\Bigg\}, \tag{C.1}$$

where $D_1 = D_1(z,p_\perp)$, with $p_\perp = |\boldsymbol{p}_\perp|$ as adopted through the present thesis.

By appropriate Dirac projection, $\Delta^{[\Gamma]} = Tr[\Gamma\Delta]$, one can single out the various sectors of the fragmentation functions. In particular, $\Gamma = \not{n}^+/2$ projects out the D sector, relative to an unpolarized quark, that is the unpolarized D_1 and the polarizing $D_{1T}^\perp$ fragmentation functions:

$$\mathrm{Tr}\left[\frac{\not{n}^+}{2}\,\Delta(z,\boldsymbol{k}_T)\right] = D_1 - D_{1T}^\perp\,\frac{\epsilon^{\mu\nu\rho\sigma}n_\mu^- k_{T\nu}P_{T\rho}^h n_\sigma^+}{M_h} = D_1 + D_{1T}^\perp\,\frac{(\hat{\boldsymbol{p}}_q\times\boldsymbol{p}_\perp)\cdot\boldsymbol{P}^h}{zM_h}\,, \tag{C.2}$$

where $n_\pm$ are two auxiliary lightlike vectors, and the second equality holds in frames where $\boldsymbol{n}^-$ and the direction $\hat{\boldsymbol{p}}_q$ of the quark momentum point in opposite directions. By choosing $\Gamma = \not{n}^+\gamma_5/2$ we select the contribution from a longitudinal polarized quark, the G sector, that is

$$\mathrm{Tr}\left[\frac{\not{n}^+}{2}\gamma_5\,\Delta(z,\boldsymbol{k}_T)\right] = P_L^h\,G_{1L} + G_{1T}\,\frac{\boldsymbol{k}_T\cdot\boldsymbol{P}_T^h}{M_h} = P_L^h\,G_{1L} - P_T^h\,\frac{p_\perp}{zM_h}\,G_{1T}\,\cos\left(\phi'_{S_h}-\phi_h\right), \tag{C.3}$$

where the angle ϕ'_{S_h} is the azimuthal angle of the hadron spin in the quark helicity frame. Finally, to obtain the H sector, relative to the fragmentation of a transversely polarized quark, we use the projector $\Gamma = i\sigma^{\rho\sigma}\gamma_5\,n_\rho^+P_\sigma^q/2$, with $P^{q\mu} = (0,\cos\phi_{s_q},\sin\phi_{s_q},0)$:

$$\begin{aligned}
&\mathrm{Tr}\left[\frac{1}{2}i\sigma^{\rho\sigma}\gamma_5\,n_\rho^+P_\sigma^q\,\Delta(z,\boldsymbol{k}_T)\right]\\
&\quad= H_{1T}\,\boldsymbol{P}_T^h\cdot\boldsymbol{P}^q + \left(P_L^h H_{1L}^\perp + H_{1T}^\perp\,\frac{\boldsymbol{k}_T\cdot\boldsymbol{P}_T^h}{M_h}\right)\frac{\boldsymbol{k}_T\cdot\boldsymbol{P}^q}{M_h} - H_1^\perp\frac{\epsilon^{\mu\nu\rho\sigma}n_\mu^-k_{T\nu}P_\rho^q n_\sigma^+}{M_h}\\
&\quad= P_T^h\left[H_1\,\cos(\phi'_{S_h}-\phi_{s_q}) + \frac{p_\perp^2}{2z^2M_h^2}H_{1T}^\perp\cos(\phi_{s_q}+\phi'_{S_h}-2\phi_h)\right]\\
&\quad- P_L^h\,\frac{p_\perp}{zM_h}H_{1L}^\perp\,\cos(\phi_{s_q}-\phi_h) + H_1^\perp\,\frac{(\hat{\boldsymbol{p}}_q\times\boldsymbol{p}_\perp)\cdot\boldsymbol{P}^q}{zM_h}\,,
\end{aligned} \tag{C.4}$$

with

$$H_1 = H_{1T} + \frac{p_\perp^2}{2z^2 M_h^2} H_{1T}^\perp \,. \tag{C.5}$$

To obtain the relation between the $D_{\lambda_q \lambda_q'}^{\lambda_h, \lambda_h'}$ fragmentation functions, including the TMD-FFs in the notation adopted here, and those of the Amsterdam group, one has to take into account that, while the first ones are given fixing the polarization vector of the hadron, the others are given at fixed quark polarization. By properly exploiting Eqs. (2.43), (2.44) and (2.50) and Eqs. (C.2)-(C.4), we get

$$D_{h/q} = D_{++}^{++} + D_{--}^{++} = D_1(z, p_\perp) \tag{C.6}$$

$$\Delta D_{S_Y/q}^h = \Delta^N D_{h^\uparrow/q} = -2\,\mathrm{Im} D_{++}^{+-} = \frac{p_\perp}{z M_h} D_{1T}^\perp(z, p_\perp) \tag{C.7}$$

$$\Delta D_{S_Z/s_L}^{h/q} = D_{++}^{++} - D_{--}^{++} = G_{1L}(z, p_\perp) \tag{C.8}$$

$$\Delta D_{S_X/s_L}^{h/q} = 2\,\mathrm{Re} D_{+-}^{++} = -\frac{p_\perp}{z M_h} G_{1T}(z, p_\perp) \tag{C.9}$$

$$\Delta D_{S_Z/s_T}^{h/q} = 2\,\mathrm{Re} D_{++}^{+-} = -\frac{p_\perp}{z M_h} H_{1L}^\perp(z, p_\perp) \tag{C.10}$$

$$\Delta^N D_{h/q^\uparrow} = 4\,\mathrm{Im} D_{+-}^{++} = \frac{2p_\perp}{z M_h} H_1^\perp(z, p_\perp) \tag{C.11}$$

$$\frac{1}{2}[\Delta D_{S_X/s_T} + \Delta^- D_{S_Y/s_T}] = D_{+-}^{+-} = H_1(z, p_\perp) \tag{C.12}$$

$$\frac{1}{2}[\Delta D_{S_X/s_T} - \Delta^- D_{S_Y/s_T}] = D_{-+}^{+-} = \frac{p_\perp^2}{2z^2 M_h^2} H_{1T}^\perp(z, p_\perp) \,. \tag{C.13}$$

To complete this comparison we observe that by inserting Eqs. (C.5), (C.7), (C.12) and (C.13) into Eqs. (2.57) and (2.59) we get

$$P_X^h \hat{D}_{h/q, s_T} = \Delta \hat{D}_{S_X/s_T}^{h/q}(z, \boldsymbol{p}_\perp) = \left[H_{1T}(z, p_\perp) + \frac{p_\perp^2}{z^2 M_h^2} H_{1T}^\perp(z, p_\perp) \right] \cos(\phi_{s_q} - \phi_h) \tag{C.14}$$

$$P_Y^h \hat{D}_{h/q, s_T} = \Delta \hat{D}_{S_Y/s_T}^{h/q}(z, \boldsymbol{p}_\perp) = \frac{p_\perp}{z M_h} D_{1T}^\perp(z, p_\perp) + H_{1T}(z, p_\perp) \sin(\phi_{s_q} - \phi_h) \,, \tag{C.15}$$

showing that H_{1T} and $H_{1T}^{\perp}$ are combinations of hadron polarized fragmentation functions.

Appendix D.

Tensorial analysis

A useful tool to exploit the integrals over $p_{\perp 2}$ involved in the convolutions $\mathcal{C}[w\Delta D\Delta\bar{D}]$ appearing in Section 2.5 is a simple tensorial decomposition, a procedure already developed in Ref. [28] for the general helicity formalism in SIDIS.

All the integrals can be indeed reduced to a linear combination of the following convolutions:

$$T^i = \frac{1}{P_{1T}} \int d^2\boldsymbol{p}_{\perp 2}\, p^i_{\perp 2}\, \Delta D^{h_1}(z_1, p_{\perp 1})\, \Delta D^{h_2}(z_2, p_{\perp 2}) \tag{D.1}$$

$$T^{ij} = \frac{1}{P^2_{1T}} \int d^2\boldsymbol{p}_{\perp 2}\, p^i_{\perp 2} p^j_{\perp 2}\, \Delta D^{h_1}(z_1, p_{\perp 1})\, \Delta D^{h_2}(z_2, p_{\perp 2}) \tag{D.2}$$

$$T^{ijk} = \frac{1}{P^3_{1T}} \int d^2\boldsymbol{p}_{\perp 2}\, p^i_{\perp 2} p^j_{\perp 2} p^k_{\perp 2}\, \Delta D^{h_1}(z_1, p_{\perp 1})\, \Delta D^{h_2}(z_2, p_{\perp 2}) \tag{D.3}$$

$$T^{ijkl} = \frac{1}{P^4_{1T}} \int d^2\boldsymbol{p}_{\perp 2}\, p^i_{\perp 2} p^j_{\perp 2} p^k_{\perp 2} p^l_{\perp 2}\, \Delta D^{h_1}(z_1, p_{\perp 1})\, \Delta D^{h_2}(z_2, p_{\perp 2})\,, \tag{D.4}$$

where we have denoted by $\Delta D^{h_{1,2}}$ any fragmentation function (depending only on the moduli of the intrinsic transverse momenta) appearing in the definition of the particular structure function F one is considering and where the upper index of $p_{\perp 2}$ can be $i = x, y$ (hadron frame):

$$p^x_{\perp 2} = p_{\perp 2} \cos\varphi_2 \qquad p^y_{\perp 2} = p_{\perp 2} \sin\varphi_2\,. \tag{D.5}$$

Notice that we have normalized each tensor by a suitable power of P_{1T} and that T^i, T^{ij}, T^{ijk} and T^{ijkl} are symmetric, rank 1, 2, 3, 4 Euclidean tensors, respectively. Bearing in mind that $\boldsymbol{p}_{\perp 1}$ is not independent and can be expressed in terms of $\boldsymbol{p}_{\perp 2}$ and $\boldsymbol{P}_{1T}$ (see Eq. (2.26)) , we have, in a completely general way, that the convolutions depend only on P_{1T} and ϕ_1, i.e. the measured modulus and azimuthal phase of the final observed hadron transverse momentum:

$$T^i = \frac{P^i_{1T}}{P_{1T}}\, S_1(P_{1T}) \tag{D.6}$$

$$T^{ij} = \frac{P^i_{1T} P^j_{1T}}{P^2_{1T}}\, S_2(P_{1T}) + \delta^{ij}\, S_3(P_{1T}) \tag{D.7}$$

$$T^{ijk} = \frac{P^i_{1T} P^j_{1T} P^k_{1T}}{P^3_{1T}}\, S_4(P_{1T}) + \frac{1}{P_{1T}}\left(P^i_{1T}\delta^{jk} + P^j_{1T}\delta^{ik} + P^k_{1T}\delta^{ij}\right) S_5(P_{1T}) \tag{D.8}$$

$$\begin{aligned} T^{ijkl} = {} & \frac{P^i_{1T} P^j_{1T} P^k_{1T} P^l_{1T}}{P^4_{1T}}\, S_6(P_{1T}) + \frac{1}{P^2_{1T}}\left(P^k_{1T}P^l_{1T}\delta^{ij} + P^l_{1T}P^j_{1T}\delta^{ik} + P^k_{1T}P^j_{1T}\delta^{il} + P^i_{1T}P^l_{1T}\delta^{jk}\right. \\ & \left. + P^i_{1T}P^k_{1T}\delta^{jl} + P^i_{1T}P^j_{1T}\delta^{kl}\right) S_7(P_{1T}) + \left(\delta^{ij}\delta^{kl} + \delta^{il}\delta^{jk} + \delta^{ik}\delta^{jl}\right) S_8(P_{1T})\,, \end{aligned} \tag{D.9}$$

where the tensorial structure is given by the components of $\boldsymbol{P}_{1T}$

$$P^X_{1T} = P_{1T}\cos\phi_1\,;\; P^Y_{1T} = P_{1T}\sin\phi_1 \tag{D.10}$$

while S_1–S_8 are eight scalar functions which can only depend on P_{1T} (modulus), and can be determined directly by contracting Eqs. (D.6)-(D.9) with suitable symmetric tensorial structures. One then finds

$$S_1(P_{1T}) = \frac{1}{P_{1T}} \int d^2\boldsymbol{p}_{\perp 2}\, (\boldsymbol{p}_{\perp 2}\cdot\hat{\boldsymbol{P}}_{1T})\, \Delta D^{h_1}\, \Delta D^{h_2} \tag{D.11}$$

$$S_2(P_{1T}) = \frac{1}{P^2_{1T}} \int d^2\boldsymbol{p}_{\perp 2}\, [2(\boldsymbol{p}_{\perp 2}\cdot\hat{\boldsymbol{P}}_{1T})^2 - p^2_{\perp 2}]\, \Delta D^{h_1}\, \Delta D^{h_2} \tag{D.12}$$

$$S_3(P_{1T}) = \frac{1}{P^2_{1T}} \int d^2\boldsymbol{p}_{\perp 2}\, [p^2_{\perp 2} - (\boldsymbol{p}_{\perp 2}\cdot\hat{\boldsymbol{P}}_{1T})^2]\, \Delta D^{h_1}\, \Delta D^{h_2} \tag{D.13}$$

$$S_4(P_{1T}) = \frac{1}{P_{1T}^3}\int d^2\boldsymbol{p}_{\perp 2}\,[4(\boldsymbol{p}_{\perp 2}\cdot\hat{\boldsymbol{P}}_{1T})^3 - 3p_{\perp 2}^2(\boldsymbol{p}_{\perp 2}\cdot\hat{\boldsymbol{P}}_{1T})]\,\Delta D^{h_1}\,\Delta D^{h_2} \tag{D.14}$$

$$S_5(P_{1T}) = \frac{1}{P_{1T}^3}\int d^2\boldsymbol{p}_{\perp 2}\,[p_{\perp 2}^2(\boldsymbol{p}_{\perp 2}\cdot\hat{\boldsymbol{P}}_{1T}) - (\boldsymbol{p}_{\perp 2}\cdot\hat{\boldsymbol{P}}_{1T})^3]\,\Delta D^{h_1}\,\Delta D^{h_2} \tag{D.15}$$

$$S_6(P_{1T}) = \frac{1}{P_{1T}^4}\int d^2\mathbf{p}_{\perp 2}\Big[8(\boldsymbol{p}_{\perp 2}\cdot\hat{\boldsymbol{P}}_{1T})^4 - 8(\boldsymbol{p}_{\perp 2}\cdot\hat{\boldsymbol{P}}_{1T})^2\,p_{\perp 2}^2 + p_{\perp 2}^4\Big]\,\Delta D^{h_1}\,\Delta D^{h_2} \tag{D.16}$$

$$S_7(P_{1T}) = \frac{1}{3P_{1T}^4}\int d^2\boldsymbol{p}_{\perp 2}\Big[-4(\boldsymbol{p}_{\perp 2}\cdot\hat{\boldsymbol{P}}_{1T})^4 + 5(\boldsymbol{p}_{\perp 2}\cdot\hat{\boldsymbol{P}}_{1T})^2\,p_{\perp 2}^2 - p_{\perp 2}^4\Big]\,\Delta D^{h_1}\,\Delta D^{h_2} \tag{D.17}$$

$$S_8(P_{1T}) = \frac{1}{3P_{1T}^4}\int d^2\boldsymbol{p}_{\perp 2}\Big[(\boldsymbol{p}_{\perp 2}\cdot\hat{\boldsymbol{P}}_{1T})^4 - 2(\boldsymbol{p}_{\perp 2}\cdot\hat{\boldsymbol{P}}_{1T})^2\,p_{\perp 2}^2 + p_{\perp 2}^4\Big]\,\Delta D^{h_1}\,\Delta D^{h_2}\,. \tag{D.18}$$

From the above relations we can get

$$\int d^2\boldsymbol{p}_{\perp 2}\,\cos\varphi_2\,\Delta D^{h_1}\,\Delta D^{h_2} = \cos\phi_1\int d^2\boldsymbol{p}_{\perp 2}\,(\hat{\boldsymbol{p}}_{\perp 2}\cdot\hat{\boldsymbol{P}}_{1T})\,\Delta D^{h_1}\,\Delta D^{h_2} \tag{D.19}$$

$$\int d^2\boldsymbol{p}_{\perp 2}\,\sin\varphi_2\,\Delta D^{h_1}\,\Delta D^{h_2} = \sin\phi_1\int d^2\boldsymbol{p}_{\perp 2}\,(\hat{\boldsymbol{p}}_{\perp 2}\cdot\hat{\boldsymbol{P}}_{1T})\,\Delta D^{h_1}\,\Delta D^{h_2} \tag{D.20}$$

$$\begin{aligned}&\int d^2\boldsymbol{p}_{\perp 2}\,\cos^2\varphi_2\,\Delta D^{h_1}\,\Delta D^{h_2}\\ &\quad= \frac{1}{2}\int d^2\boldsymbol{p}_{\perp 2}\Big\{1+\cos 2\phi_1\,[2(\hat{\boldsymbol{p}}_{\perp 2}\cdot\hat{\boldsymbol{P}}_{1T})^2 - 1]\Big\}\,\Delta D^{h_1}\,\Delta D^{h_2}\end{aligned} \tag{D.21}$$

$$\begin{aligned}&\int d^2\boldsymbol{p}_{\perp 2}\,\sin^2\varphi_2\,\Delta D^{h_1}\,\Delta D^{h_2}\\ &\quad= \frac{1}{2}\int d^2\boldsymbol{p}_{\perp 2}\Big\{1-\cos 2\phi_1\,[2(\hat{\boldsymbol{p}}_{\perp 2}\cdot\hat{\boldsymbol{P}}_{1T})^2 - 1]\Big\}\,\Delta D^{h_1}\,\Delta D^{h_2}\end{aligned} \tag{D.22}$$

$$\int d^2\boldsymbol{p}_{\perp 2}\, \cos\varphi_2\, \sin\varphi_2\, \Delta D^{h_1}\, \Delta D^{h_2}$$
$$= \cos\phi_1\, \sin\phi_1 \int d^2\boldsymbol{p}_{\perp 2}\, [2(\hat{\boldsymbol{p}}_{\perp 2}\cdot\hat{\boldsymbol{P}}_{1T})^2 - 1]\, \Delta D^{h_1}\, \Delta D^{h_2} \tag{D.23}$$

$$\int d^2\boldsymbol{p}_{\perp 2}\, \cos^3\varphi_2\, \Delta D^{h_1}\, \Delta D^{h_2}$$
$$= \cos^3\phi_1 \int d^2\boldsymbol{p}_{\perp 2}\, [4(\hat{\boldsymbol{p}}_{\perp 2}\cdot\hat{\boldsymbol{P}}_{1T})^3 - 3(\hat{\boldsymbol{p}}_{\perp 2}\cdot\hat{\boldsymbol{P}}_{1T})]\, \Delta D^{h_1}\, \Delta D^{h_2}$$
$$+ 3\cos\phi_1 \int d^2\boldsymbol{p}_{\perp 2}\, [(\hat{\boldsymbol{p}}_{\perp 2}\cdot\hat{\boldsymbol{P}}_{1T}) - (\hat{\boldsymbol{p}}_{\perp 2}\cdot\hat{\boldsymbol{P}}_{1T})^3]\, \Delta D^{h_1}\, \Delta D^{h_2} \tag{D.24}$$

$$\int d^2\boldsymbol{p}_{\perp 2}\, \sin^3\varphi_2\, \Delta D^{h_1}\, \Delta D^{h_2}$$
$$= \sin^3\phi_1 \int d^2\boldsymbol{p}_{\perp 2}\, [4(\hat{\boldsymbol{p}}_{\perp 2}\cdot\hat{\boldsymbol{P}}_{1T})^3 - 3(\hat{\boldsymbol{p}}_{\perp 2}\cdot\hat{\boldsymbol{P}}_{1T})]\, \Delta D^{h_1}\, \Delta D^{h_2}$$
$$+ 3\sin\phi_1 \int d^2\boldsymbol{p}_{\perp 2}\, [(\hat{\boldsymbol{p}}_{\perp 2}\cdot\hat{\boldsymbol{P}}_{1T}) - (\hat{\boldsymbol{p}}_{\perp 2}\cdot\hat{\boldsymbol{P}}_{1T})^3]\, \Delta D^{h_1}\, \Delta D^{h_2} \tag{D.25}$$

$$\int d^2\boldsymbol{p}_{\perp 2}\, \cos^2\varphi_2 \sin\varphi_2\, \Delta D^{h_1}\, \Delta D^{h_2}$$
$$= \cos^2\phi_1 \sin\phi_1 \int d^2\boldsymbol{p}_{\perp 2}\, [4(\hat{\boldsymbol{p}}_{\perp 2}\cdot\hat{\boldsymbol{P}}_{1T})^3 - 3(\hat{\boldsymbol{p}}_{\perp 2}\cdot\hat{\boldsymbol{P}}_{1T})]\, \Delta D^{h_1}\, \Delta D^{h_2}$$
$$+ \sin\phi_1 \int d^2\boldsymbol{p}_{\perp 2}\, [(\hat{\boldsymbol{p}}_{\perp 2}\cdot\hat{\boldsymbol{P}}_{1T}) - (\hat{\boldsymbol{p}}_{\perp 2}\cdot\hat{\boldsymbol{P}}_{1T})^3]\, \Delta D^{h_1}\, \Delta D^{h_2} \tag{D.26}$$

$$\int d^2\boldsymbol{p}_{\perp 2}\, \cos\varphi_2 \sin^2\varphi_2\, \Delta D^{h_1}\, \Delta D^{h_2}$$
$$= \cos\phi_1 \sin^2\phi_1 \int d^2\boldsymbol{p}_{\perp 2}\, [4(\hat{\boldsymbol{p}}_{\perp 2}\cdot\hat{\boldsymbol{P}}_{1T})^3 - 3(\hat{\boldsymbol{p}}_{\perp 2}\cdot\hat{\boldsymbol{P}}_{1T})]\, \Delta D^{h_1}\, \Delta D^{h_2}$$
$$+ \cos\phi_1 \int d^2\boldsymbol{p}_{\perp 2}\, [(\hat{\boldsymbol{p}}_{\perp 2}\cdot\hat{\boldsymbol{P}}_{1T}) - (\hat{\boldsymbol{p}}_{\perp 2}\cdot\hat{\boldsymbol{P}}_{1T})^3]\, \Delta D^{h_1}\, \Delta D^{h_2} \tag{D.27}$$

$$
\begin{aligned}
&\int d^2\boldsymbol{p}_{\perp 2}\,\sin^4\varphi_2\,\Delta D^{h_1}\,\Delta D^{h_2}\\
&\quad=\sin^4\phi_1\int d^2\boldsymbol{p}_{\perp 2}\Big[8\big(\hat{\boldsymbol{p}}_{\perp 2}\cdot\hat{\boldsymbol{P}}_{1T}\big)^4-8\big(\hat{\boldsymbol{p}}_{\perp 2}\cdot\hat{\boldsymbol{P}}_{1T}\big)^2+1\Big]\,\Delta D^{h_1}\,\Delta D^{h_2}\\
&\quad+2\sin^2\phi_1\int d^2\boldsymbol{p}_{\perp 2}\Big[-4\big(\hat{\boldsymbol{p}}_{\perp 2}\cdot\hat{\boldsymbol{P}}_{1T}\big)^4+5\big(\hat{\boldsymbol{p}}_{\perp 2}\cdot\hat{\boldsymbol{P}}_{1T}\big)^2-1\Big]\,\Delta D^{h_1}\,\Delta D^{h_2}\\
&\quad+\int d^2\boldsymbol{p}_{\perp 2}\Big[\big(\hat{\boldsymbol{p}}_{\perp 2}\cdot\hat{\boldsymbol{P}}_{1T}\big)^4-2\big(\hat{\boldsymbol{p}}_{\perp 2}\cdot\hat{\boldsymbol{P}}_{1T}\big)^2+1\Big]\,\Delta D^{h_1}\,\Delta D^{h_2}
\end{aligned}
\tag{D.28}
$$

$$
\begin{aligned}
&\int d^2\boldsymbol{p}_{\perp 2}\,\cos^4\varphi_2\,\Delta D^{h_1}\,\Delta D^{h_2}\\
&\quad=\cos^4\phi_1\int d^2\boldsymbol{p}_{\perp 2}\Big[8\big(\hat{\boldsymbol{p}}_{\perp 2}\cdot\hat{\boldsymbol{P}}_{1T}\big)^4-8\big(\hat{\boldsymbol{p}}_{\perp 2}\cdot\hat{\boldsymbol{P}}_{1T}\big)^2+1\Big]\,\Delta D^{h_1}\,\Delta D^{h_2}\\
&\quad+2\cos^2\phi_1\int d^2\boldsymbol{p}_{\perp 2}\Big[-4\big(\hat{\boldsymbol{p}_{\perp 2}}\cdot\hat{\boldsymbol{P}}_{1T}\big)^4+5\big(\hat{\boldsymbol{p}}_{\perp 2}\cdot\hat{\boldsymbol{P}}_{1T}\big)^2-1\Big]\,\Delta D^{h_1}\,\Delta D^{h_2}\\
&\quad+\int d^2\boldsymbol{p}_{\perp 2}\Big[\big(\hat{\boldsymbol{p}}_{\perp 2}\cdot\hat{\boldsymbol{P}}_{1T}\big)^4-2\big(\hat{\boldsymbol{p}}_{\perp 2}\cdot\hat{\boldsymbol{P}}_{1T}\big)^2+1\Big]\,\Delta D^{h_1}\,\Delta D^{h_2}
\end{aligned}
\tag{D.29}
$$

$$
\begin{aligned}
&\int d^2\boldsymbol{p}_{\perp 2}\,\cos^2\varphi_2\sin^2\varphi_2\,\Delta D^{h_1}\,\Delta D^{h_2}\\
&\quad=\cos^2\phi_1\sin^2\phi_1\int d^2\boldsymbol{p}_{\perp 2}\Big[8\big(\hat{\boldsymbol{p}}_{\perp 2}\cdot\hat{\boldsymbol{P}}_{1T}\big)^4-8\big(\hat{\boldsymbol{p}}_{\perp 2}\cdot\hat{\boldsymbol{P}}_{1T}\big)^2+1\Big]\,\Delta D^{h_1}\,\Delta D^{h_2}\\
&\quad+\int d^2\boldsymbol{p}_{\perp 2}\Big[-\big(\hat{\boldsymbol{p}}_{\perp 2}\cdot\hat{\boldsymbol{P}}_{1T}\big)^4+\big(\hat{\boldsymbol{p}}_{\perp 2}\cdot\hat{\boldsymbol{P}}_{1T}\big)^2\Big]\,\Delta D^{h_1}\,\Delta D^{h_2}
\end{aligned}
\tag{D.30}
$$

$$
\begin{aligned}
&\int d^2\boldsymbol{p}_{\perp 2}\,\cos\varphi_2\sin^3\varphi_2\,\Delta D^{h_1}\,\Delta D^{h_2}\\
&\quad=\cos\phi_1\sin^3\phi_1\int d^2\boldsymbol{p}_{\perp 2}\Big[8\big(\hat{\boldsymbol{p}}_{\perp 2}\cdot\hat{\boldsymbol{P}}_{1T}\big)^4-8\big(\hat{\boldsymbol{p}}_{\perp 2}\cdot\hat{\boldsymbol{P}}_{1T}\big)^2+1\Big]\,\Delta D^{h_1}\,\Delta D^{h_2}\\
&\quad+\cos\phi_1\sin\phi_1\int d^2\boldsymbol{p}_{\perp 2}\Big[-4\big(\hat{\boldsymbol{p}}_{\perp 2}\cdot\hat{\boldsymbol{P}}_{1T}\big)^4+5\big(\hat{\boldsymbol{p}}_{\perp 2}\cdot\hat{\boldsymbol{P}}_{1T}\big)^2-1\Big]\,\Delta D^{h_1}\,\Delta D^{h_2}
\end{aligned}
\tag{D.31}
$$

$$\begin{aligned}
&\int d^2\boldsymbol{p}_{\perp 2}\, \cos^3\varphi_2 \sin\varphi_2\, \Delta D^{h_1}\, \Delta D^{h_2} \\
&\quad = \cos^3\phi_1 \sin\phi_1 \int d^2\boldsymbol{p}_{\perp 2}\Big[8\big(\hat{\boldsymbol{p}}_{\perp 2}\cdot\hat{\boldsymbol{P}}_{1T}\big)^4 - 8\big(\hat{\boldsymbol{p}}_{\perp 2}\cdot\hat{\boldsymbol{P}}_{1T}\big)^2 + 1\Big]\, \Delta D^{h_1}\, \Delta D^{h_2} \\
&\quad + \cos\phi_1 \sin\phi_1 \int d^2\boldsymbol{p}_{\perp 2}\Big[-4\big(\hat{\boldsymbol{p}}_{\perp 2}\cdot\hat{\boldsymbol{P}}_{1T}\big)^4 + 5\big(\hat{\boldsymbol{p}}_{\perp 2}\cdot\hat{\boldsymbol{P}}_{1T}\big)^2 - 1\Big]\, \Delta D^{h_1}\, \Delta D^{h_2}\,.
\end{aligned} \tag{D.32}$$

We can then reconstruct directly the following quantities appearing in Section 2.5:

$$\int d^2\boldsymbol{p}_{\perp 2}\, \cos(2\varphi_2)\, \Delta D^{h_1}\, \Delta D^{h_2} = \cos(2\phi_1) \int d^2\boldsymbol{p}_{\perp 2}\, [2(\hat{\boldsymbol{p}}_{\perp 2}\cdot\hat{\boldsymbol{P}}_{1T})^2 - 1]\, \Delta D^{h_1}\, \Delta D^{h_2} \tag{D.33}$$

$$\int d^2\boldsymbol{p}_{\perp 2}\, \sin(2\varphi_2)\, \Delta D^{h_1}\, \Delta D^{h_2} = \sin(2\phi_1) \int d^2\boldsymbol{p}_{\perp 2}\, [2(\hat{\boldsymbol{p}}_{\perp 2}\cdot\hat{\boldsymbol{P}}_{1T})^2 - 1]\, \Delta D^{h_1}\, \Delta D^{h_2} \tag{D.34}$$

$$\begin{aligned}
&\int d^2\boldsymbol{p}_{\perp 2}\, \cos(3\varphi_2)\, \Delta D^{h_1}\, \Delta D^{h_2} \\
&\quad = \cos(3\phi_1) \int d^2\boldsymbol{p}_{\perp 2}\, [4(\hat{\boldsymbol{p}}_{\perp 2}\cdot\hat{\boldsymbol{P}}_{1T})^3 - 3(\hat{\boldsymbol{p}}_{\perp 2}\cdot\hat{\boldsymbol{P}}_{1T})]\, \Delta D^{h_1}\, \Delta D^{h_2}
\end{aligned} \tag{D.35}$$

$$\begin{aligned}
&\int d^2\boldsymbol{p}_{\perp 2}\, \sin(3\varphi_2)\, \Delta D^{h_1}\, \Delta D^{h_2} \\
&\quad = \sin(3\phi_1) \int d^2\boldsymbol{p}_{\perp 2}\, [4(\hat{\boldsymbol{p}}_{\perp 2}\cdot\hat{\boldsymbol{P}}_{1T})^3 - 3(\hat{\boldsymbol{p}}_{\perp 2}\cdot\hat{\boldsymbol{P}}_{1T})]\, \Delta D^{h_1}\, \Delta D^{h_2}
\end{aligned} \tag{D.36}$$

$$\begin{aligned}
&\int d^2\boldsymbol{p}_{\perp 2}\, \cos(4\varphi_2)\, \Delta D^{h_1}\, \Delta D^{h_2} \\
&\quad = \cos(4\phi_1) \int d^2\boldsymbol{p}_{\perp 2}\Big[8\big(\hat{\boldsymbol{p}}_{\perp 2}\cdot\hat{\boldsymbol{P}}_{1T}\big)^4 - 8\big(\hat{\boldsymbol{p}}_{\perp 2}\cdot\hat{\boldsymbol{P}}_{1T}\big)^2 + 1\Big]\, \Delta D^{h_1}\, \Delta D^{h_2}
\end{aligned} \tag{D.37}$$

$$\begin{aligned}
&\int d^2\boldsymbol{p}_{\perp 2}\, \sin(4\varphi_2)\, \Delta D^{h_1}\, \Delta D^{h_2} \\
&\quad = \sin(4\phi_1) \int d^2\boldsymbol{p}_{\perp 2}\Big[8\big(\hat{\boldsymbol{p}}_{\perp 2}\cdot\hat{\boldsymbol{P}}_{1T}\big)^4 - 8\big(\hat{\boldsymbol{p}}_{\perp 2}\cdot\hat{\boldsymbol{P}}_{1T}\big)^2 + 1\Big]\, \Delta D^{h_1}\, \Delta D^{h_2}\,.
\end{aligned} \tag{D.38}$$

Appendix E.

Helicity frames

Our physical observables are computed in two kinematical configurations, the thrust and the hadron frames, with axes denoted by $\hat{\boldsymbol{x}}_L$, $\hat{\boldsymbol{y}}_L$, and $\hat{\boldsymbol{z}}_L$, where we use L to indicate a generic laboratory (LAB) frame. The helicity frame of a particle with momentum $\boldsymbol{p}$ along the direction $\hat{\boldsymbol{p}} = (\sin\theta\cos\varphi,\, \sin\theta\sin\varphi,\, \cos\theta)$ – *as defined in the laboratory frame* – can be reached by performing the rotations [80]

$$R(\varphi,\theta,0) = R_{y'}(\theta)\, R_{z_L}(\varphi)\,. \tag{E.1}$$

The first is a rotation by an angle φ around the $\hat{\boldsymbol{z}}_L$-axis and the second is a rotation by an angle θ around the new (that is, obtained after the first rotation) $\hat{\boldsymbol{y}}'$-axis. This means

$$a)\ \hat{\boldsymbol{z}} = \hat{\boldsymbol{p}} \qquad b)\ \hat{\boldsymbol{y}} = \frac{\hat{\boldsymbol{z}}_L \times \hat{\boldsymbol{p}}}{|\hat{\boldsymbol{z}}_L \times \hat{\boldsymbol{p}}|} = \hat{\boldsymbol{z}}_L \times \hat{\boldsymbol{p}}_\perp \qquad c)\ \hat{\boldsymbol{x}} = \hat{\boldsymbol{y}} \times \hat{\boldsymbol{z}}\,. \tag{E.2}$$

In the present study we are interested in the helicity frames of the final quark/antiquark as well as those of the two hadrons coming from their fragmentation. Let us describe them, starting from the relations between the parent quark and the corresponding hadron helicity frames and then focusing separately on the two configurations for a process $e^+(k^+)e^-(k^-) \to c(q_1)\, d(q_2) \to h_1(P_{h_1})h_2(P_{h_2})\, X$.

The helicity frame of a *non-collinear* hadron with momentum

$$\boldsymbol{P}_h = P_h(\sin\theta_h\cos\phi_h, \sin\theta_h\sin\phi_h, \cos\theta_h)\,,$$

as reached from the helicity frame of its parent quark, following the above procedure *a*)-*c*) in Eq. (E.2), is simply given as:

$$\hat{\boldsymbol{Z}}_h = \sin\theta_h\cos\phi_h\,\hat{\boldsymbol{x}} + \sin\theta_h\sin\phi_h\,\hat{\boldsymbol{y}} + \cos\theta_h\,\hat{\boldsymbol{z}} \equiv \hat{\boldsymbol{P}}_h \tag{E.3}$$

$$\hat{\boldsymbol{Y}}_h = -\sin\phi_h\,\hat{\boldsymbol{x}} + \cos\phi_h\,\hat{\boldsymbol{y}} \tag{E.4}$$

$$\hat{\boldsymbol{X}}_h = \cos\theta_h\cos\phi_h\,\hat{\boldsymbol{x}} + \cos\theta_h\sin\phi_h\,\hat{\boldsymbol{y}} - \sin\theta_h\,\hat{\boldsymbol{z}}\,. \tag{E.5}$$

E.1. The thrust frame

In this case the particles c and d move along the $\hat{\boldsymbol{z}}_L$ and $-\hat{\boldsymbol{z}}_L$ direction respectively. This results in the helicity frames with axes along the following directions in the laboratory frame:

$$\hat{\boldsymbol{x}}_c = \hat{\boldsymbol{x}}_L \qquad \hat{\boldsymbol{y}}_c = \hat{\boldsymbol{y}}_L \qquad \hat{\boldsymbol{z}}_c = \hat{\boldsymbol{z}}_L \tag{E.6}$$

for a quark/antiquark c moving along $+\hat{\boldsymbol{z}}_L$, and

$$\hat{\boldsymbol{x}}_d = \hat{\boldsymbol{x}}_L \qquad \hat{\boldsymbol{y}}_d = -\hat{\boldsymbol{y}}_L \qquad \hat{\boldsymbol{z}}_d = -\hat{\boldsymbol{z}}_L \tag{E.7}$$

for a quark/antiquark d moving along $-\hat{\boldsymbol{z}}_L$. From these relations we find that the helicity axes of the hadrons h_1 in the LAB frame as reached from the quark helicity frames are [using Eqs. (E.3)-(E.5) with $h = h_1$ and Eq. (E.6)]

$$\hat{\boldsymbol{Z}}_{h_1} = \sin\theta_{h_1}\cos\phi_{h_1}\,\hat{\boldsymbol{x}}_L + \sin\theta_{h_1}\sin\phi_{h_1}\,\hat{\boldsymbol{y}}_L + \cos\theta_{h_1}\,\hat{\boldsymbol{z}}_L \tag{E.8}$$

$$\hat{\boldsymbol{Y}}_{h_1} = -\sin\phi_{h_1}\,\hat{\boldsymbol{x}}_L + \cos\phi_{h_1}\,\hat{\boldsymbol{y}}_L \tag{E.9}$$

$$\hat{\boldsymbol{X}}_{h_2} = \cos\theta_{h_1}\cos\phi_{h_1}\,\hat{\boldsymbol{x}}_L + \cos\theta_{h_1}\sin\phi_{h_1}\,\hat{\boldsymbol{y}}_L - \sin\theta_{h_1}\,\hat{\boldsymbol{z}}_L \tag{E.10}$$

and the ones for the hadron h_2 [using Eqs. (E.3)-(E.5) with $h = h_2$ and Eq. (E.7)]

$$\hat{\boldsymbol{Z}}_{h_2} = \sin\theta_{h_2}\cos\phi_{h_2}\,\hat{\boldsymbol{x}}_L - \sin\theta_{h_2}\sin\phi_{h_2}\,\hat{\boldsymbol{y}}_L - \cos\theta_{h_2}\,\hat{\boldsymbol{z}}_L \tag{E.11}$$

$$\hat{\boldsymbol{Y}}_{h_2} = -\sin\phi_{h_2}\,\hat{\boldsymbol{x}}_L - \cos\phi_{h_2}\,\hat{\boldsymbol{y}}_L \tag{E.12}$$

$$\hat{\boldsymbol{X}}_{h_2} = \cos\theta_{h_2}\cos\phi_{h_2}\,\hat{\boldsymbol{x}}_L - \cos\theta_{h_2}\sin\phi_{h_2}\,\hat{\boldsymbol{y}}_L + \sin\theta_{h_2}\,\hat{\boldsymbol{z}}_L\,. \tag{E.13}$$

On the other hand, the hadron unit three-momenta as defined in the LAB frame, see Eqs. (2.15) and (2.16), are

$$\hat{\boldsymbol{P}}_{h_1} = \hat{\boldsymbol{Z}}_{h_1} = \frac{2\eta_{\perp 1}}{z_{p_1}}\cos\varphi_1\,\hat{\boldsymbol{x}}_L + \frac{2\eta_{\perp 1}}{z_{p_1}}\sin\varphi_1\,\hat{\boldsymbol{y}}_L + \beta_1\,\hat{\boldsymbol{z}}_L \tag{E.14}$$

$$\hat{\boldsymbol{P}}_{h_2} = \hat{\boldsymbol{Z}}_{h_2} = \frac{2\eta_{\perp 2}}{z_{p_2}}\cos\varphi_2\,\hat{\boldsymbol{x}}_L + \frac{2\eta_{\perp 2}}{z_{p_2}}\sin\varphi_2\,\hat{\boldsymbol{y}}_L - \beta_2\,\hat{\boldsymbol{z}}_L\,. \tag{E.15}$$

By a direct comparison between Eqs. (E.8) and (E.14) and between Eqs. (E.11) and (E.15) we then get

$$\phi_{h_1} = \varphi_1 \qquad\qquad \phi_{h_2} = 2\pi - \varphi_2\,. \tag{E.16}$$

E.2. The hadron frame

In the hadron frame the unit vectors specifying the helicity frames of the two particles c and d, as reached from the laboratory frame are:

$$\hat{\boldsymbol{z}}_c = \frac{2\eta_{\perp 2}}{z_{p_2}}\cos\varphi_2\,\hat{\boldsymbol{x}}_L + \frac{2\eta_{\perp 2}}{z_{p_2}}\sin\varphi_2\,\hat{\boldsymbol{y}}_L + \beta_2\,\hat{\boldsymbol{z}}_L \tag{E.17}$$

$$\hat{\boldsymbol{y}}_c = -\sin\varphi_2\,\hat{\boldsymbol{x}}_L + \cos\varphi_2\,\hat{\boldsymbol{y}}_L \tag{E.18}$$

$$\hat{\boldsymbol{x}}_c = \beta_2\cos\varphi_2\,\hat{\boldsymbol{x}}_L + \beta_2\sin\varphi_2\,\hat{\boldsymbol{y}}_L - \frac{2\eta_{\perp 2}}{z_{p_2}}\,\hat{\boldsymbol{z}}_L \tag{E.19}$$

$$\hat{\boldsymbol{z}}_d = -\frac{2\eta_{\perp 2}}{z_{p_2}}\cos\varphi_2\,\hat{\boldsymbol{x}}_L - \frac{2\eta_{\perp 2}}{z_{p_2}}\sin\varphi_2\,\hat{\boldsymbol{y}}_L - \beta_2\,\hat{\boldsymbol{z}}_L \tag{E.20}$$

$$\hat{\boldsymbol{y}}_d = \sin\varphi_2\,\hat{\boldsymbol{x}}_L - \cos\varphi_2\,\hat{\boldsymbol{y}}_L \tag{E.21}$$

$$\hat{\boldsymbol{x}}_d = \beta_2\cos\varphi_2\,\hat{\boldsymbol{x}}_L + \beta_2\sin\varphi_2\,\hat{\boldsymbol{y}}_L - \frac{2\eta_{\perp 2}}{z_{p_2}}\,\hat{\boldsymbol{z}}_L\,, \tag{E.22}$$

where we started from the quark-antiquark directions in the LAB frame as defined in Eqs. (2.18) and (2.19) and, then we applied the standard procedure to identify the other two axes (see Eq. (E.2)).

From the above relations one can get the expressions of the hadron helicity axes as reached from the parton helicity ones in the LAB frame. In particular, for the Z axes we find

$$\begin{aligned}\hat{\boldsymbol{Z}}_{h_1} = &\left(\sin\theta_{h_1}(\beta_2\cos\phi_{h_1}\cos\varphi_2 - \sin\phi_{h_1}\sin\varphi_2) + \frac{2\eta_{\perp 2}}{z_{p_2}}\cos\theta_{h_1}\cos\varphi_2\right)\hat{\boldsymbol{x}}_L \\ &+\left(\sin\theta_{h_1}(\beta_2\cos\phi_{h_1}\sin\varphi_2 + \sin\phi_{h_1}\cos\varphi_2) + \frac{2\eta_{\perp 2}}{z_{p_2}}\cos\theta_{h_1}\sin\varphi_2\right)\hat{\boldsymbol{y}}_L \\ &-\left(\frac{2\eta_{\perp 2}}{z_{p_2}}\sin\theta_{h_1}\cos\phi_{h_1} - \beta_2\cos\theta_{h_1}\right)\hat{\boldsymbol{z}}_L \end{aligned} \tag{E.23}$$

$$\begin{aligned}\hat{\boldsymbol{Z}}_{h_2} = &\left(\sin\theta_{h_2}(\beta_2\cos\phi_{h_2}\cos\varphi_2 + \sin\phi_{h_2}\sin\varphi_2) - \frac{2\eta_{\perp 2}}{z_{p_2}}\cos\theta_{h_2}\cos\varphi_2\right)\hat{\boldsymbol{x}}_L \\ &+\left(\sin\theta_{h_2}(\beta_2\cos\phi_{h_2}\sin\varphi_2 - \sin\phi_{h_2}\cos\varphi_2) - \frac{2\eta_{\perp 2}}{z_{p_2}}\cos\theta_{h_2}\sin\varphi_2\right)\hat{\boldsymbol{y}}_L \\ &-\left(\frac{2\eta_{\perp 2}}{z_{p_2}}\sin\theta_{h_2}\cos\phi_{h_2} + \beta_2\cos\theta_{h_2}\right)\hat{\boldsymbol{z}}_L\,, \end{aligned} \tag{E.24}$$

that have to be compared with the corresponding expressions in the LAB frame, coming from Eqs. (2.20) and (2.17),

$$\hat{\boldsymbol{Z}}_{h_1} = \frac{2\eta_{1T}}{z_{p_1}}\cos\phi_1\,\hat{\boldsymbol{x}}_L + \frac{2\eta_{1T}}{z_{p_1}}\sin\phi_1\,\hat{\boldsymbol{y}}_L + \sqrt{1 - \frac{4\eta_{1T}^2}{z_{p_1}^2}}\,\hat{\boldsymbol{z}}_L \tag{E.25}$$

$$\hat{\boldsymbol{Z}}_{h_2} = -\hat{\boldsymbol{z}}_L\,. \tag{E.26}$$

By using

$$\sin\theta_{h_{1,2}} = \frac{2\eta_{\perp 1,2}}{z_{p_{1,2}}}\,, \tag{E.27}$$

after some algebra we get

$$\cos\phi_{h_1} = \frac{\eta_{1T}}{\eta_{\perp 1}}\beta_2\cos(\phi_1-\varphi_2) - \frac{\eta_{\perp 2}}{\eta_{\perp 1}}\frac{z_{p_1}}{z_{p_2}}\sqrt{1-\frac{4\eta_{1T}^2}{z_{p_1}^2}} \simeq \frac{P_{1T}}{p_{\perp 1}}\cos(\phi_1-\varphi_2) - \frac{p_{\perp 2}}{p_{\perp 1}}\frac{z_{p_1}}{z_{p_2}} \tag{E.28}$$

$$\sin\phi_{h_1} = \frac{\eta_{1T}}{\eta_{\perp 1}}\sin(\phi_1-\varphi_2) = \frac{P_{1T}}{p_{\perp 1}}\sin(\phi_1-\varphi_2)\,, \tag{E.29}$$

together with $\phi_{h_2} = 0$.

For their role we give here the explicit expressions of the helicity axes of the hadrons h_1 and h_2 in terms of the variables in the LAB frame

$$\begin{aligned}\hat{\boldsymbol{Z}}_{h_1} &= \frac{2\eta_{1T}}{z_{p_1}}\cos\phi_1\,\hat{\boldsymbol{x}}_L + \frac{2\eta_{1T}}{z_{p_1}}\sin\phi_1\,\hat{\boldsymbol{y}}_L + \sqrt{1-\frac{4\eta_{1T}^2}{z_{p_1}^2}}\,\hat{\boldsymbol{z}}_L \\ &\simeq \frac{2\eta_{1T}}{z_{p_1}}\cos\phi_1\,\hat{\boldsymbol{x}}_L + \frac{2\eta_{1T}}{z_{p_1}}\sin\phi_1\,\hat{\boldsymbol{y}}_L + \hat{\boldsymbol{z}}_L \simeq \hat{\boldsymbol{z}}_L \end{aligned} \tag{E.30}$$

$$\hat{\boldsymbol{Y}}_{h_1} \simeq \Big(\frac{z_{p_1}}{z_{p_2}}\frac{p_{\perp 2}}{p_{\perp 1}}\sin\varphi_2 - \frac{P_{1T}}{p_{\perp 1}}\sin\phi_1\Big)\,\hat{\boldsymbol{x}}_L + \Big(\frac{P_{1T}}{p_{\perp 1}}\cos\phi_1 - \frac{z_{p_1}}{z_{p_2}}\frac{p_{\perp 2}}{p_{\perp 1}}\cos\varphi_2\Big)\,\hat{\boldsymbol{y}}_L \tag{E.31}$$

$$\hat{\boldsymbol{X}}_{h_1} \simeq \Big(\frac{P_{1T}}{p_{\perp 1}}\cos\phi_1 - \frac{z_{p_1}}{z_{p_2}}\frac{p_{\perp 2}}{p_{\perp 1}}\cos\varphi_2\Big)\,\hat{\boldsymbol{x}}_L + \Big(\frac{P_{1T}}{p_{\perp 1}}\sin\phi_1 - \frac{z_{p_1}}{z_{p_2}}\frac{p_{\perp 2}}{p_{\perp 1}}\sin\varphi_2\Big)\,\hat{\boldsymbol{y}}_L \tag{E.32}$$

$$\hat{\boldsymbol{Z}}_{h_2} = -\hat{\boldsymbol{z}}_L \tag{E.33}$$

$$\hat{\boldsymbol{Y}}_{h_2} = \sin\varphi_2\,\hat{\boldsymbol{x}}_L - \cos\varphi_2\,\hat{\boldsymbol{y}}_L \tag{E.34}$$

$$\hat{\boldsymbol{X}}_{h_2} = \cos\varphi_2\,\hat{\boldsymbol{x}}_L + \sin\varphi_2\,\hat{\boldsymbol{y}}_L\,. \tag{E.35}$$

Notice that, while the $\hat{\boldsymbol{Z}}_{h_1}$ axis does not involve any intrinsic transverse momentum dependence, special care, when carrying out the integration over the unobserved variables, is due for the transverse axes. Moreover, at the lowest order in η_{1T} the $\hat{\boldsymbol{Z}}_{h_1}$ axis almost coincides with the $\hat{\boldsymbol{z}}_L$ one.

Before concluding this section we warn the reader that the hadron helicity frames obtained directly from the LAB frame, without passing through the parton helicity frame, give a different result where, while the $\hat{\boldsymbol{Z}}$ axes coincide, the $\hat{\boldsymbol{X}}$ and $\hat{\boldsymbol{Y}}$ axes are rotated:

$$\hat{\boldsymbol{Z}}_{h_1}^{\mathrm{LAB}} = \frac{2\eta_{1T}}{z_{p_1}} \cos\phi_1 \, \hat{\boldsymbol{x}}_L + \frac{2\eta_{1T}}{z_{p_1}} \sin\phi_1 \, \hat{\boldsymbol{y}}_L + \sqrt{1 - \frac{4\eta_{1T}^2}{z_{p_1}^2}} \, \hat{\boldsymbol{z}}_L \tag{E.36}$$

$$\hat{\boldsymbol{Y}}_{h_1}^{\mathrm{LAB}} = -\sin\phi_1 \, \hat{\boldsymbol{x}}_L + \cos\phi_1 \, \hat{\boldsymbol{y}}_L = \hat{\boldsymbol{n}} \tag{E.37}$$

$$\hat{\boldsymbol{X}}_{h_1}^{\mathrm{LAB}} = \sqrt{1 - \frac{4\eta_{1T}^2}{z_{p_1}^2}} \cos\phi_1 \, \hat{\boldsymbol{x}}_L + \sqrt{1 - \frac{4\eta_{1T}^2}{z_{p_1}^2}} \cos\phi_1 \, \hat{\boldsymbol{y}}_L - \frac{2\eta_{1T}}{z_{p_1}} \, \hat{\boldsymbol{z}}_L \tag{E.38}$$

$$\hat{\boldsymbol{Z}}_{h_2}^{\mathrm{LAB}} = -\hat{\boldsymbol{z}}_L \tag{E.39}$$

$$\hat{\boldsymbol{Y}}_{h_2}^{\mathrm{LAB}} = -\hat{\boldsymbol{y}}_L \tag{E.40}$$

$$\hat{\boldsymbol{X}}_{h_2}^{\mathrm{LAB}} = \hat{\boldsymbol{x}}_L \, . \tag{E.41}$$

Appendix F.

Transverse momenta in different frames and kinematic power corrections

Here we derive the relations between the different transverse momenta, presented in Section 5.2, in the hadron frame. To do this, we work in a frame where the two final state hadrons are exactly back-to-back along the $\pm z$ direction, the fragmenting quarks have a transverse momentum with respect to the direction of their own hadrons and the photon has a transverse momentum as well. We label the momenta as follows:

- k is the four-momentum of the quark fragmenting into hadron h_1, with four-momentum P_1 and moving along $-z$;
- p is the four-momentum of the anti-quark fragmenting into the hadron h_2, with four-momentum P_2 and moving along $+z$;
- $\boldsymbol{k}_T$ and $\boldsymbol{p}_T$ are respectively the transverse momenta of the quark and the anti-quark with respect to their hadron momenta, while $\boldsymbol{k}_\perp$ and $\boldsymbol{p}_\perp$ are respectively the transverse momenta of the two hadrons with respect to their parent quark directions of motion;

- q is the four-momentum of the virtual photon and $\boldsymbol{q}_T$ is its transverse component. This one can be related to $\boldsymbol{P}_{1T}$, the transverse momentum of hadron h_1 with respect to the second hadron h_2 (see below).

By adopting light-cone coordinates where for a generic four-vector a, we have

$$a^{\pm} = \frac{a^0 \pm a^3}{\sqrt{2}}, \tag{F.1}$$

we define the quarks and photon momenta as follows [18]:

$$k = \left(\frac{k_T^2}{2k^-}, k^-, \boldsymbol{k}_T\right) \quad \text{where} \quad k_T = |\boldsymbol{k}_T| \tag{F.2}$$

$$p = \left(p^+, \frac{p_T^2}{2p^+}, \boldsymbol{p}_T\right) \quad \text{where} \quad p_T = |\boldsymbol{p}_T| \tag{F.3}$$

$$q = \left(\frac{\widetilde{Q}}{\sqrt{2}}, \frac{\widetilde{Q}}{\sqrt{2}}, \boldsymbol{q}_T\right), \tag{F.4}$$

where $\widetilde{Q}^2 = Q^2 + q_T^2$. Since $k + p = q$, we can find the values of the components of the quark momenta:

$$k^- = \frac{Q}{\sqrt{2}} + \mathcal{O}(q_T^2/Q^2); \qquad k^+ = \frac{k_T^2}{\sqrt{2}Q} + \mathcal{O}(q_T^2/Q^2) \tag{F.5}$$

$$k^0 = \frac{Q}{2}\left(1 + \frac{k_T^2}{2Q^2}\right); \qquad k^3 = -\frac{Q}{2}\left(1 - \frac{k_T^2}{2Q^2}\right) \tag{F.6}$$

$$p^+ = \frac{Q}{\sqrt{2}} + \mathcal{O}(q_T^2/Q^2); \qquad p^- = \frac{p_T^2}{\sqrt{2}Q} + \mathcal{O}(q_T^2/Q^2) \tag{F.7}$$

and that $\boldsymbol{k}_T + \boldsymbol{p}_T = \boldsymbol{q}_T$. Meanwhile the hadron momenta are defined as follows:

$$
\begin{aligned}
P_1 &= \left(\frac{M_1^2}{z_1 Q\sqrt{2}}, \frac{z_1 Q}{\sqrt{2}}, 0 \right) \\
P_2 &= \left(\frac{z_2 Q}{\sqrt{2}}, \frac{M_2^2}{z_2 Q\sqrt{2}}, 0 \right)
\end{aligned}
\tag{F.8}
$$

where we have used the light-cone momentum fractions, defined as:

$$
z_1 = \frac{P_1^-}{k^-}; \qquad z_2 = \frac{P_2^+}{p^+}\,. \tag{F.9}
$$

For massive hadrons we can introduce two further scaling variables: the energy fraction (often adopted in experimental analyses)

$$
z_{h_i} = \frac{P_i^0}{l^0} = z_i \left(1 + \frac{M_i^2}{2 z_i^2 Q^2} \right) \tag{F.10}
$$

and the longitudinal momentum fraction

$$
z_{p_i} = \frac{P_i^3}{l^3} = z_i \left(1 - \frac{M_{h_i}^2}{2 z_i^2 Q^2} \right), \tag{F.11}
$$

where we are keeping terms of order M^2/Q^2 while neglecting terms of order q_T^2/Q^2 or larger. Notice that here l is the four-momenta of the quark fragmenting into the hadron h_i.

Now we can proceed in the derivation of the relations between the transverse momenta. Firstly, we want to move to a frame where the hadron h_1 has a transverse momentum with respect to its parent quark and the quark has zero transverse momentum component. We can reach this with two subsequent rotations: $R_z(\varphi)$ and $R_{y'}(\xi, \lambda)$:

$$R_z(\varphi) = \begin{pmatrix} 1 & 0 & 0 & 0 \\ 0 & \cos\varphi & \sin\varphi & 0 \\ 0 & -\sin\varphi & \cos\varphi & 0 \\ 0 & 0 & 0 & 1 \end{pmatrix} \qquad R_{y'}(\xi,\lambda) = \begin{pmatrix} 1 & 0 & 0 & 0 \\ 0 & \xi & 0 & -\lambda \\ 0 & 0 & 1 & 0 \\ 0 & \lambda & 0 & \xi \end{pmatrix} \tag{F.12}$$

where $\xi^2 + \lambda^2 = 1$. Given that, the quark four-momentum k in the initial frame and k' in the final frame are:

$$k = \begin{pmatrix} k^0 \\ |k_T|\cos\varphi \\ |k_T|\sin\varphi \\ k^3 \end{pmatrix}, \quad k' = R_{y'}(\xi,\lambda)\, R_z(\varphi)\, k = \begin{pmatrix} k^0 \\ 0 \\ 0 \\ -k^0 \end{pmatrix}, \tag{F.13}$$

we have $\xi = -k^3/k^0$ and $\lambda = -k_T/k^0$. Applying the above rotations to the hadron four-momentum in the initial frame

$$P_1 = \begin{pmatrix} P_1^0 \\ 0 \\ 0 \\ P_1^3 \end{pmatrix}, \quad P_1' = R_{y'}(\xi,\lambda)\, R_z(\varphi)\, P_1 = \begin{pmatrix} P_1^0 \\ k_\perp \\ 0 \\ P'^3_1 \end{pmatrix}, \tag{F.14}$$

with

$$P_1^0 = \frac{z_1 Q}{2}\left(1 + \frac{M_i^2}{2z_i^2 Q^2}\right) \tag{F.15}$$

$$P_1^3 = \frac{z_1 Q}{2}\left(1 - \frac{M_i^2}{2z_i^2 Q^2}\right) \tag{F.16}$$

$$P'^3_1 = \xi P_1^3\,, \tag{F.17}$$

we obtain that $\boldsymbol{k}_\perp$, the transverse momentum of the hadron with respect to the direction of its parent quark, follows the relations:

$$|k_\perp| = -\lambda P_1^3 \tag{F.18}$$

$$\boldsymbol{k}_\perp = -\boldsymbol{k}_T z_{p_1}\,, \tag{F.19}$$

and that, for massless hadrons, reduces to the usual $\boldsymbol{k}_T = -\boldsymbol{k}_\perp / z_1$ relation. If we want to find the relation between $\boldsymbol{P}_{1T}$, the transverse momentum of h_1 with respect to h_2, and $\boldsymbol{q}_T$, the transverse momentum of the photon, we can use the following tensor $g_\perp^{\mu\nu}$ [18]:

$$\begin{aligned} g_\perp^{\mu\nu} &= g^{\mu\nu} - \hat{t}^\mu \hat{t}^\nu + \hat{z}^\mu \hat{z}^\nu \\ \hat{t}^\mu &= \frac{q^\mu}{Q} \\ \hat{z}^\mu &= 2\frac{P_2^\mu}{z_{h_2} Q} - \hat{t}^\mu. \end{aligned}$$

By applying the above tensor to the four-momentum of hadron h_1, $P_{1T}^\mu = g_\perp^{\mu\nu} P_{1\nu}$, we find the following relation

$$P_{1T}^\mu = P_1^\mu + P_2^\mu\left(2\frac{z_1}{z_{h_2}} - \frac{z_{h_1}}{z_{h_2}}\right) - z_1 q^\mu\,, \tag{F.20}$$

where we have neglected the mass of the second hadron, $M_{h_2} = 0$. Performing the calculation we find that all components but the transverse one are zero, and

so we can recover the following relation

$$\boldsymbol{P}_{1T} = -z_1 \boldsymbol{q}_T \tag{F.21}$$

where z_1 is the light-cone momentum fraction. This reduces to the usual relation $\boldsymbol{P}_{1T} = -z_{h_1} \boldsymbol{q}_T$ for massless hadrons.

Appendix G.

Convolutions and Fourier transforms

In order to exploit the CSS evolution equations, in Section 5.2 we showed how the convolutions, in k_T-space, can be written in the conjugate $\boldsymbol{b}_T$-space through Fourier transforms of TMD-FFs. We derive here all the steps to write the convolutions in this conjugate space. The first convolution we consider is F_{UU}, defined according to Eq. (5.6)

$$\mathcal{F}[\omega D\bar{D}] = \sum_q e_q^2 \int d^2\boldsymbol{k}_T d^2\boldsymbol{p}_T\, \delta^{(2)}(\boldsymbol{k}_T + \boldsymbol{p}_T - \boldsymbol{q}_T)\, \omega(\boldsymbol{k}_T, \boldsymbol{p}_T) D(z_1, \boldsymbol{k}_\perp) \bar{D}(z_2, \boldsymbol{p}_\perp)\,, \tag{G.1}$$

as follows:

$$F_{UU} = \mathcal{F}[D_1 \bar{D}_1]\,. \tag{G.2}$$

It is trivial to transform this convolution in $\boldsymbol{b}_T$-space employing the Fourier transform definition of the TMD unpolarized fragmentation function:

$$\begin{aligned} \widetilde{D}(z_1, b_T) =& \int d^2\boldsymbol{k}_T\, e^{i\boldsymbol{b}_T\cdot\boldsymbol{k}_T} D_1(z_1, k_\perp) \\ =& 2\pi \int dk_T\, k_T J_0(b_T k_T) D_1(z_1, k_\perp)\,, \end{aligned} \tag{G.3}$$

where we have used the integral representation of J_0, the Bessel function of the first kind

$$\int_0^{2\pi} d\theta \, e^{ib_T k_T \cos\theta} = 2\pi J_0(b_T k_T) \,. \tag{G.4}$$

With the above relations, the F_{UU} convolution in $\boldsymbol{b}_T$-space can be written as:

$$\begin{aligned} F_{UU} =& \mathcal{F}[D_1 \bar{D}_1] \\ =& \sum_q e_q^2 \int \frac{d^2\boldsymbol{b}_T}{(2\pi)^2} \, e^{-i\boldsymbol{b}_T\cdot\boldsymbol{q}_T} \widetilde{D}_1(z_1, b_T) \widetilde{\bar{D}}_1(z_2, b_T) \\ =& \sum_q e_q^2 \int \frac{db_T}{(2\pi)} \, b_T J_0(b_T \, q_T) \widetilde{D}_1(z_1, b_T) \widetilde{\bar{D}}_1(z_2, b_T) \\ =& \mathcal{B}_0\left[\widetilde{D}\widetilde{\bar{D}}\right] . \end{aligned} \tag{G.5}$$

The second convolution we consider is $F_{TU}^{\sin(\phi_1-\phi_S)}$, defined as follows:

$$F_{TU}^{\sin(\phi_1-\phi_{S_1})} = \mathcal{F}\left[\frac{\hat{\boldsymbol{h}}\cdot\boldsymbol{k}_T}{M_{h_1}} D_{1T}^{\perp} \bar{D}_1\right] . \tag{G.6}$$

To work out this convolution we need the Fourier transform of the unpolarized fragmentation function, presented above, and the one of the polarizing fragmentation function multiplied by k_T^i, the i-th component of the transverse

momentum of the quark with respect to the hadron direction:

$$
\begin{aligned}
&\int d^2\boldsymbol{k}_T \, \frac{k_T^i}{M_{h_1}} e^{i\boldsymbol{b}_T\cdot\boldsymbol{k}_T} D_{1T}^{\perp}(z_1, k_\perp) \\
=&\frac{-i}{M_{h_1}} \frac{\partial}{\partial b_T^i} \int d^2\boldsymbol{k}_T \, e^{i\boldsymbol{b}_T\cdot\boldsymbol{k}_T} D_{1T}^{\perp}(z_1, k_\perp) \\
=&\frac{-i}{M_{h_1}} \frac{\partial}{\partial b_T^i} \widetilde{D}_{1T}^{\perp}(z_1, b_T) = \frac{-i}{M_{h_1}} \frac{b_T^i}{b_T} \frac{\partial}{\partial b_T} \widetilde{D}_{1T}^{\perp}(z_1, b_T) \\
=&\frac{-ib_T^i}{M_{h_1}} 2 \frac{\partial}{\partial b_T^2} \widetilde{D}_{1T}^{\perp}(z_1, b_T) = ib_T^i M_{h_1} \left(-\frac{2}{M_{h_1}^2} \frac{\partial}{\partial b_T^2} \widetilde{D}_{1T}^{\perp}(z_1, b_T) \right) \\
=&ib_T^i M_{h_1} \widetilde{D}_{1T}^{\perp(1)}(z_1, b_T) \,,
\end{aligned}
\tag{G.7}
$$

where we have used, to go from the first line to the second one, the following relation

$$
k_T^i \, e^{i\boldsymbol{b}_T\cdot\boldsymbol{k}_T} = -i \frac{\partial}{\partial b_T^i} e^{i\boldsymbol{b}_T\cdot\boldsymbol{k}_T} \,, \tag{G.8}
$$

and the definition of the Fourier transform of the polarizing fragmentation function

$$
\widetilde{D}_{1T}^{\perp}(z_1, b_T) = \int d^2\boldsymbol{k}_T \, e^{i\boldsymbol{b}_T\cdot\boldsymbol{k}_T} D_{1T}^{\perp}(z_1, \boldsymbol{k}_\perp) \,. \tag{G.9}
$$

In the very last step we have introduced $\widetilde{D}_{1T}^{\perp(1)}(z_1, b_T)$, the first moment of the polarizing fragmentation function in $\boldsymbol{b}_T$-space:

$$
\widetilde{D}_{1T}^{\perp(1)}(z_1, b_T) = \left(-\frac{2}{M_{h_1}^2} \frac{\partial}{\partial b_T^2} \widetilde{D}_{1T}^{\perp}(z_1, b_T) \right) . \tag{G.10}
$$

This term can be related to the first moment in $\boldsymbol{k}_T$-space, defined as:

$$D_{1T}^{\perp(1)}(z_1) = \int d^2\boldsymbol{k}_\perp \left(\frac{\boldsymbol{k}_\perp^2}{2z_1^2 M_{h_1}^2}\right) D_{1T}^{\perp}(z_1, k_\perp)\,, \tag{G.11}$$

adopting the limit of b_T going to zero:

$$\lim_{b_T \to 0} \widetilde{D}_{1T}^{\perp(1)}(z_1, b_T) = \frac{1}{z_1^2} D_{1T}^{\perp(1)}(z_1)\,. \tag{G.12}$$

We have indeed that:

$$\begin{aligned}
\widetilde{D}_{1T}^{\perp(1)}(z_1, b_T) &= \left(-\frac{2}{M_{h_1}^2} \frac{\partial}{\partial b_T^2} \widetilde{D}_{1T}^{\perp}(z_1, b_T) \right) \\
&= -\frac{2\pi}{b_T M_{h_1}^2} \frac{\partial}{\partial b_T} \int \frac{dk_\perp\, k_\perp}{z_1^2} J_0\left(\frac{b_T k_\perp}{z_1}\right) D_{1T}^{\perp(1)}(z_1, k_\perp) \\
&= \frac{2\pi}{M_{h_1}^2 z_1^3} \int dk_\perp \frac{k_\perp^2}{b_T} J_1\left(\frac{b_T k_\perp}{z_1}\right) D_{1T}^{\perp(1)}(z_1, k_\perp)\,,
\end{aligned} \tag{G.13}$$

where we have used the following relations:

$$\begin{aligned}
\frac{\partial}{\partial b_T} J_0(a b_T) &= -a J_1(a b_T) \\
\frac{1}{2b_T} \frac{\partial}{\partial b_T} &= \frac{\partial}{\partial b_T^2}\,.
\end{aligned} \tag{G.14}$$

Then by employing the additional relation

$$\lim_{b_T \to 0} \frac{J_1(a b_T)}{b_T} = \frac{a}{2}\,, \tag{G.15}$$

we are able to find Eq. (G.12):

$$\lim_{b_T \to 0} \widetilde{D}_{1T}^{\perp(1)}(z_1, b_T) = \frac{1}{z_1^2} \int d^2\boldsymbol{k}_\perp \left(\frac{\boldsymbol{k}_\perp^2}{2z_1^2 M_h^2}\right) D_{1T}^{\perp}(z_1, k_\perp)\,. \tag{G.16}$$

Finally with the results above, we can write again the $F_{TU}^{\sin(\phi_1-\phi_S)}$ convolution in $\boldsymbol{b}_T$-space:

$$
\begin{aligned}
&F_{TU}^{\sin(\phi_1-\phi_S)} = \mathcal{F}\left[\frac{\hat{h}\cdot\boldsymbol{k}_T}{M_{h_1}} D_{1T}^{\perp}\bar{D}_1\right] \\
=&\sum_q e_q^2 \int d^2\boldsymbol{k}_T d^2\boldsymbol{p}_T\, \delta^{(2)}(\boldsymbol{k}_T+\boldsymbol{p}_T-\boldsymbol{q}_T)\, \frac{\hat{h}\cdot\boldsymbol{k}_T}{M_{h_1}} D_{1T}^{\perp}(z_1,\boldsymbol{k}_T)\bar{D}_1(z_2,\boldsymbol{p}_T) \\
=&M_{h_1}\sum_q e_q^2 \int \frac{d^2\boldsymbol{b}_T}{(2\pi)^2}\, e^{-i\boldsymbol{b}_T\cdot\boldsymbol{q}_T}(i\hat{h}\cdot\boldsymbol{b}_T)\widetilde{D}_{1T}^{\perp(1)}(z_1,b_T)\widetilde{\bar{D}}_1(z_2,b_T) \\
=&M_{h_1}\sum_q e_q^2 \int \frac{db_T}{2\pi}\, b_T^2 J_1(q_T\, b_T)\widetilde{D}_{1T}^{\perp(1)}(z_1,b_T)\widetilde{\bar{D}}_1(z_2,b_T) \\
=&M_{h_1}\mathcal{B}_1\left[\widetilde{D}_{1T}^{\perp(1)}\widetilde{\bar{D}}_1\right],
\end{aligned}
\tag{G.17}
$$

where we have used the integral definition of the J_1 Bessel function:

$$
\int_0^{2\pi} d\theta\, e^{ib_T k_T\cos\theta}\cos\theta = (2\pi i)J_1(b_T k_T)\,. \tag{G.18}
$$

G.1. Examples of Fourier transforms and first moments: Gaussian model

As a first example of parametrization for the transverse momentum dependence of FFs, we present a simple Gaussian model, and we will derive its Fourier transform and first moment. We use the following Gaussian model for a generic TMD fragmentation function:

$$
D(z_1,k_\perp) = D(z_1,0)\frac{e^{-k_\perp^2/\langle k_\perp^2\rangle_D}}{\pi\langle k_\perp^2\rangle_1}. \tag{G.19}
$$

where $\langle k_\perp^2 \rangle_1$ is the Gaussian width of the unpolarized TMD-FF. According to Eq. (G.11), its first moment is:

$$\begin{aligned} D^{(1)}(z_1) &= \int d^2\boldsymbol{k}_\perp \left(\frac{\boldsymbol{k}_\perp^2}{2z_1^2 M_h^2} \right) D(z_1, k_\perp) \\ &= D(z_1, 0) \frac{\langle k_\perp^2 \rangle_D^2}{2z_1^2 M_h^2 \langle k_\perp^2 \rangle_1} \end{aligned} \tag{G.20}$$

and the b_T-space fragmentation function is

$$\begin{aligned} \widetilde{D}(z_1, b_T) =& \int d^2\boldsymbol{k}_T \, e^{i\boldsymbol{b}_T \cdot \boldsymbol{k}_T} D_1(z_1, \boldsymbol{k}_\perp) \\ =& 2\pi \int dk_T \, k_T J_0(b_T k_T) D_1(z_1, k_\perp) \\ =& 2\pi \int \frac{dk_\perp \, k_\perp}{z_1^2} J_0\left(\frac{b_T k_\perp}{z_1} \right) D_1(z_1, k_\perp) \\ =& \frac{D_1(z_1, 0)}{z_1^2} \frac{\langle k_\perp^2 \rangle_D}{\langle k_\perp^2 \rangle_1} e^{-b_T^2 \langle k_\perp^2 \rangle_D / (4z_1^2)} \end{aligned} \tag{G.21}$$

We notice that, when $\langle k_\perp^2 \rangle_D = \langle k_\perp^2 \rangle_1$ in the case of the unpolarized fragmentation function, then

$$\lim_{b_T \to 0} \widetilde{D}(z_1, b_T) = \frac{1}{z_1^2} D_1(z_1, 0) \tag{G.22}$$

where $D_1(z_1, 0)$ coincides with $d_{j/h}$ in the OPE in Eq. (5.33). Employing the first moment definition in $\boldsymbol{b}_T$-space, Eq. (G.10), we have:

$$\begin{aligned}\widetilde{D}^{(1)}(z_1, b_T) &= \left(-\frac{2}{M_h^2}\frac{\partial}{\partial b_T^2}\widetilde{D}_{1T}^{\perp}(z_1, b_T)\right) \\ &= D(z_1, 0)\frac{1}{2z_1^4 M_h^2}\frac{\langle k_\perp^2\rangle_D^2}{\langle k_\perp^2\rangle_1} e^{-b_T^2\langle k_\perp^2\rangle_D/(4z_1^2)}\,.\end{aligned} \tag{G.23}$$

Then, using Eq. (G.12), we find:

$$\begin{aligned}\lim_{b_T\to 0}\widetilde{D}^{(1)}(z_1, b_T) &= \frac{1}{z_1^2}\left[\frac{1}{2M_h^2 z_1^2}\frac{\langle k_\perp^2\rangle_D^2}{\langle k_\perp^2\rangle_1} D(z_1, 0)\right] \\ &= \frac{1}{z_1^2} D^{(1)}(z_1)\,.\end{aligned} \tag{G.24}$$

G.2. Examples of Fourier transforms and first moments: Power Law model

The second, and last, model used to parametrize the transverse momentum dependence of FFs, of which we calculate its Fourier transform and first moment, is the the Power-Law model. This is defined as follows:

$$D(z_1, k_\perp) = D(z_1, 0)\frac{\Gamma(p)}{\pi\Gamma(p-1)}\frac{m^{2(p-1)}}{(k_\perp^2 + m^2)^p}\,. \tag{G.25}$$

Its Fourier transform is:

$$\widetilde{D}(z_1, b_T) = D(z_1, 0)\frac{2^{2-p}}{\Gamma(p-1)}\left(b_T m/z_1\right)^{p-1} K_{p-1}(b_T m/z_1)\,. \tag{G.26}$$

The integrated first moment and the first moment in $\boldsymbol{b}_T$ space are:

$$D^{(1)}(z_1) = D(z_1, 0)\frac{1}{M_h^2 z_1^2}\frac{m^2}{2(p-2)} \tag{G.27}$$

$$\widetilde{D}^{(1)}(z_1, b_T) = D(z_1, 0)\frac{2^{2-p}}{\Gamma(p-1)}\frac{m^2}{M_h^2 z_1^2}(b_T m/z_1)^{p-2} K_{p-2}(b_T m/z_1)\,. \tag{G.28}$$

Bibliography

[1] L. Dick et al. Spin Effects in the Inclusive Reactions pi+- Polarized p –> pi+- Anything at 8-GeV/c. *Phys. Lett. B*, 57:93–96, 1975.

[2] R. D. Klem, J. E. Bowers, H. W. Courant, H. Kagan, M. L. Marshak, E. A. Peterson, K. Ruddick, W. H. Dragoset, and J. B. Roberts. Measurement of Asymmetries of Inclusive Pion Production in Proton Proton Interactions at 6-GeV/c and 11.8-GeV/c. *Phys. Rev. Lett.*, 36:929–931, 1976.

[3] W. H. Dragoset, J. B. Roberts, J. E. Bowers, H. W. Courant, H. Kagan, M. L. Marshak, E. A. Peterson, K. Ruddick, and R. D. Klem. Asymmetries in Inclusive Proton-Nucleon Scattering at 11.75-GeV/c. *Phys. Rev. D*, 18:3939–3954, 1978.

[4] G. Bunce et al. Lambda0 Hyperon Polarization in Inclusive Production by 300-GeV Protons on Beryllium. *Phys. Rev. Lett.*, 36:1113–1116, 1976.

[5] D. L. Adams et al. Analyzing power in inclusive pi+ and pi- production at high x(F) with a 200-GeV polarized proton beam. *Phys. Lett. B*, 264:462–466, 1991.

[6] D. L. Adams et al. Comparison of spin asymmetries and cross-sections in pi0 production by 200-GeV polarized anti-protons and protons. *Phys. Lett. B*, 261:201–206, 1991.

[7] D. L. Adams et al. Large x(F) spin asymmetry in pi0 production by 200-GeV polarized protons. *Z. Phys. C*, 56:181–184, 1992.

[8] A. Bravar et al. Single spin asymmetries in inclusive charged pion production by transversely polarized anti-protons. *Phys. Rev. Lett.*, 77:2626–2629,

1996.

[9] J. Adams et al. Identified particle distributions in pp and Au+Au collisions at s(NN)**(1/2) = 200 GeV. *Phys. Rev. Lett.*, 92:112301, 2004.

[10] J. Adams et al. Forward neutral pion production in p+p and d+Au collisions at s(NN)**(1/2) = 200-GeV. *Phys. Rev. Lett.*, 97:152302, 2006.

[11] S. S. Adler et al. Absence of suppression in particle production at large transverse momentum in S(NN)**(1/2) = 200-GeV d + Au collisions. *Phys. Rev. Lett.*, 91:072303, 2003.

[12] S. S. Adler et al. Measurement of transverse single-spin asymmetries for mid-rapidity production of neutral pions and charged hadrons in polarized p+p collisions at s**(1/2) = 200-GeV. *Phys. Rev. Lett.*, 95:202001, 2005.

[13] I. Arsene et al. Production of mesons and baryons at high rapidity and high P(T) in proton-proton collisions at s**(1/2) = 200-GeV. *Phys. Rev. Lett.*, 98:252001, 2007.

[14] Gordon L. Kane, J. Pumplin, and W. Repko. Transverse Quark Polarization in Large p(T) Reactions, e+ e- Jets, and Leptoproduction: A Test of QCD. *Phys. Rev. Lett.*, 41:1689, 1978.

[15] Dennis W. Sivers. Single Spin Production Asymmetries from the Hard Scattering of Point-Like Constituents. *Phys. Rev. D*, 41:83, 1990.

[16] Dennis W. Sivers. Hard scattering scaling laws for single spin production asymmetries. *Phys. Rev. D*, 43:261–263, 1991.

[17] Alessandro Bacchetta, Umberto D'Alesio, Markus Diehl, and C. Andy Miller. Single-spin asymmetries: The trento conventions. *Phys. Rev.*, D70:117504, 2004.

[18] P. J. Mulders and R. D. Tangerman. The complete tree-level result up to order 1/q for polarized deep-inelastic leptoproduction. *Nucl. Phys.*, B461:197–237, 1996.

[19] Alessandro Bacchetta, Markus Diehl, Klaus Goeke, Andreas Metz, Piet J. Mulders, and Marc Schlegel. Semi-inclusive deep inelastic scattering at small transverse momentum. *JHEP*, 02:093, 2007.

[20] John C. Collins. Fragmentation of transversely polarized quarks probed in transverse momentum distributions. *Nucl. Phys. B*, 396:161–182, 1993.

[21] Daniel Boer and P.J. Mulders. Time reversal odd distribution functions in leptoproduction. *Phys. Rev. D*, 57:5780–5786, 1998.

[22] Xiang-dong Ji, Jian-Ping Ma, and Feng Yuan. QCD factorization for spin-dependent cross sections in DIS and Drell-Yan processes at low transverse momentum. *Phys. Lett. B*, 597:299–308, 2004.

[23] Xiang-dong Ji, Jian-ping Ma, and Feng Yuan. QCD factorization for semi-inclusive deep-inelastic scattering at low transverse momentum. *Phys. Rev. D*, 71:034005, 2005.

[24] John Collins. *Foundations of Perturbative QCD*. Cambridge Monographs on Particle Physics, Nuclear Physics and Cosmology. Cambridge University Press, 2011.

[25] Miguel G. Echevarria, Ahmad Idilbi, and Ignazio Scimemi. Factorization Theorem For Drell-Yan At Low q_T And Transverse Momentum Distributions On-The-Light-Cone. *JHEP*, 07:002, 2012.

[26] John C. Collins. Leading twist single transverse-spin asymmetries: Drell-Yan and deep inelastic scattering. *Phys. Lett. B*, 536:43–48, 2002.

[27] Stanley J. Brodsky, Dae Sung Hwang, Yuri V. Kovchegov, Ivan Schmidt, and Matthew D. Sievert. Single-Spin Asymmetries in Semi-inclusive Deep Inelastic Scattering and Drell-Yan Processes. *Phys. Rev. D*, 88(1):014032, 2013.

[28] M. Anselmino, M. Boglione, U. D'Alesio, S. Melis, F. Murgia, E. R. Nocera, and A. Prokudin. General Helicity Formalism for Polarized Semi-Inclusive Deep Inelastic Scattering. *Phys. Rev.*, D83:114019, 2011.

[29] S. Arnold, A. Metz, and M. Schlegel. Dilepton production from polarized hadron hadron collisions. *Phys. Rev. D*, 79:034005, 2009.

[30] Daniel Boer, R. Jakob, and P. J. Mulders. Asymmetries in polarized hadron production in e+ e- annihilation up to order 1/q. *Nucl. Phys.*, B504:345–380, 1997.

[31] M. Anselmino, M. Boglione, U. D'Alesio, E. Leader, S. Melis, and F. Murgia. The general partonic structure for hadronic spin asymmetries. *Phys. Rev. D*, 73:014020, 2006.

[32] M. Anselmino, M. Boglione, U. D'Alesio, F. Murgia, and A. Prokudin. Role of transverse momentum dependence of unpolarized parton distribution and fragmentation functions in the analysis of azimuthal spin asymmetries. *Phys. Rev.*, D98(9):094023, 2018.

[33] Y. Guan et al. Observation of Transverse $\Lambda/\bar{\Lambda}$ Hyperon Polarization in e^+e^- Annihilation at Belle. *Phys. Rev. Lett.*, 122(4):042001, 2019.

[34] John C. Collins and Andreas Metz. Universality of soft and collinear factors in hard-scattering factorization. *Phys. Rev. Lett.*, 93:252001, 2004.

[35] M. Anselmino, Daniel Boer, U. D'Alesio, and F. Murgia. Lambda polarization from unpolarized quark fragmentation. *Phys. Rev. D*, 63:054029, 2001.

[36] Kenneth J. Heller et al. Polarization of Lambdas and anti-Lambdas Produced by 400-GeV Protons. *Phys. Rev. Lett.*, 41:607, 1978. [Erratum: Phys.Rev.Lett. 45, 1043 (1980)].

[37] Leonard Gamberg, Zhong-Bo Kang, Daniel Pitonyak, Marc Schlegel, and Shinsuke Yoshida. Polarized hyperon production in single-inclusive electron-positron annihilation at next-to-leading order. *JHEP*, 01:111, 2019.

[38] Zhong-Bo Kang, Ding Yu Shao, and Fanyi Zhao. QCD resummation on single hadron transverse momentum distribution with the thrust axis. *JHEP*, 12:127, 2020.

[39] M. Boglione and A. Simonelli. Factorization of $e^+e^- \to H\,X$ cross section, differential in z_h, P_T and thrust, in the 2-jet limit. *JHEP*, 02:076, 2021.

[40] M. Boglione and A. Simonelli. Universality-breaking effects in e^+e^- hadronic production processes. *Eur. Phys. J. C*, 81(1):96, 2021.

[41] Umberto D'Alesio, Francesco Murgia, and Marco Zaccheddu. First extraction of the Λ polarizing fragmentation function from Belle e^+e^- data. *Phys. Rev. D*, 102(5):054001, 2020.

[42] M. Anselmino et al. Transversity and Collins functions from SIDIS and e+ e- data. *Phys. Rev.*, D75:054032, 2007.

[43] M. Anselmino, Daniel Boer, U. D'Alesio, and F. Murgia. Transverse lambda polarization in semiinclusive DIS. *Phys. Rev. D*, 65:114014, 2002.

[44] M. Anselmino, R. Kishore, and A. Mukherjee. Polarizing fragmentation function and the Λ polarization in e^+e^- processes. *Phys. Rev. D*, 100(1):014029, 2019.

[45] Daniel Callos, Zhong-Bo Kang, and John Terry. Extracting the transverse momentum dependent polarizing fragmentation functions. *Phys. Rev. D*, 102(9):096007, 2020.

[46] Ambar Jain, Massimiliano Procura, and Wouter J. Waalewijn. Fully-Unintegrated Parton Distribution and Fragmentation Functions at Perturbative k_T. *JHEP*, 04:132, 2012.

[47] Yiannis Makris, Felix Ringer, and Wouter J. Waalewijn. Joint thrust and TMD resummation in electron-positron and electron-proton collisions. *JHEP*, 02:070, 2021.

[48] M. Anselmino, M. Boglione, U. D'Alesio, J. O. Gonzalez Hernandez, S. Melis, F. Murgia, and A. Prokudin. Collins functions for pions from SIDIS and new e^+e^- data: a first glance at their transverse momentum dependence. *Phys. Rev.*, D92(11):114023, 2015.

[49] Daniel de Florian, Rodolfo Sassot, and Marco Stratmann. Global analysis of

fragmentation functions for pions and kaons and their uncertainties. *Phys. Rev.*, D75:114010, 2007.

[50] S. Albino, B. A. Kniehl, and G. Kramer. AKK Update: Improvements from New Theoretical Input and Experimental Data. *Nucl. Phys. B*, 803:42–104, 2008.

[51] M. Anselmino, M. Boglione, U. D'Alesio, A. Kotzinian, F. Murgia, and A. Prokudin. The Role of Cahn and Sivers effects in deep inelastic scattering. *Phys. Rev. D*, 71:074006, 2005.

[52] M. Anselmino, M. Boglione, U. D'Alesio, A. Kotzinian, S. Melis, F. Murgia, A. Prokudin, and C. Turk. Sivers Effect for Pion and Kaon Production in Semi-Inclusive Deep Inelastic Scattering. *Eur. Phys. J.*, A39:89–100, 2009.

[53] Daniel Boer, R. Jakob, and P. J. Mulders. Angular dependences in electroweak semiinclusive leptoproduction. *Nucl. Phys. B*, 564:471–485, 2000.

[54] S. Kretzer, H. L. Lai, F. I. Olness, and W. K. Tung. Cteq6 parton distributions with heavy quark mass effects. *Phys. Rev. D*, 69:114005, 2004.

[55] M. Boglione and A. Simonelli. Kinematic regions in the $e^+e^- \to h\,X$ factorized cross section in a 2-jet topology with thrust. 9 2021.

[56] Umberto D'Alesio, Francesco Murgia, and Marco Zaccheddu. General helicity formalism for two-hadron production in e^+e annihilation within a TMD approach. *JHEP*, 10:078, 2021.

[57] J. Collins, L. Gamberg, A. Prokudin, T. C. Rogers, N. Sato, and B. Wang. Relating Transverse Momentum Dependent and Collinear Factorization Theorems in a Generalized Formalism. *Phys. Rev. D*, 94(3):034014, 2016.

[58] John Collins and Ted Rogers. Understanding the large-distance behavior of transverse-momentum-dependent parton densities and the Collins-Soper evolution kernel. *Phys. Rev. D*, 91(7):074020, 2015.

[59] Daniel Boer, Zhong-Bo Kang, Werner Vogelsang, and Feng Yuan. Test of the Universality of Naive-time-reversal-odd Fragmentation Functions. *Phys.*

Rev. Lett., 105:202001, 2010.

[60] Jian-wei Qiu and George F. Sterman. Single transverse spin asymmetries. *Phys. Rev. Lett.*, 67:2264–2267, 1991.

[61] Jian-wei Qiu and George F. Sterman. Single transverse spin asymmetries in direct photon production. *Nucl. Phys. B*, 378:52–78, 1992.

[62] C. A. Aidala, B. Field, L. P. Gamberg, and T. C. Rogers. Limits on transverse momentum dependent evolution from semi-inclusive deep inelastic scattering at moderate Q. *Phys. Rev. D*, 89(9):094002, 2014.

[63] Peng Sun, Joshua Isaacson, C. P. Yuan, and Feng Yuan. Nonperturbative functions for SIDIS and Drell–Yan processes. *Int. J. Mod. Phys. A*, 33(11):1841006, 2018.

[64] F. Landry, R. Brock, Pavel M. Nadolsky, and C. P. Yuan. Tevatron Run-1 Z boson data and Collins-Soper-Sterman resummation formalism. *Phys. Rev. D*, 67:073016, 2003.

[65] Anton V. Konychev and Pavel M. Nadolsky. Universality of the Collins-Soper-Sterman nonperturbative function in gauge boson production. *Phys. Lett. B*, 633:710–714, 2006.

[66] M. Boglione, J. O. Gonzalez-Hernandez, and R. Taghavi. Transverse parton momenta in single inclusive hadron production in e^+e^- annihilation processes. *Phys. Lett.*, B772:78–86, 2017.

[67] Leonard Gamberg, Zhong-Bo Kang, Ding Yu Shao, John Terry, and Fanyi Zhao. Transverse Λ polarization in e^+e collisions. *Phys. Lett. B*, 818:136371, 2021.

[68] Thomas Becher, Matthias Neubert, Lorena Rothen, and Ding Yu Shao. Effective Field Theory for Jet Processes. *Phys. Rev. Lett.*, 116(19):192001, 2016.

[69] Thomas Becher, Matthias Neubert, Lorena Rothen, and Ding Yu Shao. Factorization and Resummation for Jet Processes. *JHEP*, 11:019, 2016. [Erratum: JHEP 05, 154 (2017)].

[70] Thomas Becher, Benjamin D. Pecjak, and Ding Yu Shao. Factorization for the light-jet mass and hemisphere soft function. *JHEP*, 12:018, 2016.

[71] Thomas Becher, Rudi Rahn, and Ding Yu Shao. Non-global and rapidity logarithms in narrow jet broadening. *JHEP*, 10:030, 2017.

[72] Simon Caron-Huot. Resummation of non-global logarithms and the BFKL equation. *JHEP*, 03:036, 2018.

[73] Zoltan Nagy and Davison E. Soper. Summing threshold logs in a parton shower. *JHEP*, 10:019, 2016.

[74] Zoltan Nagy and Davison E. Soper. What is a parton shower? *Phys. Rev. D*, 98(1):014034, 2018.

[75] M. Dasgupta and G. P. Salam. Resummation of nonglobal QCD observables. *Phys. Lett. B*, 512:323–330, 2001.

[76] Alessandro Bacchetta, Filippo Delcarro, Cristian Pisano, Marco Radici, and Andrea Signori. Extraction of partonic transverse momentum distributions from semi-inclusive deep-inelastic scattering, Drell-Yan and Z-boson production. *JHEP*, 06:081, 2017.

[77] Hans Dembinski and Piti Ongmongkolkul et al. scikit-hep/iminuit. Dec 2020.

[78] Zhong-Bo Kang, Alexei Prokudin, Nobuo Sato, and John Terry. Efficient fourier transforms for transverse momentum dependent distributions. *Comput. Phys. Commun.*, 258:107611, 2021.

[79] Kai-Bao Chen, Zuo-Tang Liang, Yan-Lei Pan, Yu-Kun Song, and Shu-Yi Wei. Isospin Symmetry of Fragmentation Functions. *Phys. Lett. B*, 816:136217, 2021.

[80] E. Leader. Spin in particle physics. *Camb. Monogr. Part. Phys. Nucl. Phys. Cosmol.*, 15:1, 2001.

List of figures

List of tables